

SUB-NYQUIST MULTICOSET AND MIMO SAMPLING: PERFECT
RECONSTRUCTION, PERFORMANCE ANALYSIS, AND NECESSARY DENSITY
CONDITIONS

BY

RAMAN C. VENKATARAMANI

B.Tech., Indian Institute of Technology, Madras, 1995
M.S.E., Johns Hopkins University, 1996

THESIS

Submitted in partial fulfillment of the requirements
for the degree of Doctor of Philosophy in Electrical Engineering
in the Graduate College of the
University of Illinois at Urbana-Champaign, 2001

Urbana, Illinois

**Sub-Nyquist Multicoset and MIMO Sampling: Perfect
Reconstruction, Performance Analysis, and Necessary Density
Conditions**

Approved by

Prof. David Munson
Prof. Pierre Moulin
Prof. Andrew Singer
Prof. Joseph Roseblatt
Prof. Yoram Bresler (Chairman)

ABSTRACT

We study two *sub-Nyquist* sampling schemes for multiband signals known as *multicoset sampling* and *multiple-input, multiple-output (MIMO) sampling*. A multiband signal is one whose Fourier transform is supported on a set $\mathcal{F} \subseteq \mathbb{R}$ consisting of a finite union of intervals. Unlike uniform sampling, multicoset sampling allows perfect reconstruction of a multiband input at sampling rates arbitrarily close to its Landau minimum rate equal to the Lebesgue measure of \mathcal{F} . We derive perfect reconstruction conditions, an explicit interpolation formula, and bounds on the aliasing error for signals not spectrally supported on \mathcal{F} . We also examine the performance of the reconstruction system when the input contains additive sample noise. Using these measures of performance, we optimize the reconstruction system. We find that optimizing these parameters improves the performance significantly. There is an increased sensitivity to errors associated with nonuniform sampling, as opposed to uniform sampling. However, these errors can be controlled by optimal design, demonstrating the potential for practical multifold reductions in sampling rate. Multicoset sampling is applicable to Fourier imaging problems like synthetic aperture radar and magnetic resonance imaging, where the objective is to image a sparse object from limited Fourier data.

We then study the MIMO sampling problem, where a set of multiband input signals is passed through a MIMO channel and the outputs are sampled nonuniformly. MIMO sampling is motivated from applications like multiuser communications and multiple source separation. MIMO sampling encompasses several sampling strategies as special cases, including multicoset sampling and Papoulis's generalized sampling. We derive necessary density conditions for stable reconstruction of the channel inputs from the output. These results generalize Landau's sampling density results to the MIMO problem. We then investigate a special case of MIMO sampling called *commensurate periodic nonuniform MIMO sampling*, for which we present reconstruction conditions. Finally, we address the problem of reconstruction FIR filter design, formulating it as a minimization and recasting as a standard semi-infinite linear program. Owing to the generality of the MIMO sampling scheme, the design algorithm readily applies to several sampling schemes for multiband signals.

To my parents

ACKNOWLEDGMENTS

I am deeply indebted to my adviser Professor Yoram Bresler for his endless support and guidance during the entire course of my doctoral study, and for making my stay here a very enjoyable one. I also extremely grateful to Professors David Munson, Pierre Moulin, Andrew Singer, and Joseph Rosenblatt for serving on my committee and for providing invaluable advice for improving my dissertation.

I would like to thank my fellow grad students Michael Gastpar, Samit, Prakash, Brian, Nitin, Dror, Ashvin, Sanjay, and Srisankar for all useful discussions, and Pete, Qi, and Jill for being the nicest officemates in CSL.

I am very thankful to my brother Shankar for the numerous interesting discussions, especially those over dinner at Medici. Finally, none of all this would have been possible without the unfailing support and encouragement of my parents and friends.

TABLE OF CONTENTS

CHAPTER	PAGE
1 INTRODUCTION	1
1.1 Sub-Nyquist Sampling of Multiband Signals	1
1.2 Layout	2
2 SUB-NYQUIST MULTICOSET SAMPLING: PERFECT RECONSTRUCTION AND ALIASING ERROR BOUNDS	4
2.1 Introduction	4
2.1.1 Nonuniform sampling	6
2.1.2 Error bounds	7
2.2 Multicoreset Sampling	8
2.3 Reconstruction	10
2.4 Error Bounds	15
2.4.1 Sup-norm of the error	16
2.4.2 L^2 -norm of the error	17
2.4.3 Performance in the presence of noise	18
2.5 Summary	18
3 OPTIMAL MULTICOSET SAMPLING AND RECONSTRUCTION	20
3.1 Introduction	20
3.2 Multicoreset Sampling	23
3.2.1 Signals and data	23
3.2.2 Definitions and notation	24
3.2.3 Error bounds	27
3.3 Optimal Reconstruction	28
3.3.1 Minimizing the aliasing error energy	29
3.3.2 Minimizing the output noise power	30
3.3.3 Minimizing the peak aliasing error	30
3.3.4 Lower bounds on ψ_∞ , ψ_2 , and ψ_n	31
3.3.5 Which criterion to optimize?	34
3.4 Optimal Sampling	36
3.4.1 Optimizing the choice of T	36
3.4.2 Sampling pattern design	38
3.5 Comparisons	39
3.5.1 Uniform sampling versus nonuniform sampling for packable \mathcal{F}	41
3.5.2 Penalty for nonpackability	42

3.6	Summary	43
4	MIMO SAMPLING: NECESSARY DENSITY CONDITIONS AND STABILITY ISSUES	44
4.1	Introduction	44
4.1.1	Problem formulation	45
4.2	Preliminaries	47
4.2.1	Stable sampling and consistency	48
4.2.2	Notions of sampling density	52
4.3	Necessary Density Conditions	54
4.3.1	A comparison theorem	55
4.3.2	Density conditions for stable sampling	63
4.3.3	Density conditions for consistent reconstruction	76
4.4	Summary	84
5	SAMPLING THEOREMS FOR UNIFORM AND PERIODIC NONUNIFORM MIMO SAMPLING OF MULTIBAND SIGNALS	86
5.1	Introduction	86
5.1.1	Problem formulation	87
5.2	Preliminaries	88
5.3	Sampling and Reconstruction Models	89
5.4	Perfect Reconstruction	94
5.4.1	Stable sampling	96
5.4.2	Conditions for perfect reconstruction	98
5.4.3	Existence of continuous solutions	102
5.5	Summary	106
6	FILTER DESIGN FOR MIMO SAMPLING AND RECONSTRUCTION	107
6.1	Introduction	107
6.2	Preliminaries	109
6.3	Sampling and Reconstruction Models	110
6.4	Conditions for Perfect Reconstruction	112
6.5	Reconstruction Filter Design	117
6.5.1	The cost function	120
6.5.2	Semi-infinite linear program formulation	123
6.5.3	Design example	125
6.6	Summary	129
7	CONCLUSION	132
7.1	Directions for Future Research	134
7.1.1	Sampling pattern design and asymptotic analysis	134
7.1.2	Sufficient density conditions	134

APPENDIX A PROOFS AND CALCULATIONS	136
A.1 Proof of Lemma 2.1	136
A.2 Proof of Theorem 2.1	137
A.3 Proof of Theorem 2.2	137
A.4 Proof of Theorem 2.3	139
A.5 Proof of Theorem 2.4	141
A.6 Proof of Theorem 2.5	142
A.7 Proof of Lemma 3.1	143
A.8 Proof of Lemma 3.2	144
A.9 Proof of Theorem 3.3	146
A.10 Proof of Proposition 4.1	147
A.11 Proof of Proposition 4.2	148
A.12 Proof of Proposition 4.3	149
A.13 Proof of Lemma 5.1	150
A.14 Proof of Proposition 6.3	151
APPENDIX B JUSTIFICATION FOR DISCRETE-TIME MODELS . . .	153
B.1 Channel Model	153
B.2 Reconstruction Model	155
REFERENCES	157
VITA	162

LIST OF TABLES

Table	Page
3.1	Design criteria evaluated at the candidate optimal sampling patterns: $\mathcal{C}_a = \{0, 1, 2, 13, 16\}$, $\mathcal{C}_b = \{0, 4, 7, 14, 15\}$, and $\mathcal{C}_c = \{0, 1, 2, 8, 17\}$. The boxed entries are optimal in their respective rows.
3.2	Normalized error gain constant η_∞ for $2 \leq p \leq 5$
6.1	Cost functions $\bar{C}_0(\boldsymbol{\alpha}_o^0)$ and $\bar{C}_1(\boldsymbol{\alpha}_o^1)$ at optimality for FIR reconstruction filters of length $2\tau + 1$, $1 \leq \tau \leq 6$

LIST OF FIGURES

Figure	Page
2.1 Spectrum of a nonpackable multiband signal.	5
2.2 Two sampling patterns for $(L, p) = (5, 3)$: (a) $\mathcal{C} = \{0, 1, 2\}$, and (b) $\mathcal{C} = \{0, 1, 3\}$	9
2.3 (a) Indicator function of the spectral support \mathcal{F} of span $1/T = 5$. (b) Left-hand side of Eq. (2.10). (c) Active spectral subcells.	13
2.4 Multicoset sampling and reconstruction. The block “I” is an ideal sinc interpolator.	15
3.1 Model for multicoset sampling.	24
3.2 Multicoset sampling and reconstruction. The block “I” is an ideal sinc interpolator.	27
3.3 Normalized error gain constants η_2 and η_n shown as functions of the number of multicoset samples p in each period.	40
4.1 MIMO sampling.	45
4.2 $K(f)$	74
4.3 Typical spectra of the channel inputs and outputs.	74
5.1 Models for MIMO sampling and reconstruction.	87
5.2 Example multiband input spectra $X_0(f)$, and $X_1(f)$ to a MIMO channel with $R = 2$	90
5.3 Commensurate periodic nonuniform sampling sets.	93
5.4 Smallest and largest eigenvalues of $\mathbf{S}(f)$	106
6.1 Discrete-time model for the MIMO channel.	108
6.2 Discrete-time model for MIMO reconstruction.	108
6.3 Indicator function of the spectral support \mathcal{F}	125
6.4 Magnitude and phase responses of the optimal FIR filters $H_1[\nu]$ and $H_2[\nu]$	127
6.5 Approximation error $\ \mathbf{T}^{rs}[\nu]\ $ at optimality.	128
6.6 (a) Spectral support of $X_1[\nu]$, and (b) spectral support of $X_2[\nu]$	128
6.7 Optimal costs (a) $\bar{C}_0(\boldsymbol{\alpha}_o^0)$, and (b) $\bar{C}_1(\boldsymbol{\alpha}_o^1)$ for FIR reconstruction filters of length $2\tau + 1$, $1 \leq \tau \leq 6$	130
B.1 Discrete-time model for the MIMO channel.	155
B.2 Discrete-time model for MIMO reconstruction.	156

CHAPTER 1

INTRODUCTION

1.1 Sub-Nyquist Sampling of Multiband Signals

The classical sampling theorem, attributed to Whittaker, Kotelnikov, and Shannon, states that a low-pass signal can be recovered perfectly from its samples taken at a finite rate. Shannon’s original statement [1, pp. 11] of the classical sampling theorem is that “if a function $f(t)$ contains no frequencies higher than W cycles per second, it is completely determined by giving its ordinates at a series of points spaced $1/2W$ seconds apart.” Since Shannon’s paper, there has been a long history of research in the area producing several important results in sampling of multiband signals and nonuniform sampling [2–5]. The term *multiband* generally refers to a signal whose spectrum is supported on a set $\mathcal{F} \subseteq \mathbb{R}$ consisting of a finite union of finite intervals. Sometimes, however, \mathcal{F} is any real measurable set of finite measure.

In the context of multiband sampling, Landau [6, 7] proved a fundamental result that the sampling density needed for stable sampling and reconstruction of a signal is lower bounded by the Lebesgue measure of the spectral support. Landau’s result applies to any arbitrary nonuniform sampling scheme and arbitrary spectral support of finite measure. We can see offhand that a multiband signal can be recovered from its uniform samples if the sampling rate is large enough to prevent aliasing. The smallest such rate is called the *Nyquist rate*. For many signals, especially those whose spectral supports are sparse, the Landau minimum rate is significantly smaller than the Nyquist rate, and it is worth exploring efficient representations for such signals using low sampling rates. This motivates the study of *sub-Nyquist sampling* and the desire to approach Landau’s minimum sampling rate. Naturally, one needs to sample the signal nonuniformly to hope for sub-Nyquist sampling. Thus, the emphasis in this dissertation is to explore the advantages of nonuniform sampling which has to be addressed by more complex reconstruction systems, instead of its role as a “necessary evil” in much of the previous work.

From a practical perspective, sub-Nyquist sampling is essential in many Fourier imaging applications such as synthetic aperture radar (SAR) and magnetic resonance imaging (MRI), where the physics of the problem gives us measurements of an unknown sparse object in its Fourier domain [8–11]. The problem is to recover the unknown object from these measurements. Very often, there is a cost associated with acquisition of samples, and it becomes desirable to sample minimally and exploit the sparsity (i.e., multiband structure) in the object to form its image. The Fourier imaging problem is precisely a dual of the sub-Nyquist sampling problem with the roles of frequency and space interchanged.

In this dissertation, we investigate several issues pertaining to two sub-Nyquist sampling schemes: *multicoset sampling* and *multiple-input multiple-output (MIMO) sampling*. Multicoset sampling is essentially a periodic nonuniform sampling scheme that allows us to approach Landau’s lower bound on the sampling density asymptotically as the period of the sampling pattern goes to infinity. We study the perfect reconstruction problem for multicoset sampling of multiband signals. We investigate the performance of multicoset sampling, and ways to optimize it.

MIMO sampling is a very general sampling scheme where a set of multiband signals undergoes time-invariant filtering through a MIMO channel, and the outputs are subsequently sampled nonuniformly. Again, the objective is to recover the inputs from the output samples. The spectral supports of the inputs need not all be the same. This sampling scheme is motivated by problems in multichannel deconvolution, where MIMO channels occur naturally. Nonetheless, MIMO sampling is equally important from a theoretical viewpoint, as it encompasses a large class of sampling schemes including Papoulis’s generalized sampling [12], multicoset sampling, and vector sampling [13]. Our main contributions are necessary density results for MIMO sampling. These results are generalizations of Landau’s classical density results [6, 7] for sampling and interpolation of multiband signals. We also provide theorems (sufficient conditions) for perfect reconstruction reconstruction, and address the design of optimal finite impulse response (FIR) reconstruction filters.

1.2 Layout

This dissertation is organized as follows. Chapters 2 and 3 deal with multicoset sampling of multiband signals, and Chapters 4, 5, and 6 deal with MIMO sampling of multiband signals. The term *multiband signal* always refers to one whose spectral support is a finite union of finite disjoint intervals, except in the context of necessary density results (Chapter 4), where they can

be arbitrary measurable sets of finite measure. The chapters are written such that each chapter may be read independently of the others. In every chapter, we introduce necessary definitions and notation, and review some relevant results from the previous chapters.

In Chapter 2, we investigate the sub-Nyquist multicaset sampling of multiband signals. We derive perfect reconstruction conditions and present an explicit interpolation equation. We also study the performance analysis of the multicaset sampling scheme which includes bounds on the aliasing error due to signal mismodeling, and sensitivity to noise as inferred from the noise amplification factor when the sample measurements are contaminated by white noise. These performance measures indicate that some multicaset sampling patterns are better than others for a given class of multiband signals. Based on these results we investigate, in Chapter 3, the problem of optimal sampling and reconstruction. Specifically, we show how to choose the optimal reconstruction filters, the optimal base sampling period, and examine briefly the problem of optimal sampling pattern design. We also study the suitability of multicaset sampling for the so-called packable class of signals for which uniform sampling at the Landau minimum density is possible.

In Chapter 4, we formulate the problem of MIMO sampling of multiband signals. We first introduce some definitions pertaining to sampling stability and notions of lower and upper sampling density, and then we derive necessary conditions for stable sampling using the mathematical framework of Hilbert spaces. These results include lower bounds on the sampling densities of the sampling sets, and conditions on certain singular values of the channel transfer function matrix. We also derive similar conditions for the dual problem of *consistent reconstruction*, which is an analogue of the *interpolation* problem in [6]. All these results are generalizations of Landau's density results for classical multiband sampling.

In Chapter 5, we examine a special case of MIMO sampling where the channel outputs are sampled either uniformly or on periodic nonuniform sampling sets. We present necessary and sufficient conditions for stable and perfect reconstruction. Using these results we solve the reconstruction filter design problem in Chapter 6. We present discrete time models for the MIMO channel and conditions for perfect reconstruction for this problem. We formulate the design problem as a minimization of an appropriate cost function, and then recast it as a semi-infinite linear program. We solve it numerically for a few design examples. Finally, we present concluding remarks and areas of possible future work in Chapter 7.

CHAPTER 2

SUB-NYQUIST MULTICOSET SAMPLING: PERFECT RECONSTRUCTION AND ALIASING ERROR BOUNDS

2.1 Introduction

The classical sampling theorem states that a signal occupying a finite range in the frequency domain can be represented by its samples taken at a finite rate. Often attributed to Whittaker, Kotelnikov, and Shannon, a more precise statement of this so-called WKS sampling theorem is that a real lowpass signal, whose Fourier transform is limited to the range $(-f_0, f_0)$, can be recovered from its samples taken uniformly at the rate $f_s = 2f_0$ (the Nyquist rate) or higher [1].

Sampling a signal $x(t)$ uniformly at f_s causes the resulting spectrum to contain multiple copies of the original spectrum $X(f)$ located with uniform spacing of f_s between adjacent copies. Hence, the choice $f_s \geq 2f_0$ guarantees no overlaps in the sampled spectrum, and thus allows recovery of the original signal by a lowpass filtering operation. This is the key idea behind the classical sampling theorem. For efficient sampling, it is desirable to attain the lowest sampling rate possible, and this is characterized by the absence of gaps or overlaps [14] in the spectrum of the sampled signal. Unfortunately, in the case of bandpass signals, it is not always possible to eliminate gaps in the sampled spectrum. However, it is possible to minimize them. Some results on bandpass sampling can be found in [2, 3]. Thus, while uniform sampling theorems work well for lowpass, they are quite inefficient for representing certain bandpass signals and, more generally, for multiband signals, i.e., signals containing several bands in the frequency domain. We refer the reader to Papoulis [12] and Jerri's tutorial [4] for some generalizations of the WKS sampling theorem.

To quantify the sampling efficiency for signals with a given spectral support \mathcal{F} , we define its spectral span $[\mathcal{F}]$ as the smallest interval containing \mathcal{F} , and its spectral occupancy as $\Omega = \mu(\mathcal{F})/\mu([\mathcal{F}])$, where $\mu(\cdot)$ denotes the Lebesgue measure. The Nyquist rate f_{nyq} for signals with

spectral support \mathcal{F} is defined as the smallest uniform sampling rate that guarantees no aliasing, i.e.,

$$f_{\text{nyq}} = \inf\{\theta > 0 : \mathcal{F} \cap (n\theta \oplus \mathcal{F}) = \emptyset, \forall n \in \mathbb{Z} \setminus \{0\}\},$$

where

$$\theta \oplus \mathcal{F} \stackrel{\text{def}}{=} \{\theta + f : f \in \mathcal{F}\}$$

is the translation of the set \mathcal{F} by θ . Then, the Nyquist sampling rate satisfies $\mu(\mathcal{F}) \leq f_{\text{nyq}} \leq \mu([\mathcal{F}])$. We say that \mathcal{F} tessellates \mathbb{R} or \mathcal{F} is *packable* if $f_{\text{nyq}} = \mu(\mathcal{F})$, and *nonpackable* otherwise ($f_{\text{nyq}} > \mu(\mathcal{F})$). In other words, the Nyquist rate for nonpackable signals exceeds the total length of its spectral support. At the other extreme is the case $f_{\text{nyq}} = \mu([\mathcal{F}])$ (*totally nonpackable*), where uniform sampling cannot exploit the presence of gaps in \mathcal{F} .

The general case of interest here is that of \mathcal{F} being nonpackable such that the Nyquist rate for sampling $x(t)$ with spectral support \mathcal{F} is $f_{\text{nyq}} > \mu(\mathcal{F})$. On the other hand, Landau [6] showed that the sampling rate of an arbitrary sampling scheme for the class of multiband signals with spectral support \mathcal{F} is lower bounded by the quantity $\mu(\mathcal{F})$, which may be significantly smaller than the Nyquist rate. Thus, the spectral occupancy Ω is a measure of the efficiency of Landau's lower bound over the Nyquist rate. Because Ω can be low for certain nonpackable signals (in fact, it is easy to construct examples of nonpackable \mathcal{F} with arbitrarily small Ω), uniform sampling is highly inefficient for such signals. Figure 2.1 illustrates a typical case of such a nonpackable multiband signal. The Nyquist rate for this signal is $f_{\text{nyq}} = \mu([\mathcal{F}]) = 4$ (hence \mathcal{F} is totally nonpackable), whereas the Landau lower bound is $\mu(\mathcal{F}) = 2$. The spectral occupancy for this signal is $\Omega = 0.5$, suggesting that it might be possible to sample and reconstruct the signal twice as efficiently as sampling at the Nyquist rate. In this chapter, we examine the problem of efficient sampling of nonpackable signals.

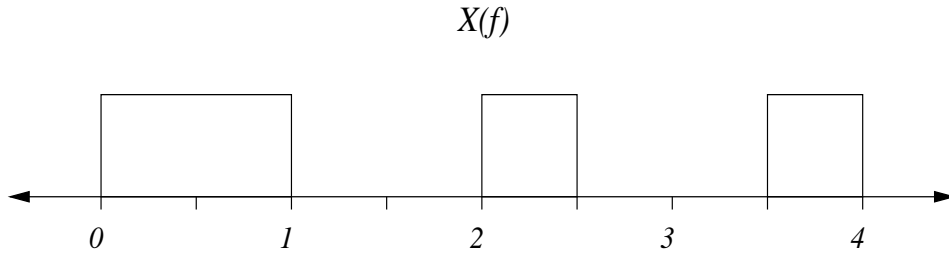


Figure 2.1 Spectrum of a nonpackable multiband signal.

Our results apply to the class of continuous complex-valued bandlimited signals of finite energy with spectral support \mathcal{F} , namely, $\mathcal{B}(\mathcal{F}) = \{x \in L^2(\mathbb{R}) \cap C(\mathbb{R}) : X(f) = 0, f \notin \mathcal{F}\}$, where $X(f)$ is the Fourier transform of $x(t)$.

2.1.1 Nonuniform sampling

Uniform sampling is not well suited for nonpackable signals. However, it turns out that there is a clever way of sampling the signal $x(t)$ called *multicoset sampling* or *periodic nonuniform sampling* at a rate lower than the Nyquist rate, that captures enough information to recover $x(t)$ exactly. Multicoset sampling and reconstruction from the samples will be described more fully in the following sections. First, we survey some known work on nonuniform sampling. Kahn and Liu [15] show how to represent and reconstruct signals from a multiple-channel sampling scheme. They provide conditions for exact reconstruction from the sampling trains and relate it to the maximum number of overlaps. Their sampling scheme, which is essentially a filter bank, is more general than nonuniform sampling since their “analysis filters” are not required to be simple delays. They express the reconstruction as the solution to a matrix equation, but do not provide an explicit interpolation formula. Cheung and Marks [16, 17] show that multicoset sampling allows sampling of 2-D signals below their Nyquist density. A similar treatment for 1-D and 2-D signals was done by Feng and Bresler [18], and Bresler and Feng [19], respectively, in the broader context of spectrum blind sampling. Filter bank theory and periodic nonuniform sampling is also used to obtain sampling rate reductions in [20–23]. Shenoy [24] and Higgins [25] apply multicoset sampling to multiband signals that do not tessellate under translation. Their results indicate that signals with certain spectral supports require a *single* interpolation filter as opposed to *more than one* in the other analyses of the problem. In other words, the sampling expansion is composed of time-translates of a single function. Simplicity of its implementation is an obvious advantage of their scheme. However, because it only works for a restricted class of signals, we do not consider their scheme here, focusing instead on multicoset sampling.

Herley and Wong [23], following [15], use filter bank theory instead, to suggest a sampling scheme for minimum rate sampling. They choose the analysis filters of the filter bank to be simple delays, i.e., $H_i(z) = z^{-i}$, and then show that some of the analysis channel outputs can be discarded, and yet, the input signal can be reconstructed from the other channels. It is clear that the reconstruction is performed by processing subsamples (obtained nonuniformly) of the original sample train at the Nyquist rates. As the number of channels goes to infinity, the average sampling rate converges to Landau’s minimum sampling rate, as expected. In fact, all of the schemes proposed in [15–18, 23] achieve the Landau minimum rate asymptotically. Although we do not adopt a filter bank approach and use a different notation, the work in [23] will be the basis for all the analysis here.

In this chapter, we continue along the lines of [23] to examine the problem of nonuniform sampling. First, we present some new results about the sampling and reconstruction

scheme itself. Herley and Wong [23] suggest using an iterative projection onto convex sets algorithm (POCS) to design the reconstruction filters, rather than derive an explicit reconstruction formula. Unlike their analysis, we provide exact expressions for the interpolation filters, or equivalently the explicit reconstruction formula for the sampling scheme. Beyond their obvious practical advantage, these expressions are useful for analytical purposes. For instance, they are useful for (a) analyzing the reconstruction error of the system; (b) quantifying the effects of signal mismodeling, i.e., computing the aliasing error and output noise; and (c) optimizing the system for the given class of signals.

2.1.2 Error bounds

Bounds on sensitivity to mismodeling of the signal are important to any sampling scheme. They are particularly important for the sampling schemes considered here because these schemes achieve what is impossible with other schemes: approach the Landau lower bound arbitrarily closely. This raises the question of a possibly increased sensitivity to signal mismodeling and sample noise, leading to an increased reconstruction error. Using our new explicit reconstruction formula, we derive bounds on the peak amplitude or the energy of the error signal. We compute bounds on the aliasing error for input signals in the class of functions $\mathcal{B}([\mathcal{F}])$, which is larger than the class $\mathcal{B}(\mathcal{F})$. We find that the upper bound on the peak aliasing error takes the form

$$\sup_t |x(t) - \hat{x}(t)| \leq \psi_\infty \int_{[\mathcal{F}] \setminus \mathcal{F}} |X(f)| df,$$

as it usually does for various other schemes. The bounding constant ψ_∞ can be used as a performance measure of the system. Different systems can be compared based on their corresponding bounding constants. In particular, Beaty and Higgins [26] derive a similar bound on the aliasing error for packable signals. The bounding constant for their case is $\psi_\infty = 2$. We also derive a bound on the energy of the aliasing error which takes the form

$$\|x - \hat{x}\|_2 \leq \psi_2 \sqrt{\int_{[\mathcal{F}] \setminus \mathcal{F}} |X(f)|^2 df}.$$

Finally, we derive an expression for the output noise power when the input is contaminated by additive white sample noise with variance σ^2 :

$$\langle E|x(t) - \tilde{x}(t)|^2 \rangle_t = \psi_n \sigma^2.$$

It turns out that the constants ψ_∞ , ψ_2 , and ψ_n depend on some parameters that are free to be chosen. An optimal choice of these free parameters would minimize ψ_∞ , ψ_2 , or ψ_n . These results can then applied to the design of sampling patterns, and this problem is addressed in Chapter 3.

2.2 Multicoset Sampling

We begin with a few definitions essential to the development and analysis of the sampling scheme. The class of continuous complex-valued of finite energy, bandlimited to a real set \mathcal{F} (consisting of a finite union of bounded intervals) is denoted by $\mathcal{B}(\mathcal{F})$:

$$\mathcal{B}(\mathcal{F}) = \{x \in L^2(\mathbb{R}) \cap C(\mathbb{R}) : X(f) = 0, f \notin \mathcal{F}\}, \quad \mathcal{F} = \bigcup_{i=1}^n [a_i, b_i), \quad (2.1)$$

where

$$X(f) = \int_{-\infty}^{\infty} x(t) \exp(-j2\pi ft) dt$$

is the Fourier transform of $x(t)$. The *span of \mathcal{F}* , denoted by $[\mathcal{F}]$, represents the convex hull of \mathcal{F} , i.e., the smallest interval containing \mathcal{F} .

Let $x \in \mathcal{B}(\mathcal{F})$. We shall assume, with no loss of generality, that $\inf \mathcal{F} = 0$. In multicoset sampling, we first pick a suitable the sampling period T (such that uniform sampling of x at rate $1/T$ causes no aliasing), and an integer $L > 0$. We then sample the input signal $x(t)$ nonuniformly at $t = (nL + c_i)T$ for $1 \leq i \leq p$, $n \in \mathbb{Z}$. The set $\{c_i\}$ contains p distinct integers chosen from the set $\mathcal{L} \stackrel{\text{def}}{=} \{0, 1, \dots, L-1\}$. The sampling process just described can be viewed as first sampling the signal at the *base sampling rate* of $1/T$ and then discarding all but p samples in every block of L samples periodically. The samples that are retained in each block are specified by $\{c_i\}$. The base sampling rate could be chosen equal to the Nyquist rate, i.e., $1/T = f_{\text{nyq}}$, but never lower. However, we choose $1/T = \mu([\mathcal{F}])$, because, sampling at this rate always guarantees no aliasing for any \mathcal{F} .

For a given c_i , it is clear that the coset of sampling instants $t = (nL + c_i)T$, $n \in \mathbb{Z}$ is uniform with inter-sample spacing equal to LT . We call this the *i th active coset*. We refer to the set $\mathcal{C} = \{c_i : 1 \leq i \leq p\}$ as an (L, p) *sampling pattern*, and the integer L as the period of the pattern. Figure 2.2 shows two multicoset sampling patterns corresponding to parameters $(L, p) = (5, 3)$. All other patterns for these parameters can be obtained by cyclic shifts of the patterns shown, namely $\mathcal{C} = \{0, 1, 2\}$ and $\mathcal{C} = \{0, 1, 3\}$. Patterns related to each other by cyclic shifts with or without reflections are essentially equivalent to each other in terms of the associated reconstruction problems and their measures of performance.

Now, consider the following L discrete-time sequences obtained by zeroing out all samples $\{x(nT)\}$ except those at $t = (mL + l)T$, $m \in \mathbb{Z}$:

$$\underline{x}_l(n) \stackrel{\text{def}}{=} x(nT) \sum_{m \in \mathbb{Z}} \delta(n - (mL + l)), \quad 0 \leq l < L,$$

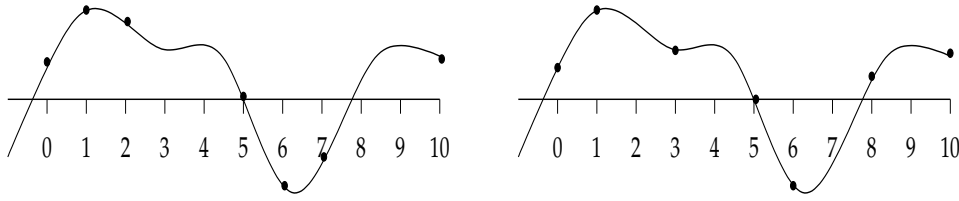


Figure 2.2 Two sampling patterns for $(L, p) = (5, 3)$: (a) $\mathcal{C} = \{0, 1, 2\}$, and (b) $\mathcal{C} = \{0, 1, 3\}$.

where $\delta(0) = 1$ and $\delta(n) = 0$ for $n \neq 0$. It is clear that the sequence $\underline{x}_{c_i}(n)$ contains the samples of the i th active coset with samples separated by $L - 1$ interleaving zeros. It is straightforward to verify that the discrete-time Fourier transform of the l th sequence is

$$\begin{aligned} \underline{X}_l(e^{j2\pi fT}) &= \sum_{n=-\infty}^{\infty} \underline{x}_l(n) \exp(-j2\pi n fT) \\ &= \frac{1}{LT} \sum_{r \in \mathbb{Z}} X\left(f + \frac{r}{LT}\right) \exp\left(\frac{j2\pi r l}{L}\right), \end{aligned} \quad (2.2)$$

which, using the fact that $X(f) = 0$ for $f \notin [0, 1/T)$, gives us

$$\underline{X}_l(e^{j2\pi fT}) = \frac{1}{LT} \sum_{r=0}^{L-1} X_r(f) \exp\left(\frac{j2\pi r l}{L}\right), \quad f \in \mathcal{F}_0, \quad (2.3)$$

where $X_r(f)$ is defined as

$$X_r(f) \stackrel{\text{def}}{=} X\left(f + \frac{r}{LT}\right) \chi(f \in \mathcal{F}_0), \quad (2.4)$$

$$\mathcal{F}_0 \stackrel{\text{def}}{=} \left[0, \frac{1}{LT}\right), \quad (2.5)$$

and $\chi(f \in \mathcal{H})$ denotes the indicator function of a set \mathcal{H} :

$$\chi(f \in \mathcal{H}) \stackrel{\text{def}}{=} \begin{cases} 1 & \text{if } f \in \mathcal{H}, \\ 0 & \text{if } f \notin \mathcal{H}. \end{cases}$$

In other words, the *spectral component* $X_r(f)$ is obtained by first using an ideal bandpass filter to extract the signal in the frequency range $r/LT \leq f < r + 1/LT$ and then performing a frequency-shift to the left by r/LT units. Denoting the inverse Fourier transform of $X_r(f)$ by $x_r(t)$, it is evident from the above definition that

$$x(t) = \sum_{r=0}^{L-1} x_r(t) \exp\left(\frac{j2\pi r t}{LT}\right). \quad (2.6)$$

The following is another result that can be deduced from Eq. (2.2) (or directly from the definition of $\underline{x}_l(nT)$):

$$\underline{X}_l(e^{j2\pi(f+r/(LT))T}) = e^{-j2\pi l r/L} \underline{X}_l(e^{j2\pi fT}), \quad r \in \mathbb{Z}. \quad (2.7)$$

We use Eqs. (2.6) and (2.7) later in deriving the reconstruction equations. We now let $l = c_i$, $i = 1, 2, \dots, p$ in Eq. (2.3) to get

$$\underline{X}_{c_i}(e^{j2\pi fT}) = \frac{1}{LT} \sum_{r=0}^{L-1} \exp\left(\frac{j2\pi c_i r}{L}\right) X_r(f), \quad f \in \mathcal{F}_0. \quad (2.8)$$

This is the main equation relating the spectral components $X_r(f)$ to the information contained in the observed samples. Note that Eq. (2.8) for $f \in \mathcal{F}_0$, contains all the relevant information present in the samples since, from Eq. (2.7), $X_{c_i}(e^{j2\pi ft})$ is essentially “periodic” with period $1/LT$. Reconstruction of the original signal $x(t)$ is achieved if we recover its spectral components $\{x_r(t)\}$.

2.3 Reconstruction

We now focus on the problem of reconstructing $x \in \mathcal{B}(\mathcal{F})$ from its multicoset samples. Herley and Wong [23] considered the analogous problem for real signals, but did not, however, provide an explicit reconstruction formula or system. We shall derive the reconstruction equations formally and devise a multirate system to perform the reconstruction.

Our objective is to invert Eq. (2.8) to obtain $X_r(f)$. The recovery of $x(t)$ is then merely an application of Eq. (2.6). Notice that, if \mathcal{C} and \mathcal{F} satisfy certain conditions, the inversion of Eq. (2.8) can be accomplished even though there are fewer equations (p) than unknowns (L) for each $f \in \mathcal{F}_0$. This is possible because the sampled signal belongs to $\mathcal{B}(\mathcal{F})$, which is smaller than $\mathcal{B}([\mathcal{F}])$.

Let \mathcal{F} be the union of n bounded intervals as in Eq. (2.1), with the additional assumption that

$$0 = a_1 < b_1 < a_2 < b_2 < \dots < a_n < b_n = \frac{1}{T}$$

holds, with no loss of generality. Consider the finite set Γ defined below:

$$\Gamma \stackrel{\text{def}}{=} \left\{ a_i - \frac{\lfloor LT a_i \rfloor}{LT} : 1 \leq i \leq n \right\} \cup \left\{ b_i - \frac{\lfloor LT b_i \rfloor}{LT} : 1 \leq i \leq n \right\}, \quad (2.9)$$

where $\lfloor \cdot \rfloor$ is the floor function. Let $\Gamma = \{\gamma_1, \gamma_2, \dots, \gamma_M\}$ be the elements of Γ arranged in increasing order. We have $\gamma_1 = 0$ as a consequence of $a_1 = 0$. We define $\gamma_{M+1} = 1/LT$ to obtain

$$0 = \gamma_1 < \gamma_2 < \dots < \gamma_{M+1} = \frac{1}{LT},$$

and a collection of intervals $\{\mathcal{I}_m\}$ that partitions the set \mathcal{F}_0

$$\mathcal{I}_m = [\gamma_m, \gamma_{m+1}), \quad 1 \leq m \leq M.$$

We prove the following fact involving the indicator function of \mathcal{F} and the sets $\{\mathcal{I}_m\}$ in Appendix A:

Lemma 2.1. *For each $r \in \mathcal{L}$ and $m \in \{1, 2, \dots, M\}$ the function $\chi(f + r/LT \in \mathcal{F})$ is constant on the interval \mathcal{I}_m .*

Equivalently, the theorem states that each *subcell* of the form $(r/LT) \oplus \mathcal{I}_m$, $r \in \mathcal{L}$ is either fully contained in \mathcal{F} or disjoint from it. This interpretation of the theorem motivates the following definition of the *spectral index sets* \mathcal{K}_m and their complements \mathcal{K}_m^c for $m \in \{1, 2, \dots, M\}$:

$$\mathcal{K}_m \stackrel{\text{def}}{=} \left\{ r \in \mathcal{L} : \frac{r}{LT} \oplus \mathcal{I}_m \subset \mathcal{F} \right\} \quad \text{and} \quad \mathcal{K}_m^c \stackrel{\text{def}}{=} \mathcal{L} \setminus \mathcal{K}_m.$$

The index set \mathcal{K}_m tells us which subcells in the collection $\{(r/LT) \oplus \mathcal{I}_m : r \in \mathcal{L}\}$ are “active”, while \mathcal{K}_m^c indicates which of them are not. The following theorem, which is a restatement of the main theorem in [23] using our notation, provides a necessary condition for reconstruction:

Theorem 2.1. *Equation (2.8) admits a unique solution for $X_r(f)$ only if the indicator function of \mathcal{F} satisfies*

$$q(f) \stackrel{\text{def}}{=} \sum_{r=0}^{L-1} \chi\left(f + \frac{r}{LT} \in \mathcal{F}\right) \leq p, \quad f \in \mathcal{F}_0. \quad (2.10)$$

Furthermore, an equality in Eq. (2.10) is necessary for attaining Landau’s lower bound on the sampling rate.

To make the dissertation self-contained, we provide a proof of Theorem 2.1 in Appendix A. Equation (2.10) reduces to

$$p \geq \max_m q_m, \quad \text{where} \quad q_m = q(f), \quad f \in \mathcal{I}_m \quad (2.11)$$

because $q(f)$ is constant on each \mathcal{I}_m by Lemma 2.1. Evidently, q_m is the cardinality of the set \mathcal{K}_m . We denote the elements of \mathcal{K}_m and \mathcal{K}_m^c by $\{k_m(l) : 1 \leq l \leq q_m\}$ and $\{k_m^c(l) : 1 \leq l \leq L - q_m\}$, respectively. Later, we shall see that for a suitable choice of \mathcal{C} , Eq. (2.11) is also sufficient for unique reconstruction. In the following example, we show how to construct the relevant \mathcal{K} -sets for the spectrum illustrated in Figure 2.3.

Example 2.1. Let the spectral support of our class of signals be $\mathcal{F} = [0, 1.3) \cup [2.7, 3.7) \cup [4.5, 5)$. Comparing this with Eq. (2.1), we find that

$$a_1 = 0, \quad a_2 = 2.7, \quad a_3 = 4.5, \quad b_1 = 1.3, \quad b_2 = 3.7, \quad \text{and} \quad b_3 = 5.$$

The indicator function $\chi(f \in \mathcal{F})$ of the set \mathcal{F} is shown in Figure 2.3(a). The length of \mathcal{F} is $\mu(\mathcal{F}) = 2.8$ and its span is $[\mathcal{F}] = [0, 5)$. It can be checked easily that \mathcal{F} is nonpackable and

hence the Nyquist rate for signals in $\mathcal{B}(\mathcal{F})$ is $1/T = \mu[\mathcal{F}] = 5$. Yet Landau's lower bound gives a rate of 2.8 and the corresponding occupancy is $\Omega = 2.8/5 = 0.56$. Suppose we pick $L = 5$. We see that Eq. (2.9) yields $\Gamma \equiv \{\gamma_0, \gamma_1, \gamma_2, \gamma_3\} = \{0, 0.3, 0.5, 0.7\}$, containing $M = 4$ elements, from which we construct sets \mathcal{I}_m that partition $\mathcal{F}_0 = [0, 1/LT) = [0, 1)$:

$$\mathcal{I}_1 = [0, 0.3), \quad \mathcal{I}_2 = [0.3, 0.5), \quad \mathcal{I}_3 = [0.5, 0.7), \quad \mathcal{I}_4 = [0.7, 1).$$

The following are immediately apparent:

$$\begin{array}{lll} q_1 = 3, & \mathcal{K}_1 = \{0, 1, 3\}, & \mathcal{K}_1^c = \{2, 4\}. \\ q_2 = 2, & \mathcal{K}_2 = \{0, 3\}, & \mathcal{K}_2^c = \{1, 2, 4\}. \\ q_3 = 3, & \mathcal{K}_3 = \{0, 3, 4\}, & \mathcal{K}_3^c = \{1, 2\}. \\ q_4 = 3, & \mathcal{K}_4 = \{0, 2, 4\}, & \mathcal{K}_4^c = \{1, 3\}. \end{array}$$

Figure 2.3(b) shows the left-hand side of Eq. (2.10) plotted on the interval $[0, 1)$. Note that this function is piecewise constant, equal to q_m on each of the intervals $\{\mathcal{I}_m\}$ which are color-coded for convenience. Figure 2.3(c) shows the indicator function of \mathcal{F} color-coded to show the active subcells derived by translating \mathcal{I}_m .

In direct analogy to Eq. (2.4), we define

$$X_{k_m(l)}(f) \stackrel{\text{def}}{=} X\left(f + \frac{k_m(l)}{LT}\right)\chi(f \in \mathcal{I}_m). \quad (2.12)$$

However, beware of this definition since it is not equal to Eq. (2.4) evaluated at $r = k_m(l)$. The extra factor of $\chi(f \in \mathcal{I}_m)$ in Eq. (2.12) makes it different. The *spectral component* $X_{k_m(l)}(f)$ is obtained by shifting the values of $X(f)$ on the subcell $(k_m(l)/LT) \oplus \mathcal{I}_m$ to the origin. For each m , we define a $p \times q_m$ matrix \mathbf{A}_m , and vectors $\mathbf{y}(\mathbf{f}) \in \mathbb{C}^p$, $\mathbf{x}_m^+(\mathbf{f}) \in \mathbb{C}^{q_m}$, and $\mathbf{x}_m^-(\mathbf{f}) \in \mathbb{C}^{L-q_m}$ as follows:

$$\begin{aligned} [\mathbf{y}(\mathbf{f})]_i &= T\sqrt{L}\underline{X}_{c_i}(e^{j2\pi fT})\chi(f \in \mathcal{F}_0), \\ [\mathbf{x}_m^+(\mathbf{f})]_l &= X_{k_m(l)}(f), \\ [\mathbf{x}_m^-(\mathbf{f})]_l &= X_{k_m^c(l)}(f), \\ [\mathbf{A}_m]_{il} &= \frac{1}{\sqrt{L}} \exp\left(\frac{j2\pi c_i k_m(l)}{L}\right). \end{aligned} \quad (2.13)$$

Note that \mathbf{A}_m is the submatrix of the $L \times L$ DFT matrix \mathbf{W}_L obtained by extracting its rows indexed by \mathcal{C} , and columns indexed by \mathcal{K}_m . We denote this by $\mathbf{A}_m = \mathbf{W}_L(\mathcal{C}, \mathcal{K})$. Next, using

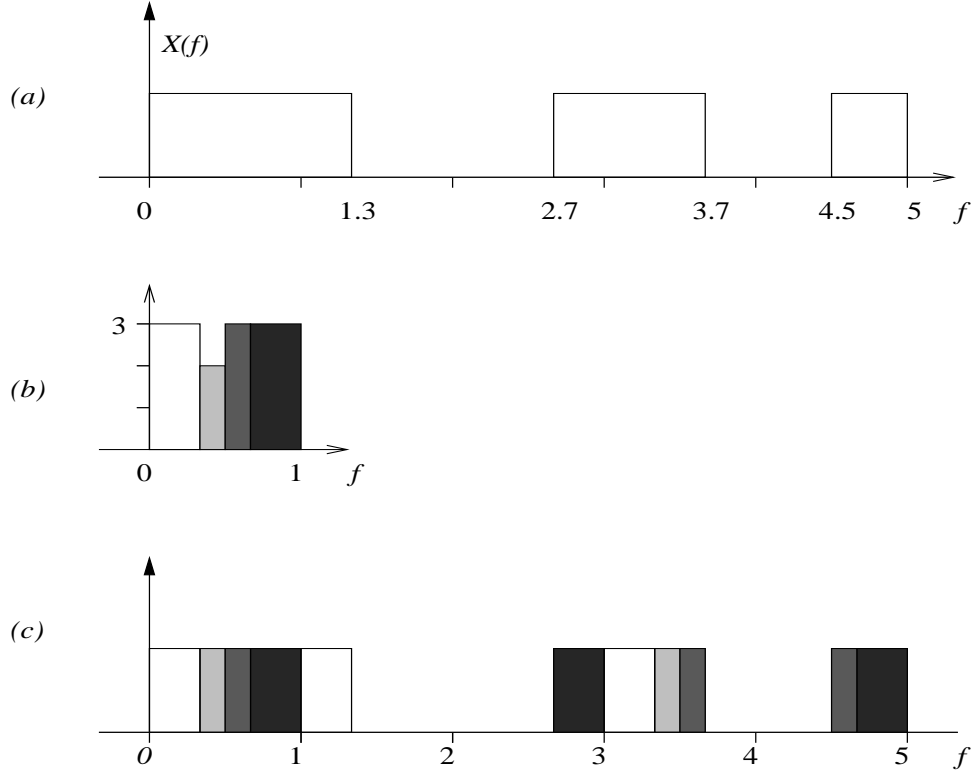


Figure 2.3 (a) Indicator function of the spectral support \mathcal{F} of span $1/T = 5$. (b) Left-hand side of Eq. (2.10). (c) Active spectral subcells.

the fact that $\mathbf{x}_m^-(f) = 0$ whenever $x \in \mathcal{B}(\mathcal{F})$, we can rewrite Eq. (2.8) in matrix form over each subcell \mathcal{I}_m as follows:

$$\mathbf{y}(f) = \mathbf{A}_m \mathbf{x}_m^+(f), \quad \forall f \in \mathcal{I}_m, \quad 1 \leq m \leq M. \quad (2.14)$$

At this point, we introduce the following two definitions that characterize the sampling pattern \mathcal{C} , of size p , in terms of the $L \times L$ DFT matrix \mathbf{W}_L .

Definition 2.1. Given an index set \mathcal{K} with $|\mathcal{K}| = q \leq p$, we call \mathcal{C} a \mathcal{K} -reconstructive sampling pattern if the matrix $\mathbf{W}_L(\mathcal{C}, \mathcal{K})$ has full column rank.

Definition 2.2. A pattern \mathcal{C} with $|\mathcal{C}| = p \geq q$ is (p, q) universal if the matrix $\mathbf{W}_L(\mathcal{C}, \mathcal{K})$ has full column rank for every index set of q elements, i.e., whenever $|\mathcal{K}| = q$. A (p, p) -universal pattern is simply called universal.

For fixed values of p and q , the second definition is stronger than the first. For every L and $p \leq L$, there always exists a (p, p) universal pattern. The *bunched sampling pattern* $\mathcal{C} = \{0, 1, \dots, p-1\}$ is one such example because the resulting matrix $\mathbf{A} = \mathbf{W}_L(\mathcal{C}, \mathcal{K})$ is

a Vandermonde matrix for any choice of \mathcal{K} . This guarantees $\text{rank}(\mathbf{A}) = q$ for *any* spectral support with $q \leq p$ active cells.

Equation (2.11), along with the assumption that \mathbf{A}_m has full rank for each m (i.e., \mathcal{C} being \mathcal{K}_m -reconstructive for each m) is necessary and sufficient for reconstruction. A simpler sufficient condition is universality of \mathcal{C} . For convenience we assume throughout that \mathcal{C} is universal. This guarantees the existence of a left-inverse \mathbf{A}_m^{-1} of \mathbf{A}_m . Therefore, inverting Eq. (2.14) gives

$$\begin{aligned} \mathbf{x}_m^+(f) &= \mathbf{A}_m^{-1} \mathbf{y}(f) \\ \mathbf{x}_m^-(f) &= \mathbf{C}_m \mathbf{y}(f) \end{aligned} \quad f \in \mathcal{I}_m, m \in \{1, \dots, M\}, \quad (2.15)$$

where, in order that $\mathbf{x}_m^-(f) = 0$ hold, \mathbf{C}_m is any $(L - q_m) \times p$ matrix satisfying

$$\mathbf{C}_m \mathbf{A}_m = \mathbf{0} \quad (2.16)$$

for each m . The matrices \mathbf{A}_m^{-1} and \mathbf{C}_m are nonunique unless $p = q_m$. In other words, there is some freedom that can be used in designing a reconstruction system. The actual choice of matrices does not affect the reconstruction, but does influence the bounds on aliasing error as described later. This suggests that finding the optimal matrices is of interest. These equations specify all the information required to reconstruct the spectrum $X(f)$ on all its spectral subcells, and hence $x(t)$ itself.

The interpolation equation may be calculated from Eq. (2.15) in a rather messy but straightforward manner. The result is summarized in the following theorem, which we prove in Appendix A.

Theorem 2.2. *Let $x \in \mathcal{B}(\mathcal{F})$ be sampled on an (L, p) multicoset pattern \mathcal{C} . Let \mathcal{K}_m , $m = 1, 2, \dots, M$ denote the spectral index sets of \mathcal{F} . Then, if \mathcal{C} is \mathcal{K}_m -reconstructive for each m , $x(t)$ can be uniquely interpolated from its multicoset samples according to the following formula:*

$$\begin{aligned} x(t) &= \sum_{i=1}^p \sum_{n=-\infty}^{\infty} \underline{x}_{c_i}(nT) \phi_i(t - nT) \\ &\equiv \sum_{i=1}^p \sum_{j=-\infty}^{\infty} x((c_i + Lj)T) \phi_i(t - (c_i + Lj)T), \end{aligned} \quad (2.17)$$

where the functions $\phi_i(t)$, $i = 1, \dots, p$ have Fourier transforms $\Phi_i(f)$ that are piecewise constant on $[\mathcal{F}]$:

$$\Phi_i(f) = \begin{cases} T\sqrt{L}[\mathbf{A}_m^{-1}]_{li} e^{j2\pi \frac{c_i k_m(l)}{L}} & \text{if } f \in k_m(l)/(LT) \oplus \mathcal{I}_m, \\ T\sqrt{L}[\mathbf{C}_m]_{li} e^{j2\pi \frac{c_i k_m^c(l)}{L}} & \text{if } f \in k_m^c(l)/(LT) \oplus \mathcal{I}_m. \end{cases} \quad (2.18)$$

Corollary 2.1. *The result in Theorem 2.2 holds if $\max_m q_m \leq p$, and \mathcal{C} is universal.*

Theorem 2.2 also holds for multicoset sampling of wide sense stationary stochastic processes if the infinite summation in Eq. (2.17) is interpreted as converging to the left-hand side in the mean square sense. The analysis for this problem is similar to the classical analysis for lowpass sampling of wide sense stationary processes [27].

The reconstruction scheme is illustrated in Figure 2.4. In the figure, $\Psi_i(z)$ is a digital filter whose impulse response is $\phi_i(nT)$. The filters used are ideal. In practice, causal, possibly FIR approximations are used, introducing some delay and distortion. The analysis of the resulting error is analogous to the truncation error in classical cardinal series expansion and is beyond the scope of this dissertation. However, we do consider the FIR filter design problem in Chapter 6. In the rest of the chapter, we assume that the filters are ideal and concentrate on the aliasing errors due to signal mismodeling.

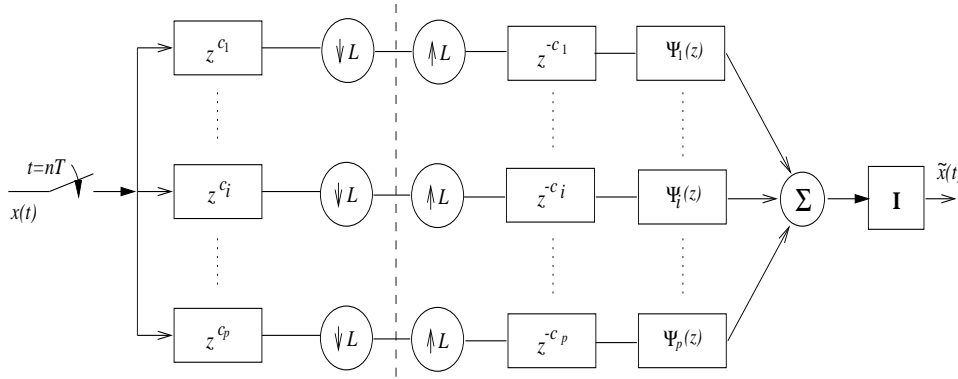


Figure 2.4 Multicoset sampling and reconstruction. The block “I” is an ideal sinc interpolator.

2.4 Error Bounds

For a system designed to sample and reconstruct signals in $\mathcal{B}(\mathcal{F})$, it is necessary that Eq. (2.11) hold. In this case the reconstruction of $x(t)$ would be exact. However, if $x \notin \mathcal{B}(\mathcal{F})$ then the signal $\tilde{x}(t)$ reconstructed using the right-hand side of Eq. (2.17) would be in error. For example, this would happen if, while designing the system, we underestimate the spectral support of signals we expect to encounter; i.e., if we choose to ignore certain frequencies that contain negligible signal energy. The purpose of this section is to obtain bounds on the aliasing error $e(t) = \tilde{x}(t) - x(t)$ resulting from an underestimation of the spectral support.

In the following analysis $X(f)$ need not vanish on $[\mathcal{F}] \setminus \mathcal{F}$, although we assume, for simplicity, that $X(f) = 0$ for $f \notin [\mathcal{F}]$. In other words, the spectral span $[\mathcal{F}]$ is specified correctly, but the

multiband structure to which $x(t)$ is bandlimited within $[\mathcal{F}]$ may be misspecified. We shall first derive bounds on the sup-norm and the L^2 norm of the aliasing error $e(t)$ for the nonuniform sampling process described in the last section.

Recall that $\mathcal{K}_m^c = \{k_m^c(l) : 1 \leq l \leq L - q_m\}$ tells us exactly which spectral subcells in the collection $\{(r/LT) \oplus \mathcal{I}_m : r \in \mathcal{L}\}$ are inactive. Now, for each $m \in \{1, 2, \dots, M\}$, let $\mathbf{B}_m = \mathbf{W}_L(\mathcal{C}, \mathcal{K}_m)$ denote the $p \times (L - q_m)$ submatrix of the $L \times L$ DFT matrix \mathbf{W}_L , whose rows and columns are indexed by \mathcal{C} and \mathcal{K}_m^c , respectively, i.e.,

$$[\mathbf{B}_m]_{il} = \frac{1}{\sqrt{L}} \exp\left(\frac{j2\pi c_i k_m^c(l)}{L}\right). \quad (2.19)$$

We can then rewrite Eq. (2.8) in matrix form as

$$\mathbf{y}(f) = \mathbf{A}_m \mathbf{x}_m^+(f) + \mathbf{B}_m \mathbf{x}_m^-(f), \quad f \in \mathcal{I}_m, \quad (2.20)$$

where $\mathbf{x}_m^-(f)$ is the $(L - q_m) \times 1$ vector defined in Eq. (2.13). Note that if $x(t) \in \mathcal{B}(\mathcal{F})$, then $\mathbf{x}_m^-(f)$ would vanish. Denoting the reconstructed signal by $\tilde{x}(t)$, it follows immediately from Eqs. (2.15), (2.16), and (2.20) that

$$\begin{aligned} \tilde{\mathbf{x}}_m^+(f) &= \mathbf{x}_m^+(f) + \mathbf{A}_m^{-1} \mathbf{B}_m \mathbf{x}_m^-(f), \\ \tilde{\mathbf{x}}_m^-(f) &= \mathbf{C}_m \mathbf{B}_m \mathbf{x}_m^-(f) \end{aligned} \quad (2.21)$$

for $f \in \mathcal{I}_m$, where $\tilde{\mathbf{x}}_m^+(f)$ and $\tilde{\mathbf{x}}_m^-(f)$ have definitions analogous to $\mathbf{x}_m^+(f)$ and $\mathbf{x}_m^-(f)$, respectively. Define matrices \mathbf{D}_m and \mathbf{F}_m (of sizes $q_m \times (L - q_m)$ and $(L - q_m) \times (L - q_m)$, respectively) for each m as follows:

$$\begin{aligned} \mathbf{D}_m &= \mathbf{A}_m^{-1} \mathbf{B}_m, \\ \mathbf{F}_m &= \mathbf{C}_m \mathbf{B}_m - \mathbf{I}. \end{aligned} \quad (2.22)$$

These definitions will be used in the following subsections, where we present bounds on the peak aliasing error, the aliasing error energy and evaluate the performance of the system in the presence of input noise.

2.4.1 Sup-norm of the error

The following theorem provides the time-domain expression for the aliasing error.

Theorem 2.3. *The aliasing error $e(t)$ takes the form*

$$e(t) = \sum_{m=1}^M \sum_{l=1}^{L-q_m} \eta_{m,l}(t) x_{k_m^c(l)}(t),$$

where $\eta_{m,l}(t)$ for each $1 \leq m \leq M$ and $1 \leq l \leq L - q_m$ are continuous, LT -periodic functions defined as

$$\eta_{m,l}(t) = \sum_{r=1}^{L-q_m} [\mathbf{F}_m]_{rl} e^{\frac{j2\pi k_m^c(r)t}{LT}} + \sum_{r=1}^{q_m} [\mathbf{D}_m]_{rl} e^{\frac{j2\pi k_m(r)t}{LT}}.$$

Furthermore, the peak value of $e(t)$ satisfies the tight bound

$$\sup_t |e(t)| \leq \psi \int_{[\mathcal{F}] \setminus \mathcal{F}} |X(f)| df, \quad \psi \stackrel{\text{def}}{=} \max_m \left(\max_{1 \leq l \leq L-q_m, t \in [0, LT]} |\eta_{m,l}(t)| \right).$$

We prove this theorem in Appendix A. The tightness of this bound is proved by demonstrating an input signal that satisfies the equality in the bound. Note that the constant ψ can be bounded from above as follows:

$$\begin{aligned} \psi &= \max_{m,l,t} \left| \sum_{r=1}^{L-q_m} [\mathbf{F}_m]_{rl} \exp\left(\frac{j2\pi k_m^c(r)t}{LT}\right) + \sum_{r=1}^{q_m} [\mathbf{D}_m]_{rl} \exp\left(\frac{j2\pi k_m(r)t}{LT}\right) \right| \\ &\leq \max_m \left[\max_l \left(\sum_{r=1}^{L-q_m} |[\mathbf{F}_m]_{rl}| + \sum_{r=1}^{q_m} |[\mathbf{D}_m]_{rl}| \right) \right] \\ &= \max_m \left\| \begin{pmatrix} \mathbf{D}_m \\ \mathbf{F}_m \end{pmatrix} \right\|_1, \end{aligned}$$

where $\|\cdot\|_1$ is the maximum-column-sum norm for matrices (or the ℓ_1 norm for column vectors.) Hence, we obtain the weaker, but more tractable bound

$$\sup_t |e(t)| \leq \psi_\infty \int_{[\mathcal{F}] \setminus \mathcal{F}} |X(f)| df, \quad \text{where } \psi_\infty = \max_m \left\| \begin{pmatrix} \mathbf{D}_m \\ \mathbf{F}_m \end{pmatrix} \right\|_1. \quad (2.23)$$

2.4.2 L^2 -norm of the error

Theorem 2.4. *The energy of the aliasing error is bounded by*

$$\begin{aligned} \int_{-\infty}^{\infty} e^2(t) dt &\leq \max_m [\lambda_{\max}(\mathbf{F}_m^* \mathbf{F}_m + \mathbf{D}_m^* \mathbf{D}_m)] \mathcal{E}_{\text{out}}, \\ \int_{-\infty}^{\infty} e^2(t) dt &\geq \min_m [\lambda_{\min}(\mathbf{F}_m^* \mathbf{F}_m + \mathbf{D}_m^* \mathbf{D}_m)] \mathcal{E}_{\text{out}}, \end{aligned}$$

with both bounds being tight, where \mathcal{E}_{out} is the out-of-band energy:

$$\mathcal{E}_{\text{out}} = \int_{[\mathcal{F}] \setminus \mathcal{F}} |X(f)|^2 df.$$

Once again, the proof can be found in Appendix A. We are particularly interested in the upper bound on the L^2 -norm of the error

$$\|e\|_2 = \sqrt{\int |e(t)|^2 dt}.$$

It is clearly related to the spectral norm of the matrix composed of \mathbf{F}_m and \mathbf{D}_m as

$$\|e\|_2 \leq \psi_2 \sqrt{\mathcal{E}_{\text{out}}}, \quad \text{where} \quad \psi_2 = \max_m \left\| \begin{pmatrix} \mathbf{D}_m \\ \mathbf{F}_m \end{pmatrix} \right\|_2. \quad (2.24)$$

2.4.3 Performance in the presence of noise

We now consider the effect of additive white sample noise representing, for example, quantization noise or sensor measurement noise associated with obtaining samples. We assume that the input signal is a wide sense stationary process with its power spectral density supported on \mathcal{F} . The sampled signal can be modeled as

$$\bar{x}(nT) = x(nT) + w(nT),$$

where $w(n)$ is a noise process with $E[w(mT)w(nT)] = \sigma^2\delta(m-n)$, and $x(t)$ is the actual signal we would like to be sampling. Owing to its linearity, Eq. (2.17) directly gives us the following expression for the output noise $\tilde{w}(t)$ which is independent of $x(t)$:

$$\tilde{w}(t) = \sum_{i=1}^p \sum_{j=-\infty}^{\infty} w((c_i + Lj)T) \phi_i(t - (c_i + Lj)T).$$

We now have the following result for the noise power amplification, which is proved in Appendix A.

Theorem 2.5. *The output noise $\tilde{w}(t)$ is periodically stationary, with average power given by*

$$\langle E|\tilde{w}(t)|^2 \rangle_t = \sigma^2 \psi_n, \quad \text{where} \quad \psi_n = T \sum_{m=1}^M \eta(\mathcal{I}_m) (\|\mathbf{A}_m^{-1}\|_F^2 + \|\mathbf{C}_m\|_F^2),$$

and $\|\cdot\|_F$ denote the Frobenius norm.

2.5 Summary

In this chapter, we have presented the analysis of a scheme for sampling multiband signals below the Nyquist rate. The sampling scheme uses multicoset sampling and achieves the Landau minimum sampling rate in the limit $L \rightarrow \infty$, where L is the period of the sampling pattern.

However, for many spectra, the minimum rate can be achieved for a finite L . Typically, this scheme is useful for sampling signals with sparse and nonpackable spectra.

We determined necessary and sufficient conditions for reconstructing multiband signals from their multicoset samples and derived an explicit reconstruction formula. There are free parameters in the reconstruction equation when the Landau minimum rate is not achieved for the particular value of L . We computed bounds on the aliasing error occurring in the event that the signal lies outside the valid class of multiband signals, and the sensitivity of the system to input sample noise. The constants in the bounds and the noise-sensitivity factor reveal that some sampling patterns are better than others. In other words, these bounds, which quantify the goodness of sampling patterns, can be viewed as cost functions to minimize to optimize the sampling pattern and the choice of free parameters in the reconstruction formula.

CHAPTER 3

OPTIMAL MULTICOSET SAMPLING AND RECONSTRUCTION

3.1 Introduction

There has been a long history of research [2–5] devoted to sampling theory, with perhaps the most fundamental and important piece of work in this area being the classical sampling theorem. Also known as the Whittaker-Kotelnikov-Shannon (WKS) theorem, it states that a lowpass signal bandlimited to the frequencies $(-f_0, f_0)$ can be reconstructed perfectly from its samples taken uniformly at no less than the Nyquist rate of $2f_0$ [1]. Another important result in sampling theory due to Landau is a lower bound on the sampling density required for any sampling scheme that allows perfect reconstruction [6]. For multiband signals, this fundamental lower bound is given by the total length (measure) of support of the Fourier transform of the signal. Landau’s bound applies to an arbitrarily sampling scheme: uniform or not, and the minimum rate may not be achievable except asymptotically. Landau’s bound is often much lower than the corresponding Nyquist rate. This motivates the study of *sub-Nyquist sampling* of multiband signals and their perfect reconstruction, c.f. [15–18, 20, 24, 28].

From a practical viewpoint, sub-Nyquist sampling is very important in several Fourier imaging applications such as sensor array imaging, SAR and MRI, where the physics of the problem provides us samples of the unknown sparse object in its Fourier domain [8–11]. Our objective then, is to reconstruct the object from the Fourier data. Often times, it is expensive or physically impossible to collect many samples, and it becomes necessary to sample minimally and exploit the sparsity (i.e., multiband structure) in the object to form its image. These problems are, of course, duals to the problem considered here since the sparsity is in the spatial domain and sparse sampling in the frequency domain.

For a given signal $x(t)$, its *spectral support* \mathcal{F} is defined as the set of frequencies where the Fourier transform $X(f)$ does not vanish, and the *spectral span* $[\mathcal{F}]$ is defined as the smallest

interval containing \mathcal{F} . We consider here only spectral supports that can be expressed as a finite union of finite intervals, called *bands*. The set of multiband signals bandlimited to \mathcal{F} is denoted by $\mathcal{B}(\mathcal{F})$. Landau’s lower bound for these signals is $\mu(\mathcal{F})$, where $\mu(\cdot)$ denotes the Lebesgue measure. However, in general, the Nyquist rate f_{nyq} for sampling $x \in \mathcal{B}(\mathcal{F})$ without aliasing (overlap between translates of \mathcal{F} by multiples of f_{nyq}) is equal to the width of its spectral span: $f_{\text{nyq}} = [\mathcal{F}]$. Hence, for multiband signals with sparse spectral supports $[\mathcal{F}]$, the Nyquist rate can be much larger than the lower bound $\mu(\mathcal{F})$.

A favorable case is when the widths of the bands and the gaps between them satisfy special relationships, so that there is no overlap between uniform translates of \mathcal{F} by multiples of a quantity $f_0 < \mu([\mathcal{F}])$. In these cases, when the spectral support is *packable*, $f_{\text{nyq}} = f_0 < \mu([\mathcal{F}])$. The most favorable situation of these is when \mathcal{F} tiles the real line under uniform translations, i.e., is packable without gaps, or “ \mathcal{F} is an explosion of the interval” [2]. In this (very special) case, $f_{\text{nyq}} = \mu(\mathcal{F})$, i.e., Landau’s lower bound is achievable by uniform sampling.

Instead, the case of interest to us in this chapter is the general case, with $\mu(\mathcal{F}) < f_{\text{nyq}} \leq \mu([\mathcal{F}])$. Without loss of generality, we focus on the extreme (worst) case of *nonpackable* \mathcal{F} , such that $f_{\text{nyq}} = \mu([\mathcal{F}])$.¹ For such multiband signals, it has been shown that perfect reconstruction is possible from *nonuniformly* spaced samples taken at a sub-Nyquist average rate approaching the Landau lower bound [15–18, 20, 28]. This discussion and intentional use of nonuniform sampling are fundamentally distinct from other extensive recent work on nonuniform sampling in which it is usually regarded as a “necessary evil,” imposed by sampling jitter or other physical limitations [29–32]. In fact, the work in [29–32] typically addresses signals with lowpass spectral supports, which, being packable, are best sampled uniformly, as we show later.

We note that the related problem of perfect reconstruction in filter banks (c.f. [33]) is fundamentally different from the problem considered here. In the filter bank work, all samples at the Nyquist rate are assumed available, and the analysis stage can be designed together with the synthesis stage. In contrast, in our problem, Nyquist-rate acquisition is too expensive or even impossible, and only the minimum number of samples of the continuous time signal is acquired. As shown later, the filter bank interpretation for this is that the analysis filters are restricted to the form of z^{-k} where $k \in \mathbb{Z}$.

Given the obvious advantages of such reduced sampling rates (e.g., by a factor of 10, in one of the examples in this chapter), one would expect extensive use and applications of these methods. However, a very high sensitivity to errors has been observed in some cases [16, 18]. In fact, it

¹Intermediate cases with $\mu(\mathcal{F}) < f_{\text{nyq}} < [\mathcal{F}]$ are reduced to this case by first sampling the signal at f_{nyq} and then considering the problem of further downsampling the discrete-time signal, which now has a nonpackable spectral support.

turns out that unless the sampling and reconstruction system is very carefully designed and optimized, the sensitivity to small errors can be so great, that although perfect reconstruction is possible with perfect data, the signal is corrupted beyond recognition in most practical situations.

The goal of this chapter is to explore these limitations and develop systematic design methods to minimize the sampling rate and at the same time to minimize the error sensitivity of the system. This will provide the necessary tools for practical applications of minimum-rate sub-Nyquist sampling. We consider the problem of periodic nonuniform sampling and reconstruction of multiband signals. We focus primarily on the results presented in Chapter 2, where we derived an explicit reconstruction formula and a multirate realization for a sampling scheme called *multicoset sampling* that allows us to approach the Landau minimum rate arbitrarily closely. As an important tool for systematic feasibility evaluation and design of the system, we derived estimates of the error resulting from signal mismodeling. More precisely, we derived bounds on (a) the peak value and energy of the aliasing error resulting when the input signal $x(t)$ lies in $\mathcal{B}([\mathcal{F}])$, rather than $\mathcal{B}(\mathcal{F})$, and (b) the output noise variance when the input samples contain additive white noise of variance σ^2 .

In this chapter, we use these various bounds to optimize the performance of the sub-Nyquist sampling and reconstruction system by minimizing the sensitivity bounds. It turns out that the reconstruction system that provides perfect reconstruction of signals $x(t) \in \mathcal{B}(\mathcal{F})$ in the modeled class has free parameters, which can be chosen to optimize the sensitivity bounds. We present closed-form, or otherwise efficient approximation numerical algorithms to solve these optimization problems. Likewise, we use the bounds to determine the best sampling pattern among all patterns that achieve a given sampling rate for a given \mathcal{F} .

In addition, we solve the problem of an optimal choice of the base sampling frequency to minimize the average sampling rate achievable by a design with a given sampling period L . This allows us to minimize the sampling rate for a given system complexity, rather than asymptotically, with $L \rightarrow \infty$. This problem is related to the problem of pairing band-edges of \mathcal{F} [28]. We provide a simple algorithm to solve the problem, whether or not Landau's lower bound is attainable for the particular \mathcal{F} and choice of L .

We derive additional relationships and bounds that allow us to quantify the performance loss in terms of increased error sensitivity due to nonpackability of the spectral support, and compare uniform and nonuniform sampling patterns for packable spectra. Not surprisingly perhaps, we find that uniform sampling is more suitable for packable spectra. Most importantly however, we find that the sensitivity penalty for sub-Nyquist sampling of signals with nonpackable spectra

can be controlled by optimal design, and by backing off slightly from the minimum rate. The resulting low error sensitivities with multifold reductions from the Nyquist rate in our numerical examples suggest that these techniques have considerable practical potential.

3.2 Multicoset Sampling

3.2.1 Signals and data

Let the class of continuous complex-valued signals of finite energy, bandlimited to a subset \mathcal{F} of the real line (consisting of a finite union of bounded intervals) be denoted by $\mathcal{B}(\mathcal{F})$:

$$\mathcal{B}(\mathcal{F}) = \{x(t) \in L^2(\mathbb{R}) \cap C(\mathbb{R}) : X(f) = 0, f \notin \mathcal{F}\}, \quad \mathcal{F} = \bigcup_{i=1}^n [a_i, b_i],$$

where

$$X(f) = \int_{\mathbb{R}} x(t) \exp(-j2\pi ft) dt.$$

The *span of \mathcal{F}* , denoted by $[\mathcal{F}]$, is the convex hull of \mathcal{F} or the smallest interval containing \mathcal{F} .

Definition 3.1. The spectral support \mathcal{F} is said to be packable at rate f_0 if

$$\mathcal{F} \cap (\mathcal{F} \oplus nf_0) = \emptyset, \quad \forall n \in \mathbb{Z} \setminus \{0\},$$

where \oplus is the translation operator defined by

$$f \oplus \mathcal{F} = \{f + x : x \in \mathcal{F}\}$$

for any real set \mathcal{F} and $f \in \mathbb{R}$.

In other words, \mathcal{F} is packable at rate f_0 if signals with spectral support \mathcal{F} can be sampled uniformly at rate f_0 without inducing aliasing. Hence, \mathcal{F} is always packable at rate $\mu([\mathcal{F}])$. We call \mathcal{F} *nonpackable* if it is not packable at any rate smaller than $\mu([\mathcal{F}])$. We assume that \mathcal{F} is nonpackable and that $\inf \mathcal{F} = a_1 = 0$ and $\sup \mathcal{F} = b_n$: there is no loss of generality here because any signal spectrum whose span $[\mathcal{F}]$ is known can be shifted to the origin by multiplication of the signal in the time domain by a suitable complex exponential. Since multiplication and sampling in the time domain commute, we are justified in making the assumption.

We now describe multicoset sampling. Given a bandlimited signal $x \in \mathcal{B}(\mathcal{F})$, we obtain its samples taken on a periodic nonuniform grid consisting of the sampling locations $(nL + c_i)T$, for $n \in \mathbb{Z}$ and $i = 1, \dots, p$, where $\{c_i\}$ is a set of p distinct integers in the set $\mathcal{L} = \{0, 1, \dots, L - 1\}$, and $1/T$ is the *base frequency* which is at least equal to the Nyquist rate for $x(t)$: $1/T \geq \mu([\mathcal{F}])$. This is illustrated in Figure 3.1. In Section 3.4, we address the problems of selecting the optimal base frequency $1/T$ and sampling pattern $\{c_i\}$.

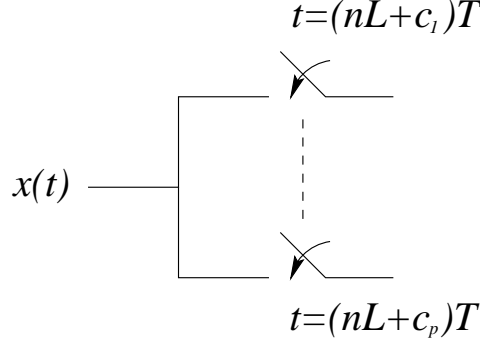


Figure 3.1 Model for multicoset sampling.

3.2.2 Definitions and notation

This section is largely a collection of definitions and notations needed to describe the various error bounds derived in Chapter 2. For any real set $\mathcal{S} \in \mathbb{R}$, denote its indicator function by

$$\chi(f \in \mathcal{S}) \stackrel{\text{def}}{=} \begin{cases} 1 & \text{if } f \in \mathcal{S}, \\ 0 & \text{otherwise,} \end{cases}$$

and for the given spectral support $\mathcal{F} = \bigcup_i [a_i, b_i)$, define the finite set

$$\Gamma \stackrel{\text{def}}{=} \left\{ a_i - \frac{\lfloor LT a_i \rfloor}{LT} : 1 \leq i \leq n \right\} \cup \left\{ b_i - \frac{\lfloor LT b_i \rfloor}{LT} : 1 \leq i \leq n \right\}, \quad (3.1)$$

where $\lfloor \cdot \rfloor$ is the floor function. Suppose $\Gamma = \{\gamma_1, \gamma_2, \dots, \gamma_M\}$ is the enumeration of the elements of Γ in increasing order, then $\gamma_1 = 0$ as a consequence of $a_1 = 0$. Furthermore, defining $\gamma_{M+1} = 1/(LT)$, we see that

$$0 = \gamma_1 < \gamma_2 < \dots < \gamma_{M+1} = (LT)^{-1},$$

and a collection of intervals $\{\mathcal{I}_m\}$ that partitions the set $\mathcal{F}_0 = [0, 1/(LT))$ is given by

$$\mathcal{I}_m = [\gamma_m, \gamma_{m+1}), \quad 1 \leq m \leq M.$$

As discussed in Chapter 2, the reason we partition \mathcal{F}_0 in this manner is that $\chi(f \in \mathcal{F})$ is constant (either 0 or 1) for $f \in \mathcal{I}_m \oplus r/(LT)$, and each pair of indices m and r . In other words each *subcell* of the form $\mathcal{I}_m \oplus r/(LT)$, for $l \in \mathcal{L}$ and $1 \leq m \leq M$ is either disjoint from or fully contained in \mathcal{F} . Now define *spectral index sets* \mathcal{K}_m and their complements $\bar{\mathcal{K}}_m$ for $m \in \{1, 2, \dots, M\}$ as follows:

$$\mathcal{K}_m \stackrel{\text{def}}{=} \left\{ r \in \mathcal{L} : \frac{r}{LT} \oplus \mathcal{I}_m \subset \mathcal{F} \right\}, \quad \bar{\mathcal{K}}_m = \mathcal{L} \setminus \mathcal{K}_m.$$

The set \mathcal{K}_m contains the indices of subcells in the collection $\{r/(LT) \oplus \mathcal{I}_m : r \in \mathcal{L}\}$ that are contained in \mathcal{F} . The following example illustrates the construction of these sets.

Example 3.1. Suppose we want to design sampling patterns for a class of bandlimited signals $\mathcal{B}(\mathcal{F})$ with

$$\mathcal{F} = \left[0, \frac{21}{400}\right) \cup \bigcup_{m=1}^{19} \left[\frac{21m}{400}, \frac{21m}{400} + \frac{1}{400}\right),$$

which is nonpackable with $[\mathcal{F}] = [0, 1)$ and $\Omega = 0.1$. Hence, the Nyquist rate equals $\mu([\mathcal{F}]) = 1$, and the Landau minimum rate is $\mu(\mathcal{F}) = 0.1$. For the choice $L = 20$, we find that $M = 19$ and $\Gamma = \{m/200 : m = 0, \dots, 19\}$. Hence, the subcells in $\mathcal{F}_0 = [0, 1/20)$ and the spectral index sets are given by

$$\mathcal{I}_m = \begin{cases} [0, 2/400) & \text{if } m = 1, \\ [M/400, (m+1)/400) & 2 \leq m \leq 19, \end{cases}$$

$$\mathcal{K}_m = \begin{cases} \{0, 1\} & \text{if } m = 1, \\ \{0, m\} & 2 \leq m \leq 19. \end{cases}$$

Denote the number of elements of \mathcal{K}_m by $q_m = |\mathcal{K}_m|$. Then $|\bar{\mathcal{K}}_m| = L - q_m$. Observe that $q(f) = q_m$ for all $f \in \mathcal{I}_m$, where

$$q(f) \stackrel{\text{def}}{=} \sum_{r=0}^{L-1} \chi\left(f + \frac{r}{LT} \in \mathcal{F}\right), \quad f \in \mathcal{F}_0. \quad (3.2)$$

Next, define the following matrices for each m :

$$\begin{aligned} \mathbf{A}_m &= \mathbf{W}_L(\mathcal{C}, \mathcal{K}_m) \quad \text{of size: } p \times q_m, \\ \mathbf{B}_m &= \mathbf{W}_L(\mathcal{C}, \bar{\mathcal{K}}_m) \quad \text{of size: } p \times (L - q_m), \end{aligned} \quad (3.3)$$

where \mathbf{W}_L is the $L \times L$ unitary DFT matrix whose (m, n) entry is $\mathbf{W}_{L, mn} = 1/\sqrt{L} \exp(j2\pi mn/L)$, and $\mathbf{W}_L(\mathcal{C}, \mathcal{K})$ denotes the submatrix of \mathbf{W}_L obtained by selecting its rows indexed by \mathcal{C} and columns by \mathcal{K} . Observe that \mathbf{A}_m and \mathbf{B}_m satisfy

$$\mathbf{A}_m \mathbf{A}_m^* + \mathbf{B}_m \mathbf{B}_m^* = \mathbf{I}. \quad (3.4)$$

These matrices play an important role in the error bounds, as we shall see later. A necessary and sufficient condition for reconstruction of every signal $x \in \mathcal{B}(\mathcal{F})$ is the existence of left-inverses \mathbf{A}_m^{-1} for each \mathbf{A}_m such that $\mathbf{A}_m^{-1} \mathbf{A}_m = \mathbf{I}$. This in turn requires that \mathbf{A}_m have full rank for each $1 \leq m \leq M$. This motivates the definition of two notions of goodness that characterize sampling patterns.

Definition 3.2. Given an index set \mathcal{K} with $|\mathcal{K}| = q \leq p$, we call \mathcal{C} a \mathcal{K} -reconstructive sampling pattern if the matrix $\mathbf{W}_L(\mathcal{C}, \mathcal{K})$ has full column rank.

Definition 3.3. A pattern \mathcal{C} with $|\mathcal{C}| = p \geq q$ is (p, q) universal if the matrix $\mathbf{W}_L(\mathcal{C}, \mathcal{K})$ has full column rank for every index set \mathcal{K} of q elements, i.e., whenever $|\mathcal{K}| = q$. A (p, p) -universal pattern is simply called *universal*.

The existence of a universal pattern is demonstrated by the *bunched sampling pattern* $\mathcal{C} = \{0, 1, \dots, p-1\}$. It is universal because the resulting matrix $\mathbf{W}(\mathcal{C}, \mathcal{K})$ has a Vandermonde structure for any $|\mathcal{K}| = p$. A (p, q) universal pattern is \mathcal{K} -reconstructive for every \mathcal{K} with $|\mathcal{K}| \leq q$, so that the second definition is stronger than the first for fixed p and q . Therefore, as shown in Chapter 2, the set \mathcal{C} has to be \mathcal{K}_m -reconstructive for each m , for perfect reconstruction. However, for simplicity we assume in the rest of this chapter that \mathcal{C} is universal with $p \geq \max_m q_m$. This automatically satisfies the reconstruction condition. In view of Eq. (3.2), this condition reduces to $p \geq \max_f q(f)$. Hence, the average sampling rate f_{avg} satisfies

$$f_{\text{avg}} = \frac{p}{LT} \geq \frac{1}{LT} \max_{f \in \mathcal{F}_0} \sum_{r=0}^{L-1} \chi\left(f + \frac{r}{LT} \in \mathcal{F}\right). \quad (3.5)$$

The equality in Eq. (3.5) is achieved for universal sampling patterns \mathcal{C} with $p = \max_m q_m$. The condition $p \geq \max_m q_m$ guarantees that \mathbf{A}_m has full column rank for each m . Under this condition, we obtain the following explicit reconstruction formula for $x(t)$ from its multicoset samples:

$$x(t) = \sum_{i=1}^p \sum_{j=-\infty}^{\infty} x((c_i + Lj)T) \phi_i(t - (c_i + Lj)T),$$

where the functions $\phi_i(t)$, $i = 1, \dots, p$ are (nonunique) interpolation filters. These filters can be parameterized in terms of matrices \mathbf{A}_m^{-1} of size $q_m \times p$ and \mathbf{C}_m of size $(L - q_m) \times p$, defined by:

$$\mathbf{A}_m^{-1} \mathbf{A}_m = \mathbf{I}_{q_m} \quad \text{and} \quad \mathbf{C}_m \mathbf{A}_m = \mathbf{0}. \quad (3.6)$$

It is clear that these matrices are nonunique if $p > q_m$, and this reflects the nonuniqueness of the interpolation filters. A multirate realization of the reconstruction scheme is illustrated in Figure 3.2. The analysis part, to the left of the broken line, is a model for the multicoset sampling process of the continuous-time signal (Figure 3.1). In other words, the simple structure of the analysis part of the filter bank is dictated by the assumption that only samples on the multicoset grid are available, while the synthesis part has a fully general structure. The digital

filters $\Psi_i(z)$, $i = 1, \dots, p$ on the synthesis side are related to the interpolation filters by:

$$\Psi_i(z) = \sum_{n \in \mathbb{Z}} \phi_i(nT) z^{-n}.$$

The exact expressions for these interpolation filters in terms of \mathbf{A}_m^L and \mathbf{C}_m are given in Chapter 2. We summarize the bounds below, as they will be the basis for all the results in this chapter.

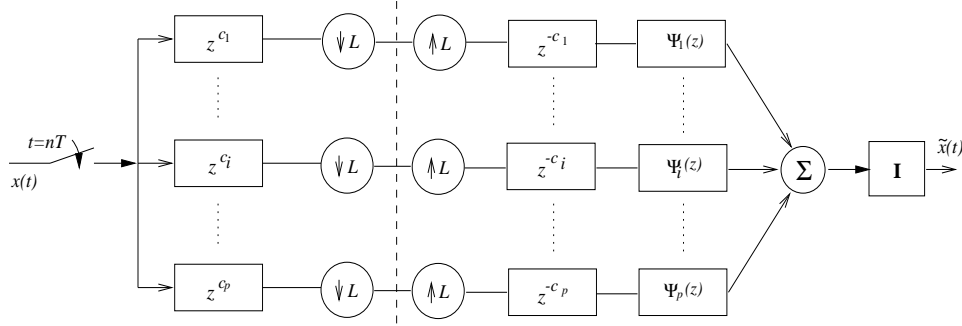


Figure 3.2 Multicoset sampling and reconstruction. The block “I” is an ideal sinc interpolator.

All our error bounds are expressed in terms of \mathbf{A}_m^{-1} , \mathbf{C}_m and \mathbf{S}_m defined as:

$$\mathbf{S}_m = \begin{pmatrix} \mathbf{A}_m^{-1} \mathbf{B}_m \\ \mathbf{C}_m \mathbf{B}_m - \mathbf{I}_{q_m} \end{pmatrix}. \quad (3.7)$$

3.2.3 Error bounds

Assume that $x(t)$ lies in $\mathcal{B}([\mathcal{F}])$ rather than in the class of signals for which it was designed, namely $\mathcal{B}(\mathcal{F})$. Thus $x(t)$ has out-of-band frequency components. This causes the reconstructed signal $\tilde{x}(t)$ to be in error, which for simplicity we call the *aliasing error*. The following are some error bounds derived in Chapter 2. The peak value of $e(t)$ is bounded:

$$\sup_t |e(t)| \leq \psi_\infty \int_{[\mathcal{F}] \setminus \mathcal{F}} |X(f)| df, \quad \text{where } \psi_\infty = \max_m \|\mathbf{S}_m\|_1, \quad (3.8)$$

while the energy of $e(t)$ and an upper bound on it are given by

$$\int_{-\infty}^{\infty} |e(t)|^2 dt = \sum_{m=1}^M \int_{\mathcal{I}_m} (\mathbf{x}_m^-(f))^* (\mathbf{S}_m^* \mathbf{S}_m) \mathbf{x}_m^-(f) df, \quad (3.9)$$

$$\int_{-\infty}^{\infty} |e(t)|^2 dt \leq \psi_2^2 \int_{[\mathcal{F}] \setminus \mathcal{F}} |X(f)|^2 df, \quad \psi_2 = \max_m \|\mathbf{S}_m\|_2. \quad (3.10)$$

where $\mathbf{x}_m^-(f)$, defined for $f \in \mathcal{I}_m$, are vectors containing the out-of-band signal components:

$$\mathbf{x}_m^-(f) = \left\{ X\left(f + \frac{k}{LT}\right) : k \in \bar{\mathcal{K}}_m \right\}, \quad f \in \mathcal{I}_m.$$

Suppose the input samples $x(nT)$ contain additive white noise $w(n)$ with variance σ^2 representing, for instance, sensor noise or quantization error associated with sampling. Then the corresponding output noise has average power equal to

$$\langle E|\tilde{w}(t)|^2 \rangle_t = \sigma^2 \psi_n, \quad \psi_n = T \sum_{m=1}^M \mu(\mathcal{I}_m) (\|\mathbf{A}_m^{-1}\|_F^2 + \|\mathbf{C}_m\|_F^2). \quad (3.11)$$

The bounds in Eqs. (3.10) and (3.11) are tight because there exist nonzero input signals that satisfy the bounds with equality, however Eq. (3.8) need not be a tight bound. All three bounds depend only on a measure of the out-of-band signal content, which is either the magnitude of the spectrum $|X(f)|$ or its square integrated over the out-of-band region $[\mathcal{F}] \setminus \mathcal{F}$.

3.3 Optimal Reconstruction

The multiplying constants ψ_∞ , ψ_2 in the bounds in Eqs. (3.8) and (3.10) are nondecreasing functions of the 1- and 2-norms, respectively, of the matrix \mathbf{S}_m for each m . Hence, our problem is to ensure that \mathbf{S}_m has the smallest norm possible for each m . This is clearly a collection of mutually independent problems. So, for the sake of readability, we drop the index m everywhere from now on with the understanding that the solution needs to be applied to each m . Given sampling pattern \mathcal{C} and a spectral index set \mathcal{K} , our objective is to pick appropriate matrices \mathbf{A}^{-1} and \mathbf{C} that satisfy $\mathbf{A}^{-1}\mathbf{A} = \mathbf{I}$ and $\mathbf{C}\mathbf{A} = \mathbf{0}$ (viz. Eq. (3.6)) and minimize the norm of

$$\mathbf{S} = \begin{pmatrix} \mathbf{A}^{-1}\mathbf{B} \\ \mathbf{C}\mathbf{B} - \mathbf{I} \end{pmatrix}, \quad (3.12)$$

where “norm” means either $\|\cdot\|_2$ (spectral norm) or $\|\cdot\|_1$ (maximum-column-sum norm). The other possibility is to minimize the output noise power in Eq. (3.11). A close look at this expression reveals that we need to minimize (for each fixed m) the quantity $\|\mathbf{A}^{-1}\|_F^2 + \|\mathbf{C}\|_F^2$ over all valid matrices \mathbf{A}^{-1} and \mathbf{C} .

Note that if $p = q$, the matrix \mathbf{A} is square and hence the left-inverse \mathbf{A}^{-1} is unique. Also the only matrix \mathbf{C} that would satisfy $\mathbf{C}\mathbf{A} = \mathbf{0}$ is trivial, namely $\mathbf{C} = \mathbf{0}$. In other words, there are no free parameters when $p = q$. Therefore, the reconstruction system only needs to be optimized when $p > q$. We assume that $p > q_m$ in the rest of the section. The other point to note is that the optimization needs to be carried out for each value of the index m , the subscript we have chosen to omit. We will see in a moment that the selection of the best \mathbf{A} and \mathbf{C} to minimize (a) the spectral norm of \mathbf{S} , and (b) the output noise power in Eq. (3.11) can be solved analytically. Minimizing the quantity $\|\mathbf{S}\|_1$ is a little harder however, requiring the use of numerical methods.

3.3.1 Minimizing the aliasing error energy

The following lemmas (whose proofs can be found in Appendix A) address the problem of minimizing the bounding constant ψ_2 for the aliasing error energy in Eq. (3.10):

Lemma 3.1. *The solution \mathbf{X}_\star to the problem*

$$\min_{\mathbf{X}} \|\mathbf{R} + \mathbf{X}\mathbf{Q}\|_2,$$

for given \mathbf{R} and \mathbf{Q} with compatible dimensions, is $\mathbf{X}_\star = -\mathbf{R}\mathbf{Q}^\dagger$, where \mathbf{Q}^\dagger is the pseudo-inverse of \mathbf{Q} . Furthermore, \mathbf{X}_\star simultaneously minimizes all singular values of $\mathbf{R} + \mathbf{X}\mathbf{Q}$.

Lemma 3.2. *Let $(\mathbf{A} \ \mathbf{B})$ be a $p \times L$ submatrix of the $L \times L$ DFT matrix \mathbf{W} whose entries are $W_{mn} = \exp(-j2\pi mn/L)$, with possible rearrangements of the columns. Suppose that \mathbf{A} , with $q \leq p$ columns, has full rank. Then the minimization of the largest singular value of \mathbf{S} ,*

$$\min \|\mathbf{S}\|_2 \equiv \min \left\| \begin{pmatrix} \mathbf{A}^{-1}\mathbf{B} \\ \mathbf{C}\mathbf{B} - \mathbf{I} \end{pmatrix} \right\|, \quad (3.13)$$

performed over all matrices \mathbf{A}^{-1} and \mathbf{C} that satisfy $\mathbf{A}^{-1}\mathbf{A} = \mathbf{I}$ and $\mathbf{C}\mathbf{A} = \mathbf{0}$, has the solution

$$\mathbf{A}_\star^{-1} = \mathbf{A}^\dagger = (\mathbf{A}^*\mathbf{A})^{-1}\mathbf{A}^* \quad \text{and} \quad \mathbf{C}_\star = \mathbf{B}^*(\mathbf{I} - \mathbf{A}\mathbf{A}^\dagger), \quad (3.14)$$

and the corresponding minimum value of the objective function is

$$\|\mathbf{S}_\star\|_2 = \begin{cases} \sqrt{\lambda_{\max}((\mathbf{A}^*\mathbf{A})^{-1})} & \text{if } p < L, \\ 0 & \text{if } p = L. \end{cases} \quad (3.15)$$

Furthermore, the solution in Eq. (3.14) simultaneously minimizes all singular values of \mathbf{S} , and therefore also its Frobenius norm.

Next we address the problem of optimizing the actual reconstruction in terms of the aliasing error energy.

Theorem 3.1. *The choice of optimal matrices \mathbf{A}_\star^{-1} and \mathbf{C}_\star in Lemma 3.2 minimizes the actual aliasing error energy for each $x(t) \in \mathcal{B}([\mathcal{F}])$ as well as the aliasing error bound in Eq. (3.10).*

Proof. Equation (3.14) clearly minimizes the constant ψ_2 in Eq. (3.10), or equivalently the bound itself. Moreover, Lemma 3.2 says that the solution in Eq. (3.14) minimizes all the eigenvalues of $\mathbf{S}^*\mathbf{S}$. Hence, $\mathbf{S}^*\mathbf{S} - \mathbf{S}_\star^*\mathbf{S}_\star$ is nonnegative definite for any feasible \mathbf{S} . Examining the expression for the actual aliasing error energy (Eq. (3.9)), we see that the quantity in Eq. (3.14) is indeed the best solution. \square

Remark. Suppose that $p < L$. Then for the choice $\mathbf{A}^{-1} = \mathbf{A}^\dagger$ and $\mathbf{C} = \mathbf{0}$, Eq. (3.12) yields $\mathbf{S} = \begin{pmatrix} \mathbf{A}^\dagger \mathbf{B} \\ -\mathbf{I} \end{pmatrix}$, whose spectral norm can be shown to be

$$\begin{aligned} \|\mathbf{S}\|_2 &= \sqrt{\lambda_{\max}(\mathbf{A}^\dagger \mathbf{B} (\mathbf{A}^\dagger \mathbf{B})^* + \mathbf{I})} = \sqrt{\lambda_{\max}(\mathbf{A}^\dagger (\mathbf{A}^\dagger)^*)} \\ &= \sqrt{\lambda_{\max}((\mathbf{A}^* \mathbf{A})^{-1})} \equiv \|\mathbf{S}_\star\|_2. \end{aligned}$$

using Eq. (3.4). Thus the pair $(\mathbf{A}^{-1}, \mathbf{C}) = (\mathbf{A}^\dagger, \mathbf{0})$ produces the optimal constant multiplier ψ_2 in Eq. (3.10), but does not minimize the actual aliasing error energy. In other words these matrices produce the same worst case, but not the same case-by-case performance as the optimal matrices in Eq. (3.14).

3.3.2 Minimizing the output noise power

We seek the optimal matrices \mathbf{A}^{-1} and \mathbf{C} that satisfy $\mathbf{A}^{-1} \mathbf{A} = \mathbf{I}$ and $\mathbf{C} \mathbf{A} = \mathbf{0}$ and minimize ψ_n in Eq. (3.11), or equivalently, $\|\mathbf{A}^{-1}\|_F^2 + \|\mathbf{C}\|_F^2$. This is a fairly easy problem because \mathbf{C} and \mathbf{A}^{-1} are independent of each other and the objective function is separable. Therefore, we need to compute $\min_{\mathbf{A}^{-1}} \|\mathbf{A}^{-1}\|_F^2$ and $\min_{\mathbf{C}} \|\mathbf{C}\|_F^2$ individually. For the second term $\mathbf{C}_\star = \mathbf{0}$ is clearly the unique solution, while for the first term, we use the representation $\mathbf{A}^{-1} \equiv \mathbf{A}^\dagger + \mathbf{X} \mathbf{P}$ where \mathbf{P} is the projection operator onto the null space of \mathbf{A}^* , namely $\mathbf{P} \stackrel{\text{def}}{=} (\mathbf{I} - \mathbf{A} \mathbf{A}^\dagger) = (\mathbf{I} - \mathbf{A} (\mathbf{A}^* \mathbf{A})^{-1} \mathbf{A}^*)$. This representation is justified in the proof of Lemma 3.2 in Appendix A. This yields the following minimization

$$\min_{\mathbf{A}^{-1}} \|\mathbf{A}^{-1}\|_F^2 = \min_{\mathbf{X}} \|\mathbf{A}^\dagger + \mathbf{X} \mathbf{P}\|_F^2.$$

Applying Lemma 3.1, we obtain the minimizing solution $\mathbf{X}_\star = -\mathbf{A}^\dagger \mathbf{P}^\dagger \equiv -\mathbf{A}^\dagger \mathbf{P} = \mathbf{0}$. Therefore, $\mathbf{A}_\star^{-1} = \mathbf{A}^\dagger$. Finally,

$$\|\mathbf{A}^\dagger\|_F = [\text{tr}(\mathbf{A}^\dagger (\mathbf{A}^\dagger)^*)]^{1/2} = \sqrt{\text{tr}((\mathbf{A}^* \mathbf{A})^{-1})}. \quad (3.16)$$

3.3.3 Minimizing the peak aliasing error

The relevant quantity to minimize in order to obtain the tightest bound in Eq. (3.8) is the 1-norm of the matrix \mathbf{S} defined in Eq. (3.12):

$$\min_{\mathbf{C}, \mathbf{A}^{-1}} \left\| \begin{pmatrix} \mathbf{A}^{-1} \mathbf{B} \\ \mathbf{C} \mathbf{B} - \mathbf{I} \end{pmatrix} \right\|_1 \quad \text{subject to} \quad \begin{pmatrix} \mathbf{A}^{-1} \\ \mathbf{C} \end{pmatrix} \mathbf{A} = \begin{pmatrix} \mathbf{I} \\ \mathbf{0} \end{pmatrix}. \quad (3.17)$$

The problem of choosing \mathbf{A}^{-1} and \mathbf{C} to minimize $\|\mathbf{S}\|_1$, unlike the spectral or Frobenius norms of \mathbf{S} cannot be solved analytically. We resort to numerical methods instead. As shown in the

proof of Lemma 3.2, we can represent \mathbf{A}^{-1} and \mathbf{C} as follows:

$$\mathbf{A}^{-1} = \mathbf{A}^\dagger + \mathbf{X}_1 \mathbf{P} \quad \text{and} \quad \mathbf{C} = \mathbf{X}_2 \mathbf{P}, \quad (3.18)$$

where \mathbf{X}_1 is a $q \times p$ matrix, and \mathbf{X}_2 a $(L - q) \times p$ matrix. We can now rewrite Eq. (3.17) in an unconstrained form as

$$\min_{\mathbf{X}_1, \mathbf{X}_2} \left\| \begin{pmatrix} \mathbf{A}^\dagger \mathbf{B} \\ -\mathbf{I} \end{pmatrix} + \begin{pmatrix} \mathbf{X}_1 \\ \mathbf{X}_2 \end{pmatrix} \mathbf{P} \mathbf{B} \right\|_1 \equiv \min_{\mathbf{X}} \|\mathbf{S}_0 + \mathbf{X} \mathbf{M}\|_1, \quad (3.19)$$

where $\mathbf{S}_0 = \begin{pmatrix} \mathbf{A}^\dagger \mathbf{B} \\ -\mathbf{I} \end{pmatrix}$, $\mathbf{X} = \begin{pmatrix} \mathbf{X}_1 \\ \mathbf{X}_2 \end{pmatrix}$, and $\mathbf{M} = \mathbf{P} \mathbf{B}$. This problem may be solved approximately using a linear program. We first rewrite Eq. (3.19) as follows

$$\min d \quad \text{subject to} \quad d \geq \|\mathbf{z}_i\|_1, \quad \mathbf{Z} = \mathbf{S}_0 + \mathbf{X} \mathbf{M}.$$

Each constraint $\|\mathbf{z}\|_1 \leq d$ can be approximated by the set of linear inequalities:

$$\begin{aligned} \sum_{k=1}^K u_{mik} \exp(-j2\pi k/K) &= z_{mi}, \quad \forall m, i \\ \sum_{m=1}^L \sum_{k=1}^K u_{mik} &\leq d, \quad \forall i \\ u_{mik} &\geq 0, \quad \forall m, i, k. \end{aligned}$$

This region is clearly a subset of $\|\mathbf{z}_i\| \leq d$, but it can be verified easily that it is a superset of the region $\|\mathbf{z}_i\| \leq d/\cos(\pi/K)$. Hence, the approximate linear program produces an answer that is accurate to within a factor of $\cos(\pi/K)$ of the correct answer. Hence, the normalized error is bounded by $1 - \cos(\pi/K) \leq \pi^2/(2K^2)$, and the approximation is quite good for moderately large K . This is essentially like approximating circles by K -sided polygons. The optimization in Eq. (3.19) can also be solved using semi-infinite linear programming [34].

3.3.4 Lower bounds on ψ_∞ , ψ_2 , and ψ_n

The choice of sampling pattern \mathcal{C} that minimizes the optimal constants ψ_∞ , ψ_2 , and ψ_n is a difficult problem. It is therefore useful to know, even before attempting such a design, how small these constants can be made. In this section we present lower-bounds on these ‘‘error gain constants’’ $\|\mathbf{S}\|_2$, $\|\mathbf{A}^{-1}\|_F$, and $\|\mathbf{S}\|_1$. These are the relevant quantities that affect the bounds in Eqs. (3.8), (3.10), and the noise power in Eq. (3.11). All bounds presented here are independent of the sampling pattern and only depend on L , p , and q .

Suppose we denote the (real positive) eigenvalues of the $q \times q$ matrix $\mathbf{A}^* \mathbf{A}$ by $\lambda_1, \lambda_2, \dots, \lambda_q$ in decreasing order. Then we have from Eq. (3.15) that

$$\|\mathbf{S}\|_2^2 \geq \|\mathbf{S}_*\|_2^2 = \lambda_{\max}((\mathbf{A}^* \mathbf{A})^{-1}) = \frac{1}{\lambda_q}, \quad (3.20)$$

where \mathbf{S}_* is optimized to obtain the lowest aliasing error energy. Of course $\lambda_q > 0$, since \mathbf{A} is assumed to have full rank. Notice that we can use the fact that $|\mathbf{A}_{ij}| = 1/\sqrt{L}$ to bound the average eigenvalue $\bar{\lambda}_{\text{am}} = \text{tr}(\mathbf{A}^* \mathbf{A})/q$:

$$\bar{\lambda}_{\text{am}} = \frac{1}{q} \sum_{i=1}^q \sum_{j=1}^p |\mathbf{A}_{ij}|^2 = \frac{p}{L}. \quad (3.21)$$

This result along with Eq. (3.20) and $\lambda_q \leq \bar{\lambda}_{\text{am}}$ yields

$$\|\mathbf{S}\|_2 \geq \sqrt{\frac{L}{p}}. \quad (3.22)$$

Our next bound on $\|\mathbf{A}^\dagger\|_F$ provides an estimate for the worst-case output noise power. Equation (3.16) implies that

$$\|\mathbf{A}^\dagger\|_F^2 = \text{tr}((\mathbf{A}^* \mathbf{A})^{-1}) = \sum_{i=1}^q \lambda_i^{-1} = q/\bar{\lambda}_{\text{hm}},$$

where $\bar{\lambda}_{\text{hm}}$ is the harmonic mean of the eigenvalues. Using the standard inequality $\bar{\lambda}_{\text{hm}} \leq \bar{\lambda}_{\text{am}}$ and Eq. (3.21), we immediately obtain

$$\|\mathbf{A}^\dagger\|_F^2 = \text{tr}((\mathbf{A}^* \mathbf{A})^{-1}) \geq \frac{qL}{p}. \quad (3.23)$$

We refer the reader to [35] for some stronger bounds on the eigenvalues of these matrices, but they hold only for special sampling patterns and bandpass spectral supports. Our next theorem concerns the tightness of the bounds in Eqs. (3.22) and (3.23):

Theorem 3.2. *The bounds in Eqs. (3.22) and (3.23) are tight in the sense that they hold when \mathcal{C} is a uniform sampling pattern and \mathcal{F} is packable corresponding to \mathcal{C} .*

Proof. Assume that $\mathcal{C} = \{0, a, 2a, \dots, (p-1)a\}$, i.e., $c_i = (i-1)a$, where $a = L/p$ is an integer. This corresponds to subsampling $x(nT)$ by a factor of a . Let \mathcal{I}_m and \mathcal{K}_m denote the spectral subcells and index sets corresponding to \mathcal{F} . Let m be a fixed index and $\mathcal{K}_m = \{k_1, k_2, \dots, k_{q_m}\}$. We see that packability of \mathcal{F} implies that $k_i - k_j$ cannot be a multiple of p , for $i \neq j$. Otherwise, the subcells $\mathcal{I}_m \oplus (k_i/LT)$ and $\mathcal{I}_m \oplus (k_j/LT)$ would overlap in the spectrum of $x(nT)$ when subsampled by $a = L/p$. Therefore, the (i, l) entry of \mathbf{A}_m is

$$\mathbf{A}_{m,il} = \frac{1}{\sqrt{L}} \exp\left(j2\pi \frac{(i-1)ak_l}{L}\right) = \frac{1}{\sqrt{ap}} \exp\left(j2\pi \frac{(i-1)\kappa_l}{p}\right),$$

where $\kappa_l \in \{0, 1, \dots, p-1\}$ is such that $\kappa_l \equiv k_l \pmod{p}$. Evidently $\{\kappa_l\}$ are distinct because \mathcal{F} is packable. We see that $\sqrt{a}\mathbf{A}_m$ is a submatrix of the $p \times p$ DFT matrix consisting of *all* its rows and q of its columns. It immediately follows that $\lambda_{\max}(\mathbf{A}_m^* \mathbf{A}_m) = 1/a = L/p$ and $\text{tr}(\mathbf{A}_m^* \mathbf{A}_m) = q_m/a = q_m L/p$. Hence, the optimal matrices satisfy $\|\mathbf{S}_{m^*}\|_2 = \sqrt{L/p}$ and $\|\mathbf{A}^\dagger\|_F^2 = q_m L/p$. \square

Finally, we provide a lower-bound on $\|\mathbf{S}\|_1$ just as in the case of the spectral norm. From the definition of the 1-norm we have

$$\|\mathbf{S}\|_1 = \max_s \sum_{r=1}^L |\mathbf{S}_{rs}| \geq \max_s \left(\sum_{r=1}^L |\mathbf{S}_{rs}|^2 \right)^{\frac{1}{2}},$$

where the last step follows from the positivity of terms in the sum. Therefore,

$$\begin{aligned} \|\mathbf{S}\|_1 &\geq \left(\max_s \sum_{r=1}^L |\mathbf{S}_{rs}|^2 \right)^{\frac{1}{2}} \geq \left(\frac{1}{L-q} \sum_{s=1}^{L-q} \sum_{r=1}^L |\mathbf{S}_{rs}|^2 \right)^{\frac{1}{2}} \\ &= \frac{1}{\sqrt{L-q}} \|\mathbf{S}\|_F. \end{aligned} \quad (3.24)$$

Observe that $\|\mathbf{S}\|_F^2 = \|\mathbf{A}^{-1}\mathbf{B}\|_F^2 + \|\mathbf{CB} - \mathbf{I}\|_F^2 \geq \|\mathbf{A}^\dagger\mathbf{B}\|_F^2 + \|\mathbf{B}^*\mathbf{PB} - \mathbf{I}\|_F^2$ which follows from the fact that the solution in Eq. (3.14) minimizes the Frobenius norm of \mathbf{S} . Therefore,

$$\begin{aligned} \|\mathbf{S}\|_F^2 &\geq \text{tr}(\mathbf{A}^\dagger \mathbf{B} \mathbf{B}^* (\mathbf{A}^\dagger)) + \text{tr}((\mathbf{B}^* \mathbf{P} \mathbf{B} - \mathbf{I})^2) \\ &= \text{tr}((\mathbf{A}^* \mathbf{A})^{-1} - \mathbf{I}) + \text{tr}(\mathbf{I} - \mathbf{B}^* \mathbf{P} \mathbf{B}). \end{aligned}$$

The expressions in the last step were obtained using the facts that $\mathbf{B}\mathbf{B}^* = \mathbf{I} - \mathbf{A}\mathbf{A}^*$ and $(\mathbf{I} - \mathbf{B}^*\mathbf{P}\mathbf{B})$ is a projection operator. These are justified in the proof of Lemma 3.2. Therefore, using the identities

$$\mathbf{P}\mathbf{B}\mathbf{B}^* = \mathbf{P}(\mathbf{I} - \mathbf{A}\mathbf{A}^*) = \mathbf{P}$$

and

$$\text{tr}(\mathbf{P}) = \text{tr}(\mathbf{I} - \mathbf{A}\mathbf{A}^\dagger) = p - \text{tr}(\mathbf{A}^\dagger \mathbf{A}) = p - q$$

we conclude that

$$\begin{aligned} \|\mathbf{S}\|_F^2 &\geq \text{tr}((\mathbf{A}^* \mathbf{A})^{-1}) - q + (L - q) - \text{tr}(\mathbf{P}\mathbf{B}\mathbf{B}^*) \\ &= \text{tr}((\mathbf{A}^* \mathbf{A})^{-1}) - q + (L - q) - (p - q). \end{aligned}$$

Combining the last inequality with Eqs. (3.24) and (3.23) we finally obtain

$$\|\mathbf{S}\|_1 \geq \frac{1}{\sqrt{(L-q)}} \sqrt{\frac{qL}{p} - q + L - p} = \sqrt{\frac{(L-p)(q+p)}{(L-q)p}}. \quad (3.25)$$

When $p = q$, we can obtain a stronger bound than Eq. (3.25) when $p = q$. Observe that the matrices \mathbf{A}^{-1} and $\mathbf{C} = \mathbf{0}$ are unique. Therefore,

$$\|\mathbf{S}\|_1 = \left\| \begin{pmatrix} \mathbf{A}^{-1}\mathbf{B} \\ -\mathbf{I} \end{pmatrix} \right\|_1 = 1 + \|\mathbf{A}^{-1}\mathbf{B}\|_1 \geq 1 + \frac{\|\mathbf{B}\|_1}{\|\mathbf{A}\|_1} = 2. \quad (3.26)$$

This bound, although applicable only for $p = q$, is indeed stronger than Eq. (3.25), whose right-hand side evaluates to $\sqrt{2}$ for $p = q$.

3.3.5 Which criterion to optimize?

As seen in Section 3.3, each of the three criteria leads to a different optimal choice for \mathbf{A}^{-1} and \mathbf{C} . Furthermore, the computation of those matrices is more difficult in one of the cases (minimizing the peak error). Therefore, the following question arises: suppose that \mathbf{A}^{-1} and \mathbf{C} are chosen to optimize one of the criteria. Then, how far from the optimum would the other criteria be for this choice? First of all, it is not fair to compare the optimum matrices corresponding to the criteria ψ_2 and ψ_n because the two problems have different underlying settings: the error energy is due to input signal mismodeling, while the output noise power is due to additive sample noise. Yet, we have seen that the “least-squares” solution \mathbf{A}^\dagger is the optimal choice for \mathbf{A}^{-1} for both criteria, although the optimal choices for \mathbf{C} are different. However, it is more meaningful to compare the optimal matrices for the criteria ψ_2 and ψ_∞ because the two problems are similar: the imperfections in the input signal in both cases are due to mismodeling. It is therefore reasonable to expect the optimal matrices that minimize $\|\mathbf{S}\|_1$ to be close to those that minimize $\|\mathbf{S}\|_2$ for which, of course, we have the analytical least-squares solution in Eq. (3.14). A question that springs to the mind is whether or not the least-squares solution is a good enough approximation to the exact solution for the 1-norm problem. The answer partially lies in the following result, which is a bound on the improvement factor that the solution to Eq. (3.19) can offer over the least-squares solution in Eq. (3.14). Observe that Eq. (3.19) can be rewritten in a slightly different constrained form as

$$\begin{aligned} \min \|\mathbf{S}\|_1 \quad \text{subject to} \quad & \mathbf{S}\boldsymbol{\xi} = \mathbf{S}_{\text{ls}}\boldsymbol{\xi}, \quad \forall \boldsymbol{\xi} \text{ such that } \mathbf{P}\mathbf{B}\boldsymbol{\xi} = \mathbf{0}, \\ & \text{where } \mathbf{S}_{\text{ls}} = \begin{pmatrix} \mathbf{A}^\dagger\mathbf{B} \\ \mathbf{B}^*\mathbf{P}\mathbf{B} - \mathbf{I} \end{pmatrix}, \end{aligned} \quad (3.27)$$

because we can write $(\mathbf{S} - \mathbf{S}_{\text{ls}}) = \mathbf{X}\mathbf{P}\mathbf{B}$ for a suitable \mathbf{X} owing to the fact that $\mathbf{A}^{-1} = \mathbf{A}^\dagger + \mathbf{X}_1\mathbf{P}$ and $\mathbf{C} = \mathbf{X}_2\mathbf{P}$ for suitable \mathbf{X}_1 and \mathbf{X}_2 . Note that \mathbf{S}_{ls} is the optimal matrix for the 2-norm minimization. Therefore, Eq. (3.27) yields

$$\|\mathbf{S}\|_1 \|\boldsymbol{\xi}\|_1 \geq \|\mathbf{S}_{\text{ls}}\boldsymbol{\xi}\|_1, \quad \forall \boldsymbol{\xi} \in N(\mathbf{P}\mathbf{B}) \implies \|\mathbf{S}\|_1 \geq \max_{\substack{\boldsymbol{\xi} \in N(\mathbf{P}\mathbf{B}) \\ \boldsymbol{\xi} \neq \mathbf{0}}} \frac{\|\mathbf{S}_{\text{ls}}\boldsymbol{\xi}\|_1}{\|\boldsymbol{\xi}\|_1}. \quad (3.28)$$

where $N(\cdot)$ denotes the null space. In the proof of Lemma 3.2, we show that $N(\mathbf{P}\mathbf{B}) = R(\mathbf{K})$ where $\mathbf{K} \stackrel{\text{def}}{=} (\mathbf{I} - \mathbf{B}^*\mathbf{P}\mathbf{B})$ is an orthonormal projector. Furthermore $\mathbf{S}_{\text{ls}}\mathbf{K} = \mathbf{S}_{\text{ls}}$ is easy to check. Hence, for ease of computation, we can weaken the bound in Eq. (3.28) by maximizing over the set consisting of the $L - q$ columns of \mathbf{K} , rather than the subspace $N(\mathbf{P}\mathbf{B}) = R(\mathbf{K})$. Thus, letting $\{\mathbf{k}_i\}$ denote the columns of \mathbf{K} , we obtain

$$\|\mathbf{S}\|_1 \geq \max_i \frac{\|\mathbf{S}_{\text{ls}}\mathbf{k}_i\|_1}{\|\mathbf{k}_i\|_1} \geq \frac{\max_i \|\mathbf{S}_{\text{ls}}\mathbf{k}_i\|_1}{\max_i \|\mathbf{k}_i\|_1} = \frac{\|\mathbf{S}_{\text{ls}}\mathbf{K}\|_1}{\|\mathbf{K}\|_1} = \frac{\|\mathbf{S}_{\text{ls}}\|_1}{\|\mathbf{K}\|_1},$$

implying that $\|\mathbf{S}_{\text{ls}}\|_1 \leq \|\mathbf{S}\|_1 \|\mathbf{K}\|_1$. In other words, using the least-squares solution in Eq. (3.14) instead of the solution to Eq. (3.19) cannot amplify $\|\mathbf{S}\|_1$ by a factor of more than $\|\mathbf{K}\|_1 \geq 1$.

We can apply these results to the norms of \mathbf{S}_m and \mathbf{A}_m^{-1} for each m to obtain lower bounds on (a) the constants present Eqs. (3.8) and (3.10); and (b) the average output noise power in Eq. (3.11). Without explicitly deriving them, we summarize the bounds below in terms of Ω , L , p and $q' = \max_m q_m$:

$$\begin{aligned} \|e\|_\infty &\leq \psi_\infty \int_{[\mathcal{F}] \setminus \mathcal{F}} |X(f)| df, \\ \|e(t)\|_2 &\leq \psi_2 \left(\int_{[\mathcal{F}] \setminus \mathcal{F}} |X(f)|^2 df \right)^{\frac{1}{2}}, \\ \langle E|\tilde{w}(t)|^2 \rangle_t &= \psi_n \sigma^2, \end{aligned}$$

where

$$\psi_\infty = \max_m \|\mathbf{S}_m\|_1 \geq \sqrt{\frac{(L-p)(q'+p)}{(L-q')p}}, \quad (3.29)$$

$$\psi_2 = \max_m \|\mathbf{S}_m\|_2 \geq \sqrt{\frac{L}{p}}, \quad (3.30)$$

$$\psi_n = T \sum_m \mu(\mathcal{I}_m) \|\mathbf{A}_m^\dagger\|_F^2 \geq \Omega \frac{L}{p}. \quad (3.31)$$

In each of the first two equations, we have a lower bound and an upper bound that cannot be combined. However, note that the bounds for $\|e(t)\|_\infty$ or $\|e(t)\|_2$ are tight. Hence, the lower bounds on ψ_∞ and ψ_2 tell us how large the aliasing error can be in the worst cases for the corresponding bounds. However, they do not tell how large or small the errors in other cases. Also note that the constants ψ_ω , ($\omega = 2, n, \infty$) decrease as expected for a fixed $\{q_m\}$ when p is increased. If we increase L , p , and q_m in such a way that p/L and q/L remain constant (as would happen if one attempts to approach the Landau rate by increasing L), we find that these bounds are invariant. These bounds represent errors inherent to any sampling procedure, whether uniform or not, for any multiband signals, packable or not. In Section 3.5, we study the

increase in error sensitivity incurred for nonpackable signals that are sampled at a sub-Nyquist rate.

3.4 Optimal Sampling

In this section, we discuss two important issues pertaining to optimal sampling, namely, determining the optimal base sampling frequency and sampling pattern design. The first one is concerned with choosing the period T that produces the lowest average sampling rate for given \mathcal{F} and L . The second issue is concerned with finding a good sampling pattern \mathcal{C} that optimizes the aliasing error bounds or sensitivity to noise. Our study of this latter problem is somewhat numerical in nature.

3.4.1 Optimizing the choice of T

In all our previous analysis, we set the base sampling frequency $1/T = f_{\text{nyq}}$ for convenience. This is equivalent to sampling the original signal uniformly at the Nyquist rate prior to discarding some samples. Clearly, we could have chosen a slightly larger rate than the Nyquist rate and still obtained similar results. In this section, we examine the problem of choosing, for given L and \mathcal{F} , the optimal value T_* for T that minimizes the average sampling rate. We also provide a polynomial-time algorithm to find T_* , whose value may be larger than $1/f_{\text{nyq}}$, and we show this by example. This problem is related to that of pairing band edges that Herley and Wong [28] suggest. They provide a necessary and sufficient condition on the band edge frequencies a_i and b_i of the spectral support \mathcal{F} , for achieving the Landau minimum rate. They also show that for sufficiently large L , with LT fixed, the minimum rate can be approached arbitrarily closely. In our case, however, we fix L as it determines the complexity of the reconstruction. Our variable is T , and the problem is to compute the optimal base sampling frequency $1/T$

All the results derived for the specific case $1/T = f_{\text{nyq}}$, the Nyquist rate, extend to the general case $1/T \geq f_{\text{nyq}}$ provided that we replace the spectral span $[\mathcal{F}]$ everywhere by $[0, 1/T)$. We already know that for given L and T , the smallest average sampling rate (equal to $\max_m q_m/(LT)$) is given by the right-hand side of Eq. (3.5):

$$f_{\text{avg}}(T, L) = \frac{1}{LT} \max_{f \in [0, \frac{1}{LT})} \sum_{r=0}^{L-1} \chi\left(f + \frac{r}{LT} \in \mathcal{F}\right).$$

Therefore, we seek the solution to

$$T_\star = \arg \min_{0 < T \leq T_0} f_{\text{avg}}(T, L), \quad \text{where } T_0 = \frac{1}{f_{\text{nyq}}}, \quad (3.32)$$

for a fixed L . For spectral supports expressible as $\mathcal{F} = \bigcup_{i=1}^n [a_i, b_i)$, we have seen that the construction of the sets \mathcal{I}_m and \mathcal{K}_m can be done in polynomial time. Therefore, the computation of $f_{\text{avg}}(T, L)$ requires polynomial time also. The minimization in Eq. (3.32), however, is performed over a continuous parameter T . The following theorem allows us to transform the minimization problem to an exhaustive search over a finite set of values for T .

Theorem 3.3. *For a spectral support of the form $\mathcal{F} = \bigcup_{i=1}^n [a_i, b_i)$, the optimum T_\star in Eq. (3.32) must satisfy*

$$\frac{1}{LT_\star} = \frac{b_j - a_i}{k}$$

for some integers i, j and k such that $1 \leq i \leq j \leq n$, and $0 < k \leq LT_0(b_j - a_i) \leq L$.

The proof can be found in Appendix A. Theorem 3.3 enables us to generate no more than $n(n+1)(L-1)/2$ possible candidates for T_\star , which may then be used to minimize the average sampling rate. It turns out that $T_\star = T_0$ is optimal for the spectral support \mathcal{F} of Example 2.1. However, as the following example shows, spectral supports exist for which $T = T_0$ is highly suboptimal:

Example 3.2. For a given L , consider the spectral support,

$$\mathcal{F} = \bigcup_{r=0}^{L-1} [r, r + \epsilon) \cup [L - \epsilon, L),$$

where $\epsilon < 1/(L+1)$ is a small positive number. For the choice $T = T_0 = 1/L$ we have $1/(LT) = 1$ and

$$\sum_{r=0}^{L-1} \chi\left(f + \frac{r}{LT} \in \mathcal{F}\right) = \begin{cases} L & \text{if } 0 \leq f < \epsilon, \\ 0 & \text{if } \epsilon \leq f < 1 - \epsilon, \\ 1 & \text{if } 1 - \epsilon \leq f < 1. \end{cases}$$

Since L pieces of the spectrum overlap, we require $p = L$ and this makes the average sampling rate equal to $p/(LT) = L$. Next, for the optimal choice $T = T_\star = (L(1 + \epsilon))^{-1}$ we have

$$\sum_{r=0}^{L-1} \chi\left(f + \frac{r}{LT} \in \mathcal{F}\right) = \begin{cases} 1 & \text{if } f \in [0, \epsilon) \cup [1 - L\epsilon, 1 - L\epsilon + \epsilon) \cup [1 - L\epsilon + 2\epsilon, 1 + \epsilon), \\ 0 & \text{if } f \in [\epsilon, 1 - L\epsilon) \cup [1 - L\epsilon + \epsilon, 1 - L\epsilon + 2\epsilon). \end{cases}$$

Therefore, $p_\star = 1$ is required and the average sampling rate $p_\star/(LT) = (1 + \epsilon)$. Hence, the choice $T = T_\star$ can improve the sampling rate over the choice $T = T_0$ by a factor of $L/(1 + \epsilon)$, which is nearly as large as it can get because this factor never exceeds L , as shown below:

$$\frac{p_\star}{LT_\star} \geq \frac{p_\star}{LT_0} \geq \frac{1}{L} \left(\frac{p}{LT_0} \right),$$

which follows from $T_\star \leq T_0$ and $p_\star \geq 1 \geq p/L$. Although Example 3.2 is an extreme situation, it shows that optimizing T may be of significance, with the largest gains occurring typically for signals with sparse spectral supports.

3.4.2 Sampling pattern design

We now examine the problem of designing good sampling patterns. We propose to use the following minimizations as empirical design criteria:

$$\mathcal{C}_\star = \arg \min_{\mathcal{C}} \psi_\omega(\mathcal{C}, \{\mathcal{K}_m\}_{m=1}^M) \quad \text{for } \omega = 2, \infty, n,$$

where $\psi_\omega(\mathcal{C}, \{\mathcal{K}_m\})$ are $\max_m \|\mathbf{S}_{\star m}\|_2$, $\max_m \|\mathbf{S}_{\star m}\|_1$, and $T \sum_m \mu(\mathcal{I}_m) \|\mathbf{A}_m^\dagger\|_F^2$ for $\omega = 1, 2, n$, respectively, and the subscript “ \star ” denotes optimality of \mathbf{S}_m with respect to the matrices \mathbf{A}_m^{-1} and \mathbf{C}_m , which is discussed in the previous section. The functions $\psi_\omega(\mathcal{C}, \{\mathcal{K}_m\})$ are invariant under cyclic shifts of \mathcal{C} in $\{0, 1, \dots, L - 1\}$, and this follows easily from the definitions of these functions.

Example 3.1 (Continued). For the chosen spectral support and $L = 20$, we have $q_m = 2$ for all m . Hence, $p \geq 2$ is necessary and sufficient for perfect reconstruction from the multicoset samples. For example, an exhaustive search over all sampling patterns for $p = 5$ yields

$$\begin{aligned} \psi_{2\star} &= \min_{\mathcal{C}} \psi_2(\mathcal{C}, \{\mathcal{K}_m\}) = 2.9032 \text{ at } \mathcal{C}_a = \{0, 1, 2, 13, 16\}, \\ \psi_{n\star} &= \min_{\mathcal{C}} \psi_n(\mathcal{C}, \{\mathcal{K}_m\}) = 0.4769 \text{ at } \mathcal{C}_b = \{0, 4, 7, 14, 15\}, \\ \psi_{\infty\star} &= \min_{\mathcal{C}} \psi_\infty(\mathcal{C}, \{\mathcal{K}_m\}) = 2.2583 \text{ at } \mathcal{C}_c = \{0, 1, 2, 8, 17\}, \end{aligned}$$

where $\min_{\mathcal{C}} \psi_\infty(\mathcal{C}, \{\mathcal{K}_m\})$ is computed using the approximate linear program formulation with $K = 12$, and hence cannot be claimed to be truly optimal. In this example, the three design criteria produce different optimal sampling patterns. Table 3.1 shows the three objective functions evaluated for each of these three candidate optimal patterns. It is evident that none of the three candidate sampling patterns is simultaneously optimal for all three design criteria. However all three candidates solutions are close to optimal for each of the criteria, and we lose

little in terms of optimality by restricting our attention to any one of the criteria. For example, we can pick ψ_n as it is the easiest to compute.

Let $\psi_{2\star} = \min_{\mathcal{C}} \psi_2(\mathcal{C}, \{\mathcal{K}_m\})$ and $\psi_{n\star} = \min_{\mathcal{C}} \psi_n(\mathcal{C}, \{\mathcal{K}_m\})$ denote the optimal constants for a given p . Define the following quantities

$$\eta_2 = \psi_{2\star} \sqrt{\frac{p}{L}}, \quad \eta_n = \psi_{n\star} \frac{p}{\Omega L}, \quad \eta_\infty = \psi_{\infty\star} \sqrt{\frac{(L - q')p}{(L - p)(q' + p)}},$$

which are obtained by normalizing the quantities $\psi_{2\star}$, $\psi_{n\star}$, and $\psi_{\infty\star}$ by their lower bounds in Eqs. (3.29), (3.30), and (3.31). Figure 3.3 illustrates (for $2 \leq p \leq 20$) the behavior of η_2 and η_n . These are computed by first finding $\psi_{2\star}$ and $\psi_{n\star}$ using an exhaustive search algorithm over all sampling patterns of size p , followed by normalization. Due to the higher computational complexity, we computed η_∞ only for $2 \leq p \leq 5$ as summarized in Table 3.2.

Table 3.1 Design criteria evaluated at the candidate optimal sampling patterns: $\mathcal{C}_a = \{0, 1, 2, 13, 16\}$, $\mathcal{C}_b = \{0, 4, 7, 14, 15\}$, and $\mathcal{C}_c = \{0, 1, 2, 8, 17\}$. The boxed entries are optimal in their respective rows.

Criterion	$\mathcal{C} = \mathcal{C}_a$	$\mathcal{C} = \mathcal{C}_b$	$\mathcal{C} = \mathcal{C}_c$
ψ_2	2.9032	3.0641	3.5241
ψ_n	0.4811	0.4769	0.4918
ψ_∞	2.3929	2.6479	2.2583

Table 3.2 Normalized error gain constant η_∞ for $2 \leq p \leq 5$.

p	2	3	4	5
η_∞	9.8256	3.3764	2.3049	2.0908

Figure 3.3 shows that the optimal error gain constants η_2 and η_n approach their lower bounds rather quickly when p is increased. This behavior suggests the following design recommendation: for given \mathcal{F} with occupancy Ω and given L , choose $p = L\Omega + 1$ or $p = L\Omega + 2$. This results in sampling rate p/L slightly larger than Ω , but provides significant reduction in error sensitivities. Table 3.2 shows that η_∞ also approaches its lower bound but more slowly.

3.5 Comparisons

The goal of this section is to compare uniform and nonuniform sampling below the Nyquist rate for packable and nonpackable supports \mathcal{F} . Some of the comparisons are numerical examples.

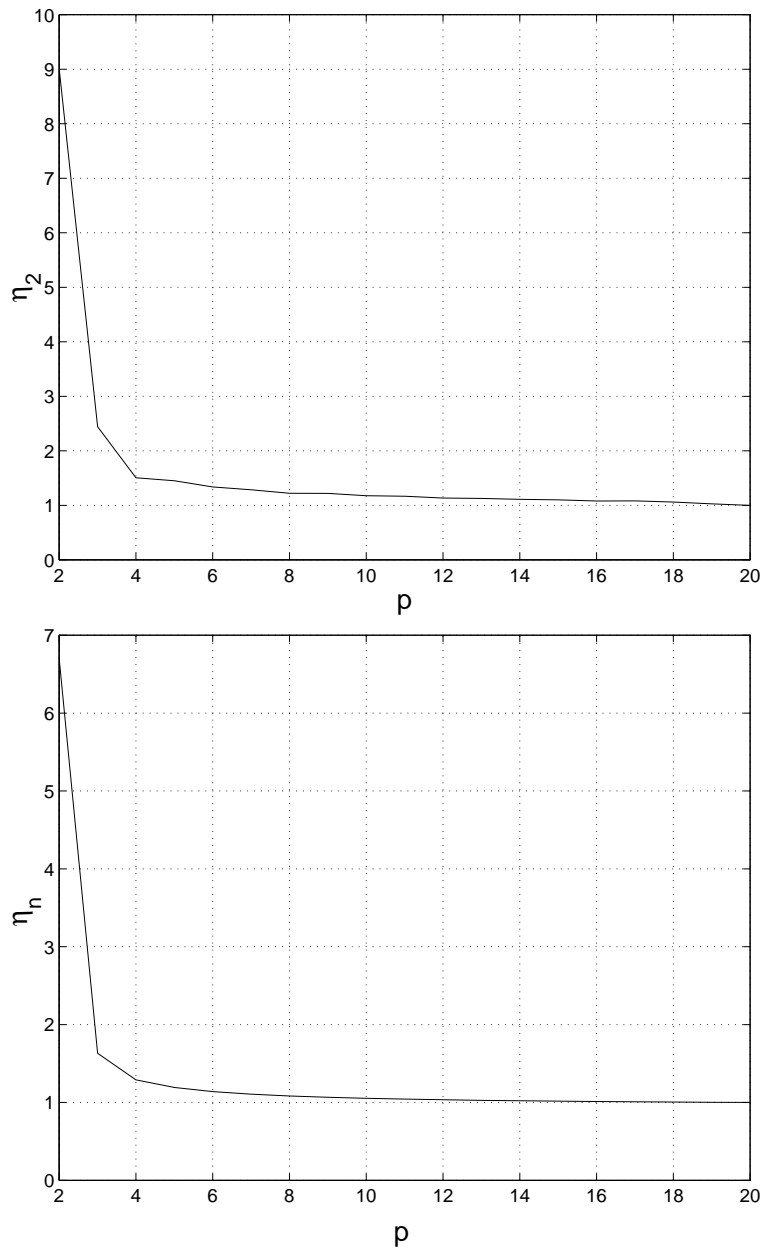


Figure 3.3 Normalized error gain constants η_2 and η_n shown as functions of the number of multiset samples p in each period.

We shall the following two questions: (a) For packable spectra, both uniform and nonuniform sampling at the same average rate is possible. How does the reconstruction error compare between the two options? (b) What is the penalty for nonpackability: given $\mathcal{F}^{(1)}$ packable and $\mathcal{F}^{(2)}$ nonpackable, such that $\mu(\mathcal{F}^{(1)}) = \mu(\mathcal{F}^{(2)})$, which are sampled at the same rate—uniformly and nonuniformly, respectively—how do the error bounds compare?

3.5.1 Uniform sampling versus nonuniform sampling for packable \mathcal{F}

Recall that a signal $x \in \mathcal{B}(\mathcal{F})$ is packable at rate $1/T' < \mu([\mathcal{F}])$ if $\mathcal{F} \cap (\mathcal{F} \oplus n/T') = \emptyset$ for all $n \neq 0$. Dodson and Silva [36] proved the following sampling theorem for packable signals.

Theorem 3.4. *Suppose \mathcal{F} is packable at rate $1/T'$ for some $T' > 0$, then $x \in \mathcal{B}(\mathcal{F})$ has the sampling representation*

$$x(t) = \sum_{m \in \mathbb{Z}} x(mT') \varphi(t - mT'; \mathcal{F}), \quad (3.33)$$

with the sum converging uniformly and absolutely for $t \in \mathbb{R}$.

The following theorem, due to Beaty and Higgins [26], is a bound on the peak value of the aliasing error for signals with finite energy and packable \mathcal{F} .

Theorem 3.5. *Suppose that $x(t) \in L^2(\mathbb{R}) \cap C(\mathbb{R})$ with $X(f) \in L^1(\mathbb{R})$ is sampled at the rate $1/T'$ that satisfies $\mathcal{F} \cap ((n/T') \oplus \mathcal{F}) = \emptyset, \forall n \neq 0$. Then the aliasing error $e(t)$ satisfies*

$$|e(t)| \leq 2 \int_{\mathbb{R} \setminus \mathcal{F}} |X(f)| df. \quad (3.34)$$

Incidentally, this equation is identical to the bound for the aliasing error in classical Shannon sampling of lowpass signals. Although valid for all $x \in F$, Eq. (3.34) will be used only for the class signals $x \in \mathcal{B}([\mathcal{F}])$ in order to compare with the bound in Eq. (3.8) which applies to signals in $\mathcal{B}([\mathcal{F}])$. It turns out that uniform patterns are indeed the best patterns suited for packable spectra because the aliasing error bounds in Eqs. (3.8) and (3.34) have identical forms, with the only difference being the premultiplying constants: the constant is 2 in Eq. (3.34), but $\max_m \|\mathbf{S}_m\|_1$ in Eq. (3.8). Since the lower bound in Eq. (3.26) implies that $\psi_\infty = \max_m \|\mathbf{S}_m\|_1 \geq 2$ for $p = \max q_m$, we see that for packable signals uniform sampling is most appropriate. Theorem 3.2 verifies this claim for the other two performance criteria because the constants ψ_2 and ψ_n attain their respective lower bounds for uniform sampling. In summary, for packable signals, uniform sampling is the best.

3.5.2 Penalty for nonpackability

What is the penalty in error sensitivity for Nonpackability? Unfortunately the answer to this question is not easy to deduce analytically. From various numerical computations, it seems that there is a price to pay for nonpackability of \mathcal{F} . We provide an example here to support the conjecture.

Example 3.2. Consider spectral supports $\mathcal{F}^{(1)}$, $\mathcal{F}^{(2)}$ and $\mathcal{F}^{(3)}$:

$$\begin{aligned}\mathcal{F}^{(1)} &= [0, 7), \\ \mathcal{F}^{(2)} &= [0, 3) \cup [5, 6) \cup [12, 13) \cup [14, 16), \\ \mathcal{F}^{(3)} &= [0, 3) \cup [6, 8) \cup [13, 16).\end{aligned}$$

For $L = 16$ and base sampling rate $1/T = 16$, all their subcell decompositions contain only one subcell, i.e., $M = 1$. The corresponding index sets are $\mathcal{K}_1^{(1)} = \{0 \rightarrow 7\}$, $\mathcal{K}_1^{(2)} = \{0 \rightarrow 2, 5, 11, 12, 14, 15\}$, and $\mathcal{K}_1^{(3)} = \{0 \rightarrow 2, 6, 7, 13 \rightarrow 15\}$. The spectral supports have the same measure, and the \mathcal{K} -sets have $q = 8$ elements each. While $\mathcal{K}^{(1)}$ and $\mathcal{K}^{(2)}$ are packable, $\mathcal{K}^{(3)}$ is not. Upon minimizing the quantity $\psi_\omega(\mathcal{C}, \mathcal{K}^{(i)})$ (using a forward selection greedy algorithm) for $i = 1, 2, 3$, and $\omega = n, 2, \infty$, we obtain the following optimal sampling patterns $\mathcal{C}_{\star\omega}^{(i)}$ of size $p = 8$ (corresponding to half the Nyquist rate) and objective functions $\psi_{\star\omega}^{(i)} \stackrel{\text{def}}{=} \psi_{\star\omega}(\mathcal{C}_{\star\omega}^{(i)}, \{\mathcal{K}_m^{(i)}\})$:

- For $i = 1, 2$, we obtain $\mathcal{C}_{\star n}^{(i)} = \mathcal{C}_{\star 2}^{(i)} = \mathcal{C}_{\star\infty}^{(i)} = \{1, 3, 5, 7, 9, 11, 13, 15\}$ with the corresponding objective functions being $\psi_{\star n}^{(i)} = 1.0$, $\psi_{\star 2}^{(i)} = 1.4142$, and $\psi_{\star\infty}^{(i)} = 2.0$. Note that these values agree with the results of Theorem 3.2.
- For $i = 3$, we obtain $\mathcal{C}_{\star n}^{(3)} = \mathcal{C}_{\star 2}^{(3)} = \{2, 4, 5, 6, 9, 12, 14, 15\}$, and $\mathcal{C}_{\star\infty}^{(3)} = \{1, 4, 5, 6, 9, 12, 13, 14\}$. The objective functions take the values $\psi_{\star n}^{(3)} = 1.9291$, $\psi_{\star 2}^{(3)} = 3.3598$, and $\psi_{\star\infty}^{(3)} = 4.8284$ at optimality.

Hence, the price to pay to sample a signal with a nonpackable spectrum at the Landau rate manifests itself in the output noise and aliasing error bounds: they are larger for nonpackable spectra.

Remark. Example 3.2 also illustrates the point made in the last subsection that uniform sampling is generally better suited for packable signals than nonuniform patterns. The fact that the sampling patterns for the packable spectra, $(\mathcal{C}_{\star\omega}^{(1)}$ and $\mathcal{C}_{\star\omega}^{(2)})$ turn out to be uniform clearly supports the claim.

3.6 Summary

We presented solutions to the problems of optimal sub-Nyquist sampling and reconstruction. We showed how to determine optimal matrices to obtain the best performance in terms of the aliasing error bounds or the noise sensitivity (the measures of performance) that were derived in Chapter 2. We provided explicit solutions for most of these problems.

The error bounds reveal a dependence on the sampling pattern \mathcal{C} . We examined the problem of designing sampling patterns that optimize the performance measures. We used an exhaustive search algorithm in one example and a forward selection greedy algorithm in another to pick optimal sampling patterns for a few design examples. An exhaustive search over all sampling patterns is computationally very expensive for even moderately large L , while a greedy search is not guaranteed to produce the best pattern. Nevertheless, the greedy algorithm did produce very good results. The problem of designing sampling patterns efficiently is still an open problem. We also showed how to choose the optimal base sampling frequency that minimizes the average sampling rate for a given sampling period L . This is an important issue because sampling at a base frequency equal to the Nyquist rate may be severely suboptimal for certain spectral supports.

We made comparisons to determine whether nonuniform sampling is appropriate for packable signals. Our findings are that (a) for packable spectral supports, uniform sampling pattern yields a better performance than a general nonuniform sampling pattern, and (b) for non-packable signals, where uniform sampling is not applicable, there is a penalty associated with nonuniform sampling. The error bounds are larger for this case relative to uniform sampling of a packable signal of the same occupancy. We find that the sensitivity penalties (error gain constants) for sub-Nyquist sampling of signals with nonpackable spectra can be controlled by optimal design and by backing off slightly from the minimum rate. The resulting low error sensitivities and the significant reduction in the sampling rate over the Nyquist rate of our numerical examples suggest that these techniques have considerable practical potential. Most of the results presented for 1-D signals should be extensible to two and higher dimensions with little difficulty. In contrast, determining the optimal base sampling lattice in higher dimensions would be a harder problem.

CHAPTER 4

MIMO SAMPLING: NECESSARY DENSITY CONDITIONS AND STABILITY ISSUES

4.1 Introduction

Multichannel deconvolution or multichannel separation of a convolutive mixture is an important problem arising in several applications and has attracted substantial interest recently. The problem, simply stated, deals with a MIMO channel whose outputs can be observed, and the primary goal is to invert or equalize the channel to recover the original input signals. In general, the channel inputs have overlapping spectra and share a common bandwidth. For example, the problem of separation multiple speakers in a room with multiple microphones is an acoustic source separation problem. The various acoustic sources can be modeled as multiband signals with overlapping spectra, and the microphone signals can be modeled as the outputs of a linear MIMO channel. Multiuser or multiaccess communications, multichannel image restoration, and geophysical data processing are examples of other applications where MIMO equalization arises [37–43].

We assume that the channel characteristics are either known or can be estimated accurately using known test input signals. In practice, digital processing is used to perform the channel inversion, whereas the channel inputs and outputs are continuous-time signals. Consequently, the channel outputs need to be sampled prior to processing. In other words, the objective is to reconstruct the channel inputs from the sampled output signals. Therefore, the MIMO channel inversion problem can be restated as one in sampling theory, and we call this sampling scheme *MIMO sampling*. We shall study this problem entirely from the perspective of sampling theory, although the problem could, equally well, be viewed as one of channel equalization.

4.1.1 Problem formulation

MIMO sampling can be described as follows. Let $x_r(t)$, $r = 1, \dots, R$, be a collection of multiband signals whose spectral supports are measurable sets $\mathcal{F}_r \subseteq \mathbb{R}$ of finite measure. These R signals are the inputs to a MIMO channel consisting of linear time-invariant filters (see Figure 4.1) producing P output signals $y_p(t)$, $p = 1, \dots, P$. In other words

$$y_p = \sum_{r=1}^R g_{pr} * x_r, \quad p = 1, \dots, P,$$

where $*$ denotes convolution, and $g_{pr} \in L^2(\mathbb{R})$ are the channel filter impulse responses. The outputs $y_p(t)$ are subsequently sampled on either a uniform or a nonuniform grid $\Lambda_p = \{\lambda_{np} : n \in \mathbb{Z}\}$. We then attempt to reconstruct the channel inputs from the output samples. This sampling scheme is very general and subsumes various other sampling schemes as special cases. For instance Papoulis's generalized sampling [12] is essentially a single-input, multiple-output (SIMO) sampling scheme, i.e., $R = 1$. A natural generalization of Papoulis's sampling expansion to vector valued inputs considered by Seidner and Feder [13] is also a special case where all input channels have identical lowpass spectra, i.e., $\mathcal{F}_r = [-B, B]$. See [44] for an interesting SIMO sampling scheme applicable to general signal spaces including wavelet and spline spaces. However, we restrict our attention to multiband signal spaces alone.

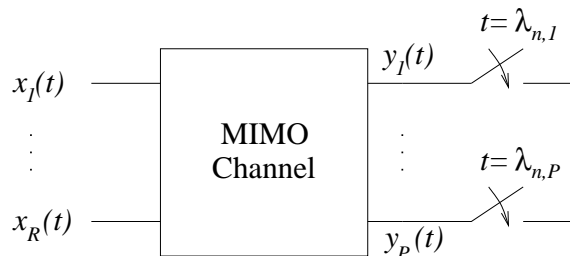


Figure 4.1 MIMO sampling.

Landau [6, 7] proved the following fundamental result for sampling and interpolation of multiband signals. Let $X(f)$ denote the Fourier transform of a signal $x(t)$, and

$$\mathcal{B}(\mathcal{F}) = \{x \in L^2(\mathbb{R}^d) \cap C(\mathbb{R}^d) : X(f) = 0, \forall f \notin \mathcal{F}\},$$

the class of continuous $L^2(\mathbb{R}^d)$ signals bandlimited to a measurable $\mathcal{F} \subseteq \mathbb{R}^d$. Suppose that a function $x \in \mathcal{B}(\mathcal{F})$ with $\mathcal{F} \subseteq \mathbb{R}^d$ is sampled at a discrete set of points $\Lambda = \{\lambda_n : n \in \mathbb{Z}\} \subseteq \mathbb{R}^d$. Then, for stable reconstruction of $x(t)$ from its samples $x(\lambda_n)$, it is necessary that the density of Λ be no less than the measure of \mathcal{F} , i.e., Λ must be sufficiently dense in order to

stably reconstruct the input. A dual problem is that of interpolation where we seek necessary conditions on Λ that guarantee that

$$\exists x \in \mathcal{B}(\mathcal{F}) \quad \text{s.t.} \quad x(\lambda_n) = c_n \quad (4.1)$$

whenever $\{c_n\} \in l^2$. Equation (4.1) is called the *interpolation condition*, and a necessary condition for this problem is that the density of Λ be no more than the measure of \mathcal{F} . Roughly speaking, the samples of $x(t)$ on the set Λ can take arbitrary values only if Λ is sufficiently sparse. Alternatively, the density of Λ can be interpreted as a lower bound on the *size* of the class of multiband signals with spectral support \mathcal{F} , in which a solution to the interpolation problem is guaranteed to exist, where “size” refers to the Lebesgue measure of the spectral support \mathcal{F} .

Gröchenig and Razafinjatovo [45] recently provided a simpler proof of Landau’s result. Their technique also allowed them to prove necessary density conditions for some derivative sampling schemes. However, all their results, unlike Landau’s, are applicable only when the boundary of the set \mathcal{F} has zero measure. The purpose of this chapter is to extend the idea of [45] to prove more general results for MIMO sampling while removing the restriction on the boundaries of the spectral supports. We consider only single variate functions in our analysis ($d = 1$), and the results easily extend to multivariate functions. The questions that we address are the following: (a) what are the necessary density conditions on the sampling densities of $\{\Lambda_p\}$ for stable reconstruction of the MIMO inputs $x_r \in \mathcal{B}(\mathcal{F}_r)$ from the MIMO output samples $\{y_p(\lambda_{np})\}$? and (b) what are the necessary conditions on the sampling densities of $\{\Lambda_p\}$ such that

$$\exists x_r \in \mathcal{B}(\mathcal{F}_r) \quad \text{s.t.} \quad y_p(\lambda_{np}) = c_{np} \quad (4.2)$$

for any sequence $\{c_{np} : n \in \mathbb{Z}, p = 1, \dots, P\} \in l^2$? Problem (b) is analogous to Landau’s interpolation problem for classical single input sampling, and Eq. (4.2) is the analogue of the interpolation condition in Eq. (4.1). However, we call Eq. (4.2) the *consistency condition*¹ rather than the *interpolation condition*. Roughly speaking, this condition implies that the channel outputs on the sets Λ_p can take arbitrary values, and this requires that Λ_p be sufficiently sparse. Equivalently, these conditions can be interpreted as minimum size requirements on the sets \mathcal{F}_r .

Note that although the sampling theorems for special cases considered in [12, 13] provide sufficient densities for uniform or periodic sampling, these are not shown to be necessary for arbitrary, nonuniform sampling of the channel outputs. In Section 4.2, we introduce some

¹Equation (4.2) does not describe an interpolation problem because the multichannel samples are not samples of the input signals themselves.

notation and review some mathematical background. In Section 4.3, we establish necessary conditions on $\{\Lambda_p\}$ for stable MIMO sampling and consistent MIMO reconstruction. For stable reconstruction, we prove that the sum of densities of Λ_p is lower bounded by the sum of the measures \mathcal{F}_r . Similarly, for the consistency problem, the sum of densities of Λ_p is upper bounded by the sum of the measures of \mathcal{F}_r . Apart from these natural generalizations of Landau's results, we also derive necessary conditions on the joint density for each subcollection of sampling sets, as well as conditions on the channel transfer function. These bounds provide an outer bound on the region of achievable densities. We provide examples to illustrate the results.

4.2 Preliminaries

The class of continuous $L^2(\mathbb{R})$ signals bandlimited to a measurable $\mathcal{F} \subseteq \mathbb{R}$ is denoted by

$$\mathcal{B}(\mathcal{F}) = \{x \in L^2(\mathbb{R}) \cap C(\mathbb{R}) : X(f) = 0, \forall f \notin \mathcal{F}\}, \quad (4.3)$$

where $X(f)$ is the Fourier transform of a signal $x(t)$:

$$X(f) = \int_{\mathbb{R}} x(t)e^{-j2\pi ft} dt.$$

The space $\mathcal{B}(\mathcal{F})$ is a separable Hilbert space. Let $\mu(\cdot)$ denote the Lebesgue measure, and $\chi(\cdot)$, the indicator function. For instance, $\chi(f \in \mathcal{F})$ takes the value 1 on the set \mathcal{F} , and 0 elsewhere. Let $\phi_{\mathcal{F}}(t)$ denote the inverse Fourier transform of $\chi(f \in \mathcal{F})$:

$$\phi_{\mathcal{F}}(t) = \int_{\mathcal{F}} e^{j2\pi ft} df.$$

Denote the time-shift operator by Θ_{τ} , i.e., $\Theta_{\tau}f(t) = f(t - \tau)$. Let \emptyset denote the empty set, and \mathcal{S}^c , the complement of a set \mathcal{S} in the appropriate universal set.

We now introduce some notation pertaining to matrices. We denote the class of complex-valued matrices of size $M \times N$ by $\mathbb{C}^{M \times N}$. Let $\mathbf{e}_r \in \mathbb{C}^{R \times 1}$ denote the r th standard basis vectors, i.e., \mathbf{e}_r has a 1 at the r th position, and zeros elsewhere. For a given matrix \mathbf{A} , let \mathbf{A}^H denote its conjugate-transpose, $\mathbf{A}_{\mathcal{R}, \mathcal{C}}$, its submatrix corresponding to rows indexed by the set \mathcal{R} and columns by the set \mathcal{C} . Also let $\mathbf{A}_{\bullet, \mathcal{C}}$ denote the submatrix formed by keeping all rows of \mathbf{A} , but only columns indexed by \mathcal{C} , and let $\mathbf{A}_{\mathcal{R}, \bullet}$ denote the submatrix formed by retaining rows indexed by \mathcal{R} and all columns. We use a similar notation for vectors. Hence, $\mathbf{X}_{\mathcal{R}}$ is the subvector of \mathbf{X} corresponding to rows indexed by \mathcal{R} . We always apply the subscripts before superscripts. So $\mathbf{A}_{\mathcal{R}, \mathcal{C}}^H$ is the conjugate-transpose of $\mathbf{A}_{\mathcal{R}, \mathcal{C}}$. When dealing with singleton index sets: $\mathcal{R} = \{r\}$ or $\mathcal{C} = \{c\}$, we omit the curly braces for readability. Therefore, $\mathbf{A}_{r, \bullet}$ and $\mathbf{A}_{\bullet, c}$ are the r th row and

the c th column of \mathbf{A} , respectively. Let $\lambda_{\max}(\mathbf{A})$ and $\lambda_{\min}(\mathbf{A})$ denote the largest and smallest eigenvalues of \mathbf{A} . Let $\sigma_{\max}(\mathbf{A})$ denote the largest singular value of matrix \mathbf{A} , and $\sigma_{\min}(\mathbf{A})$, the smallest *nonzero* singular value of a \mathbf{A} if $\mathbf{A} \neq \mathbf{0}$. If $\mathbf{A} = \mathbf{0}$, we take $\sigma_{\min}(\mathbf{A}) = \infty$. The following proposition, which is proved in Appendix A, is used later to characterize the region of achievable densities.

Proposition 4.1. *Let $\mathbf{G} \in \mathbb{C}^{R \times \rho}$, and let \mathcal{A} and \mathcal{B} be subsets of $\{1, \dots, R\}$. Then*

$$\text{rank}(\mathbf{G}_{\mathcal{A}, \bullet}) + \text{rank}(\mathbf{G}_{\mathcal{B}, \bullet}) \geq \text{rank}(\mathbf{G}_{\mathcal{A} \cup \mathcal{B}, \bullet}) + \text{rank}(\mathbf{G}_{\mathcal{A} \cap \mathcal{B}, \bullet}). \quad (4.4)$$

4.2.1 Stable sampling and consistency

The following material on frames is standard (c.f. [2, 46]). Let \mathcal{H} is a separable Hilbert space equipped with an inner product $\langle \cdot, \cdot \rangle$. A sequence $\{\psi_n\} \subseteq \mathcal{H}$ is called a *frame* if there exist constants $A, B > 0$ such that

$$A\|x\|^2 \leq \sum_n |\langle \psi_n, x \rangle|^2 \leq B\|x\|^2, \quad (4.5)$$

for all $x \in \mathcal{H}$. The constants A and B are called the lower and upper *frame bounds*. If $A = B$, then the frame is a *tight frame*. The frame operator S , defined as

$$Sx = \sum_n \langle x, \psi_n \rangle \psi_n, \quad \forall x \in \mathcal{H},$$

is a bounded linear operator satisfying $AI \leq S \leq BI$, where I is the identity operator. Let $\tilde{\psi}_n = S^{-1}\psi_n$. Then $\{\tilde{\psi}_n\}$ is also a frame (the *dual frame*) for \mathcal{H} with frame bounds B^{-1} and A^{-1} . Then any $x \in \mathcal{H}$ can be expanded as

$$x = \sum_n \langle x, \tilde{\psi}_n \rangle \psi_n = \sum_n \langle x, \psi_n \rangle \tilde{\psi}_n. \quad (4.6)$$

If $\{\psi_n\}$ is a frame, then for any sequence $\{c_n\} \in \ell^2$, we have

$$\left\| \sum_n c_n \psi_n \right\|^2 \leq B \sum_n |c_n|^2. \quad (4.7)$$

A sequence $\{\psi_n\} \subseteq \mathcal{H}$ is called a *Riesz basis* if it is fully equivalent to an orthonormal basis for \mathcal{H} , i.e., if there exists a bounded invertible operator T and an orthonormal basis $\{e_n\}$ such that $\psi_n = Te_n$. A Riesz basis is a frame, and hence Eqs. (4.6) and (4.7) hold. In fact, for a Riesz basis, we can replace Eq. (4.7) by the following stronger condition:

$$A \sum_n |c_n|^2 \leq \left\| \sum_n c_n \psi_n \right\|^2 \leq B \sum_n |c_n|^2. \quad (4.8)$$

Conversely, if $\{\psi_n\}$ is a complete sequence in \mathcal{H} , then it is a Riesz basis for \mathcal{H} whenever Eq. (4.8) holds for finite sequences [46]. The dual frame $\{\tilde{\psi}_n\}$ of a Riesz basis $\{\psi_n\}$ is called the *biorthogonal basis* of $\{\psi_n\}$, and it is also a Riesz basis for \mathcal{H} .

A sequence $\{\psi_n\} \subseteq \mathcal{H}$ is called a *Riesz-Fischer* sequence if the *moment problem*

$$\langle x, \psi_n \rangle = c_n \quad (4.9)$$

has a solution $x \in \mathcal{H}$ whenever $\{c_n\} \in \ell^2$. If $\{\psi_n\}$ is a Riesz-Fischer sequence, then there exists a solution x to Eq. (4.9) such that

$$\|x\|^2 \leq \frac{1}{a} \|c\|^2$$

for some $a > 0$ called the bound of the Riesz-Fischer sequence. A necessary and sufficient condition for $\{\psi_n\}$ to be a Riesz-Fischer sequence with bound a is that

$$\left\| \sum_n c_n \psi_n \right\|^2 \geq a \sum_n |c_n|^2 \quad (4.10)$$

for every finite sequence $\{c_n\}$. Finally, note that the moment problem in Eq. (4.9) has a unique solution if $\{\psi_n\}$ is a *complete* Riesz-Fischer sequence in \mathcal{H} . Every Riesz basis is a Riesz-Fischer sequence, but the converse is not true. However, if a Riesz-Fischer sequence is also a frame, then it is a Riesz basis. The notions of frames and Riesz-Fischer sequences are used in much of our analysis in Section 4.3.

In the context of classical multiband sampling, the class of input signals is the separable Hilbert space $\mathcal{H} = \mathcal{B}(\mathcal{F})$ having the following inner product:

$$\langle x, y \rangle = \int_{\mathbb{R}} x(t) \overline{y(t)} dt, \quad \forall x, y \in \mathcal{B}(\mathcal{F}).$$

Obviously, the norm on \mathcal{H} is defined as $\|x\| = \sqrt{\langle x, x \rangle}$.

A discrete set $\Lambda = \{\lambda_n : n \in \mathbb{Z}\}$ is called a *stable set of sampling* for $\mathcal{B}(\mathcal{F})$ if there exist $A, B > 0$ such that

$$A\|x\|^2 \leq \sum_{n \in \mathbb{Z}} |x(\lambda_n)|^2 \leq B\|x\|^2, \quad \forall x \in \mathcal{B}(\mathcal{F}). \quad (4.11)$$

First notice that $x(\lambda_n) = \langle x, \Theta_{\lambda_n} \phi_{\mathcal{F}} \rangle$. Using this fact and Eq. (4.11), we see that $\{\Theta_{\lambda_n} \phi_{\mathcal{F}} : n \in \mathbb{Z}\}$ is a frame for $\mathcal{B}(\mathcal{F})$ with frame bounds A and B . Denoting its dual frame by $\{\tilde{\phi}_n\}$ and using Eq. (4.6), we obtain the following interpolation equation to reconstruct x :

$$x = \sum_{n \in \mathbb{Z}} \langle x, \Theta_{\lambda_n} \phi_{\mathcal{F}} \rangle \tilde{\phi}_n = \sum_{n \in \mathbb{Z}} x(\lambda_n) \tilde{\phi}_n. \quad (4.12)$$

The following argument shows that Eq. (4.12) is a stable reconstruction formula. Suppose that a perturbation $\{\delta z_n\} \in l^2$ is added to $z_n = x(\lambda_n)$. Then, owing to linearity of Eq. (4.12), the resulting perturbation δx in the reconstruction is given by

$$\delta x = \sum_{n \in \mathbb{Z}} \delta z_n \tilde{\phi}_n.$$

Using Eq. (4.7) and noting that the upper frame bound for the dual frame is $1/A$, it follows that

$$\|\delta x\|^2 = \left\| \sum_n b_n \tilde{\phi}_n \right\|^2 \leq \frac{1}{A} \sum_n |b_n|^2. \quad (4.13)$$

Finally, from Eqs. (4.11) and (4.13) we conclude that

$$\frac{\|\delta x\|}{\|x\|} \leq \sqrt{\frac{B}{A}} \frac{\|\delta z\|}{\|z\|}.$$

The ratio $K = \sqrt{B/A} \geq 1$ is called the *condition number* of the sampling scheme, and K^2 is a bound on the amplification of the normalized perturbation energy. Similarly, it can be shown that a perturbation of δx in $x \in \mathcal{H}$ produces a perturbation of $\delta z \in l^2$ in $z_n = x(\lambda_n)$ such that

$$\frac{\|\delta z\|}{\|z\|} \leq \sqrt{\frac{B}{A}} \frac{\|\delta x\|}{\|x\|}.$$

Thus, the stability condition in Eq. (4.11) guarantees that the errors in the sampled signal or its samples cannot produce arbitrarily large errors in the reconstructed signal.

The set Λ is called a *set of interpolation* if there exists $x \in \mathcal{B}(\mathcal{F})$ such that $x(\lambda_n) = c_n$ whenever $\{c_n\} \in l^2$. This condition is clearly equivalent to $\{\Theta_{\lambda_n} \phi_{\mathcal{F}} : n \in \mathbb{Z}\}$ being a Riesz-Fischer sequence in $\mathcal{B}(\mathcal{F})$. Finally, if Λ is a set of both sampling and interpolation, then $\{\Theta_{\lambda_n} \phi_{\mathcal{F}} : n \in \mathbb{Z}\}$ is a Riesz basis for $\mathcal{B}(\mathcal{F})$. The theory of frames thus provides a convenient tool to study sampling [47].

We shall now generalize the above notions of stable sampling and interpolation for the MIMO problem. Recall that the channel input and output signals are related to each other as

$$\mathbf{y}(t) = \mathbf{g} * \mathbf{x}(t) = \int_{\mathbb{R}} \mathbf{g}(t - \tau) \mathbf{x}(\tau) d\tau,$$

where \mathbf{x} is the input vector whose components are multiband signals $x_r \in \mathcal{B}(\mathcal{F}_r)$, and \mathbf{y} is the channel output in vector form. The class of input signals is the separable Hilbert space

$$\mathcal{H} = \mathcal{B}(\mathcal{F}_1) \times \cdots \times \mathcal{B}(\mathcal{F}_R) \quad (4.14)$$

equipped with the inner product

$$\langle \mathbf{x}, \mathbf{z} \rangle = \int_{\mathbb{R}} \mathbf{z}^H(t) \mathbf{x}(t) dt = \sum_{r=1}^R \int_{\mathbb{R}} \overline{z_r(t)} x_r(t) dt, \quad \forall \mathbf{x}, \mathbf{z} \in \mathcal{H}. \quad (4.15)$$

The norm on \mathcal{H} is clearly defined as $\|\mathbf{x}\| = \sqrt{\langle \mathbf{x}, \mathbf{x} \rangle}$. In the rest of this chapter let \mathcal{R} and \mathcal{P} denote index sets for the components of the channel inputs and outputs, i.e.,

$$\mathcal{R} = \{1, \dots, R\} \quad \text{and} \quad \mathcal{P} = \{1, \dots, P\}.$$

Suppose that

$$\mathcal{C}_f = \{r : f \in \mathcal{F}_r\}, \tag{4.16}$$

then it is clear that $\mathbf{X}_{\mathcal{C}_f}(f)$ captures all the nonzero elements of $\mathbf{X}(f)$. Hence, the channel output in the frequency domain can be expressed as

$$\mathbf{Y}(f) = \mathbf{G}(f)\mathbf{X}(f) = \mathbf{G}_{\bullet, \mathcal{C}_f}(f)\mathbf{X}_{\mathcal{C}_f}(f), \tag{4.17}$$

where $\mathbf{G}(f)$, the Fourier transform of $\mathbf{g}(t)$, is called the *channel transfer function matrix*.

Definition 4.1. A collection of discrete sets $\Lambda_p = \{\lambda_{np} : n \in \mathbb{Z}\}$, $p \in \mathcal{P}$ is called a *stable collection of MIMO sampling* with respect to $\mathbf{G}(f)$ for the space \mathcal{H} if there exist $A, B > 0$ such that

$$A\|\mathbf{x}\|^2 \leq \sum_{p=1}^P \sum_{n \in \mathbb{Z}} |y_p(\lambda_{np})|^2 \leq B\|\mathbf{x}\|^2 \tag{4.18}$$

for every $\mathbf{x} \in \mathcal{H}$, where $\mathbf{Y}(f) = \mathbf{G}(f)\mathbf{X}(f)$.

It is clear that we can write $y_p(\lambda_{np}) = \langle \mathbf{x}, \Theta_{\lambda_{np}} \boldsymbol{\psi}_p \rangle$ for appropriate $\boldsymbol{\psi}_p \in \mathcal{H}$. In fact a simple calculation reveals that

$$\boldsymbol{\Psi}_p(f) = \sum_{r=1}^R \overline{G_{pr}(f)} \chi(f \in \mathcal{F}_r) \mathbf{e}_r, \tag{4.19}$$

where \mathbf{e}_r is the r th standard basis vector.

Now, Eq. (4.18) is equivalent to the condition that $\{\Theta_{\lambda_{np}} \boldsymbol{\psi}_p : n \in \mathbb{Z}, p \in \mathcal{P}\}$ is a frame for \mathcal{H} . This observation, as in the case of classical sampling, implies that we can perform the reconstruction of the channel inputs from the output samples using the dual frame as the set of interpolating functions. Also, the stability condition in Eq. (4.18) guarantees that the errors in the sampled signal or its samples do not produce arbitrarily large errors in the reconstructed signals. The *condition number* for the MIMO sampling scheme is $K = \sqrt{B/A} \geq 1$.

Definition 4.2. A collection of discrete sets $\Lambda_p = \{\lambda_{np} : n \in \mathbb{Z}\}$, $p \in \mathcal{P}$ is called a *collection of consistent reconstruction* with respect to $\mathbf{G}(f)$ for the space \mathcal{H} if there exists a solution $\mathbf{x} \in \mathcal{H}$ to the problem $y_p(\lambda_{np}) = c_{np}$ for every $\{c_{np}\} \in l^2$, where $\mathbf{Y}(f) = \mathbf{G}(f)\mathbf{X}(f)$.

Equivalently, $\{\Lambda_p : p \in \mathcal{P}\}$ is a collection of consistent reconstruction with respect to $\mathbf{G}(f)$ for the space \mathcal{H} if $\{\Theta_{\lambda_{np}} \psi_p : n \in \mathbb{Z}, p \in \mathcal{P}\}$ is a Riesz-Fischer sequence in \mathcal{H} . For any finite sequence $\{c_{np}\}$, observe that

$$\begin{aligned} \left\| \sum_{n,p} c_{np} \Theta_{\lambda_{np}} \psi_p \right\|^2 &= \max_{\mathbf{x} \in \mathcal{B}_{\mathcal{H}}} \left| \sum_{n,p} c_{np} \langle \mathbf{x}, \Theta_{\lambda_{np}} \psi_p \rangle \right|^2 \\ &= \max_{\mathbf{x} \in \mathcal{B}_{\mathcal{H}}} \left| \sum_{n,p} c_{np} y_p(\lambda_{np}) \right|^2, \end{aligned}$$

where $B_{\mathcal{H}} = \{\mathbf{x} \in \mathcal{H} : \|\mathbf{x}\| \leq 1\}$ is the unit ball in \mathcal{H} . In view of Eq. (4.10), it is clear that

$$\{\Theta_{\lambda_{np}} \psi_p : n \in \mathbb{Z}, p \in \mathcal{P}\}$$

is a Riesz-Fischer sequence in \mathcal{H} if and only if

$$\max_{\mathbf{x} \in \mathcal{B}_{\mathcal{H}}} \left| \sum_{n,p} c_{np} y_p(\lambda_{np}) \right|^2 \geq a \sum_{n,p} |c_{np}|^2 \quad (4.20)$$

for every finite sequence $\{c_{np}\}$. It turns out that the above characterization of consistent MIMO reconstruction is easier to use than Definition 4.2. Finally, we point out that if a collection of discrete sets $\Lambda_p = \{\lambda_{np} : n \in \mathbb{Z}\}$, $p \in \mathcal{P}$ is a collection of both stable sampling and consistent reconstruction, then $\{\Theta_{\lambda_{np}} \psi_p : n \in \mathbb{Z}, p \in \mathcal{P}\}$ is a Riesz basis for \mathcal{H} .

4.2.2 Notions of sampling density

A discrete subset $\Lambda = \{\lambda_n : n \in \mathbb{Z}\} \subseteq \mathbb{R}$ is called uniformly discrete with separation δ if

$$|\lambda_m - \lambda_n| \geq 2\delta, \quad \forall m \neq n.$$

Let the maximum and minimum number of sampling points of Λ found in any interval of length 2γ be denoted by

$$\nu_{\gamma}^+(\Lambda) = \sup_{\tau \in \mathbb{R}} \#(\Lambda \cap B_{\gamma}(\tau)) \quad \text{and} \quad \nu_{\gamma}^-(\Lambda) = \inf_{\tau \in \mathbb{R}} \#(\Lambda \cap B_{\gamma}(\tau)), \quad (4.21)$$

respectively, where $\#(\mathcal{S})$ denotes the cardinality of a set \mathcal{S} , and

$$B_{\gamma}(\tau) = \{\sigma \in \mathbb{R} : |\sigma - \tau| \leq \gamma\}$$

is a closed interval of length 2γ centered at t . For a discrete set Λ , the upper and lower densities are defined as

$$D^+(\Lambda) = \limsup_{\gamma \rightarrow \infty} \frac{\nu_{\gamma}^+(\Lambda)}{2\gamma} \quad \text{and} \quad D^-(\Lambda) = \liminf_{\gamma \rightarrow \infty} \frac{\nu_{\gamma}^-(\Lambda)}{2\gamma}, \quad (4.22)$$

respectively. See [47] for several other notions of density for nonuniform sampling. Although traditionally written as “lim inf” and “lim sup,” the limits in Eq. (4.22) can be replaced by simple limits [47]. If the lower and upper densities coincide, this density is called the *uniform density* and is denoted by $D(\Lambda)$. Note that this does not mean that the sampling points in Λ are uniformly spaced. Any large interval of size l contains approximately $lD(\Lambda)$ points of Λ . If Λ is uniformly discrete, then $D^+(\Lambda)$ is finite. However, the converse statement is not true, but the following is a slightly weaker result that generally suffices:

Proposition 4.2. *A discrete set Λ has $D^+(\Lambda) < \infty$ if and only if Λ can be expressed as a union K uniformly discrete sets $\{\Lambda_k : k = 0, \dots, K - 1\}$, such that $D^\pm(\Lambda_k) = D^\pm(\Lambda)/K$. The smallest such K is given by*

$$K_0(\Lambda) = \inf_{\delta > 0} \nu_\delta^+(\Lambda).$$

In addition, for any $\epsilon > 0$, we can choose K such that each Λ_k has a separation of $\delta > 0$ satisfying

$$D^+(\Lambda) \leq \frac{K}{2\delta} \leq D^+(\Lambda) + \epsilon.$$

Proposition 4.2 is proved in Appendix A.

When dealing with a collection of sampling sets, as in the MIMO setting, it is useful to define *joint densities* for the collection. These are generalizations of the densities defined earlier.

Definition 4.3. Given a finite collection of discrete sets Λ_p , $p = 1, \dots, P$, their *joint upper and lower densities* are defined as

$$D^+(\Lambda_1, \dots, \Lambda_P) = \limsup_{\gamma \rightarrow \infty} \frac{\nu_\gamma^+(\Lambda_1, \dots, \Lambda_P)}{2\gamma}, \quad (4.23)$$

$$D^-(\Lambda_1, \dots, \Lambda_P) = \liminf_{\gamma \rightarrow \infty} \frac{\nu_\gamma^-(\Lambda_1, \dots, \Lambda_P)}{2\gamma}, \quad (4.24)$$

respectively, where

$$\nu_\gamma^+(\Lambda_1, \dots, \Lambda_P) = \sup_{\tau \in \mathbb{R}} \sum_{p=1}^P \#(\Lambda_p \cap B_\gamma(\tau)),$$

$$\nu_\gamma^-(\Lambda_1, \dots, \Lambda_P) = \inf_{\tau \in \mathbb{R}} \sum_{p=1}^P \#(\Lambda_p \cap B_\gamma(\tau))$$

are the maximum and minimum number of sampling points of the collection $\{\Lambda_p : p = 1, \dots, P\}$ found in any interval of length 2γ .

If these densities coincide, then $\{\Lambda_1, \dots, \Lambda_P\}$ has uniform joint density of

$$D(\Lambda_1, \dots, \Lambda_P) = D^\pm(\Lambda_1, \dots, \Lambda_P).$$

If each Λ_p has uniform density, then so does the collection $\{\Lambda_1, \dots, \Lambda_P\}$. However, the converse is not true. From these definitions it is clear that

$$D^+(\Lambda_1, \dots, \Lambda_P) \leq \sum_{p=1}^P D^+(\Lambda_p),$$

$$D^-(\Lambda_1, \dots, \Lambda_P) \geq \sum_{p=1}^P D^-(\Lambda_p).$$

Moreover, if each Λ_p has uniform density, the collection $\{\Lambda_p\}$ also has uniform joint densities given by

$$D(\Lambda_1, \dots, \Lambda_P) = \sum_{p=1}^P D(\Lambda_p).$$

We use the above properties later without explicitly stating them. The following proposition is proved in Appendix A.

Proposition 4.3. *The lim sup in Eq. (4.23) and the lim inf in Eq. (4.24) can be replaced by simple limits. In fact,*

$$\nu_\gamma^+(\Lambda_1, \dots, \Lambda_P) \geq 2\gamma D^+(\Lambda_1, \dots, \Lambda_P), \quad (4.25)$$

$$\nu_\gamma^-(\Lambda_1, \dots, \Lambda_P) \leq 2\gamma D^-(\Lambda_1, \dots, \Lambda_P) \quad (4.26)$$

for all $\gamma > 0$.

4.3 Necessary Density Conditions

Our aim in this section is to prove necessary density conditions for MIMO sampling of multiband signals. These results are analogous to Landau's density result for nonuniform sampling of multiband signals [6, 7]. Gröchenig and Razafinjatoivo [45] provided a simpler proof of Landau's result, and their ideas were based on a method due to Ramanathan and Steger [48]. This idea allowed them to prove some results for derivative sampling. With some modifications, the results in [45] can also be extended to SIMO sampling and interpolation. However, these results apply only to signals in the class of multiband signals $\mathcal{B}(\mathcal{F})$ for which $\mu(\partial\mathcal{F}) = 0$, i.e., the boundary of \mathcal{F} has measure zero. Most sets of practical interest satisfy this condition, while several pathological sets such as nowhere dense sets are excluded. Unfortunately, the

condition also excludes some reasonable sets. For example, let $\mathcal{F} = [0, 1] \cap Q^c$, where Q is the set of rationals. Then $\partial\mathcal{F} = [0, 1]$, implying that $\mu(\partial\mathcal{F}) = 1$. But $\mathcal{B}(\mathcal{F}) = \mathcal{B}([0, 1])$ since \mathcal{F} differs from $[0, 1]$ by a set of measure zero. In other words their results do not apply to some elementary classes of signals under a simple disguise.

4.3.1 A comparison theorem

In this section we present the main technical result, which is a modification of a similar comparison theorem presented in [45]. We use the theorem to compute necessary density conditions for the stable MIMO sampling and consistent reconstruction. However, the theorem is very general, involving arbitrary signal spaces, and can potentially be used for proving necessary density conditions for sampling problems in wavelet or spline spaces.

Lemma 4.1. *Let $h \in \mathcal{B}([\nu_1, \nu_2])$. Then,*

$$h^\#(t) \stackrel{\text{def}}{=} \sup_{|\tau-t| \leq 1} |h(\tau)|,$$

satisfies $h^\# \in L^2(\mathbb{R})$ and $\|h^\#\|^2 \leq C\|h\|^2$ for some $C = C(\nu_2 - \nu_1) > 0$ that depends only on the difference $(\nu_2 - \nu_1)$. Moreover, if $\Lambda = \{\lambda_m : m \in \mathbb{Z}\} \subseteq \mathbb{R}$ is a discrete set with $D^+(\Lambda) < \infty$, then

$$\sum_{|\lambda_n - \sigma| \geq \Gamma} |h(\lambda_n)|^2 \leq C' \int_{|t-\sigma| \geq \Gamma-1} |h^\#(t)|^2 dt \quad (4.27)$$

for all $\sigma \in \mathbb{R}$, $\Gamma \geq 0$, and some $C' = C'(\Lambda) > 0$. In particular

$$\sum_{n \in \mathbb{Z}} |h(\lambda_n)|^2 \leq C' C \|h\|^2.$$

Proof. For every $\eta > 0$, let $S_\eta(f)$ be a Schwartz function such that $S_\eta(f) = 1$ for $f \in [0, \eta]$. Define $C(\eta) = \|s_\eta^\#\|_1^2$. Then $S(f) = S_{\nu_2 - \nu_1}(f - \nu_1)$ is also a Schwartz function such that $S(f) = 1$ on $[\nu_1, \nu_2]$. Since $h \in \mathcal{B}([\nu_1, \nu_2])$, we have $h = h * s$. Hence,

$$\begin{aligned} h^\#(t) &= \sup_{\tau \in B_1(t)} \left| \int_{\mathbb{R}} s(\tau - \sigma) h(\sigma) d\sigma \right| \\ &\leq \int_{\mathbb{R}} \sup_{\tau \in B_1(t)} |s(\tau - \sigma)| \cdot |h(\sigma)| d\sigma \\ &= \int_{\mathbb{R}} s^\#(t - \sigma) |h(\sigma)| d\sigma = s^\# * |h|. \end{aligned}$$

Clearly $s^\#(t) \in L^1(\mathbb{R})$ because $s(t)$ is a rapidly decaying function of t . Therefore,

$$\|h^\#\| \leq \|s^\# * |h|\| \leq \|s^\#\|_1 \cdot \|h\|,$$

holds for all $h \in \mathcal{B}(\mathcal{F})$. It is clear that $\|s^\#\|_1^2 = \|s_{\nu_2 - \nu_1}^\#\|_1^2 = C(\nu_2 - \nu_1)$. Thus $\|h^\#\|^2 \leq C(\nu_2 - \nu_1)\|h\|^2$. Suppose $D^+(\Lambda) < \infty$, then by Proposition 4.2 we can express Λ as a union of K uniformly discrete sets $\{\Lambda_k : k = 1, \dots, K\}$ each with separation $\delta > 0$. Without loss of generality, assume that $\delta < 1$. Let the elements of Λ_k be denoted by $\{\lambda_{nk} : n \in \mathbb{Z}\}$. Then, for any $\sigma \in \mathbb{R}$, we have

$$\begin{aligned} \sum_{|\lambda_n - \sigma| \geq \Gamma} |h(\lambda_n)|^2 &= \sum_{k=1}^K \sum_{|\lambda_{nk} - \sigma| \geq \Gamma} |h(\lambda_{nk})|^2 \\ &\leq \sum_{k=1}^K \sum_{|\lambda_{nk} - \sigma| \geq \Gamma} \frac{1}{2\delta} \int_{|t - \lambda_{nk}| \leq \delta} |h^\#(t)|^2 dt \end{aligned}$$

because $|h(\lambda_n)| \leq h^\#(t)$ for all t such that $|t - \lambda_{nk}| \leq \delta \leq 1$. Thus,

$$\begin{aligned} \sum_{|\lambda_n - \sigma| \geq \Gamma} |h(\lambda_n)|^2 &\leq \frac{1}{2\delta} \sum_{k=1}^K \int_{|t - \sigma| \geq \Gamma - \delta} |h^\#(t)|^2 dt \\ &\leq \frac{K}{2\delta} \int_{|t - \sigma| \geq \Gamma - 1} |h^\#(t)|^2 dt. \end{aligned}$$

This bound has the required form if we set $C' = K/(2\delta)$ that, evidently, depends only on Λ . \square

Lemma 4.1 says that the samples of a bandlimited signal on a sampling set of finite upper density cannot be arbitrarily large. As we shall see later, it is a simple but powerful result.

We now introduce a few quantities relevant to the main result that follows shortly. Define the following separable Hilbert spaces:

$$\begin{aligned} \mathcal{H}_\beta &= (\mathcal{B}([- \beta, \beta]))^R, \quad \beta > 0, \\ \mathcal{H}_\infty &= (L^2(\mathbb{R}))^R, \end{aligned}$$

and let the inner product on both spaces be defined as in Eq. (4.15). Note that \mathcal{H}_β is the space of vector functions whose R components are bandlimited to the frequencies $[-\beta, \beta]$. Let $P_S : \mathcal{H}_\infty \rightarrow \mathcal{S}$ denote the orthogonal projection operator onto a closed subspace $\mathcal{S} \subseteq \mathcal{H}_\infty$.

Definition 4.4. A subspace $\mathcal{S} \subseteq \mathcal{H}_\infty$ is called *shift-invariant* if $\Theta_\sigma \mathbf{x} \in \mathcal{S}$ for all $\sigma \in \mathbb{R}$ whenever $\mathbf{x} \in \mathcal{S}$.

Evidently \mathcal{H}_∞ and \mathcal{H}_β are shift-invariant spaces. We write $\mathbf{x} \perp \mathcal{S}$ whenever $\langle \mathbf{x}, \mathbf{z} \rangle = 0$ for all $\mathbf{z} \in \mathcal{H}_\beta$. The following properties of a closed shift-invariant subspace $\mathcal{S} \subseteq \mathcal{H}_\infty$ can be verified easily.

Proposition 4.4. *Suppose that $\mathbf{x} \in \mathcal{H}_\beta$, $\sigma \in \mathbb{R}$, and $\mathcal{S} \subseteq \mathcal{H}_\infty$ is a closed shift-invariant subspace. Then (a) $\mathbf{x} \perp \mathcal{S} \implies \Theta_\sigma \mathbf{x} \perp \mathcal{S}$, and (b) $P_{\mathcal{S}} \Theta_\sigma \mathbf{x} = \Theta_\sigma P_{\mathcal{S}} \mathbf{x}$, i.e., translation commutes with orthogonal projection onto \mathcal{S} .*

Proof. (a) Suppose that $\mathbf{x} \perp \mathcal{S}$. Then $\langle \Theta_\sigma \mathbf{x}, \mathbf{z} \rangle = \langle \mathbf{x}, \Theta_{-\sigma} \mathbf{z} \rangle = 0$ whenever $\mathbf{z} \in \mathcal{S}$ and $\sigma \in \mathbb{R}$ because $\Theta_{-\sigma} \mathbf{z} \in \mathcal{S}$. Hence, $\Theta_\sigma \mathbf{x} \perp \mathcal{S}$. To prove (b), note $P_{\mathcal{S}} \Theta_\sigma \mathbf{x} - \Theta_\sigma P_{\mathcal{S}} \mathbf{x} \in \mathcal{S}$. For arbitrary $\mathbf{z} \in \mathcal{S}$, we have

$$\begin{aligned} \langle P_{\mathcal{S}} \Theta_\sigma \mathbf{x} - \Theta_\sigma P_{\mathcal{S}} \mathbf{x}, \mathbf{z} \rangle &= \langle P_{\mathcal{S}} \Theta_\sigma \mathbf{x}, \mathbf{z} \rangle - \langle \Theta_\sigma P_{\mathcal{S}} \mathbf{x}, \mathbf{z} \rangle \\ &= \langle \Theta_\sigma \mathbf{x}, P_{\mathcal{S}} \mathbf{z} \rangle - \langle \mathbf{x}, P_{\mathcal{S}} \Theta_{-\sigma} \mathbf{z} \rangle \\ &= \langle \Theta_\sigma \mathbf{x}, \mathbf{z} \rangle - \langle \mathbf{x}, \Theta_{-\sigma} \mathbf{z} \rangle = 0, \end{aligned}$$

proving that $P_{\mathcal{S}} \Theta_\sigma \mathbf{x} = \Theta_\sigma P_{\mathcal{S}} \mathbf{x}$. □

Lemma 4.2. *Let $\mathcal{S} \subseteq \mathcal{H}_\infty$ be a closed subspace, and $\Sigma \subseteq \mathbb{R}$. Then,*

$$\limsup_{\beta \rightarrow \infty} \sup_{\sigma \in \Sigma} \|\Theta_\sigma \mathbf{x} - P_{\mathcal{S}} \Theta_\sigma P_{\mathcal{H}_\beta} \mathbf{x}\| \leq \sup_{\sigma \in \Sigma} \|\Theta_\sigma \mathbf{x} - P_{\mathcal{S}} \Theta_\sigma \mathbf{x}\|$$

for all $\mathbf{x} \in \mathcal{H}_\infty$.

Proof. For any $\mathbf{x} \in \mathcal{H}_\infty$ and $\epsilon > 0$, there exists $\beta_0 > 0$ such that

$$\|\mathbf{x} - P_{\mathcal{H}_\beta} \mathbf{x}\| = \int_{|f| \geq \beta} \|\mathbf{X}(f)\|^2 df \leq \epsilon, \quad \forall \beta \geq \beta_0 \quad (4.28)$$

because $\mathbf{X}(f)$ is square-integrable. Now, using the fact that $P_{\mathcal{S}}$ is a projection operator we obtain

$$\begin{aligned} \|\Theta_\sigma \mathbf{x} - P_{\mathcal{S}} \Theta_\sigma P_{\mathcal{H}_\beta} \mathbf{x}\| &\leq \|\Theta_\sigma \mathbf{x} - P_{\mathcal{S}} \Theta_\sigma \mathbf{x}\| + \|P_{\mathcal{S}} \Theta_\sigma \mathbf{x} - P_{\mathcal{S}} \Theta_\sigma P_{\mathcal{H}_\beta} \mathbf{x}\| \\ &\leq \|\Theta_\sigma \mathbf{x} - P_{\mathcal{S}} \Theta_\sigma \mathbf{x}\| + \|\Theta_\sigma \mathbf{x} - \Theta_\sigma P_{\mathcal{H}_\beta} \mathbf{x}\| \\ &= \|\Theta_\sigma \mathbf{x} - P_{\mathcal{S}} \Theta_\sigma \mathbf{x}\| + \|\mathbf{x} - P_{\mathcal{H}_\beta} \mathbf{x}\| \end{aligned}$$

for all $\sigma \in \Sigma$. In view of Eq. (4.28) and the above inequality, we conclude that

$$\limsup_{\beta \rightarrow \infty} \sup_{\sigma \in \Sigma} \|\Theta_\sigma \mathbf{x} - P_{\mathcal{S}} P_{\mathcal{H}_\beta} \Theta_\sigma \mathbf{x}\| \leq \sup_{\sigma \in \Sigma} \|\Theta_\sigma \mathbf{x} - P_{\mathcal{S}} \Theta_\sigma \mathbf{x}\| + \epsilon.$$

The result follows immediately because $\epsilon > 0$ is arbitrary. □

Theorem 4.1 (Comparison Theorem). *Let \mathcal{H}_S and \mathcal{H}_L be closed subspaces of \mathcal{H}_∞ , and let $\Sigma_1, \dots, \Sigma_Q$, and $\Lambda_1, \dots, \Lambda_P$ be discrete subsets of \mathbb{R} such that all $D^+(\Lambda_p) < \infty$. Suppose that $\mathbf{s}_1, \dots, \mathbf{s}_Q$ and $\mathbf{l}_1, \dots, \mathbf{l}_P$ are such that*

$$\{\Theta_\sigma \mathbf{s}_q : \sigma \in \Sigma_q, q = 1, \dots, Q\} \subseteq \mathcal{H}_S$$

is a Riesz-Fischer sequence in \mathcal{H}_S with bound $a > 0$, and that

$$\{\Theta_\lambda \mathbf{l}_p : \lambda \in \Lambda_p, p = 1, \dots, P\} \subseteq \mathcal{H}_L$$

is a frame for \mathcal{H}_L . Then

$$D^\pm(\Lambda_1, \dots, \Lambda_P) \geq D^\pm(\Sigma_1, \dots, \Sigma_Q) - \sum_{q=1}^Q \alpha_q D^+(\Sigma_q), \quad (4.29)$$

if all $D^+(\Sigma_q) < \infty$, where

$$\alpha_q = \frac{1}{\sqrt{a}} \sup_{\sigma \in \Sigma_q} \|\Theta_\sigma \mathbf{s}_q - P_{\mathcal{H}_L} \Theta_\sigma \mathbf{s}_q\|.$$

In particular, $D^+(\Sigma_q) < \infty$ is guaranteed whenever all $\alpha_q < 1$.

Let $\Sigma_q = \{\sigma_{nq} : n \in \mathbb{Z}\}$ and $\Lambda_p = \{\lambda_{np} : n \in \mathbb{Z}\}$ be enumerations of the discrete sampling sets Σ_q and Λ_p , and $\Sigma'_q \subseteq \Sigma_q$, a finite subset of Σ_q . Define

$$\mathcal{H}'_S = \text{span}\{\Theta_\sigma \mathbf{s}_q : \sigma \in \Sigma'_q, q \in \mathcal{Q}\}, \quad (4.30)$$

where $\mathcal{Q} = \{1, \dots, Q\}$. Then \mathcal{H}'_S is a closed finite dimensional subspace of \mathcal{H}_S . Since

$$\{\Theta_\sigma \mathbf{s}_q : \sigma \in \Sigma_q, q \in \mathcal{Q}\}$$

is a Riesz-Fischer sequence with bound a , we have from Eq. (4.10) that

$$\left\| \sum_{q=1}^Q \sum_{n \in \mathcal{N}_q} c_{nq} \Theta_{\sigma_{nq}} \mathbf{s}_q \right\|^2 \geq a \sum_{q=1}^Q \sum_{n \in \mathcal{N}_q} |c_{nq}|^2,$$

where

$$\mathcal{N}_q = \{n : \sigma_{nq} \in \Sigma'_q\}$$

is a finite set. In other words, $\{\Theta_\sigma \mathbf{s}_q : \sigma \in \Sigma'_q, q \in \mathcal{Q}\}$ is a (Riesz) basis for \mathcal{H}'_S , with lower frame bound a . Then its biorthogonal basis, denoted by $\{\tilde{\mathbf{s}}_{nq} : n \in \mathcal{N}_q, q \in \mathcal{Q}\}$, has an upper frame bound of $1/a$, and hence Eq. (4.8) implies that

$$\|\tilde{\mathbf{s}}_{nq}\|^2 \leq 1/a. \quad (4.31)$$

By hypothesis, $\{\Theta_\lambda \mathbf{l}_p : \lambda \in \Lambda_p, p \in \mathcal{P}\}$ is a frame for \mathcal{H}_L . Denoting its dual frame by $\{\tilde{\mathbf{l}}_{np} : n \in \mathbb{Z}, p \in \mathcal{P}\} \subseteq \mathcal{H}_L$ and using Eq. (4.7), we obtain

$$\left\| \sum_{n,p} c_{np} \tilde{\mathbf{l}}_{np} \right\|^2 \leq B \sum_{n,p} |c_{np}|^2 \quad (4.32)$$

for all $\{c_{np}\} \in l^2$ and some constant $B > 0$. Now, define the following finite-dimensional subspaces:

$$\begin{aligned}\mathcal{W}_\gamma^S(\tau) &= \text{span}\{\Theta_\sigma \mathbf{s}_q : \sigma \in B_\gamma(\tau) \cap \Sigma'_q, q \in \mathcal{Q}\} \subseteq \mathcal{H}'_S, \\ \mathcal{W}_\gamma^L(\tau) &= \text{span}\{\tilde{\mathbf{l}}_{np} : n \in \mathcal{I}_p(\gamma, \tau), p \in \mathcal{P}\} \subseteq \mathcal{H}_L,\end{aligned}$$

where

$$\mathcal{I}_p(\gamma, \sigma) = \{n : \lambda_{np} \in B_\gamma(\sigma)\}, \quad \gamma > 0, \tau \in \mathbb{R}. \quad (4.33)$$

Also let $P_\gamma^S(\tau) : \mathcal{H}_\infty \rightarrow \mathcal{W}_\gamma^S(\tau)$ and $P_\gamma^L(\tau) : \mathcal{H}_\infty \rightarrow \mathcal{W}_\gamma^L(\tau)$ denote orthogonal projection operators onto these subspaces. Before presenting the proof Theorem 4.1, we introduce some additional definitions and prove some preliminary results.

Lemma 4.3 (Homogeneous Approximation Property). *Let $\mathbf{f} \in \mathcal{H}_\beta$ for some $\beta > 0$ and $\epsilon' > 0$. Then there exists $\Gamma = \Gamma(\mathbf{f}, \epsilon', \{\mathbf{l}_p\}) > 0$ such that*

$$\sup_{\sigma \in B_\gamma(\tau)} \|(I - P_{\gamma+\Gamma}^L(\tau))P_{\mathcal{H}_L}\Theta_\sigma \mathbf{f}\| \leq \epsilon'$$

for all $\gamma \geq 0$ and $\tau \in \mathbb{R}$.

Proof. Let $\sigma \in B_\gamma(\tau)$. Then, using Eq. (4.33) and the triangle inequality, we have

$$\mathcal{I}_p(\Gamma, \sigma) \subseteq \mathcal{I}_p(\gamma + \Gamma, \tau), \quad \forall \Gamma > 0. \quad (4.34)$$

Expanding $P_{\mathcal{H}_L}\Theta_\sigma \mathbf{f}$ with respect to the dual frame $\{\tilde{\mathbf{l}}_{np}\}$, we obtain

$$\begin{aligned}P_{\mathcal{H}_L}\Theta_\sigma \mathbf{f} &= \sum_{p=1}^P \sum_{n \in \mathbb{Z}} \langle P_{\mathcal{H}_L}\Theta_\sigma \mathbf{f}, \Theta_{\lambda_{np}} \mathbf{l}_p \rangle \tilde{\mathbf{l}}_{np} \\ &= \sum_{p=1}^P \sum_{n \in \mathbb{Z}} \langle \Theta_\sigma \mathbf{f}, \Theta_{\lambda_{np}} \mathbf{l}_p \rangle \tilde{\mathbf{l}}_{np},\end{aligned}$$

where the last step follows because $\Theta_{\lambda_{np}} \mathbf{l}_p \in \mathcal{H}_L$. Using the above representation, and the fact that $P_{\gamma+\Gamma}^L(\tau)$ is an orthogonal projection, we have

$$\begin{aligned}\|(I - P_{\gamma+\Gamma}^L(\tau))P_{\mathcal{H}_L}\Theta_\sigma \mathbf{f}\| &\leq \left\| P_{\mathcal{H}_L}\Theta_\sigma \mathbf{f} - \sum_{p=1}^P \sum_{n \in \mathcal{I}_p(\gamma+\Gamma, \tau)} \langle \Theta_\sigma \mathbf{f}, \Theta_{\lambda_{np}} \mathbf{l}_p \rangle \tilde{\mathbf{l}}_{np} \right\| \\ &= \left\| \sum_{p=1}^P \sum_{n \notin \mathcal{I}_p(\gamma+\Gamma, \tau)} \langle \Theta_\sigma \mathbf{f}, \Theta_{\lambda_{np}} \mathbf{l}_p \rangle \tilde{\mathbf{l}}_{np} \right\|.\end{aligned}$$

Combining this with Eq. (4.32) we get

$$\begin{aligned} \|(I - P_{\gamma+\Gamma}^L(\tau))P_{\mathcal{H}_L}\Theta_\sigma\mathbf{f}\|^2 &\leq B \sum_{p=1}^P \sum_{n \notin \mathcal{I}_p(\gamma+\Gamma, \tau)} |\langle \Theta_\sigma\mathbf{f}, \Theta_{\lambda_{np}}\mathbf{l}_p \rangle|^2 \\ &\leq B \sum_{p=1}^P \sum_{n \notin \mathcal{I}_p(\Gamma, \sigma)} |\langle \Theta_\sigma\mathbf{f}, \Theta_{\lambda_{np}}\mathbf{l}_p \rangle|^2, \end{aligned}$$

where the last step follows from Eq. (4.34). Letting $\overleftarrow{l}_{p,r}(t) = \overline{l_{p,r}(-t)}$ and

$$h_p(t) = \sum_{r=1}^R f_r * \overleftarrow{l}_{p,r}(t) = \sum_{r=1}^R \int_{\mathbb{R}} \overline{l_{p,r}(\tau-t)} f_r(\tau) d\tau,$$

where the bar denotes complex conjugation, we obtain

$$\|(I - P_{\gamma+\Gamma}^L(\tau))P_{\mathcal{H}_L}\Theta_\sigma\mathbf{f}\|^2 \leq B \sum_{p=1}^P \sum_{n \notin \mathcal{I}_p(\Gamma, \sigma)} |h_p(\lambda_{np} - \sigma)|^2.$$

Observe that $h_p \in \mathcal{B}[-\beta, \beta]$ because $\mathbf{f} \in \mathcal{H}_\beta$. By hypotheses, the sets $\{\Lambda_p\}$ have finite upper densities. Hence, applying Lemma 4.1, we obtain

$$\begin{aligned} \|(I - P_{\gamma+\Gamma}^L(\tau))P_{\mathcal{H}_L}\Theta_\sigma\mathbf{f}\|^2 &\leq BC' \sum_{p=1}^P \int_{|t-\sigma| \geq \Gamma-1} |h_p^\#(t-\sigma)|^2 dt \\ &= BC' \sum_{p=1}^P \int_{|t| \geq \Gamma-1} |h_p^\#(t)|^2 dt \end{aligned} \quad (4.35)$$

for some $C' = C'(\{\Lambda_p\}) > 0$ and all $\sigma \in B_\gamma(\tau)$. Since each $h_p^\# \in L^2(\mathbb{R})$, the right-hand side of Eq. (4.35) can be made smaller than ϵ' for sufficiently large Γ . The choice of Γ clearly depends only on ϵ' , \mathbf{f} , $\{\mathbf{l}_p : p \in \mathcal{P}\}$, and $\{\Lambda_p : p \in \mathcal{P}\}$. It depends on β through \mathbf{f} . \square

The homogenous approximation property roughly states that if we choose $\Gamma > 0$ sufficiently large then, for every σ such that $|\sigma - \tau| \leq \gamma$, the projection of $\Theta_\sigma\mathbf{f}$ onto \mathcal{H}_L can be approximated well by a vector in $\mathcal{W}_{\gamma+\Gamma}^L(\tau)$. The approximation is homogenous in the sense that the choice of Γ does not depend on σ , τ , or γ .

Proof of the Comparison Theorem. Define

$$\mathbf{s}'_{q\sigma\beta} = P_{\mathcal{H}_L}\Theta_\sigma P_{\mathcal{H}_\beta}\mathbf{s}_q, \quad \beta > 0, \sigma \in \mathbb{R}.$$

Let $\Gamma = \Gamma(\epsilon, \beta)$ be chosen such that the homogeneous approximation property (Lemma 4.3) holds for $\epsilon' = \epsilon\sqrt{a}$ and $\mathbf{f} = P_{\mathcal{H}_\beta}\mathbf{s}_q$ for each q . We write $\Gamma = \Gamma(\epsilon, \beta)$ to show its dependence

on these parameters. However, Γ also depends on $\{\mathbf{s}_q\}$, $\{\mathbf{l}_p\}$, a , and $\{\Lambda_p\}$, but we do not state these explicitly because they are fixed quantities. Therefore,

$$\|(I - P_{\gamma+\Gamma}^L(\tau))\mathbf{s}'_{q\sigma\beta}\| \leq \epsilon\sqrt{a} \quad (4.36)$$

for all $\gamma \geq 0$, $\tau \in \mathbb{R}$, and $\sigma \in B_\gamma(\tau)$. Define

$$\mathbf{s}''_{q\sigma\beta} = \Theta_\sigma \mathbf{s}_q - \mathbf{s}'_{q\sigma\beta} = \Theta_\sigma \mathbf{s}_q - P_{\mathcal{H}_L} \Theta_\sigma P_{\mathcal{H}_\beta} \mathbf{s}_q.$$

Then, using Eq. (4.36), we obtain

$$\begin{aligned} \|(I - P_{\gamma+\Gamma}^L(\tau))\Theta_\sigma \mathbf{s}_q\| &\leq \|(I - P_{\gamma+\Gamma}^L(\tau))\mathbf{s}'_{q\sigma\beta}\| + \|(I - P_{\gamma+\Gamma}^L(\tau))\mathbf{s}''_{q\sigma\beta}\| \\ &\leq \epsilon\sqrt{a} + \|\mathbf{s}''_{q\sigma\beta}\| \end{aligned} \quad (4.37)$$

for all $\gamma \geq 0$, $\tau \in \mathbb{R}$, and $\sigma \in B_\gamma(\tau)$. Let $T_\gamma(\tau) : \mathcal{W}_\gamma^S(\tau) \rightarrow \mathcal{W}_\gamma^S(\tau)$ be defined as $T_\gamma(\tau) = P_\gamma^S(\tau)P_{\gamma+\Gamma}^L(\tau)$. We shall compute lower and upper bounds on the real part of the trace of $T_\gamma(\tau)$. First observe that

$$\Re \operatorname{tr} T_\gamma(\tau) = \sum_{q=1}^Q \sum_{\sigma_{nq} \in \Sigma'_q \cap B_\gamma(\tau)} \Re \langle T_\gamma(\tau) \Theta_{\sigma_{nq}} \mathbf{s}_q, \tilde{\mathbf{s}}_{nq} \rangle, \quad (4.38)$$

where $\Re(\cdot)$ denotes the real part. We can rewrite each term in the summation as

$$\begin{aligned} \Re \langle T_\gamma(\tau) \Theta_{\sigma_{nq}} \mathbf{s}_q, \tilde{\mathbf{s}}_{nq} \rangle &= \Re \langle P_{\gamma+\Gamma}^L(\tau) \Theta_{\sigma_{nq}} \mathbf{s}_q, P_\gamma^S(\tau) \tilde{\mathbf{s}}_{nq} \rangle \\ &= \Re \langle \Theta_{\sigma_{nq}} \mathbf{s}_q, P_\gamma^S(\tau) \tilde{\mathbf{s}}_{nq} \rangle + \Re \langle (P_{\gamma+\Gamma}^L(\tau) - I) \Theta_{\sigma_{nq}} \mathbf{s}_q, P_\gamma^S(\tau) \tilde{\mathbf{s}}_{nq} \rangle \\ &= 1 + \Re \langle (P_{\gamma+\Gamma}^L(\tau) - I) \Theta_{\sigma_{nq}} \mathbf{s}_q, P_\gamma^S(\tau) \tilde{\mathbf{s}}_{nq} \rangle \\ &\geq 1 - \|(P_{\gamma+\Gamma}^L(\tau) - I) \Theta_{\sigma_{nq}} \mathbf{s}_q\| \|\tilde{\mathbf{s}}_{nq}\|. \end{aligned}$$

Since $\sigma_{nq} \in B_\gamma(\tau)$, we can use Eqs. (4.31) and (4.37) and the above inequality to obtain

$$\Re \langle T_\gamma(\tau) \Theta_{\sigma_{nq}} \mathbf{s}_q, \tilde{\mathbf{s}}_{nq} \rangle \geq 1 - \frac{(\epsilon\sqrt{a} + \|\mathbf{s}''_{q,\sigma_{nq},\beta}\|)}{\sqrt{a}} \geq 1 - \epsilon - \alpha'_q(\beta), \quad (4.39)$$

where

$$\alpha'_q(\beta) = \frac{1}{\sqrt{a}} \sup_{\sigma \in \Sigma_q} \|\mathbf{s}''_{q\sigma\beta}\| = \frac{1}{\sqrt{a}} \sup_{\sigma \in \Sigma_q} \|\Theta_\sigma \mathbf{s}_q - P_{\mathcal{H}_L} \Theta_\sigma P_{\mathcal{H}_\beta} \mathbf{s}_q\|. \quad (4.40)$$

In view of Eq. (4.40) and Lemma 4.2, we have

$$\limsup_{\beta \rightarrow \infty} \alpha'_q(\beta) \leq \frac{1}{\sqrt{a}} \sup_{\sigma \in \Sigma_q} \|\Theta_\sigma \mathbf{s}_q - P_{\mathcal{H}_L} \Theta_\sigma \mathbf{s}_q\| = \alpha_q. \quad (4.41)$$

Combining Eqs. (4.38) and (4.39) gives us a lower bound on the real part of the trace of $T_\gamma(\tau)$:

$$\Re \operatorname{tr} T_\gamma(\tau) \geq \sum_{q=1}^Q (1 - \epsilon - \alpha'_q(\beta)) \#(\Sigma'_q \cap B_\gamma(\tau)). \quad (4.42)$$

For the upper bound, observe that $\|T_\gamma(\tau)\| \leq \|P_\gamma^S(\tau)\| \|P_{\gamma+\Gamma}^L(\tau)\| \leq 1$. Therefore,

$$\Re \operatorname{tr} T_\gamma(\tau) \leq \operatorname{rank} T_\gamma(\tau) \leq \dim \mathcal{W}_{\gamma+\Gamma}^L(\tau) \leq \sum_{p=1}^P \#(\Lambda_p \cap B_{\gamma+\Gamma}(\tau)). \quad (4.43)$$

Combining Eqs. (4.42) and (4.43), we obtain

$$\sum_{p=1}^P \#(\Lambda_p \cap B_{\gamma+\Gamma}(\tau)) \geq \sum_{q=1}^Q (1 - \epsilon - \alpha'_q(\beta)) \#(\Sigma'_q \cap B_\gamma(\tau)) \quad (4.44)$$

for all $\gamma, \beta \geq 0$, $\tau \in \mathbb{R}$, and $\Gamma > \Gamma(\epsilon, \beta)$. Suppose that $D^+(\Sigma_q) < \infty$ for all q , then any interval of Σ_q is guaranteed to contain a finite number of points. So, we can take $\Sigma'_q = \Sigma_q \cap [-T, T]$.

Dividing Eq. (4.44) by 2γ and letting $T \rightarrow \infty$ we get

$$\frac{1}{2\gamma} \sum_{p=1}^P \#(\Lambda_p \cap B_{\gamma+\Gamma}(\tau)) \geq \frac{1}{2\gamma} \sum_{q=1}^Q (1 - \epsilon - \alpha'_q(\beta)) \#(\Sigma_q \cap B_\gamma(\tau)). \quad (4.45)$$

Taking the supremum (or infimum) of Eq. (4.45) over τ and letting $\gamma \rightarrow \infty$, we obtain

$$D^\pm(\Lambda_1, \dots, \Lambda_P) \geq (1 - \epsilon) D^\pm(\Sigma_1, \dots, \Sigma_Q) - \sum_{q=1}^Q \alpha'_q(\beta) D^+(\Sigma_q).$$

Since $\epsilon, \beta > 0$ are arbitrary, we obtain

$$D^\pm(\Lambda_1, \dots, \Lambda_P) \geq D^\pm(\Sigma_1, \dots, \Sigma_Q) - \sum_{q=1}^Q \limsup_{\beta \rightarrow \infty} \alpha'_q(\beta) D^+(\Sigma_q).$$

Using Eq. (4.41), we obtain the desired inequality in Eq. (4.29). Now suppose that $D^+(\Sigma_q) < \infty$ is not a given hypotheses, but all $\alpha_q < 1$. Then, from Eq. (4.41), we conclude that $1 - \epsilon - \alpha'_q(\beta) > 0$ for all q and some $\epsilon, \beta > 0$. Under this condition, Eq. (4.44) implies $1 - \epsilon - \alpha'_q(\beta) > 0$ for all q and some $\epsilon, \beta > 0$, and hence

$$\#(\Sigma'_q \cap B_\gamma(\tau)) \leq \frac{1}{(1 - \epsilon - \alpha'_q(\beta))} \sum_{p=1}^P \#(\Lambda_p \cap B_{\gamma+\Gamma}(\tau)), \quad q \in \mathcal{Q}. \quad (4.46)$$

The right-hand side of this expression is finite because $D^+(\Lambda_p) < \infty$. If any interval $\mathcal{I} = B_\gamma(\tau)$ contained infinitely many points of Σ_q , then exists a $\Sigma'_q \subseteq \Sigma_q$ such that \mathcal{I} contains an arbitrarily large (but finite) number of points of Σ'_q . This would clearly violate Eq. (4.46). Thus each

interval contains finitely many points of Σ_q . Letting $\Sigma'_q = \Sigma_q \cap [-T, T]$ with $T \rightarrow \infty$ in Eq. (4.46), taking the supremum of this equation over τ , and then letting $\gamma \rightarrow \infty$ produces $D^+(\Sigma_q) < \infty$ because the sets Λ_p have finite upper densities. \square

Note that \mathcal{H}_L and \mathcal{H}_S are arbitrary subspaces in \mathcal{H}_∞ . However, the comparison theorem is most powerful when we let the spaces be nearly the same. In this case, the coefficients α_q would be small, thereby yielding the following density bound:

$$D^\pm(\Lambda_1, \dots, \Lambda_P) \geq D^\pm(\Sigma_1, \dots, \Sigma_Q) - \epsilon,$$

where $\epsilon > 0$ is a small quantity representing the summation in Eq. (4.29) involving the terms α_q . The import of this statement is roughly that a frame, being an overcomplete sequence in a Hilbert space \mathcal{H} , is “denser” (contains more vectors) than a Riesz-Fischer sequence \mathcal{H} . By using an appropriate limiting argument, we can then show that $\epsilon > 0$ can be made arbitrarily small, yielding

$$D^\pm(\Lambda_1, \dots, \Lambda_P) \geq D^\pm(\Sigma_1, \dots, \Sigma_Q).$$

We illustrate the use of this theorem in the next section, where we derive necessary density conditions for the MIMO sampling problem.

4.3.2 Density conditions for stable sampling

Theorem 4.1 now allows us to prove the necessary density results for stable sampling in the MIMO setting.

Theorem 4.2. *Suppose that \mathcal{F}_r , $r \in \mathcal{R}$ are real sets of finite measure, and Λ_p , $p \in \mathcal{P}$ are discrete sets with $D^+(\Lambda_p) < \infty$ that constitute a stable collection of MIMO sampling with respect to $\mathbf{G}(f)$ for $\mathcal{H} = \mathcal{B}(\mathcal{F}_1) \times \dots \times \mathcal{B}(\mathcal{F}_R)$. Then for every $\Pi \subseteq \mathcal{P}$,*

$$D^-(\{\Lambda_p : p \in \Pi\}) \geq \sum_{r=1}^R \mu(\mathcal{F}_r) - \int_{\mathbb{R}} \text{rank}(\mathbf{G}_{\Pi^c, \mathcal{C}_f}(f)) df, \quad (4.47)$$

where $\mathcal{C}_f = \{r : f \in \mathcal{F}_r\}$ and Π^c denotes the complement of Π in \mathcal{P} . Furthermore, if

$$\text{ess inf}_{f \in \mathcal{F}} \sigma_{\min}(\mathbf{G}_{\Pi^c, \mathcal{C}_f}(f)) = 0, \quad \mathcal{F} = \bigcup_{r \in \mathcal{R}} \mathcal{F}_r, \quad (4.48)$$

for some $\Pi \neq \mathcal{P}$, then the inequality in Eq. (4.47) is strict.

Proof. Note that \mathcal{F} is the set where \mathcal{C}_f is not empty. Let $\Pi \subseteq \mathcal{P}$ be a fixed subset. We consider two cases: first suppose that either $\Pi = \mathcal{P}$ or Eq. (4.48) does not hold. In this case take $\mathcal{D}_0 = \emptyset$.

Otherwise $\Pi \neq \mathcal{P}$, so we can define

$$K = \max_{p \in \Pi^c} C'(\Lambda_p)C(1), \quad (4.49)$$

where C' and C are quantities defined in Lemma 4.1. Let $\epsilon_0 > 0$ be such that $K\epsilon_0^2 \leq A/2$, where A is the lower stability bound in Eq. (4.18). Since Eq. (4.48) is satisfied in the second case, there exists a set \mathcal{D}_0 such that $\mu(\mathcal{D}_0) > 0$ and

$$\sigma_{\min}(\mathbf{G}_{\Pi^c, \mathcal{C}_f}(f)) \leq \epsilon_0, \quad \forall f \in \mathcal{D}_0. \quad (4.50)$$

Without loss of generality, assume that $\mathcal{D}_0 \subseteq [\nu, \nu + 1]$ for some $\nu \in \mathbb{R}$. In fact, Eq. (4.50) is satisfied in both cases. Let the cardinality of the set \mathcal{C}_f be denoted by $|\mathcal{C}_f|$, i.e.,

$$|\mathcal{C}_f| = \sum_{r=1}^R \chi(f \in \mathcal{F}_r). \quad (4.51)$$

Let the dimension of the null space of $\mathbf{G}_{\Pi^c, \mathcal{C}_f}(f)$ be denoted by

$$\rho(f) = |\mathcal{C}_f| - \text{rank}(\mathbf{G}_{\Pi^c, \mathcal{C}_f}(f)), \quad (4.52)$$

and let the columns of $\mathbf{U}'(f) \in \mathbb{C}^{|\mathcal{C}_f| \times \rho(f)}$ form an orthonormal basis for the null space of $\mathbf{G}_{\Pi^c, \mathcal{C}_f}(f)$. For $f \in \mathcal{D}_0$, let $\mathbf{U}''(f) \in \mathbb{C}^{|\mathcal{C}_f| \times 1}$ be a unit-norm right singular vector of $\mathbf{G}_{\Pi^c, \mathcal{C}_f}(f)$ corresponding to its smallest nonzero singular value. We can always choose $\mathbf{U}'(f)$ and $\mathbf{U}''(f)$ to be measurable functions. Clearly, $\mathbf{U}''(f)$ is orthogonal to the columns of $\mathbf{U}'(f)$ for $f \in \mathcal{D}_0$. Therefore,

$$\mathbf{U}(f) = \begin{cases} [\mathbf{U}'(f) \ \mathbf{U}''(f)] & \text{if } f \in \mathcal{D}_0, \\ \mathbf{U}'(f) & \text{otherwise,} \end{cases}$$

has orthonormal columns for all f . Let \mathcal{G}_r be the set where $\mathbf{U}(f)$ contains r columns, i.e.,

$$\mathcal{G}_r = \{f : \rho(f) + \chi(f \in \mathcal{D}_0) = r\}, \quad r \in \mathcal{R}. \quad (4.53)$$

The sets $\{\mathcal{G}_r\}$ are clearly disjoint sets of finite measure. Therefore, for any $\delta > 0$, there exist finite collection of disjoint intervals $\{\mathcal{I}_{rk} : r \in \mathcal{R}, k = 1, \dots, K_r\}$ such that the sets

$$\mathcal{G}'_r \stackrel{\text{def}}{=} \bigcup_{k=1}^{K_r} \mathcal{I}_{rk}, \quad r \in \mathcal{R} \quad (4.54)$$

approximate \mathcal{G}_r in the sense that $\mu(\mathcal{G}'_r \cap \mathcal{G}_r^c) \leq \delta/R^2$ and $\mu(\mathcal{G}'_r^c \cap \mathcal{G}_r) \leq \delta/R^2$. It follows that

$$\sum_{r=1}^R r \mu(\mathcal{G}'_r \cap \mathcal{G}_r^c) \leq \sum_{r=1}^R \frac{r\delta}{R^2} \leq \delta. \quad (4.55)$$

It is also clear that $|\mu(\mathcal{G}'_r) - \mu(\mathcal{G}_r)| \leq \delta/R^2$. Consequently, we have

$$\left| \sum_{r=1}^R r\mu(\mathcal{G}_r) - \sum_{r=1}^R r\mu(\mathcal{G}'_r) \right| \leq \delta. \quad (4.56)$$

Now, define $\mathbf{W}^r(f) \in \mathbb{C}^{R \times r}$ on \mathcal{G}'_r for each r as follows:

$$\mathbf{W}^r(f) = \begin{cases} \mathbf{I}_{\bullet, \mathcal{C}_f} \mathbf{U}(f) & \text{if } f \in \mathcal{G}'_r \cap \mathcal{G}_r, \\ (e_1, \dots, e_r) & \text{if } f \in \mathcal{G}'_r \cap \mathcal{G}_r^c, \end{cases} \quad (4.57)$$

where \mathbf{I} is the $R \times R$ identity matrix. Note that the columns of $\mathbf{W}^r(f)$ form an orthonormal set of vectors for each $f \in \mathcal{G}'_r$. For each $r \in \mathcal{R}$, let k and m be indices such that $1 \leq k \leq K_r$ and $1 \leq m \leq r$. For convenience let $q(r, k, m)$ denote an invertible mapping from the triplet (r, k, m) to a single index q :

$$q(r, k, m) : \{(r, k, m) : r \in \mathcal{R}, k = 1, \dots, K_r, m = 1, \dots, r\} \rightarrow \mathcal{Q},$$

where $\mathcal{Q} = \{1, \dots, Q\}$ and

$$Q = \sum_{r=1}^R rK_r.$$

In the rest of the proof, assume that q, r, k , and m are related to each other by $q = q(r, k, m)$. We shall now define several quantities with the intention of eventually using Theorem 4.1 to derive the necessary density conditions. Let $\{\mathbf{s}_q\} \subseteq \mathcal{H}_\infty$ be defined as follows in terms of their Fourier transforms:

$$\mathbf{s}_q(f) = \begin{cases} \mathbf{W}_{\bullet, m}^r(f) / \sqrt{\mu(\mathcal{I}_{rk})} & \text{if } f \in \mathcal{I}_{rk}, \\ \mathbf{0} & \text{otherwise,} \end{cases} \quad (4.58)$$

where $\mathbf{W}_{\bullet, m}^r(f)$ is the m th column of $\mathbf{W}^r(f)$. The sampling set

$$\Sigma_q \stackrel{\text{def}}{=} \left\{ \frac{n}{\mu(\mathcal{I}_{rk})} : n \in \mathbb{Z} \right\}. \quad (4.59)$$

has uniform density of $\mu(\mathcal{I}_{rk})$. Since the intervals \mathcal{I}_{rk} are disjoint, and $\{\mathbf{W}_{\bullet, m}^r(f) : m = 1, \dots, r\}$ is a set of orthonormal vectors for each r and f , it follows that $\{\Theta_{\sigma_{nq}} \mathbf{s}_q : q \in \mathcal{Q}, n \in \mathbb{Z}\}$ is an orthonormal sequence. Let \mathcal{H}_S be the closure of the span of this orthonormal sequence, i.e.,

$$\mathcal{H}_S = \overline{\text{span}\{\Theta_{\sigma_{nq}} \mathbf{s}_q : q \in \mathcal{Q}, n \in \mathbb{Z}\}} \subseteq \mathcal{H}_\infty. \quad (4.60)$$

Then clearly $\{\Theta_{\sigma_{nq}} \mathbf{s}_q : q \in \mathcal{Q}, n \in \mathbb{Z}\}$ is an orthonormal Riesz basis for \mathcal{H}_S with lower frame bound $a = 1$. In particular, it is a Riesz-Fischer sequence with bound $a = 1$.

Now define

$$\mathcal{H}_L = \{\mathbf{x} \in \mathcal{H} : \mathbf{X}_{\mathcal{C}_f}(f) = \mathbf{U}(f)\mathbf{U}^H(f)\mathbf{X}_{\mathcal{C}_f}(f) \text{ a.e.}\}. \quad (4.61)$$

where ‘‘a.e.’’ stands for almost everywhere. It is obvious that \mathcal{H}_L is a shift-invariance subspace. To see that \mathcal{H}_L is closed, consider the following argument. Let $\{\mathbf{x}^i\} \in \mathcal{H}_L$ be a sequence converging to $\mathbf{x}^\infty \in \mathcal{H}_\infty$. Then we have

$$\mathbf{X}_{\mathcal{C}_f}^i(f) = \mathbf{U}(f)\mathbf{U}^H(f)\mathbf{X}_{\mathcal{C}_f}^i(f) \text{ a.e.}$$

Also, $\mathbf{X}^i(f)$ converges to $\mathbf{X}^\infty(f)$ in the L^2 sense. Hence, there exists a subsequence $\{i_j\}$ such that as $j \rightarrow \infty$, we have $\mathbf{X}^{i_j}(f) \rightarrow \mathbf{X}^\infty(f)$ a.e. Therefore,

$$\mathbf{U}(f)\mathbf{U}^H(f)\mathbf{X}_{\mathcal{C}_f}^\infty(f) = \lim_{j \rightarrow \infty} \mathbf{U}(f)\mathbf{U}^H(f)\mathbf{X}_{\mathcal{C}_f}^{i_j}(f) = \mathbf{X}_{\mathcal{C}_f}^\infty(f) \text{ a.e.,}$$

or equivalently $\mathbf{x}_\infty \in \mathcal{H}_L$, proving that \mathcal{H}_L is closed.

Suppose that $\mathbf{x} \in \mathcal{H}_L$. Then using Eqs. (4.17) and (4.61) we see that

$$\mathbf{Y}_{\Pi^c}(f) = \mathbf{G}_{\Pi^c, \mathcal{C}_f}(f)\mathbf{X}_{\mathcal{C}_f}(f) = \mathbf{G}_{\Pi^c, \mathcal{C}_f}(f)\mathbf{U}(f)\mathbf{U}^H(f)\mathbf{X}_{\mathcal{C}_f}(f).$$

Using the definitions of $\mathbf{U}(f)$ and $\mathbf{U}''(f)$, we conclude that

$$\mathbf{Y}_{\Pi^c}(f) = \mathbf{0}, \quad f \notin \mathcal{D}_0, \quad (4.62)$$

$$\begin{aligned} \|\mathbf{Y}_{\Pi^c}(f)\| &= \|\mathbf{G}_{\Pi^c, \mathcal{C}_f}(f)\mathbf{U}''(f)\mathbf{U}''^H(f)\mathbf{X}_{\mathcal{C}_f}(f)\| \\ &\leq \epsilon_0\|\mathbf{X}(f)\|, \quad f \in \mathcal{D}_0. \end{aligned} \quad (4.63)$$

Equations (4.62) and (4.63) imply that $\|\mathbf{Y}_{\Pi^c}(f)\| \leq \epsilon_0\|\mathbf{X}(f)\|$. Hence,

$$\int_{\mathbb{R}} \|\mathbf{Y}_{\Pi^c}(f)\|^2 df \leq \epsilon_0^2\|\mathbf{x}\|^2. \quad (4.64)$$

We also see that for each $p \in \Pi^c$, $Y_p(f)$ is supported on $\mathcal{D}_0 \subseteq [\nu, \nu + 1]$. Applying Lemma 4.1 to y_p , $p \in \Pi^c$ and using Eq. (4.64) yields

$$\sum_{p \in \Pi^c} \sum_{n \in \mathbb{Z}} |y_p(\lambda_{np})|^2 \leq K \int_{\mathbb{R}} \|\mathbf{Y}_{\Pi^c}(f)\|^2 df \leq K\epsilon_0^2\|\mathbf{x}\|^2, \quad (4.65)$$

where K is the constant defined in Eq. (4.49). Combining Eq. (4.65) with the first inequality in the sampling stability condition in Eq. (4.18), we obtain

$$\sum_{p \in \Pi} \sum_{n \in \mathbb{Z}} |y_p(\lambda_{np})|^2 \geq (A - K\epsilon_0^2)\|\mathbf{x}\|^2 \geq \frac{A}{2}\|\mathbf{x}\|^2, \quad \forall \mathbf{x} \in \mathcal{H}_L, \quad (4.66)$$

where the second inequality above follows from the choice of ϵ_0 . From Eq. (4.18), we obviously also have

$$\sum_{p \in \Pi} \sum_{n \in \mathbb{Z}} |y_p(\lambda_{np})|^2 \leq B \|\mathbf{x}\|^2, \quad \forall \mathbf{x} \in \mathcal{H}_L \quad (4.67)$$

because $\mathcal{H}_L \subseteq \mathcal{H}$. Combining Eqs. (4.66) and (4.67), we obtain

$$\frac{A}{2} \|\mathbf{x}\|^2 \leq \sum_{p \in \Pi} \sum_{n \in \mathbb{Z}} |y_p(\lambda_{np})|^2 \leq B \|\mathbf{x}\|^2, \quad \forall \mathbf{x} \in \mathcal{H}_L. \quad (4.68)$$

Let $\mathbf{l}_p = P_{\mathcal{H}_L} \boldsymbol{\psi}_p$, where $\boldsymbol{\psi}_p$ is defined in Eq. (4.19). Recall that \mathcal{H}_L is shift-invariant. Hence, using Proposition 4.4, we obtain

$$\Theta_{\lambda_{np}} \mathbf{l}_p = \Theta_{\lambda_{np}} P_{\mathcal{H}_L} \boldsymbol{\psi}_p = P_{\mathcal{H}_L} \Theta_{\lambda_{np}} \boldsymbol{\psi}_p \in \mathcal{H}_L. \quad (4.69)$$

Also,

$$\langle \mathbf{x}, \Theta_{\lambda_{np}} \mathbf{l}_p \rangle = \langle \mathbf{x}, P_{\mathcal{H}_L} \Theta_{\lambda_{np}} \boldsymbol{\psi}_p \rangle = \langle \mathbf{x}, \Theta_{\lambda_{np}} \boldsymbol{\psi}_p \rangle = y_p(\lambda_{np}), \quad \forall \mathbf{x} \in \mathcal{H}_L. \quad (4.70)$$

It follows from Eqs. (4.68), (4.69), and (4.70) that $\{\Theta_{\lambda_{np}} \mathbf{l}_p : p \in \Pi, n \in \mathbb{Z}\}$ is a frame for \mathcal{H}_L . Having verified all the required hypotheses, we can now apply Theorem 4.1 to obtain the following inequality relating the densities of $\{\Lambda_p : p \in \Pi\}$ and $\{\Sigma_q : q \in \mathcal{Q}\}$:

$$D^-(\{\Lambda_p : p \in \Pi\}) \geq D^-(\Sigma_1, \dots, \Sigma_Q) - \sum_{q \in \mathcal{Q}} \alpha_q D^+(\Sigma_q), \quad (4.71)$$

where

$$\alpha_q = \frac{1}{\sqrt{a}} \sup_{\sigma \in \Sigma_q} \|\Theta_{\sigma} \mathbf{s}_q - P_{\mathcal{H}_L} \Theta_{\sigma} \mathbf{s}_q\|.$$

Since \mathcal{H}_L is shift-invariant, we can use Proposition 4.4 to obtain

$$\alpha_q = \frac{1}{\sqrt{a}} \sup_{\sigma \in \Sigma_q} \|\Theta_{\sigma} \mathbf{s}_q - \Theta_{\sigma} P_{\mathcal{H}_L} \mathbf{s}_q\| = \frac{1}{\sqrt{a}} \|\mathbf{s}_q - P_{\mathcal{H}_L} \mathbf{s}_q\| = \|\mathbf{s}_q - P_{\mathcal{H}_L} \mathbf{s}_q\|,$$

where the last line follows because $a = 1$. We shall estimate α_q in a moment, but first, define $\mathbf{v}_q \in \mathcal{H}$ as follows:

$$\mathbf{V}_q(f) = \begin{cases} \mathbf{S}_q(f) & \text{if } f \in \mathcal{I}_{rk} \cap \mathcal{G}_r, \\ \mathbf{0} & \text{otherwise.} \end{cases} \quad (4.72)$$

For all $f \in \mathcal{I}_{rk} \cap \mathcal{G}_r$, we use Eqs. (4.57), (4.58) and (4.72) to conclude that

$$\mathbf{U}(f) \mathbf{U}^H(f) \mathbf{V}_q(f) = \frac{\mathbf{U}(f) \mathbf{U}^H(f) \mathbf{U}_{\bullet, m}(f)}{\sqrt{\mu(\mathcal{I}_{rk})}} = \frac{\mathbf{U}_{\bullet, m}(f)}{\sqrt{\mu(\mathcal{I}_{rk})}} = \mathbf{V}_q(f).$$

This proves that $\mathbf{v}_q \in \mathcal{H}_L$. Therefore, $\alpha_q \leq \|\mathbf{s}_q - \mathbf{v}_q\|$. Using Parseval's Theorem and Eqs. (4.58) and (4.72) we obtain

$$\alpha_q \leq \left(\int \|\mathbf{S}_q(f) - \mathbf{V}_q(f)\|^2 df \right)^{\frac{1}{2}} = \left(\int_{\mathcal{I}_{rk} \cap \mathcal{G}_r^c} \left\| \frac{\mathbf{W}_{\bullet, m}^r(f)}{\sqrt{\mu(\mathcal{I}_{rk})}} \right\|^2 df \right)^{\frac{1}{2}}.$$

Since $\mathbf{W}_{\bullet, n}^r(f)$ is a normal vector, we arrive at the following estimate for α_q :

$$\alpha_q \leq \sqrt{\frac{\mu(\mathcal{I}_{rk} \cap \mathcal{G}_r^c)}{\mu(\mathcal{I}_{rk})}}. \quad (4.73)$$

Combining Eqs. (4.71) and (4.73) and using the fact that Σ_q has a uniform density of $\mu(\mathcal{I}_{rk})$, we obtain

$$\begin{aligned} D^-(\{\Lambda_p : p \in \Pi\}) &\geq \sum_{r, m, k} \mu(\mathcal{I}_{rk}) - \sum_{r, m, k} \alpha_q \mu(\mathcal{I}_{rk}) \\ &\geq \sum_r r \mu(\mathcal{G}'_r) - \sum_{r, k} r \sqrt{\mu(\mathcal{I}_{rk} \cap \mathcal{G}_r^c) \mu(\mathcal{I}_{rk})}. \end{aligned}$$

Using the Cauchy-Schwarz inequality, we obtain

$$\begin{aligned} D^-(\{\Lambda_p : p \in \Pi\}) &\geq \sum_r r \mu(\mathcal{G}'_r) - \left(\sum_{rk} r \mu(\mathcal{I}_{rk} \cap \mathcal{G}_r^c) \right)^{\frac{1}{2}} \left(\sum_{rk} r \mu(\mathcal{I}_{rk}) \right)^{\frac{1}{2}} \\ &= \sum_r r \mu(\mathcal{G}'_r) - \left(\sum_r r \mu(\mathcal{G}'_r \cap \mathcal{G}_r^c) \right)^{\frac{1}{2}} \left(\sum_r r \mu(\mathcal{G}'_r) \right)^{\frac{1}{2}}. \end{aligned} \quad (4.74)$$

Now, Eqs. (4.55), (4.56), and (4.74) imply that

$$D^-(\{\Lambda_p : p \in \Pi\}) \geq \left[\sum_r r \mu(\mathcal{G}_r) \right] - \delta - \left[\delta \left(\delta + \sum_r r \mu(\mathcal{G}_r) \right) \right]^{\frac{1}{2}}. \quad (4.75)$$

Meanwhile, using Eqs. (4.51), (4.52) and (4.53), and the definition of the Lebesgue integral, we obtain

$$\begin{aligned} \sum_{r=1}^R r \mu(\mathcal{G}_r) &= \int_{\mathbb{R}} [\rho(f) + \chi(f \in \mathcal{D}_0)] df \\ &= \mu(\mathcal{D}_0) + \int_{\mathbb{R}} [|\mathcal{C}_f| - \text{rank}(\mathbf{G}_{\Pi^c, \mathcal{C}_f}(f))] df \\ &= \mu(\mathcal{D}_0) + \sum_{r=1}^R \mu(\mathcal{F}_r) - \int_{\mathbb{R}} \text{rank}(\mathbf{G}_{\Pi^c, \mathcal{C}_f}(f)) df. \end{aligned} \quad (4.76)$$

Putting together Eqs. (4.75) and (4.76), and letting $\delta \rightarrow 0$ yields

$$D^-(\{\Lambda_p : p \in \Pi\}) \geq \mu(\mathcal{D}_0) + \sum_{r=1}^R \mu(\mathcal{F}_r) - \int_{\mathbb{R}} \text{rank}(\mathbf{G}_{\Pi^c, \mathcal{C}_f}(f)) df.$$

This proves Eq. (4.47). Finally, recall that if Eq. (4.48) is satisfied for some $\Pi \neq \mathcal{P}$, then $\mu(\mathcal{D}_0) > 0$, proving that the strict inequality in Eq. (4.47) holds in this case. \square

Theorem 4.2 is a generalization of Landau's classical result to the MIMO sampling problem. Letting $\Pi = \mathcal{P}$ in Eq. (4.47), we obtain

$$D^-(\Lambda_1, \dots, \Lambda_P) \geq \sum_{r=1}^R \mu(\mathcal{F}_r). \quad (4.77)$$

In other words, the combined sampling density on all the output channels must be no less than the combined bandwidth of all the input signals. Theorem 4.2 also provides lower bounds on the joint densities of subcollections of $\{\Lambda_p\}$, and some of them may even be strict inequalities.

In Eq. (4.47), the joint density $D^-(\{\Lambda_p : p \in \Pi\})$ is interpreted as an upper bound on the "signal information" captured by the samples of y_p on those sampling sets. The bound on the joint density of $\{\Lambda_p : p \in \Pi\}$ depends only on the $\mathbf{G}_{\Pi^c, \mathcal{C}_f}(f)$, i.e., the submatrix of $\mathbf{G}(f)$ whose rows are indexed by the complement of Π and columns by \mathcal{C}_f . Note that $G_{pr}(f)$ is irrelevant for $f \notin \mathcal{F}_r$ because $X_r(f)$ vanishes outside \mathcal{F}_r . This explains restriction of the columns to the set $\mathcal{C}_f = \{r : f \in \mathcal{F}_r\}$. Suppose that the outputs $y_p(t)$, $p \in \Pi^c$ are completely known for all $t \in \mathbb{R}$. Then $\mathbf{Y}_{\Pi^c}(f) = \mathbf{G}_{\Pi^c, \mathcal{C}_f}(f)\mathbf{X}_{\mathcal{C}_f}(f)$ is also known for all f . Then $\text{rank}(\mathbf{G}_{\Pi^c, \mathcal{C}_f}(f))$ is the number of independent components of $\mathbf{X}(f)$ that can be determined from $\mathbf{Y}_{\Pi^c}(f)$ alone. Consequently,

$$\int_{\mathbb{R}} \text{rank}(\mathbf{G}_{\Pi^c, \mathcal{C}_f}(f))$$

is a measure of input signal information that can be captured by knowing the outputs $y_p(t)$, $p \in \Pi^c$ completely (for all t). The additional signal information required from the samples of $\{y_p(\lambda_{np}) : p \in \Pi\}$ is indicated by the difference of the two terms in Eq. (4.47). This also explains why Eq. (4.47) depend only on $G_{pr}(f)$ for $p \in \Pi^c$.

Next, if some singular value of $\mathbf{G}_{\Pi^c, \mathcal{C}_f}(f)$ takes arbitrarily small nonzero values, then there is not enough information in $\mathbf{Y}_{\Pi^c}(f) = \mathbf{G}_{\Pi^c, \mathcal{C}_f}(f)\mathbf{X}_{\mathcal{C}_f}(f)$ to stably recover $\text{rank}(\mathbf{G}_{\Pi^c, \mathcal{C}_f}(f))$ independent components of $\mathbf{X}(f)$. Therefore, the information contained in the samples of $y_p(t)$ must be a little bit more than right-hand side of Eq. (4.47) for stable reconstruction, and this explains the strictness of the bound.

The following corollary shows that stability of sampling requires an additional condition on the channel transfer function matrix $\mathbf{G}(f)$.

Corollary 4.1. *Suppose that the hypotheses of Theorem 4.2 are satisfied, and let $\mathcal{F} = \bigcup_{r \in \mathcal{R}} \mathcal{F}_r$. Then*

$$\text{ess inf}_{f \in \mathcal{F}} \lambda_{\min}(\mathbf{G}_{\Pi^c, \mathcal{C}_f}^H(f)\mathbf{G}_{\Pi^c, \mathcal{C}_f}(f)) > 0, \quad (4.78)$$

for every $\Pi \subset \mathcal{P}$, $\Pi \neq \mathcal{P}$ such that $D^-(\{\Lambda_p : p \in \Pi\}) = 0$. In particular,

$$\text{ess inf}_{f \in \mathcal{F}} \lambda_{\min}(\mathbf{G}_{\bullet, \mathcal{C}_f}^H(f)\mathbf{G}_{\bullet, \mathcal{C}_f}(f)) > 0. \quad (4.79)$$

Proof. From Theorem 4.2 and Eq. (4.51) we have

$$D^-(\{\Lambda_p : p \in \Pi\}) \geq \sum_{r=1}^R \mu(\mathcal{F}_r) - \int_{\mathbb{R}} \text{rank}(\mathbf{G}_{\Pi^c, \mathcal{C}_f}(f)) df \geq \sum_{r=1}^R \mu(\mathcal{F}_r) - \int_{\mathbb{R}} |\mathcal{C}_f| df \geq 0.$$

If $D^-(\{\Lambda_p : p \in \Pi\}) = 0$, both the inequalities above must, in fact, be equalities. In particular, Eq. (4.47) holds with an equality, which implies that

$$\text{ess inf}_{f \in \mathcal{F}} \sigma_{\min}(\mathbf{G}_{\Pi^c, \mathcal{C}_f}(f)) > 0,$$

by Theorem 4.2. We also have $\text{rank}(\mathbf{G}_{\Pi^c, \mathcal{C}_f}(f)) = |\mathcal{C}_f|$, implying that

$$\lambda_{\min}(\mathbf{G}_{\Pi^c, \mathcal{C}_f}^H(f) \mathbf{G}_{\Pi^c, \mathcal{C}_f}(f)) = [\sigma_{\min}(\mathbf{G}_{\Pi^c, \mathcal{C}_f}(f))]^2.$$

Now Eq. (4.78) follows by combining the last two observations. Applying this result to $\Pi = \emptyset$, we obtain Eq. (4.79). \square

Equation (4.79), which states that the singular values of $\mathbf{G}_{\bullet, \mathcal{C}_f}(f)$ are uniformly bounded away from the origin, must always hold for stable MIMO sampling. In fact, even if all outputs $y_p(t)$ are known for all t , we cannot stably recover the channel inputs unless Eq. (4.79) holds because this condition is necessary to satisfy the lower stability bound in Eq. (4.18). In particular, a more elementary necessary condition that emerges from Eq. (4.79) is that $P \geq |\mathcal{C}_f|$ a.e.; i.e., the number of channels cannot be less than the number of overlapping input spectral supports at any frequency. Next $D^-(\{\Lambda_p : p \in \Pi\}) = 0$ implies that the output samples on the sampling sets $\{\Lambda_p : p \in \Pi\}$ are too sparse to contain any signal information. Therefore, we must rely entirely on the outputs samples taken on $\{\Lambda_p : p \in \Pi^c\}$ to achieve stable reconstruction. The validity of Eq. (4.78) can be seen using the same argument that we used to justify Eq. (4.79).

The following theorem provides another necessary condition for stable sampling.

Theorem 4.3. *Under the hypotheses of Theorem 4.2,*

$$\text{ess sup}_{f \in \mathcal{F}} \sigma_{\max}(\mathbf{G}_{\Pi^+, \mathcal{C}_f}(f)) < \infty, \quad (4.80)$$

where $\Pi^+ = \{p \in \mathcal{P} : D^+(\Lambda_p) > 0\}$ and $\mathcal{F} = \bigcup_{r \in \mathcal{R}} \mathcal{F}_r$.

Proof. Suppose that Eq. (4.80) fails to hold, then some entries of $\mathbf{G}_{\Pi^+, \mathcal{C}_f}(f)$ are necessarily unbounded on \mathcal{F} . So let $p_o \in \Pi^+$ and $r_o \in \mathcal{R}$ be indices such that for every $\epsilon > 0$, there exists

$$\mathcal{G} \subseteq \mathcal{F}_{r_o} \cap \{f : |G_{p_o, r_o}(f)|^2 \geq 1/\epsilon\},$$

satisfying $\mu(\mathcal{G}) > 0$. Without loss of generality assume that $\mu(\mathcal{G}) < \infty$. Let $\{\mathcal{I}_k : k = 1, \dots, K\}$ be a finite collection of disjoint intervals such that

$$\mathcal{G}' = \bigcup_{k=1}^K \mathcal{I}_k,$$

satisfies $\mu(\mathcal{G}' \cap \mathcal{G}^c) \leq \delta$ and $\mu(\mathcal{G}'^c \cap \mathcal{G}) \leq \delta$, where $\delta = \epsilon\mu(\mathcal{G})/(1 + \epsilon)$. It follows easily that $\mu(\mathcal{G}') \geq \mu(\mathcal{G}) - \delta$. Now at least one interval \mathcal{I}_k satisfies

$$\frac{\mu(\mathcal{I}_k \cap \mathcal{G}^c)}{\mu(\mathcal{I}_k)} \leq \epsilon. \quad (4.81)$$

Otherwise, we would have

$$\mu(\mathcal{G}' \cap \mathcal{G}^c) = \sum_{k=1}^K \mu(\mathcal{I}_k \cap \mathcal{G}^c) > \sum_{k=1}^K \epsilon\mu(\mathcal{I}_k) = \epsilon\mu(\mathcal{G}') \geq \epsilon(\mu(\mathcal{G}) - \delta) = \delta,$$

violating our assumption that $\mu(\mathcal{G}' \cap \mathcal{G}^c) \leq \delta$. So, let \mathcal{I}_k denote an interval that satisfies Eq. (4.81). Define $\gamma = 1/(2\mu(\mathcal{I}_k))$. Since $D^+(\Lambda_{p_o}) > 0$, Proposition 4.3 and Eq. (4.21) imply that there exists $\tau \in \mathbb{R}$ such that

$$\#(\Lambda_{p_o} \cap B_\gamma(\tau)) \geq 2\gamma(D^+(\Lambda_{p_o})/2). \quad (4.82)$$

Define

$$X_{r_o}(f) = \begin{cases} e^{-j2\pi f\tau}/G_{p_o, r_o}(f) & \text{if } f \in \mathcal{I}_k \cap \mathcal{G}, \\ 0 & \text{otherwise,} \end{cases}$$

and $X_r(f) = 0$ for all $r \neq r_o$. Then, we clearly have

$$\|\mathbf{x}\|^2 \leq \epsilon\mu(\mathcal{I}_k). \quad (4.83)$$

Using Eq. (4.17), we conclude that

$$Y_{p_o}(f) = e^{-j2\pi f\tau} \chi(f \in \mathcal{I}_k \cap \mathcal{G}) = e^{-j2\pi f\tau} [\chi(f \in \mathcal{I}_k) - \chi(f \in \mathcal{I}_k \cap \mathcal{G}^c)],$$

whose inverse Fourier transform is

$$y_{p_o}(t) = \mu(\mathcal{I}_k) \text{sinc}(\mu(\mathcal{I}_k)(t - \tau)) e^{-j2\pi f_0(t - \tau)} - \phi_{\mathcal{I}_k \cap \mathcal{G}^c}(t - \tau), \quad t \in \mathbb{R}, \quad (4.84)$$

where $\text{sinc}(t) = \sin(\pi t)/(\pi t)$ and f_0 is the midpoint of \mathcal{I}_k . Note that

$$\sup_t |\phi_{\mathcal{I}_k \cap \mathcal{G}^c}(t)| \leq \mu(\mathcal{I}_k \cap \mathcal{G}^c) \leq \epsilon\mu(\mathcal{I}_k). \quad (4.85)$$

Then, for all t such that $|t - \tau| \leq \gamma = 1/(2\mu(\mathcal{I}_k))$, it follows from Eqs. (4.84) and (4.85) that

$$|y_{p_o}(t)| \geq \mu(\mathcal{I}_k)(\text{sinc}(1/2) - \epsilon). \quad (4.86)$$

Using Eqs. (4.82) and (4.86), we obtain

$$\begin{aligned} \sum_{p=1}^P \sum_{n \in \mathbb{Z}} |y_p(\lambda_{np})|^2 &\geq \sum_{n \in \mathbb{Z}} |y_{p_o}(\lambda_{np_o})|^2 \geq \sum_{\lambda \in \Lambda_{p_o} \cap B_\gamma(\tau)} |y_{p_o}(\lambda)|^2 \\ &\geq 2\gamma(D^+(\Lambda_{p_o})/2) [\mu(\mathcal{I}_k)(\text{sinc}(1/2) - \epsilon)]^2 \\ &= \frac{1}{2} D^+(\Lambda_{p_o}) \mu(\mathcal{I}_k) [\text{sinc}(1/2) - \epsilon]^2. \end{aligned}$$

Combining this result with Eq. (4.83), we conclude that

$$\sum_{p=1}^P \sum_{n \in \mathbb{Z}} |y_p(\lambda_{np})|^2 \geq \frac{1}{2\epsilon} D^+(\Lambda_{p_o}) [\text{sinc}(1/2) - \epsilon]^2 \|\mathbf{x}\|^2.$$

Since $\epsilon > 0$ is arbitrary, and $\mathbf{x} \in \mathcal{H}$ is nonzero, the above conclusion violates the second inequality of the stability condition Eq. (4.18), proving the necessity of Eq. (4.80). \square

In Theorem 4.3, suppose that $D^+(\Lambda_p) = 0$ for some $p \in \mathcal{P}$. Then the samples of y_p on Λ_p are too sparse to provide any useful information. Consequently, the p th row of the $\mathbf{G}(f)$ is irrelevant. Thus, Π^+ is the set of outputs whose samples are sufficiently dense to provide information about the inputs. Now, Eq. (4.80) can be interpreted as being equivalent to the upper stability bound in Eq. (4.18) for stable sampling.

We can view the set of densities

$$\{D^-(\{\Lambda_p : p \in \Pi\}) : \Pi \subseteq \mathcal{P}, \Pi \neq \emptyset\}$$

as a point in \mathbb{R}^{2^P-1} . However, if the sampling sets have uniform densities², then

$$D^-(\{\Lambda_p : p \in \Pi\}) = \sum_{p \in \Pi} D(\Lambda_p),$$

i.e., the joint densities become linearly related to each other, and they can all be described in terms of the individual densities. The resulting density space is now \mathbb{R}^P , which has a much smaller dimension. In general, we are interested in constructing stable sampling sets whose lower and upper densities are the smallest possible. Obviously, it becomes desirable to achieve minimum density sampling with sampling sets of uniform densities.

²Recall that a sampling set need not have uniform sample spacing in order to have uniform density.

Definition 4.5. The *density region for stable sampling* is defined as the collection of all (d_1, \dots, d_P) such that stable MIMO sampling is realizable using sampling sets $\{\Lambda_p\}$ of uniform densities $D(\Lambda_p) = d_p$, $p \in \mathcal{P}$.

Suppose that every Λ_p has uniform density $D(\Lambda_p) = d_p$, then the sampling density conditions in Eq. (4.47) reduce to

$$\sum_{p \in \Pi} d_p \geq \theta_S(\Pi), \quad \forall \Pi \subseteq \mathcal{P}, \quad (4.87)$$

$$\theta_S(\Pi) = \sum_{r=1}^R \mu(\mathcal{F}_r) - \int_{\mathbb{R}} \text{rank}(\mathbf{G}_{\Pi^c, \mathcal{C}_f}(f)) df.$$

Since Eq. (4.87) is a set of necessary conditions whose sufficiency is unknown, the region specified by Eq. (4.87) is generally an outer bound on the density region. It is clear that $\theta_S(\emptyset) = 0$ and $\theta_S(\Pi_1) \leq \theta_S(\Pi_2)$ whenever $\Pi_1 \subseteq \Pi_2$. Using Proposition 4.1, it is an easy exercise to show that

$$\theta_S(\Pi_1) + \theta_S(\Pi_2) \leq \theta_S(\Pi_1 \cup \Pi_2) + \theta_S(\Pi_1 \cap \Pi_2), \quad \forall \Pi_1, \Pi_2 \subseteq \mathcal{P}.$$

These properties of $\theta_S(\Pi)$ imply that the outer bound on the density region specified by the system of inequalities in Eq. (4.87) forms a contra-polymatroid [49, 50]. Consequently, every constraint in Eq. (4.87) is active, i.e., the equality in each constraint in Eq. (4.87) holds for some point in the region.

We now present a simple example to illustrate the necessary conditions for stable MIMO sampling.

Example 4.1. Consider a MIMO channel with $R = 2$ inputs and $P = 2$ outputs having the following transfer function matrix:

$$\mathbf{G}(f) = \begin{bmatrix} 1 & K(f) \\ 0 & 1 \end{bmatrix},$$

where $K(f) = (1 - 2f/3)\chi(f \in [0, 1.5])$ is shown in Figure 4.2. Let $\mathcal{F}_1 = [-1, 1)$ and $\mathcal{F}_2 = [0, 2)$ be the input spectral supports. Figure 4.3 illustrates the input and output spectra for a typical set of channel inputs.

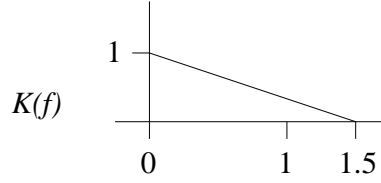


Figure 4.2 $K(f)$.

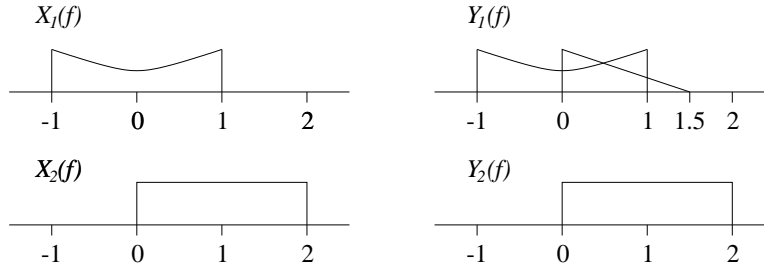


Figure 4.3 Typical spectra of the channel inputs and outputs.

We seek conditions on the sampling sets Λ_1 and Λ_2 for stable MIMO sampling with respect to $\mathbf{G}(f)$. We have $\mathcal{F} = \mathcal{F}_1 \cup \mathcal{F}_2 = [-1, 2]$ and

$$\mathbf{C}_f = \{r : f \in \mathcal{F}_r\} = \begin{cases} \{1\} & \text{if } f \in [-1, 0), \\ \{1, 2\} & \text{if } f \in [0, 1), \\ \{2\} & \text{if } f \in [1, 2), \\ \emptyset & \text{otherwise.} \end{cases}$$

It is easy to check that Eq. (4.80) is satisfied regardless of Π^+ . Also

$$\sigma_{\min}(\mathbf{G}_{\bullet, \mathcal{C}_f}(f)) = \frac{[2 + K^2(f)] - \sqrt{[2 + K^2(f)] - 4}}{2}.$$

This quantity is uniformly bounded from below because $K(f)$ is a bounded function. Hence, the necessary condition in Eq. (4.79) is satisfied. Applying Theorem 4.2, we obtain the following

density conditions:

$$\begin{aligned}
D^-(\Lambda_1, \Lambda_2) &\geq \mu(\mathcal{F}_1) + \mu(\mathcal{F}_2) = 4 \\
D^-(\Lambda_1) &\geq \mu(\mathcal{F}_1) + \mu(\mathcal{F}_2) - \int_{\mathbb{R}} \text{rank}(\mathbf{G}_{2, \mathcal{C}_f}(f)) df \\
&= 4 - \int_{[-1,0]} 0 df - \int_{[0,1]} 1 df - \int_{[1,2]} 1 df = 2 \\
D^-(\Lambda_2) &\geq \mu(\mathcal{F}_1) + \mu(\mathcal{F}_2) - \int_{\mathbb{R}} \text{rank}(\mathbf{G}_{1, \mathcal{C}_f}(f)) df \\
&= 4 - \int_{[-1,0]} 1 df - \int_{[0,1]} 1 df - \int_{[1,2]} \chi(K(f) \neq 0) df \\
&= 1.5.
\end{aligned}$$

Now, a simple calculation reveals that

$$\sigma_{\min}(\mathbf{G}_{1, \mathcal{C}_f}(f)) = \begin{cases} 1 & \text{if } f \in [-1, 0), \\ \sqrt{1 + K^2(f)} & \text{if } f \in [0, 1), \\ |K(f)| & \text{if } f \in [1, 2). \end{cases}$$

Clearly, this quantity takes arbitrarily small values in the vicinity of $f = 1.5$, where $K(f)$ vanishes. Hence, the bound on $D^-(\Lambda_2)$ is indeed a strict inequality. Another calculation reveals that³

$$\sigma_{\min}(\mathbf{G}_{2, \mathcal{C}_f}(f)) = \begin{cases} \infty & \text{if } f \in [-1, 0), \\ 1 & \text{if } f \in [0, 1), \\ 1 & \text{if } f \in [1, 2). \end{cases}$$

Hence, we cannot guarantee that the bound on $D^-(\Lambda_1)$ is a strict inequality. Thus, we obtain the following conditions on the joint densities:

$$D^-(\Lambda_1, \Lambda_2) \geq 4, \quad D^-(\Lambda_1) \geq 2, \quad \text{and} \quad D^-(\Lambda_2) > 1.5.$$

We shall now explain the above bounds intuitively. First of all, we can interpret Landau's classical sampling density result as follows: the sampling density must be no less than the number of *units of signal information*, where a unit of signal information, roughly speaking, equals the information contained in a unit bandwidth of a signal spectrum. In other words, sampling at unit density provides no more than one unit of signal information. In the MIMO

³Recall that we take $\sigma_{\min}(\mathbf{A}) = \infty$ if $\mathbf{A} = \mathbf{0}$.

problem, the condition $D^-(\Lambda_1, \Lambda_2) \geq 4$ is a natural generalization of Landau's result because the combined bandwidth of the input signals is 4 units.

Next, from at Figure 4.3, we see that $Y_2(f)$ is unaffected by $X_1(f)$. Therefore, $X_1(f)$ on the set $[-1, 0)$ must be reconstructed from the samples of y_2 alone. In order to reconstruct $X_1(f)$ and $X_2(f)$ on $[0, 1)$, it is clearly necessary that $Y_1(f)$ and $Y_2(f)$ on $[0, 1)$ be reconstructible from their samples. Now, $X_2(f)$ on $[1.5, 2)$ must be reconstructed based entirely on $Y_2(f)$. Combining all these observations, we see that the samples of y_1 contain enough information to reconstruct $Y_1(f)$ on $[-1, 1)$, while the samples of y_2 contain enough information to reconstruct $Y_2(f)$ on $[0, 1) \cup [1.5, 2)$. This explains that $D^-(\Lambda_1) \geq 2$ and that $D^-(\Lambda_2) \geq 1.5$. Suppose that $D^-(\Lambda_2) = 1.5$, then roughly speaking, there is just enough information in the samples of y_2 to reconstruct $Y_2(f)$ on $[0, 1) \cup [1.5, 2)$. Consequently, we must reconstruct $Y_2(f) = X_2(f)$ for all $f \in [1, 1.5)$ based entirely on the samples of y_1 . Now, $Y_1(f) = K(f)X_2(f)$ for $f \in [1, 1.5)$, where $K(f)$ takes arbitrarily small values on $[1, 1.5)$. Hence, this inversion cannot be accomplished stably, justifying the need for $D^-(\Lambda_2) > 1.5$.

Finally, we point out that we can have undersampling at each output and yet can be able to reconstruct all the inputs jointly from the available information. For instance, we do not need $D^-(\Lambda_1) \geq 2.5$, even though y_1 has a bandwidth of 2.5. To see this, we construct a sampling scheme for which the densities $(d_1, d_2) = (2, 2)$ are *achievable*, where $d_p = D(\Lambda_p)$, i.e., Λ_p has a uniform density of d_p . Let Λ_1 and Λ_2 be uniform sampling lattices:

$$\Lambda_1 = \Lambda_2 = \{n/2 : n \in \mathbb{Z}\}.$$

Clearly, $y_2 = x_2$ can be reconstructed stably. Now, the samples of x_1 on Λ_1 can be computed as follows:

$$x_1(\lambda_{n1}) = y_1(\lambda_{n1}) - k * x_2(\lambda_{n1}),$$

because $x_2(t)$ is known for all t . Thus, x_2 can also be reconstructed stably. However, it is not immediately clear whether all densities satisfying the necessary conditions are achievable, or how to achieve them.

4.3.3 Density conditions for consistent reconstruction

We now present the necessary condition for consistent MIMO reconstruction, which is a dual problem to the one of stable sampling.

Theorem 4.4. *Suppose that \mathcal{F}_r , $r \in \mathcal{R}$ are real sets of finite measure, and Λ_p , $p \in \mathcal{P}$ are discrete sets that constitute a collection of consistent reconstruction with respect to $\mathbf{G}(f)$ for*

$\mathcal{H} = \mathcal{B}(\mathcal{F}_1) \times \cdots \times \mathcal{B}(\mathcal{F}_R)$. Then for every $\Pi \subseteq \mathcal{P}$,

$$D^+(\{\Lambda_p : p \in \Pi\}) \leq \int_{\mathbb{R}} \text{rank}(\mathbf{G}_{\Pi, \mathcal{C}_f}(f)) df, \quad (4.88)$$

where $\mathcal{C}_f = \{r : f \in \mathcal{F}_r\}$. Furthermore, if

$$\text{ess inf}_{f \in \mathcal{F}} \sigma_{\min}(\mathbf{G}_{\Pi, \mathcal{C}_f}(f)) = 0, \quad \mathcal{F} = \bigcup_{r \in \mathcal{R}} \mathcal{F}_r, \quad (4.89)$$

for some $\Pi \neq \emptyset$, then the inequality in Eq. (4.88) is strict.

Proof. First note that the consistency condition implies that

$$\{\Theta_{\lambda_{np}} \psi_p : p \in \Pi, n \in \mathbb{Z}\}, \quad (4.90)$$

is a Riesz-Fischer sequence in \mathcal{H} , where ψ_p is defined in Eq. (4.19). Let $\Pi \subseteq \mathcal{P}$ be a fixed subset. Consider the following two cases. First suppose that either $\Pi = \emptyset$, or $D^+(\Lambda_p) = \infty$ for some $p \in \Pi$, or Eq. (4.89) does not hold: in this case take $\mathcal{D}_0 = \emptyset$. Otherwise, $D^+(\Lambda_p) < \infty$ for all $p \in \Pi \neq \emptyset$. So, we can define

$$K = \max_{p \in \Pi} C'(\Lambda_p)C(1) < \infty, \quad (4.91)$$

where C' and C are quantities defined in Lemma 4.1. Since Eq. (4.89) is satisfied in the second case, we can find a set \mathcal{D}_0 such that $\mu(\mathcal{D}_0) > 0$, and

$$\sigma_{\min}(\mathbf{G}_{\Pi, \mathcal{C}_f}(f)) \leq \epsilon_0, \quad \forall f \in \mathcal{D}_0. \quad (4.92)$$

where $\epsilon_0 > 0$ is such that $K\epsilon_0^2 \leq a/4$, and a is the bound for the Riesz-Fischer sequence in Eq. (4.90). Assume without loss of generality that $\mathcal{D}_0 \subseteq [\nu, \nu + 1]$ for some $\nu \in \mathbb{R}$. Thus, Eq. (4.92) is satisfied in both cases. Let the dimension of the range space of $\mathbf{G}_{\Pi, \mathcal{C}_f}^H(f)$ be denoted by

$$\rho(f) = \text{rank}(\mathbf{G}_{\Pi, \mathcal{C}_f}(f)), \quad (4.93)$$

and let the columns of $\mathbf{U}'(f) \in \mathbb{C}^{|\mathcal{C}_f| \times \rho(f)}$ form an orthonormal basis for the range space of $\mathbf{G}_{\Pi, \mathcal{C}_f}^H(f)$. Note that $\rho(f)$ is defined differently from $\rho(f)$ in the proof of Theorem 4.2. For $f \in \mathcal{D}_0$, let $\mathbf{U}''(f) \in \mathbb{C}^{|\mathcal{C}_f| \times 1}$ be a unit-norm right singular vector of $\mathbf{G}_{\Pi, \mathcal{C}_f}(f)$ corresponding to its smallest nonzero singular value. There is no loss of generality in assuming that the first column of $\mathbf{U}'(f)$ equals $\mathbf{U}''(f)$ for all $f \in \mathcal{D}_0$. Hence, for $f \in \mathcal{D}_0$, we can write

$$\mathbf{U}'(f) = [\mathbf{U}''(f) \ \mathbf{U}(f)],$$

for some $\mathbf{U}(f)$. For $f \notin \mathcal{D}_0$, let $\mathbf{U}(f) = \mathbf{U}'(f)$. The columns of $\mathbf{U}(f)$ are clearly orthonormal. Note that $\mathbf{U}'(f)$ and $\mathbf{U}''(f)$ can be assumed to be measurable. The matrix $\mathbf{U}(f)$ has r columns for $f \in \mathcal{G}_r$, where

$$\mathcal{G}_r = \{f : \rho(f) - \chi(f \in \mathcal{D}_0) = r\}, \quad r \in \mathcal{R}. \quad (4.94)$$

Each \mathcal{G}_r has finite measure. Since the sets $\{\mathcal{G}_r\}$ are disjoint, we can find, as in the proof of Theorem 4.2, a collection of disjoint intervals $\{\mathcal{I}_{rk} : r \in \mathcal{R}, k = 1, \dots, K_r\}$ and sets \mathcal{G}'_r as in Eq. (4.54) such that Eqs. (4.55) and (4.56) hold. In the rest of the proof, assume that $q = q(r, k, m)$ for some invertible index-mapping as in the proof of Theorem 4.2. Define $\mathbf{W}^r(f) \in \mathbb{C}^{R \times r}$, $\mathbf{S}_q(f)$, and Σ_q exactly as in Eqs. (4.57), (4.58), and (4.59), respectively. Also let \mathcal{H}_S be the closed subspace of \mathcal{H}_∞ defined as in Eq. (4.60). Using arguments similar to those in Theorem 4.2, we see that

$$\{\Theta_{\sigma_{nq}} \mathbf{s}_q : q \in \mathcal{Q}, n \in \mathbb{Z}\}$$

is an orthonormal Riesz basis for \mathcal{H}_S . In particular, it is a frame for \mathcal{H}_S . It is also easily verified that \mathcal{H}_S is a shift-invariant subspace of \mathcal{H}_∞ .

Now, $\{\Theta_{\lambda_{np}} \psi_p : p \in \Pi, n \in \mathbb{Z}\}$, being a subcollection of the set in Eq. (4.90), is also a Riesz-Fischer sequence in \mathcal{H} . Let $\{c_{np}\}$, $p \in \Pi$ be some finite sequences. Then Eq. (4.20) implies that

$$\max_{\mathbf{x} \in \mathcal{B}_{\mathcal{H}}} \left| \sum_{n,p} c_{np} y_p(\lambda_{np}) \right|^2 \geq a \sum_{n,p} |c_{np}|^2. \quad (4.95)$$

Let $\mathbf{x}^\circ \in \mathcal{B}_{\mathcal{H}}$ be the maximizer of the left-hand side of Eq. (4.95), and $\mathbf{Y}^\circ(f) = \mathbf{G}(f) \mathbf{X}^\circ(f)$, its corresponding MIMO channel output. Then,

$$\left| \sum_{n,p} c_{np} y_p^\circ(\lambda_{np}) \right| \geq \sqrt{a} \|c\|. \quad (4.96)$$

Next, the subspace

$$\mathcal{H}_L = \{\mathbf{x} \in \mathcal{H} : \mathbf{X}_{c_f}(f) = \mathbf{U}(f) \mathbf{U}^H(f) \mathbf{X}_{c_f}(f) \text{ a.e.}\} \quad (4.97)$$

is closed and shift-invariant by the same argument as in the proof of Theorem 4.2. Note that

$$\mathbf{X}(f) = \mathbf{I}_{\bullet, c_f} \mathbf{U}(f) \mathbf{U}^H(f) \mathbf{I}_{c_f, \bullet} \mathbf{X}(f) \quad (4.98)$$

is an equivalent way of stating $\mathbf{x} \in \mathcal{H}_L$ because $\mathbf{X}_{c_f}(f)$ captures all the nonzero elements of $\mathbf{X}(f)$ for every $\mathbf{x} \in \mathcal{H}$. Let $\mathbf{x}' \in \mathcal{H}$ be defined as follows:

$$\mathbf{X}'_{c_f}(f) = \mathbf{U}(f) \mathbf{U}^H(f) \mathbf{X}_{c_f}^\circ(f).$$

Evidently $\mathbf{x}' \in \mathcal{H}_L$ and $\|\mathbf{x}'\| \leq 1$ because $\mathbf{U}(f)$ has orthonormal columns. Let $\mathbf{Y}'(f) = \mathbf{G}(f)\mathbf{X}'(f)$ and $\mathbf{Y}''(f) = \mathbf{Y}^\circ(f) - \mathbf{Y}'(f)$. Then for all $f \notin \mathcal{D}_0$, we have $\mathbf{U}(f) = \mathbf{U}'(f)$. Hence, using the definition of $\mathbf{U}'(f)$, we conclude that

$$\mathbf{Y}''_{\Pi}(f) = \mathbf{G}_{\Pi, \mathcal{C}_f}(f) [\mathbf{X}_{\mathcal{C}_f}^\circ(f) - \mathbf{U}'(f)\mathbf{U}'^H(f)\mathbf{X}_{\mathcal{C}_f}^\circ(f)] = \mathbf{0}. \quad (4.99)$$

For $f \in \mathcal{D}_0$, we have $\mathbf{U}(f)\mathbf{U}^H(f) = \mathbf{U}'(f)\mathbf{U}'^H(f) - \mathbf{U}''(f)\mathbf{U}''^H(f)$. Hence,

$$\begin{aligned} \|\mathbf{Y}''_{\Pi}(f)\| &= \|\mathbf{G}_{\Pi, \mathcal{C}_f}(f) [\mathbf{X}_{\mathcal{C}_f}^\circ(f) - \mathbf{U}(f)\mathbf{U}^H(f)\mathbf{X}_{\mathcal{C}_f}^\circ(f)]\| \\ &= \|\mathbf{G}_{\Pi, \mathcal{C}_f}(f)\mathbf{U}''(f)\mathbf{U}''^H(f)\mathbf{X}_{\mathcal{C}_f}^\circ(f)\| \\ &\leq \epsilon_0 \|\mathbf{X}_{\mathcal{C}_f}^\circ(f)\|. \end{aligned} \quad (4.100)$$

Combining Eqs. (4.99) and (4.100), and using $\|\mathbf{x}^\circ\| \leq 1$, we have

$$\int_{\mathbb{R}} \|\mathbf{Y}''_{\Pi}(f)\|^2 df \leq \begin{cases} \epsilon_0^2 & \text{if } \mu(\mathcal{D}_0) > 0, \\ 0 & \text{if } \mu(\mathcal{D}_0) = 0. \end{cases} \quad (4.101)$$

Notice that $Y_p''(f)$ is supported on $\mathcal{D}_0 \subseteq [\nu, \nu + 1]$ for all $p \in \Pi$. Recall that $\mu(\mathcal{D}_0) > 0$ implies that $D^+(\Lambda_p) < \infty$. In this case, we can invoke Lemma 4.1 to conclude that

$$\sum_{p \in \Pi} \sum_{n \in \mathbb{Z}} |y_p''(\lambda_{np})|^2 \leq K\epsilon_0^2, \quad (4.102)$$

where K is the constant defined in Eq. (4.91). However, if $\mu(\mathcal{D}_0) = 0$, then $\mathbf{Y}''_{\Pi}(f) = \mathbf{0}$ from Eq. (4.101), and hence, Eq. (4.102) holds trivially. In other words Eq. (4.102) always holds, and using the Cauchy-Schwarz inequality, we conclude that

$$\left| \sum_{p \in \Pi} \sum_{n \in \mathbb{Z}} c_{np} y_p''(\lambda_{np}) \right| \leq \sqrt{K}\epsilon_0 \|c\|, \quad (4.103)$$

Recall that ϵ_0 is chosen so that $K\epsilon_0^2 \leq a/4$. So, combining Eqs. (4.96) and (4.103) and noting that $y_p' = y_p^\circ - y_p''$, we obtain

$$\left| \sum_{p \in \Pi} \sum_{n \in \mathbb{Z}} c_{np} y_p'(\lambda_{np}) \right| \geq (\sqrt{a} - \sqrt{K}\epsilon_0) \|c\| \geq \frac{\sqrt{a}}{2} \|c\|.$$

Since the quantities $\{y_p'\}$ are the channel outputs corresponding to an input $\mathbf{x}' \in \mathcal{H}_L$ satisfying $\|\mathbf{x}'\| \leq 1$, we have

$$\max_{\mathbf{x}' \in \mathcal{B}_{\mathcal{H}_L}} \left| \sum_{p \in \Pi} \sum_{n \in \mathbb{Z}} c_{np} y_p(\lambda_{np}) \right|^2 \geq \frac{a}{4} \|c\|^2. \quad (4.104)$$

Define $\mathbf{l}_p = P_{\mathcal{H}_L} \psi_p$. Since \mathcal{H}_L is shift-invariant, we obtain $\Theta_{\lambda_{np}} \mathbf{l}_p \in \mathcal{H}_L$ and $y_p(\lambda_{np}) = \langle \mathbf{x}, \Theta_{\lambda_{np}} \mathbf{l}_p \rangle$ using the same argument as in Eqs. (4.69) and (4.70). Therefore, Eq. (4.104) implies that

$$\left\| \sum_{p \in \Pi} \sum_{n \in \mathbb{Z}} c_{np} \Theta_{\lambda_{np}} \mathbf{l}_p \right\|^2 \geq \frac{a}{4} \|c\|^2$$

for all finite sequences $\{c_{np}\}$, $p \in \Pi$. Then we conclude, using Eq. (4.10), that $\{\Theta_{\lambda_{np}} \mathbf{l}_p : p \in \Pi, n \in \mathbb{Z}\}$ is a Riesz-Fischer sequence in \mathcal{H}_L with bound $a/4$.

To avoid confusion, we point out that the quantities associated with the frame in this proof are \mathcal{H}_S , Σ_q , \mathbf{s}_q etc., while those associated with the Riesz-Fischer sequence are \mathcal{H}_L , Λ_p , \mathbf{l}_p etc. This is opposite from the convention adopted in the proofs of Theorems 4.1 and 4.2. We shall estimate the quantities

$$\alpha_p = \sqrt{\frac{4}{a}} \sup_{\lambda \in \Lambda_p} \|\Theta_{\lambda} \mathbf{l}_p - P_{\mathcal{H}_S} \Theta_{\lambda} \mathbf{l}_p\|$$

defined in Theorem 4.1 shortly, but first, we define $\mathbf{v}_p \in \mathcal{H}_{\infty}$ for $p \in \Pi$ as follows:

$$\mathbf{V}_p(f) = \begin{cases} \mathbf{L}_p(f) & \text{if } f \in \mathcal{G}'_r \cap \mathcal{G}_r, \text{ for some } r, \\ \mathbf{0} & \text{otherwise.} \end{cases} \quad (4.105)$$

Since $\mathbf{l}_p \in \mathcal{H}_L$, Eq. (4.98) implies that

$$\mathbf{L}_p(f) = \mathbf{I}_{\bullet, \mathcal{C}_f} \mathbf{U}(f) \mathbf{U}^H(f) \mathbf{I}_{\mathcal{C}_f, \bullet} \mathbf{L}_p(f).$$

Therefore, whenever $f \in \mathcal{G}'_r \cap \mathcal{G}_r$, we have

$$\begin{aligned} \mathbf{V}_p(f) &= \mathbf{I}_{\bullet, \mathcal{C}_f} \mathbf{U}(f) \mathbf{U}^H(f) \mathbf{I}_{\mathcal{C}_f, \bullet} \mathbf{L}_p(f) \\ &= \sum_{m=1}^r \mathbf{I}_{\bullet, \mathcal{C}_f} \mathbf{U}_{\bullet, m}(f) [\mathbf{U}_{\bullet, m}^H(f) \mathbf{I}_{\mathcal{C}_f, \bullet} \mathbf{L}_p(f)]. \end{aligned}$$

Using Eqs. (4.54), (4.58), and the above observation, we can express $\mathbf{V}_p(f)$ as a linear combination involving $\mathbf{S}_q(f)$:

$$\mathbf{V}_p(f) = \sum_{r=1}^R \sum_{k=1}^{K_r} \sum_{m=1}^r \sqrt{\mu(\mathcal{I}_{rk})} \mathbf{S}_q(f) [\mathbf{U}_{\bullet, m}^H(f) \mathbf{I}_{\mathcal{C}_f, \bullet} \mathbf{L}_p(f)] \chi(f \in \mathcal{G}_r), \quad f \in \mathbb{R}.$$

Now, the quantity $[\mathbf{U}_{\bullet, m}^H(f) \mathbf{I}_{\mathcal{C}_f, \bullet} \mathbf{L}_p(f)]$ is clearly square-integrable, and we conclude that $\mathbf{v}_p \in \mathcal{H}_S$. Recall that \mathcal{H}_S is shift-invariant. Thus, using Proposition 4.4, we obtain

$$\begin{aligned} \alpha_p &= \sqrt{\frac{4}{a}} \sup_{\lambda \in \Lambda_p} \|\Theta_{\lambda} \mathbf{l}_p - P_{\mathcal{H}_S} \Theta_{\lambda} \mathbf{l}_p\| \\ &= \frac{2}{\sqrt{a}} \|\mathbf{l}_p - P_{\mathcal{H}_S} \mathbf{l}_p\| \leq \frac{2}{\sqrt{a}} \|\mathbf{l}_p - \mathbf{v}_p\|. \end{aligned}$$

Using Parseval's theorem and Eq. (4.105), we obtain the following estimate for α_p :

$$\begin{aligned}\alpha_p &\leq \frac{2}{\sqrt{a}} \left(\int_{\mathbb{R}} \|\mathbf{L}_p(f) - \mathbf{V}_p(f)\|^2 df \right)^{\frac{1}{2}} \\ &= \frac{2}{\sqrt{a}} \left(\sum_{r=1}^R \int_{\mathcal{G}'_r \cap \mathcal{G}_r^c} \|\mathbf{L}_p(f)\|^2 df \right)^{\frac{1}{2}}.\end{aligned}$$

The last expression can be made arbitrarily small for sufficiently small δ , because each $\mathbf{L}_p(f)$ is square-integrable, and $\mu(\mathcal{G}'_r \cap \mathcal{G}_r^c) \leq \delta/R^2$. Hence, for any $\epsilon > 0$ and sufficiently small $\delta > 0$, we can guarantee that $\alpha_p \leq \epsilon$. Applying Theorem 4.1, we obtain $D^+(\Lambda_p) < \infty$ for $p \in \Pi$ and

$$D^+(\Sigma_1, \dots, \Sigma_Q) \geq D^+(\{\Lambda_p : p \in \Pi\}) - \sum_{p \in \Pi} \alpha_p D^+(\Lambda_p). \quad (4.106)$$

Using the estimate for α_p and the fact that Σ_q has a uniform density of $\mu(\mathcal{I}_{rk})$ in Eq. (4.106), we obtain

$$\begin{aligned}D^+(\{\Lambda_p : p \in \Pi\}) &\leq \sum_{r,m,k} \mu(\mathcal{I}_{rk}) + \epsilon \sum_{p \in \Pi} D^+(\Lambda_p) \\ &= \sum_{r=1}^R r\mu(\mathcal{G}'_r) + \epsilon \sum_{p \in \Pi} D^+(\Lambda_p) \\ &\leq \sum_{r=1}^R r\mu(\mathcal{G}_r) + \delta + \epsilon \sum_{p \in \Pi} D^+(\Lambda_p).\end{aligned} \quad (4.107)$$

Using Eqs. (4.93), (4.94), and the definition of the Lebesgue integral, we have

$$\sum_{r=1}^R r\mu(\mathcal{G}_r) = \int_{\mathbb{R}} [\rho(f) - \chi(f \in \mathcal{D}_0)] df = \int_{\mathbb{R}} \text{rank}(\mathbf{G}_{\Pi, \mathcal{C}_f}(f)) df - \mu(\mathcal{D}_0). \quad (4.108)$$

Combining Eqs. (4.107) and (4.108), and letting $\delta, \epsilon \rightarrow 0$, we obtain

$$D^+(\{\Lambda_p : p \in \Pi\}) \leq \int_{\mathbb{R}} \text{rank}(\mathbf{G}_{\Pi, \mathcal{C}_f}(f)) df - \mu(\mathcal{D}_0).$$

This proves Eq. (4.88). We have already demonstrated that $D^+(\Lambda_p) < \infty$. Therefore, if Eq. (4.89) is satisfied for some $\Pi \neq \emptyset$, we have $\mu(\mathcal{D}_0) > 0$, implying that the inequality in Eq. (4.88) is strict. \square

Theorem 4.4 is the generalization of Landau's necessary density condition for interpolation. In particular, if $\mathbf{G}(f)$ satisfies Eq. (4.79), then

$$\text{rank}(\mathbf{G}_{\Pi, \mathcal{C}_f}(f)) \leq |\mathcal{C}_f|.$$

Under this condition, it follows from Eq. (4.88) for $\Pi = \mathcal{P}$ that

$$D^+(\Lambda_1, \dots, \Lambda_P) \leq \sum_{r=1}^R \mu(\mathcal{F}_r), \quad (4.109)$$

which states that the joint density of Λ_p cannot exceed the combined bandwidth of the input signals. Note that Eq. (4.79) need not hold for consistent reconstruction, and we would get a stronger upper bound on the joint density than Eq. (4.109) when Eq. (4.79) does not hold. Theorem 4.4 also provides conditions on the joint densities of all subcollections of $\{\Lambda_p\}$. We have already seen that the quantity

$$\int_{\mathbb{R}} \text{rank}(\mathbf{G}_{\Pi, \mathcal{C}_f}(f)) df$$

is a measure of “signal information” contained in the samples of $\{y_p(\lambda_{np}) : p \in \Pi\}$. We can think of $y_p(\lambda_{np}) = c_{np}$ as constraints that restrict the freedom of the input \mathbf{x} . In the consistent reconstruction problem, we interpret the *constraint density* $D^+(\{\Lambda_p : p \in \Pi\})$ as a lower bound of this lost freedom measured in units of signal information. For the existence of a solution to the consistency problem, we require that the constraint density be no more than the amount of signal information present in the inputs, thereby justifying Eq. (4.88).

The following corollary is an exact dual of Corollary 4.1.

Corollary 4.2. *Suppose that the hypotheses of Theorem 4.4 are satisfied and $\mathcal{F} = \bigcup_{r \in \mathcal{R}} \mathcal{F}_r$, then*

$$\text{ess inf}_{f \in \mathcal{F}} \lambda_{\min}(\mathbf{G}_{\Pi, \mathcal{C}_f}^H(f) \mathbf{G}_{\Pi, \mathcal{C}_f}(f)) > 0, \quad (4.110)$$

for every $\Pi \subseteq \mathcal{P}$, $\Pi \neq \emptyset$ such that

$$D^+(\{\Lambda_p : p \in \Pi\}) = \sum_{r=1}^R \mu(\mathcal{F}_r). \quad (4.111)$$

Proof. From Theorem 4.4 and Eq. (4.51), we have

$$D^+(\{\Lambda_p : p \in \Pi\}) \leq \int_{\mathbb{R}} \text{rank}(\mathbf{G}_{\Pi, \mathcal{C}_f}(f)) df \leq \int_{\mathbb{R}} |\mathcal{C}_f| = \sum_{r=1}^R \mu(\mathcal{F}_r).$$

If Eq. (4.111) holds, then both the above inequalities are, in fact, equalities. Then observe that Eq. (4.88) is satisfied with an equality, implies that Eq. (4.89) fails to hold. Also, $\text{rank}(\mathbf{G}_{\Pi, \mathcal{C}_f}(f)) = |\mathcal{C}_f|$, implying that

$$\lambda_{\min}(\mathbf{G}_{\Pi, \mathcal{C}_f}^H(f) \mathbf{G}_{\Pi, \mathcal{C}_f}(f)) = [\sigma_{\min}(\mathbf{G}_{\Pi, \mathcal{C}_f}(f))]^2$$

Now Eq. (4.110) follows by combining the last two observations. □

Corollary 4.2 can be interpreted as follows. Suppose that the smallest singular value of $\mathbf{G}_{\Pi, \mathcal{C}_f}$ takes arbitrarily small values, then there are inputs with unit energy that can produce outputs y_p , $p \in \Pi$ of arbitrarily small energies. Roughly speaking, this means that we can find an l^2 sequences $\{c_{np}\}$ for which the consistency problem does not have a finite-energy solution $\mathbf{x} \in \mathcal{H}$ if we are operating at the critical sampling density, i.e., with an equality in Eq. (4.88).

Once again, we consider the case where the sampling sets have uniform densities, as it enables us to reduce the dimension of the space of densities from \mathbb{R}^{2^P-1} to \mathbb{R}^P .

Definition 4.6. The *density region for consistency* is defined as the collection of all (d_1, \dots, d_P) such that consistent MIMO reconstruction is realizable using sampling sets $\{\Lambda_p\}$ of uniform densities $D(\Lambda_p) = d_p$, $p \in \mathcal{P}$.

Suppose that every Λ_p has uniform density with $D(\Lambda_p) = d_p$, then the consistency conditions in Eq. (4.88) reduce to

$$\sum_{p \in \Pi} d_p \geq \theta_C(\Pi), \quad \forall \Pi \subseteq \mathcal{P}, \quad (4.112)$$

$$\theta_C(\Pi) = \int_{\mathbb{R}} \text{rank}(\mathbf{G}_{\Pi, \mathcal{C}_f}(f)) df.$$

As in the case of stable MIMO sampling, the above region is an outer bound on the density region for consistency. Next, observe that $\theta_C(\emptyset) = 0$ and $\theta_C(\Pi_1) \leq \theta_C(\Pi_2)$ whenever $\Pi_1 \subseteq \Pi_2$. Consequently, we can use Proposition 4.1 to show that

$$\theta_C(\Pi_1) + \theta_C(\Pi_2) \geq \theta_C(\Pi_1 \cup \Pi_2) + \theta_C(\Pi_1 \cap \Pi_2), \quad \forall \Pi_1, \Pi_2 \subseteq \mathcal{P}.$$

These properties of $\theta_C(\Pi)$ imply that the system of inequalities in Eq. (4.112) forms a polymatroid [49, 50], implying that every constraint in Eq. (4.112) is active for some point in the region.

We now present an example to illustrate the results for consistent reconstruction.

Example 4.2. Let the MIMO channel and the input spectral supports be as defined in Example 4.1. We seek necessary conditions on the sampling sets Λ_1 and Λ_2 for consistent reconstruction. Fortunately, we have already performed all the necessary calculations in Example 4.1. Applying Theorem 4.4, we obtain the following bounds on the joint densities:

$$D^+(\Lambda_1, \Lambda_2) \leq \int_{\mathbb{R}} \text{rank}(\mathbf{G}_{\bullet, \mathcal{C}_f}(f)) df = 4,$$

$$D^+(\Lambda_1) < \int_{\mathbb{R}} \text{rank}(\mathbf{G}_{1, \mathcal{C}_f}(f)) df = 2.5,$$

$$D^+(\Lambda_2) \leq \int_{\mathbb{R}} \text{rank}(\mathbf{G}_{2, \mathcal{C}_f}(f)) df = 2.$$

These inequalities can be justified as follows. The combined bandwidth of the inputs is 4, requiring $D^+(\Lambda_1, \Lambda_2) \leq 4$ for consistency. Now, if consistent reconstruction of x_1 and x_2 is possible, then in particular, we must also have consistent reconstruction (or interpolation) of y_1 and y_2 from their respective samples. Looking at Figure 4.3, pg. 74, we see that $Y_2(f) = X_2$ is bandlimited to $[0, 2)$. Therefore, by Landau's interpolation density result, we require $D^+(\Lambda_2) \leq 2$ for consistent reconstruction of y_2 . Finally, $Y_1(f)$ is bandlimited to $[-1, 2.5)$, thereby requiring $D^+(\Lambda_1) \leq 2.5$. However, $D^+(\Lambda_1) = 2.5$ is not allowed because $K(f)$ is arbitrarily small in the vicinity of $f = 1.5$.

We now show that the point $(d_1, d_2) = (2, 2)$ is achievable, where $d_p = D(\Lambda_p)$ for sampling sets $\{\Lambda_p\}$ of uniform density. Let Λ_1 and Λ_2 be defined as in Example 4.1. Let $\{c_{n1}\}$ and $\{c_{n2}\}$ be l^2 sequences. Then the problem $y_2(\lambda_{n2}) = c_{n2}$ clearly has a solution $y_2 \in \mathcal{B}([0, 2])$. Now, the sequence $d_n = k * x_2(\lambda_{n1})$ is square-summable because $K(f)$ is a bounded function, implying that

$$x_1(\lambda_{n1}) = y_1(\lambda_{n1}) - k * x_2(\lambda_{n1}) = c_{n1} - d_n,$$

also has a solution $x_1 \in \mathcal{B}([-1, 1])$. This proves that $(d_1, d_2) = (2, 2)$ is achievable.

Remark. Recall that a collection of sets that is both a collection of stable sampling and consistent reconstruction provides a Riesz basis for the space \mathcal{H} . Unfortunately, the existence of such bases is difficult to prove (or disprove) for a given \mathcal{H} . In fact, the simpler problem of finding exponential Riesz bases for $\mathcal{B}(\mathcal{F})$ is still unsolved except for special sets. For instance, the simplest case $\mathcal{F} = [a, b]$ is very well studied, and Riesz bases are easy to construct for $\mathcal{B}(\mathcal{F})$. The problem is also solved when \mathcal{F} is a finite union of intervals of whose lengths are commensurate, or an arbitrary union of two intervals [51–53]. However, even the case where \mathcal{F} is an arbitrary finite union of intervals is unsolved.

4.4 Summary

In this chapter, we formulated the MIMO sampling scheme and defined the notions of stable MIMO sampling and consistent MIMO reconstruction. These notions are generalizations of the definitions of stable sampling and interpolation for classical sampling. We also generalized the definitions of upper and lower sampling densities applicable to *collections* of sampling sets.

Strengthening an idea of Gröchenig and Razafinjato, we proved a comparison theorem, which in turn allowed us to deduce necessary density conditions for stable sampling and consistent reconstruction in the MIMO setting. For the stability of MIMO sampling, we find that a family of $2^P - 1$ bounds hold—a lower bound on the joint lower density of each nonempty

set of output sampling sets. Similarly we find that a family of $2^P - 1$ hold for the consistency problem. This time, they are upper bounds on the joint upper densities of the sampling sets. These bounds generalize density results that Landau derived for the classical sampling problem, and like Landau's results, they are fundamentally important bounds. Since the MIMO sampling scheme is extremely general, and encompasses various sampling schemes such as Papoulis's generalized sampling, and multicoset or periodic nonuniform sampling as special cases, we have automatically generated necessary conditions for all these sampling schemes.

Finally, we point out that the comparison theorem is a general and powerful result. If the relevant frames vectors, Riesz-Fischer sequences and their parent spaces are defined properly in the theorem, it has potential use for deriving density results for other class of input signals such as wavelet and spline spaces.

CHAPTER 5

SAMPLING THEOREMS FOR UNIFORM AND PERIODIC NONUNIFORM MIMO SAMPLING OF MULTIBAND SIGNALS

5.1 Introduction

The study of MIMO channel equalization is motivated by applications in multichannel deconvolution and multiple source separation. Some example applications where MIMO channels arise are multiuser or multiaccess communications, multichannel image restoration, and geophysical data processing [37–43]. In practice, the equalizer is implemented using digital signal processors. However, the MIMO channel inputs and outputs are continuous-time signals, implying that the channel outputs need to be sampled prior to processing by the digital system. Hence, the problem is equivalent to reconstructing the channel inputs from the sampled output signals. In other words, the MIMO channel inversion problem can be restated as one in sampling theory, and we call this sampling scheme *MIMO sampling*. Most work to date on multichannel deconvolution has addressed discrete-time channel models, apparently assuming that each output is sampled at the appropriate rate common Nyquist rate sufficient for reconstruction of each output. However as we demonstrate in this chapter, this is not necessary, and appropriately chosen nonuniform sampling schemes with lower average sampling density suffice for perfect reconstruction of the MIMO channel inputs.

Although motivated by real world problems, MIMO sampling is an important problem in sampling theory in its own right. Several sampling schemes can be expressed as special cases of the MIMO setting. For example, for a SIMO channel (i.e., $R = 1$), the outputs are filtered and uniformly sampled versions of a single input signal. In other words, this is precisely Papoulis's generalized sampling [12]. Additionally, if the channel filters are chosen to be pure delays, we obtain multicoset or periodic nonuniform sampling of the input which has been widely studied [14–24], as it allows us to approach the Landau minimum sampling for multiband signals [6].

Seidner and Feder [13] provide a natural generalization of Papoulis’s sampling expansions for a vector inputs whose components are bandlimited to $[-B, B]$. Their sampling scheme is clearly a special case of MIMO sampling. We deal only with multiband signal spaces, and we refer the reader to [44] for some results on multichannel sampling for general signal spaces such as wavelet and spline spaces.

We derived necessary sampling density conditions for the MIMO problem in Chapter 4. It is not clear if those conditions are sufficient, however they indicate the potential for reduction in the sampling density needed for stable sampling relative to the Nyquist rate. In this chapter, we demonstrate how to achieve stable sampling and reconstruction at rates lower than the Nyquist rate. We can think of these results as partial sufficient conditions for stable MIMO sampling, although we do not provide explicit bounds on the sampling densities themselves. These results complement our results in Chapter 4.

5.1.1 Problem formulation

Figure 5.1 illustrates the block diagram for MIMO sampling. The channel is shown to the left of the dashed line, and its inputs $x_r(t)$ are assumed to be continuous-time signals. The channel is modeled as a linear time-invariant system. The channel outputs are sampled at a uniform rate of $1/T$ to produce discrete-time sequences, $z_p[n]$. From a practical viewpoint, we can interpret this as the sampling step prior to processing digitally. The reconstruction block, shown to the right of the dashed line, inverts the MIMO channel to produce estimates $\tilde{x}_r(t)$ of the input signals. In the context of MIMO sampling, we showed in Chapter 4 that stable sampling and reconstruction of the inputs imposes lower bounds on the sampling densities on the various channels. These results are analogues of Landau’s classic minimum density results for multiband sampling [6].

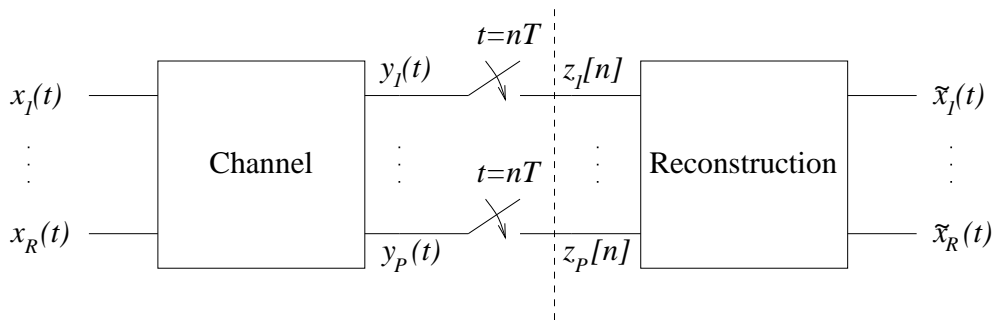


Figure 5.1 Models for MIMO sampling and reconstruction.

The problem that we address in this chapter is a special case of MIMO sampling problem introduced in Chapter 4, where the channel outputs are sampled uniformly. Even though we consider only *uniform* sampling of the MIMO channel outputs, we shall see later that this sampling scheme is fairly general, and it encompasses most periodic nonuniform sampling of the channel outputs, with sampling at different rates on different channels.

We study the following issues in this chapter: (a) the relation of stable MIMO sampling to frame theory, and (b) the necessary and sufficient conditions on the channel allowing to achieve perfect reconstruction of the inputs under uniform sampling. We focus entirely on the uniform sampling problem, with the understanding that results for the periodic nonuniform case can be obtained similarly.

This chapter is organized as follows. Section 5.2 contains some notation and definitions used in the rest of the chapter. In Section 5.3 we present models for the channel and reconstruction. The input signals are modeled as multiband signals, with different band structures. Section 5.4 deals with the problem of perfect reconstruction of the channel inputs. We explore the connection between MIMO sampling and frame theory. The computation of the frame bounds enables us to determine necessary conditions on the input signal spaces, the channel characteristics, and the sampling rate for the existence of reconstruction filters that achieves stable and perfect reconstruction of the inputs. We also present additional conditions under which there exist reconstruction filters that are continuous in the frequency domain. This, as elaborated later, is important from the viewpoint of FIR filter design.

5.2 Preliminaries

We begin with a some basic definitions and notation. We denote the Fourier transform of a continuous-time square-integrable signal $x(t)$ by

$$X(f) = \int_{\mathbb{R}} x(t)e^{-j2\pi ft} dt.$$

Similarly, for a discrete-time signal $y[n]$, we define its Fourier transform be

$$Y[\nu] = \sum_{n \in \mathbb{Z}} y[n]e^{-j2\pi\nu n}.$$

In general, we denote discrete-time and continuous-time signals (either scalar-valued or vector-valued) using lower-case letters, and their Fourier transforms by the corresponding upper-case letters. Let the class of continuous, finite-energy signals bandlimited to the set of frequencies \mathcal{F} be

$$\mathcal{B}(\mathcal{F}) = \{x \in L^2(\mathbb{R}) \cap C(\mathbb{R}) : X(f) = 0, \forall f \notin \mathcal{F}\}. \quad (5.1)$$

Denote the interior and closure of a set $\mathcal{S} \subseteq \mathbb{R}$ by $\text{int } \mathcal{S}$ and $\overline{\mathcal{S}}$, respectively, the class of complex-valued matrices of size $M \times N$ by $\mathbb{C}^{M \times N}$, the conjugate-transpose of \mathbf{A} by \mathbf{A}^H , its pseudo inverse by \mathbf{A}^\dagger . For a given matrix \mathbf{A} , let $\mathbf{A}_{\mathcal{R},\mathcal{C}}$ denotes the submatrix of \mathbf{A} corresponding to rows indexed by the set \mathcal{R} and columns by the set \mathcal{C} . The quantity $\mathbf{A}_{\bullet,\mathcal{C}}$ denotes a submatrix formed by keeping all rows of \mathbf{A} , but only columns indexed by \mathcal{C} , whereas $\mathbf{A}_{\mathcal{R},\bullet}$ denotes the submatrix formed by retaining rows indexed by \mathcal{R} and all columns. We use a similar notation for vectors. Hence, $\mathbf{X}_{\mathcal{R}}$ is the subvector of \mathbf{X} corresponding to rows indexed by \mathcal{R} . We always apply the subscripts of a matrix before the superscript. So $\mathbf{A}_{\mathcal{R},\mathcal{C}}^H$ is the conjugate-transpose of $\mathbf{A}_{\mathcal{R},\mathcal{C}}$. When dealing with singleton index sets $\mathcal{R} = \{r\}$ or $\mathcal{C} = \{c\}$, we omit the curly braces for readability. Therefore, $\mathbf{A}_{r,\bullet}$ and $\mathbf{A}_{\bullet,c}$ are the r th row and the c th column of \mathbf{A} , respectively. For convenience, we always number the rows and columns of a finite-size matrix starting from 0. For infinite-size matrices, the row and column indices range over \mathbb{Z} .

The identity matrix of size $N \times N$ is denote by \mathbf{I}_N , and the zero matrix by $\mathbf{0}$. We denote the indicator function by $\chi(\cdot)$. Finally, suppose that \mathcal{S} is a subset of \mathbb{R} or \mathbb{Z} , and a is an element of \mathbb{R} or \mathbb{Z} . Then

$$\begin{aligned}\mathcal{S} \oplus a &= \{s + a : s \in \mathcal{S}\}, \\ \mathcal{S} \ominus a &= \{s - a : s \in \mathcal{S}\}, \\ a\mathcal{S} &= \{as : s \in \mathcal{S}\}, \\ \mathcal{S} \bmod a &= \{s \bmod a : s \in \mathcal{S}\}.\end{aligned}$$

denote, respectively, the positive and negative translations, scaling, and the modulus of \mathcal{S} by a .

5.3 Sampling and Reconstruction Models

Let the input and output signals of the MIMO channel depicted in Figure 5.1 be represented in vector form as

$$\mathbf{x}(t) = \begin{pmatrix} x_0(t) \\ x_1(t) \\ \vdots \\ x_{R-1}(t) \end{pmatrix} \quad \text{and} \quad \mathbf{y}(t) = \begin{pmatrix} y_0(t) \\ y_1(t) \\ \vdots \\ y_{P-1}(t) \end{pmatrix}. \quad (5.2)$$

For convenience, define $\mathcal{R} = \{0, 1, \dots, R-1\}$ and $\mathcal{P} = \{0, 1, \dots, P-1\}$. These sets index the components of the input and the output vectors. For each $r \in \mathcal{R}$, we model $x_r(t)$ as a *multiband*

signal $x_r(t) \in \mathcal{B}(\mathcal{F}_r)$, where the spectral support \mathcal{F}_r is a finite union of disjoint intervals:

$$\mathcal{F}_r = \bigcup_{n=1}^{N_r} [a_{rn}, b_{rn}), \quad a_{r1} < b_{r1} < a_{r2} < \cdots < a_{rN_r} < b_{rN_r}. \quad (5.3)$$

The channel inputs need not have the same multiband spectral support. Figure 5.2 shows such an example for $R = 2$, which will be used throughout the chapter for illustrative purposes.

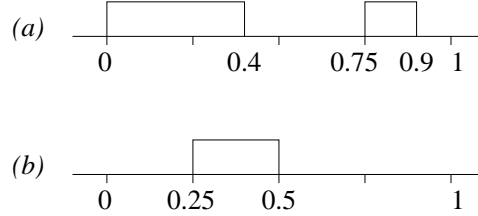


Figure 5.2 Example multiband input spectra $X_0(f)$, and $X_1(f)$ to a MIMO channel with $R = 2$.

We model the MIMO channel as a linear and shift-invariant system. Thus, we can write

$$\mathbf{y}(t) = \mathbf{g} * \mathbf{x}(t) = \int_{\mathbb{R}} \mathbf{g}(t - \tau) \mathbf{x}(\tau) d\tau,$$

where $*$ denotes convolution and

$$\mathbf{g}(t) = \begin{pmatrix} g_{0,0}(t) & \cdots & g_{0,R-1}(t) \\ \vdots & \ddots & \vdots \\ g_{P-1,0}(t) & \cdots & g_{P-1,R-1}(t) \end{pmatrix} \in \mathbb{C}^{P \times R}$$

is the impulse response matrix of the channel. Therefore,

$$\mathbf{Y}(f) = \mathbf{G}(f) \mathbf{X}(f), \quad (5.4)$$

where $\mathbf{X}(f)$, $\mathbf{Y}(f)$, and $\mathbf{G}(f)$ are the Fourier transforms of $\mathbf{x}(t)$, $\mathbf{y}(t)$, and $\mathbf{g}(t)$, respectively. In particular, $\mathbf{G}(f)$ is the *channel transfer function matrix*. The channel outputs are sampled at $t = nT$, $n \in \mathbb{Z}$, and we denote these output quantities by $z_p[n] = y_p(nT)$, or in matrix form by

$$\mathbf{z}[n] \stackrel{\text{def}}{=} \begin{pmatrix} z_0[n] \\ z_1[n] \\ \vdots \\ z_{P-1}[n] \end{pmatrix} = \mathbf{y}(nT), \quad n \in \mathbb{Z}.$$

Then, it is clear that

$$\begin{aligned}\mathbf{Z}[\nu] &= \frac{1}{T} \sum_{l \in \mathbb{Z}} \mathbf{Y}\left(\frac{\nu+l}{T}\right), \quad \nu \in [0, 1) \\ &= \frac{1}{T} \sum_{l \in \mathbb{Z}} \mathbf{G}\left(\frac{\nu+l}{T}\right) \mathbf{X}\left(\frac{\nu+l}{T}\right), \quad \nu \in [0, 1),\end{aligned}\tag{5.5}$$

where the second line follows from Eq. (5.4). We model the reconstruction block as follows:

$$\tilde{\mathbf{x}}(t) = \sum_{n \in \mathbb{Z}} \mathbf{h}(t - nT) \mathbf{z}[n],\tag{5.6}$$

where

$$\mathbf{h}(t) = \begin{pmatrix} h_{0,0}(t) & \cdots & h_{0,P-1}(t) \\ \vdots & \ddots & \vdots \\ h_{R-1,0}(t) & \cdots & h_{R-1,P-1}(t) \end{pmatrix} \in \mathbb{C}^{R \times P}.$$

It is clear from Eq. (5.6) that the entire MIMO system (consisting of the channel, the samplers and the reconstruction block) is invariant to a time-shift by a multiple of T , i.e.

$$\mathbf{x}(t) \rightarrow \tilde{\mathbf{x}}(t) \implies \mathbf{x}(t - nT) \rightarrow \tilde{\mathbf{x}}(t - nT), \quad \forall n \in \mathbb{Z}, t \in \mathbb{R}.$$

Conversely, Eq. (5.6) is the most general linear transformation that allows this invariance. Taking its Fourier transform and rewriting in matrix form yields

$$\tilde{\mathbf{X}}(f) = \mathbf{H}(f) \mathbf{Z}[fT], \quad f \in \mathbb{R},\tag{5.7}$$

where $\mathbf{H}(f)$, the Fourier transform of $\mathbf{h}(t)$, is the *reconstruction filter matrix*. Owing to the periodicity of $\mathbf{Z}[\nu]$, we can rewrite Eq. (5.7) as

$$\tilde{\mathbf{X}}\left(f + \frac{l'}{T}\right) = \mathbf{H}\left(f + \frac{l'}{T}\right) \mathbf{Z}[fT], \quad l' \in \mathbb{Z}, f \in \left[0, \frac{1}{T}\right).\tag{5.8}$$

We can now rewrite Eqs. (5.5) and (5.8) compactly as

$$\mathbf{Z}[fT] = \mathbf{G}(f) \mathbf{X}(f),\tag{5.9}$$

$$\tilde{\mathbf{X}}(f) = \mathbf{H}(f) \mathbf{Z}[fT],\tag{5.10}$$

for $f \in [0, 1/T)$, where $\mathbf{X}(f)$ and $\tilde{\mathbf{X}}(f)$ are the *modulated input and reconstructed vectors* whose entries are

$$\mathbf{X}_{Rl+r}(f) = X_r\left(f + \frac{l}{T}\right), \quad (r, l) \in \mathcal{R} \times \mathbb{Z},\tag{5.11}$$

$$\tilde{\mathbf{X}}_{Rl+r}(f) = \tilde{X}_r\left(f + \frac{l}{T}\right), \quad (r, l) \in \mathcal{R} \times \mathbb{Z},\tag{5.12}$$

while $\mathcal{G}(f)$ and $\mathcal{H}(f)$ for are the *modulated channel and reconstruction matrices* whose entries are

$$\mathcal{G}_{p, Rl+r}(f) = \frac{1}{T} G_{pr} \left(f + \frac{l}{T} \right), \quad (p, r, l) \in \mathcal{P} \times \mathcal{R} \times \mathbb{Z}, \quad (5.13)$$

$$\mathcal{H}_{Rl+r,p}(f) = H_{rp} \left(f + \frac{l}{T} \right), \quad (p, r, l) \in \mathcal{P} \times \mathcal{R} \times \mathbb{Z}. \quad (5.14)$$

Note that, even though these matrices have infinitely many columns or rows, only a finite summation is involved in Eq. (5.9) because the components of $\mathbf{X}(f)$ are bandlimited implying that only a finite number of entries in $\mathcal{X}(f)$ are nonzero. In the next section, we seek conditions on the channel and the inputs, that guarantee perfect reconstruction of the input signals, or equivalently, perfect inversion of the channel.

We consider only uniform sampling in this chapter. Fortunately, most periodic nonuniform sampling schemes can be expressed as special cases of uniform sampling. To see this, consider the following situation where the p th channel output $y_p(t)$ is sampled at

$$t \in \Lambda_p = \{nT_p + \lambda_{kp} : k = 0, \dots, K_p - 1\}.$$

The sampling patterns periods for the p th output channel is T_p , and the average sampling density of the p th output is K_p/T_p . First, consider the case where all the periods are equal, i.e., $T_p = T$. Then, we can write

$$\Lambda_p = \bigcup_{k=0}^{K_p-1} (T\mathbb{Z} + \lambda_{kp}).$$

In other words, Λ_p is composed of a union of K_p uniform sampling sets of density $1/T$. Consider a hypothetical MIMO channel whose transfer function matrix is obtained by performing the following modification to $\mathbf{G}(f)$. We replace the p th row of $\mathbf{G}(f)$, namely $\mathbf{G}_{p,\bullet}(f)$, by the following K_p rows: $\mathbf{G}_{p,\bullet}(f)e^{-j2\pi f\lambda_{kp}}$, $k = 0, \dots, K_p - 1$. The new channel matrix has $\sum_p K_p$ rows, and the samples of the new outputs taken at $t = nT$ are precisely equal to the samples of the old MIMO channel outputs taken on the periodic nonuniform sampling sets $\{\Lambda_p\}$ and reordered. Next suppose that the different channels have unequal but *commensurate* sampling periods, i.e., that the ratios of sampling periods are rational numbers: $T_p = (m_p/n_p)T$, for some $m_p, n_p \in \mathbb{N}$, and $T \in \mathbb{R}$. In this case, a common period for all the sampling sets $\{\Lambda_p\}$ is $T \prod n_p$, and an argument as before allows us to convert this to uniform sampling of the outputs of a hypothetical MIMO channel. The upshot of this argument is that most periodic nonuniform sampling (except those with non-commensurate periods) may be recast as a uniform sampling problem. Of course the price to pay is that the hypothetical MIMO channel has many more outputs. We illustrate this in the following example.

Example 5.1. Let $\mathbf{G}(f)$ be the channel transfer function matrix of a MIMO channel with $P = 2$ outputs. Let the sampling sets for the channel outputs be as depicted in Figure 5.3, i.e.,

$$\Lambda_1 = \{3n, 3n + 0.5 : n \in \mathbb{Z}\},$$

$$\Lambda_2 = \{2n : n \in \mathbb{Z}\}.$$

These sets are clearly commensurate because sampling periods $T_1 = 3$ and $T_2 = 2$ are such that T_1/T_2 is rational. A common period for the two sampling sets is obviously 6. Indeed, we have

$$\Lambda_1 = \bigcup_{k=0}^3 (6\mathbb{Z} + \lambda_{k,1}), \quad \{\lambda_{k,1} : k = 0, \dots, 3\} = \{0, 0.5, 3, 3.5\},$$

$$\Lambda_2 = \bigcup_{k=0}^2 (6\mathbb{Z} + \lambda_{k,2}), \quad \{\lambda_{k,2} : k = 0, \dots, 2\} = \{0, 2, 4\}.$$

Hence, the modified channel has six outputs and the rows of its transfer function matrix $\tilde{\mathbf{G}}(f)$ are given by

$$\tilde{\mathbf{G}}_{k,\bullet}(f) = \mathbf{G}_{0,\bullet}(f)e^{-j2\pi f\lambda_{k,1}}, \quad k = 0, 1, 2, 3,$$

$$\tilde{\mathbf{G}}_{k+4,\bullet}(f) = \mathbf{G}_{1,\bullet}(f)e^{-j2\pi f\lambda_{k,2}}, \quad k = 0, 1, 2.$$

If the outputs of the hypothetical channel are sampled uniformly at $t = 6n$, $n \in \mathbb{Z}$, we essentially obtain a reordered sequence of the samples of the original MIMO channel outputs taken on the samples sets Λ_1 and Λ_2 .

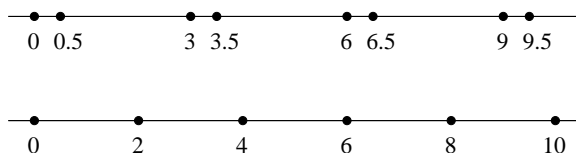


Figure 5.3 Commensurate periodic nonuniform sampling sets.

We have shown that commensurate periodic nonuniform sampling is really uniform sampling in disguise, because their equivalence is shown using the above modification trick. Therefore, the study of uniform sampling automatically provides answers to the commensurate periodic nonuniform sampling problem. In the subsequent sections, we present results for uniform MIMO sampling only.

In practice, we would usually only attempt to reconstruct a version of the set of inputs that is uniformly sampled at the corresponding Nyquist rate, and implement $\mathbf{H}(f)$ using FIR

filters. The continuous-time version could then be reconstructed by a bank of conventional digital-to-analog (D/A) converters on the reconstructed discrete-time signals. In particular, it would be desirable to use a reconstruction filter matrix $\mathbf{H}(f)$, that is continuous in f . The reason for this is roughly the following. Recall that a real function on a real compact set can be approximated arbitrarily closely (in the L^∞ sense) by polynomials if the given function is continuous. Similarly, if $\mathbf{H}(f)$ is continuous in f , we can approximate the matrix function $\mathbf{H}(f)$ arbitrarily closely in the \mathcal{H}^∞ sense by choosing sufficiently long FIR filters. Although we shall not delve into implementation issues in this chapter, we do consider both cases (*with* and *without* the continuity requirement imposed on $\mathbf{H}(f)$) in the next section, when we derive conditions for perfect reconstruction. This will be useful in Chapter 6, where we deal with FIR filter design issues.

5.4 Perfect Reconstruction

We begin with some definitions. Define the following two *spectral index sets* at frequency $f \in [0, 1/T)$:

$$\begin{aligned}\mathcal{K}_f^\circ &= \{(r, l) \in \mathcal{R} \times \mathbb{Z} : \left(f + \frac{l}{T}\right) \in \mathcal{F}_r\}, \\ \mathcal{K}_f &= \{Rl + r : (r, l) \in \mathcal{R} \times \mathbb{Z} \text{ and } \left(f + \frac{l}{T}\right) \in \mathcal{F}_r\}.\end{aligned}\tag{5.15}$$

Recall that the mapping of the pair $(r, l) \in \mathcal{R} \times \mathbb{Z}$ to a single index $Rl + r \in \mathbb{Z}$, is invertible. Hence, specifying any one of \mathcal{K}_f° and \mathcal{K}_f uniquely determines the other. Also let $\mathcal{K}_f^c = \mathbb{Z} \setminus \mathcal{K}_f$ denote the complement of \mathcal{K}_f . We now have the following proposition.

Proposition 5.1. *Suppose that sets \mathcal{F}_r , $r \in \mathcal{R}$ have multiband structure as defined in Eq. (5.3). Then \mathcal{K}_f is piecewise constant on $[0, 1/T)$, i.e., there exists a collection of disjoint intervals \mathcal{I}_m of the form $[\alpha, \beta)$, and sets \mathcal{K}_m , $m = 1, \dots, M$ such that $\mathcal{K}_f = \mathcal{K}_m$, for $f \in \mathcal{I}_m$, and*

$$\bigcup_{m=1}^M \mathcal{I}_m = \left[0, \frac{1}{T}\right).$$

This result is easily demonstrated by using an argument very similar to the one in Chapter 2 for multicoset sampling. Hence, we can write

$$\begin{aligned}\mathcal{I}_m &= [\gamma_m, \gamma_{m+1}), \quad m \in \mathcal{M}, \\ \gamma_1 &< \gamma_2 < \dots < \gamma_{M+1},\end{aligned}$$

such that $\gamma_1 = 0$ and $\gamma_{M+1} = 1/T$.

In this section, we derive the conditions on the channel and the spectral supports \mathcal{F}_r of the channel inputs for the existence of a reconstruction filter matrix $\mathbf{H}(f)$ that achieves perfect reconstruction of the inputs. We consider both cases *with* and *without* the continuity requirement imposed on the channel and reconstruction filters. As we shall see later, the continuity of $\mathbf{H}(f)$ may also require the continuity of the channel transfer function matrix $\mathbf{G}(f)$. Since our analysis in the next section will rely on the modulated channel and reconstruction matrices $\mathcal{G}(f)$ and $\mathcal{H}(f)$, the following proposition will turn out to be useful.

Proposition 5.2. *If $G_{\bullet,r}(f)$ is continuous on $\overline{\mathcal{F}_r}$ then $\mathcal{G}_{\bullet,\mathcal{K}_m}(f)$ is continuous on $\overline{\mathcal{I}_m}$ and the following “boundary condition” holds:*

$$\mathcal{G}_{\bullet,\mathcal{K}}\left(\frac{1}{T}\right) = \mathcal{G}_{\bullet,\mathcal{K} \oplus R}(0), \quad \mathcal{K} \subseteq \mathbb{Z}. \quad (5.16)$$

The quantity $\mathbf{H}(f)$ is continuous if and only if the entries of $\mathcal{H}(f)$ are continuous on $[0, 1/T]$ and satisfies the boundary condition

$$\mathcal{H}_{\mathcal{K},\bullet}\left(\frac{1}{T}\right) = \mathcal{H}_{\mathcal{K} \oplus R,\bullet}(0), \quad \mathcal{K} \subseteq \mathbb{Z}. \quad (5.17)$$

We do not care about $G_{pr}(f)$ outside the closure of the set \mathcal{F}_r because $X_r(f)$ vanishes there. This explains why the conditions for $\mathbf{G}(f)$ and $\mathbf{H}(f)$ are different in Proposition 5.2. We omit its proof since it is quite straightforward, following directly from Eqs. (5.13) and (5.14), and the definition of \mathcal{K}_m . The boundary conditions imply that the entries of the vector $\mathcal{G}_{\bullet,\mathcal{K}}(0)$ is a shifted version of those of $\mathcal{G}_{\bullet,\mathcal{K}}(1/T)$.

In the next section, we use frame theory to derive necessary and sufficient conditions for stable and perfect reconstruction of the channel inputs, but we first present a simple necessary condition. From Eq. (5.15), it is clear that all the nonzero entries of $\mathcal{X}(f)$ are captured in the subvector $\mathcal{X}_{\mathcal{K}_f}(f)$, and hence we can rewrite Eqs. (5.9) and (5.10) as

$$\tilde{\mathcal{X}}_{\mathcal{K}_f}(f) = \mathcal{H}_{\mathcal{K}_f,\bullet}(f) \mathcal{G}_{\bullet,\mathcal{K}_f}(f) \mathcal{X}_{\mathcal{K}_f}(f), \quad (5.18)$$

$$\tilde{\mathcal{X}}_{\mathcal{K}_f^c}(f) = \mathcal{H}_{\mathcal{K}_f^c,\bullet}(f) \mathcal{G}_{\bullet,\mathcal{K}_f}(f) \mathcal{X}_{\mathcal{K}_f}(f). \quad (5.19)$$

For perfect reconstruction, we require the existence of $\mathcal{H}(f)$ such that $\tilde{\mathcal{X}}(f) = \mathcal{X}(f)$ a.e. It is clear that this would happen if and only if

$$\mathcal{H}_{\mathcal{K}_f,\bullet}(f) \mathcal{G}_{\bullet,\mathcal{K}_f}(f) = \mathbf{I}_{|\mathcal{K}_f|} \quad \text{and} \quad \mathcal{H}_{\mathcal{K}_f^c,\bullet}(f) \mathcal{G}_{\bullet,\mathcal{K}_f}(f) = \mathbf{0} \quad \text{a.e.}, \quad (5.20)$$

which can be expressed more compactly as

$$\mathcal{H}(f)\mathcal{G}_{\bullet, \mathcal{K}_f}(f) = \mathbf{I}_{\bullet, |\mathcal{K}_f|}. \quad (5.21)$$

Since $\mathcal{G}_{\bullet, \mathcal{K}_f}(f) \in \mathbb{C}^{P \times |\mathcal{K}_f|}$, we require that $\mathcal{G}_{\bullet, \mathcal{K}_f}(f)$ have full column rank a.e. This condition guarantees the uniqueness of the solution to Eq. (5.21) if a solution exists. In view of Proposition 5.1, we now obtain the following necessary condition for perfect reconstruction:

$$\text{rank}(\mathcal{G}_{\bullet, \mathcal{K}_m}(f)) = |\mathcal{K}_m|, \quad \text{a.e. } f \in \mathcal{I}_m. \quad (5.22)$$

However, this condition does not address the issue of stability of reconstruction, and hence may be insufficient.

5.4.1 Stable sampling

The MIMO channel can be viewed as a linear transformation from the class of input signals to the space of its samples. The condition in Eq. (5.22) on the channel and the input signals is necessary for stable perfect reconstruction. However, it does not suffice because it does not answer the important question regarding stability of the reconstruction. In this section, we shall use frame theory to study the stability issue of sampling problem. Recall the definition of a frame:

Definition 5.1. Let \mathcal{H} be a separable Hilbert space. A sequence $\{\psi_n\} \subseteq \mathcal{H}$ is a frame if there exist constants $A, B > 0$ such that

$$A\|x\|^2 \leq \sum_n |\langle \psi_n, x \rangle|^2 \leq B\|x\|^2,$$

for all $x \in \mathcal{H}$. If $A = B$, then the frame is a tight frame.

The frame operator S , defined as

$$Sx = \sum_n \langle x, \psi_n \rangle \psi_n, \quad \forall x \in \mathcal{H},$$

is a bounded linear operator satisfying $AI \leq S \leq BI$, where I is the identity operator. Define $\tilde{\psi}_n = S^{-1}\psi_n$. Then $\{\tilde{\psi}_n\}$ is also a frame (the *dual frame*) for \mathcal{H} with frame bounds B^{-1} and A^{-1} , and any $x \in \mathcal{H}$ can be expressed as

$$x = \sum_n \langle x, \tilde{\psi}_n \rangle \psi_n = \sum_n \langle x, \psi_n \rangle \tilde{\psi}_n. \quad (5.23)$$

In the context of MIMO sampling, the relevant Hilbert space is the class of input signals:

$$\mathcal{H} = \mathcal{B}(\mathcal{F}_1) \times \cdots \times \mathcal{B}(\mathcal{F}_R).$$

The inner product and norm on \mathcal{H} are defined as

$$\begin{aligned}\langle \mathbf{x}, \mathbf{w} \rangle &= \int_{\mathbb{R}} \mathbf{w}^H(t) \mathbf{x}(t) dt, \quad \mathbf{x}, \mathbf{w} \in \mathcal{H}, \\ \|\mathbf{x}\| &= \sqrt{\langle \mathbf{x}, \mathbf{x} \rangle}.\end{aligned}$$

We now present an important definition for the stability of MIMO sampling (see Chapter 4):

Definition 5.2. The MIMO sampling scheme is called *stable* if there exist constants $A, B > 0$ such that

$$A\|\mathbf{x}\|^2 \leq \sum_{n \in \mathbb{Z}} \|z[n]\|^2 \leq B\|\mathbf{x}\|^2, \quad (5.24)$$

for all $\mathbf{x}(t) \in \mathcal{H}$.

Equation (5.24) clearly allows stable reconstruction, and to see this we recast Eq. (5.24) in a frame theoretic form. Define the diagonal matrix

$$\mathbf{J}(f) = \text{diag}(\chi(f \in \mathcal{F}_1), \dots, \chi(f \in \mathcal{F}_R)). \quad (5.25)$$

Then we have

$$\mathbf{J}(f)\mathbf{X}(f) = \mathbf{X}(f) \quad (5.26)$$

because $X_r(f)$ is supported on \mathcal{F}_r . In view of Eq. (5.26), we can rewrite $z_p[n]$ as

$$\begin{aligned}z_p[n] = y_p(nT) &= \int_{\mathbb{R}} e^{j2\pi fnT} \mathbf{G}_{p,\bullet}(f) \mathbf{X}(f) df \\ &= \int_{\mathbb{R}} e^{j2\pi fnT} \mathbf{G}_{p,\bullet}(f) \mathbf{J}(f) \mathbf{X}(f) df \\ &= \int_{\mathbb{R}} \mathbf{\Psi}_{pn}^H(f) \mathbf{X}(f) df,\end{aligned} \quad (5.27)$$

where

$$\mathbf{\Psi}_{pn}^H(f) = e^{j2\pi fnT} \mathbf{G}_{p,\bullet}(f) \mathbf{J}(f) \iff \boldsymbol{\psi}_{pn}(t) = \int_{\mathbb{R}} \mathbf{J}(f) \mathbf{G}_{p,\bullet}^H(f) e^{j2\pi f(t-nT)} df, \quad (5.28)$$

for $(p, n) \in \mathcal{P} \times \mathbb{Z}$. It is clear that $\boldsymbol{\psi}_{pn} \in \mathcal{H}$. Using Parseval's theorem and Eq. (5.28) we conclude that

$$\langle \mathbf{x}, \boldsymbol{\psi}_{pn} \rangle = \int_{\mathbb{R}} \boldsymbol{\psi}_{pn}^H(t) \mathbf{x}(t) dt = \int_{\mathbb{R}} \mathbf{\Psi}_{pn}^H(f) \mathbf{X}(f) df = z_p[n].$$

Thus $z_p[n]$ can be expressed as an inner product of \mathbf{x} and $\boldsymbol{\psi}_{pn} \in \mathcal{H}$, and consequently, Eq. (5.24) is equivalent to the condition that $\{\boldsymbol{\psi}_{pn}\}$ forms a frame for \mathcal{H} . Suppose we denote its dual frame by $\{\tilde{\boldsymbol{\psi}}_{np} : n \in \mathbb{Z}, p \in \mathcal{P}\}$, then Eq. (5.23) produces with the following reconstruction formula:

$$\mathbf{x} = \sum_{n \in \mathbb{Z}} \sum_{p \in \mathcal{P}} \langle \mathbf{x}, \boldsymbol{\psi}_{np} \rangle \tilde{\boldsymbol{\psi}}_{np} = \sum_{n \in \mathbb{Z}} \sum_{p \in \mathcal{P}} z_p[n] \tilde{\boldsymbol{\psi}}_{np}.$$

As shown in Chapter 4, the implication of stability of reconstruction is that errors in the inputs or the sampled outputs cannot produce arbitrarily large errors in the reconstructed outputs. The ratio $K = \sqrt{B/A} \geq 1$ is called the *condition number* of the sampling scheme, and K^2 is a bound on the amplification of the normalized error energy due to the reconstruction filters.

5.4.2 Conditions for perfect reconstruction

Let ess inf and ess sup denote the essential infimum and supremum, i.e.,

$$\text{ess inf } g(t) = \sup\{\gamma : g(t) \geq \gamma \text{ a.e.}\},$$

$$\text{ess sup } g(t) = \inf\{\gamma : g(t) \leq \gamma \text{ a.e.}\}.$$

for any real function g . Our next result provides necessary and sufficient conditions on the channel matrix for stable MIMO reconstruction.

Theorem 5.1. *The frame bounds for the MIMO sampling problem are given by*

$$A = T \text{ess inf}_{f \in [0, 1/T]} \lambda_{\min}(\mathcal{G}_{\bullet, \mathcal{K}_f}^H(f) \mathcal{G}_{\bullet, \mathcal{K}_f}(f)), \quad (5.29)$$

$$B = T \text{ess sup}_{f \in [0, 1/T]} \lambda_{\max}(\mathcal{G}_{\bullet, \mathcal{K}_f}^H(f) \mathcal{G}_{\bullet, \mathcal{K}_f}(f)). \quad (5.30)$$

In particular, $A > 0$ and $B < \infty$ are necessary and sufficient conditions for stable reconstruction of the MIMO inputs.

Proof. We need to compute

$$A = \inf_{\mathbf{x} \in \mathcal{B}} \sum_{n \in \mathbb{Z}} \|\mathbf{z}[n]\|^2 \quad \text{and} \quad B = \sup_{\mathbf{x} \in \mathcal{B}} \sum_{n \in \mathbb{Z}} \|\mathbf{z}[n]\|^2, \quad (5.31)$$

where \mathcal{B} is the set of input signals of unit combined energy:

$$\mathcal{B} = \{\mathbf{x} \in \mathcal{H} : \|\mathbf{x}\| = 1\}. \quad (5.32)$$

First observe that

$$\begin{aligned} \|\mathbf{x}\|^2 &= \int_{\mathbb{R}} \|\mathbf{x}(t)\|^2 dt = \int_{\mathbb{R}} \|\mathbf{X}(f)\|^2 df \\ &\stackrel{(a)}{=} \int_{[0, \frac{1}{T}]} \|\mathbf{X}(f)\|^2 df \\ &\stackrel{(b)}{=} \int_{[0, \frac{1}{T}]} \|\mathbf{X}_{\mathcal{K}_f}(f)\|^2 df, \end{aligned} \quad (5.33)$$

where the norms on the right-hand side of Eq. (5.33) are the Euclidean norms. The equality (a) above follows from Eq. (5.11), and (b) follows because $\mathcal{X}_{\mathcal{K}_f}(f)$ captures all the nonzero entries of $\mathcal{X}(f)$. Next

$$\begin{aligned} \sum_{n \in \mathbb{Z}} \|z[n]\|^2 &= \int_{\nu \in [0,1]} \|z[\nu]\|^2 d\nu \\ &\stackrel{(a)}{=} T \int_{[0, \frac{1}{T}]} \|z[TV]\|^2 df \\ &\stackrel{(b)}{=} T \int_{[0, \frac{1}{T}]} \|\mathcal{G}_{\bullet, \mathcal{K}_f}(f) \mathcal{X}_{\mathcal{K}_f}(f)\|^2 df, \end{aligned} \quad (5.34)$$

where (a) is obtained by a change of variables, and (b) from Eq. (5.9) and the fact that $\mathcal{X}_{\mathcal{K}_f}(f)$ captures all the nonzero entries of $\mathcal{X}(f)$. Therefore, Eqs. (5.31), (5.32), (5.33), and (5.34) yield

$$\begin{aligned} A &= \inf T \int_{[0, \frac{1}{T}]} \|\mathcal{G}_{\bullet, \mathcal{K}_f}(f) \mathcal{X}_{\mathcal{K}_f}(f)\|^2 df \quad \text{s.t.} \quad \int_{[0, \frac{1}{T}]} \|\mathcal{X}_{\mathcal{K}_f}(f)\|^2 df = 1, \\ B &= \sup T \int_{[0, \frac{1}{T}]} \|\mathcal{G}_{\bullet, \mathcal{K}_f}(f) \mathcal{X}_{\mathcal{K}_f}(f)\|^2 df \quad \text{s.t.} \quad \int_{[0, \frac{1}{T}]} \|\mathcal{X}_{\mathcal{K}_f}(f)\|^2 df = 1. \end{aligned}$$

Now the claimed results in Eqs. (5.29) and (5.30) follow immediately. \square

Note that a simple necessary condition for perfect reconstruction is that $P \geq |\mathcal{K}_m|$ for each $m \in \mathcal{M}$. Clearly, multiple solutions $\mathcal{H}(f)$ exist to Eq. (5.21) if $P > |\mathcal{K}_m|$ for some m . The average sampling density for this sampling scheme is P/T . Now, Eq. (5.15) implies that

$$|\mathcal{K}_f| = \sum_{r \in \mathcal{R}} \sum_{l \in \mathbb{Z}} \chi(f + l/T \in \mathcal{F}_r).$$

Hence,

$$\int_{[0, 1/T]} |\mathcal{K}_f| df = \sum_{r=1}^R \int_{\mathcal{F}_r} \chi(f \in \mathcal{F}_r) = \sum_{r=1}^R \mu(\mathcal{F}_r), \quad (5.35)$$

where $\mu(\cdot)$ denotes the Lebesgue measure. Suppose that $P = |\mathcal{K}_m|$ for all m , then Eq. (5.35) reduces to

$$\frac{P}{T} = \sum_{r=1}^R \mu(\mathcal{F}_r).$$

This value for the total sampling density coincides with the minimum density required for stable MIMO sampling (see Theorem 4.2) using any sampling scheme for the channel outputs, whether uniform or not. Also note that we have uniqueness of the reconstruction filters when $P = |\mathcal{K}_m|$.

Corollary 5.1. *Suppose that $\mathbf{G}(f)$ is such that $G_{pr}(f)$ is continuous for $f \in \overline{\mathcal{F}_r}$, and $\mathcal{G}_{\bullet, \mathcal{K}_m}(f)$ has full column rank for all $m \in \mathcal{M}$, $f \in \overline{\mathcal{I}_m} = [\gamma_m, \gamma_{m+1}]$. Then the MIMO sampling scheme is stable, i.e., $\{\psi_{pn}\}$ forms a frame.*

Proof. By Proposition 5.2, we have continuity of $\mathcal{G}_{\bullet, \mathcal{K}_m}(f)$ on the compact set $\overline{\mathcal{I}_m}$. Therefore, both the smallest and the largest eigenvalues of $\mathcal{G}_{\bullet, \mathcal{K}_m}^H(f)\mathcal{G}_{\bullet, \mathcal{K}_m}(f)$ are continuous functions on $\overline{\mathcal{I}_m}$. Since the smallest eigenvalue is strictly positive for all $f \in [0, 1/T]$ by hypothesis, it follows that the infimum in Eq. (5.29) is attained, implying that $A > 0$. Similarly, $B < \infty$ because the supremum in Eq. (5.30) is attained. \square

We illustrate the MIMO sampling result of Theorem 5.1 for a simple MIMO channel.

Example 5.2. Consider a MIMO channel with $R = 2$ inputs and $P = 4$ outputs having the following transfer function matrix:

$$\mathbf{G}(f) = \begin{pmatrix} 1 & 1 \\ 1 & 1 + e^{-j2\pi f} \\ e^{-j2\pi f} & 0.25 + e^{-j4\pi f} \\ 1 + 0.5e^{-j2\pi f} & 1 + e^{-j4\pi f} \end{pmatrix}.$$

Let the input spectra $X_1(f)$ and $X_2(f)$ have supports as illustrated in Figure 5.2, i.e.,

$$\mathcal{F}_1 = [0, 0.4) \cup [0.75, 0.9) \quad \text{and} \quad \mathcal{F}_2 = [0.25, 0.5).$$

Each output is a multiband signals supported on $\mathcal{F} = \mathcal{F}_1 \cup \mathcal{F}_2 = [0, 0.5) \cup [0.75, 0.9)$. Hence, the Nyquist rate for sampling each output is $\mu(\mathcal{F}) = 0.65$. However, we demonstrate in this example that we do not need to sample each output at the Nyquist rate to achieve perfect reconstruction. Let the sampling period be $T = 4$. For this choice, it is easy to verify that

$$\mathcal{I}_1 = [0, 0.15) \quad \text{and} \quad \mathcal{I}_2 = [0.15, 0.25).$$

Furthermore, Eq. (5.15) and Proposition 5.1 imply that

$$\mathcal{K}_f^\circ = \begin{cases} \{(0, 0), (0, 1), (0, 3), (1, 1)\}, & \text{if } f \in \mathcal{I}_1, \\ \{(0, 0), (1, 1)\}, & \text{if } f \in \mathcal{I}_2. \end{cases}$$

Therefore, $\mathcal{K}_1 = \{0, 2, 6, 3\}$ and $\mathcal{K}_2 = \{0, 3\}$. A simple calculation shows that

$$\mathcal{G}_{\bullet, \mathcal{K}_1}(f) = \frac{1}{4} \begin{pmatrix} 1 & 1 & 1 & 1 \\ 1 & 1 & 1 & 1 + e^{-j2\pi(f+1/4)} \\ e^{-j2\pi f} & e^{-j2\pi(f+1/4)} & e^{-j2\pi(f+3/4)} & 0.25 + e^{-j4\pi(f+1/4)} \\ 1 + 0.5e^{-j2\pi f} & 1 + 0.5e^{-j2\pi(f+1/4)} & 1 + 0.5e^{-j2\pi(f+3/4)} & 1 + e^{-j4\pi(f+1/4)} \end{pmatrix},$$

$$\mathcal{G}_{\bullet, \mathcal{K}_2}(f) = \frac{1}{4} \begin{pmatrix} 1 & 1 \\ 1 & 1 + e^{-j2\pi(f+1/4)} \\ e^{-j2\pi f} & 0.25 + e^{-j4\pi(f+1/4)} \\ 1 + 0.5e^{-j2\pi f} & 1 + e^{-j4\pi(f+1/4)} \end{pmatrix}.$$

It can be verified numerically that

$$\begin{aligned}\text{rank}(\mathcal{G}_{\bullet, \mathcal{K}_1}(f)) &= 4, \quad \forall f \in \overline{\mathcal{I}_1}, \\ \text{rank}(\mathcal{G}_{\bullet, \mathcal{K}_2}(f)) &= 2, \quad \forall f \in \overline{\mathcal{I}_2}.\end{aligned}$$

Since $\mathbf{G}(f)$ is continuous, we conclude using Corollary 5.1, that stable perfect reconstruction of the inputs is possible from the channel output samples. However, as we shall see in Example 5.4, the reconstruction filter matrix $\mathbf{H}(f)$ would necessarily have to be discontinuous. Finally, note that the total sampling density of the outputs is $P/T = 1$, while the minimum density, as dictated by Theorem 4.2 is $\mu(\mathcal{F}_1) + \mu(\mathcal{F}_2) = 0.8$.

In Example 5.2, we showed that the combined sampling density of 1 is achievable, but the lower bound on this density is 0.8. Therefore, we could potentially find a nonuniform MIMO sampling scheme that closes the gap. In fact, this is precisely what we are going to show in the following example.

Example 5.3. Let the inputs signal characteristics and the channel transfer function matrix be the same as in Example 5.2. We show that, using a proper nonuniform sampling strategy at the outputs, we can achieve the minimum combined sampling rate for all the output channels as stipulated by Theorem 4.2. Let the channel outputs be sampled on the sets $\Lambda_p = \{20n + \lambda_{kp} : k = 0, \dots, K_p - 1\}$, where $(K_1, K_2, K_3, K_4) = (0, 3, 5, 8)$ and

$$\{\lambda_{kp} : k = 0, \dots, K_p - 1\} = \begin{cases} \emptyset & \text{if } p = 0, \\ \{1, 8, 14\} & \text{if } p = 1, \\ \{2, 5, 8, 13, 18\} & \text{if } p = 2, \\ \{0, 2, 4, 5, 7, 8, 14, 17\} & \text{if } p = 3. \end{cases}$$

Evidently, these are all periodic nonuniform sampling sets having a common period of $T = 20$, and consisting of 16 cosets in all. Hence, the modified MIMO channel has a transfer function matrix $\tilde{\mathbf{G}}(f)$ of size 16×2 , and its rows can be worked out as in Example 5.1. Since the band edges of \mathcal{F}_1 and \mathcal{F}_2 are all multiples of 0.05, we trivially obtain $M = 1$, $\mathcal{I}_1 = [0, 0.05)$, and

$$\mathcal{K}_1 = \{0, 2, 4, 6, 8, 10, 12, 14, 30, 32, 34\} \cup \{11, 13, 15, 17, 19\}.$$

Now, $\tilde{\mathcal{G}}_{\bullet, \mathcal{K}_1}(f)$ is a continuous 16×16 matrix, whose rank is verifiable to be 16 for all f . By Corollary 5.1, we conclude that stable and perfect reconstruction of the channel inputs is possible from these periodic nonuniform MIMO samples. In fact, the stability bounds are

$A = 8.0724 \times 10^{-4}$ and $B = 3.6833$, implying that the condition number $K = \sqrt{B/A} = 67.5487$. The sampling densities of Λ_p is $d_p = K_p/T$, so that

$$(d_1, d_2, d_3, d_4) = (0, 0.15, 0.25, 0.5)$$

in an achievable point in density region for stable sampling. Obviously, they must meet all the necessary conditions for stable sampling derived in Chapter 4. In particular, the total combined sampling rate of all the outputs is $16/T = 0.8$, which is precisely equal to the minimum joint sampling density required by Theorem 4.2, namely $\mu(\mathcal{F}_1) + \mu(\mathcal{F}_2)$. We learn from this example that we need not sample the different outputs at the same rate. In fact, one of the channels is not sampled at all, unlike in Example 5.2, where, due to uniform sampling, we required samples from all channel outputs.

5.4.3 Existence of continuous solutions

Theorem 5.1 does not guarantee the existence of a continuous filter matrix $\mathbf{H}(f)$ which, as we have seen earlier, may be desirable from an implementation point of view. The following theorem shows that, under a stronger set of conditions, we can guarantee the existence of a continuous filter matrix $\mathbf{H}(f)$. We begin with a lemma.

Lemma 5.1. *Let $\mathbf{C}(f) \in \mathbb{C}^{p \times q}$ (with $p \geq q$) and $\mathbf{D}(f) \in \mathbb{C}^{r \times q}$ be continuous functions of $f \in [\alpha, \beta]$ such that $\text{rank } \mathbf{C}(f) = q$ for all f , and let $\mathbf{E}_\alpha, \mathbf{E}_\beta \in \mathbb{C}^{r \times p}$ be matrices satisfying*

$$\mathbf{E}_\alpha \mathbf{C}(\alpha) = \mathbf{D}(\alpha) \quad \text{and} \quad \mathbf{E}_\beta \mathbf{C}(\beta) = \mathbf{D}(\beta).$$

Then there exists a continuous $\mathbf{E}(f) \in \mathbb{C}^{r \times p}$ such that $\mathbf{E}(f)\mathbf{C}(f) = \mathbf{D}(f)$ for all $f \in [\alpha, \beta]$, and that $\mathbf{E}(\alpha) = \mathbf{E}_\alpha$ and $\mathbf{E}(\beta) = \mathbf{E}_\beta$ are satisfied.

The proof of Lemma 5.1 can be found in Appendix A. We can now derive the conditions for the existence of continuous reconstruction filters that achieve perfect reconstruction.

Theorem 5.2. *Suppose that the MIMO transfer function matrix $\mathbf{G}(f)$ is such that $G_{pr}(f)$ is continuous for $f \in \overline{\mathcal{F}_r}$. Then there exists a reconstruction filter matrix $\mathbf{H}(f)$ continuous in f , that achieves stable and perfect reconstruction of the MIMO channel inputs if and only if*

$$\text{rank}(\mathcal{G}_{\bullet, \mathcal{K}_m}(f)) = |\mathcal{K}_m|, \quad \forall f \in \text{int } \mathcal{I}_m = (\gamma_m, \gamma_{m+1}), \quad (5.36)$$

$$\text{rank}(\mathcal{G}_{\bullet, \mathcal{J}_m}(\gamma_m)) = |\mathcal{J}_m|, \quad m \in \mathcal{M}. \quad (5.37)$$

where

$$\begin{aligned} \mathcal{J}_m &= \mathcal{K}_m \cup \mathcal{K}_{m-1}, \quad m = 2, \dots, M, \\ \mathcal{J}_1 &= \mathcal{K}_1 \cup (\mathcal{K}_M \oplus R). \end{aligned} \quad (5.38)$$

Proof. First note that the hypotheses in this theorem are stronger than those of Corollary 5.1. Thus, stable reconstruction is guaranteed. We shall first prove the necessity of Eqs. (5.36) and (5.37). The first condition in Eq. (5.20) states that

$$\mathcal{H}_{\mathcal{K}_f, \bullet}(f) \mathcal{G}_{\bullet, \mathcal{K}_f}(f) = \mathbf{I}_{|\mathcal{K}_f|} \quad \text{a.e.} \quad (5.39)$$

So suppose that $\mathbf{H}(f)$ is a continuous solution, then Proposition 5.2 implies that $\mathcal{H}_{\mathcal{K}_m, \bullet}(f)$ and $\mathcal{G}_{\bullet, \mathcal{K}_m}(f)$ are continuous functions in the interior of \mathcal{I}_m , and, in fact, Eq. (5.39) must hold for all $f \in \text{int } \mathcal{I}_m$, not just a.e., because both sides of Eq. (5.39) are continuous functions. Now Eq. (5.36) follows immediately. Letting $f \downarrow \gamma_1 = 0$ in Eq. (5.20) and using the continuity of $\mathcal{H}(f)$ gives us

$$\mathcal{H}_{\mathcal{K}_1, \bullet}(0) \mathcal{G}_{\bullet, \mathcal{K}_1}(0) = \mathbf{I}_{q_1}, \quad \mathcal{H}_{\mathcal{K}_1^c, \bullet}(0) \mathcal{G}_{\bullet, \mathcal{K}_1}(0) = \mathbf{0}, \quad (5.40)$$

while letting $f \uparrow \gamma_{M+1} = 1/T$ instead, and using Eqs. (5.16) and (5.17), we obtain

$$\mathcal{H}_{\mathcal{K}_M \oplus R, \bullet}(0) \mathcal{G}_{\bullet, \mathcal{K}_M \oplus R}(0) = \mathbf{I}_{q_M}, \quad \mathcal{H}_{\mathcal{K}_M^c \oplus R, \bullet}(0) \mathcal{G}_{\bullet, \mathcal{K}_M \oplus R}(0) = \mathbf{0}. \quad (5.41)$$

Combining Eqs. (5.40) and (5.41), we obtain the following set of necessary conditions:

$$\mathcal{H}_{\mathcal{J}_1, \bullet}(0) \mathcal{G}_{\bullet, \mathcal{J}_1}(0) = \mathbf{I}_{|\mathcal{J}_1|}, \quad \mathcal{H}_{\mathcal{J}_1^c, \bullet}(0) \mathcal{G}_{\bullet, \mathcal{J}_1}(0) = \mathbf{0}. \quad (5.42)$$

where $\mathcal{J}_1 = \mathcal{K}_1 \cup (\mathcal{K}_M \oplus R)$. Using a similar continuity argument in the vicinity of γ_m , for $m = 2, \dots, M$ yields:

$$\mathcal{H}_{\mathcal{J}_m, \bullet}(\gamma_m) \mathcal{G}_{\bullet, \mathcal{J}_m}(\gamma_m) = \mathbf{I}_{|\mathcal{J}_m|}, \quad \mathcal{H}_{\mathcal{J}_m^c, \bullet}(\gamma_m) \mathcal{G}_{\bullet, \mathcal{J}_m}(\gamma_m) = \mathbf{0}. \quad (5.43)$$

where $\mathcal{J}_m = \mathcal{K}_m \cup \mathcal{K}_{m-1}$. Hence, Eq. (5.37) is necessary to meet conditions in Eqs. (5.42) and (5.43). To prove sufficiency of Eqs. (5.36) and (5.37), we construct an appropriate reconstruction matrix $\mathcal{H}(f)$ that is continuous in f and satisfies the boundary condition in Eq. (5.17). We first define the function $\mathcal{H}(f)$ on the following finite set of frequencies $\{\gamma_m : m \in \mathcal{M}\}$:

$$\mathcal{H}_{\mathcal{J}_m, \bullet}(\gamma_m) = \mathcal{G}_{\bullet, \mathcal{J}_m}^\dagger(\gamma_m), \quad \mathcal{H}_{\mathcal{J}_m^c, \bullet}(\gamma_m) = \mathbf{0}. \quad (5.44)$$

Then in view of Eq. (5.17), we need to define

$$\begin{aligned} \mathcal{H}_{\mathcal{J}_{M+1}, \bullet}\left(\frac{1}{T}\right) &= \mathcal{H}_{\mathcal{J}_1, \bullet}(0) = \mathcal{G}_{\bullet, \mathcal{J}_1}(0), \\ \mathcal{H}_{\mathcal{J}_{M+1}^c, \bullet}\left(\frac{1}{T}\right) &= \mathbf{0}, \end{aligned}$$

where

$$\mathcal{J}_{M+1} \stackrel{\text{def}}{=} \mathcal{J}_1 \ominus R = (\mathcal{K}_1 \ominus R) \cup \mathcal{K}_M.$$

Therefore, using Eq. (5.16), we now have

$$\mathcal{H}_{\mathcal{J}_{M+1}, \bullet} \left(\frac{1}{T} \right) = \mathcal{G}_{\bullet, \mathcal{J}_{M+1}}^\dagger \left(\frac{1}{T} \right), \quad \mathcal{H}_{\mathcal{J}_{M+1}^c, \bullet} \left(\frac{1}{T} \right) = \mathbf{0}. \quad (5.45)$$

To complete the proof, it suffices to construct a *continuous extension* $\mathcal{H}(f)$ on $[0, 1/T]$ that satisfies Eqs. (5.44) and (5.45). With the intention of applying Lemma 5.1, define the following quantities:

$$\begin{aligned} a = \gamma_m, \quad \mathbf{E}_\alpha &= \begin{pmatrix} \mathcal{H}_{\mathcal{K}_m, \bullet}(\alpha) \\ \mathcal{H}_{(\mathcal{J}_m \cup \mathcal{J}_{m+1}) \setminus \mathcal{K}_m, \bullet}(\alpha) \end{pmatrix}, & \mathbf{C}(f) &= \mathcal{G}_{\bullet, \mathcal{K}_m}(f), \\ b = \gamma_{m+1}, \quad \mathbf{E}_\beta &= \begin{pmatrix} \mathcal{H}_{\mathcal{K}_m, \bullet}(\beta) \\ \mathcal{H}_{(\mathcal{J}_m \cup \mathcal{J}_{m+1}) \setminus \mathcal{K}_m, \bullet}(\beta) \end{pmatrix}, & \mathbf{D}(f) &= \begin{pmatrix} \mathbf{I}_{|\mathcal{K}_m|} \\ \mathbf{0} \end{pmatrix}. \end{aligned}$$

Observe that $\mathbf{C}(f) = \mathcal{G}_{\bullet, \mathcal{K}_m}(f)$ has full column rank for $f \in [\gamma_m, \gamma_{m+1}]$. Moreover, using $\mathcal{K}_m \subseteq \mathcal{J}_m$, and $\mathcal{K}_m \subseteq \mathcal{J}_{m+1}$, it follows from Eq. (5.44) that

$$\mathbf{E}_\alpha \mathbf{C}(\alpha) = \begin{pmatrix} \mathbf{I}_{|\mathcal{K}_m|} \\ \mathbf{0} \end{pmatrix} = \mathbf{D}(\alpha) \quad \text{and} \quad \mathbf{E}_\beta \mathbf{C}(\beta) = \begin{pmatrix} \mathbf{I}_{|\mathcal{K}_m|} \\ \mathbf{0} \end{pmatrix} = \mathbf{D}(\beta).$$

Thus, we have verified all the technical conditions required in Lemma 5.1, and we are guaranteed a continuous solution

$$\mathbf{E}(f) = \begin{pmatrix} \mathcal{H}_{\mathcal{K}_m, \bullet}(f) \\ \mathcal{H}_{(\mathcal{J}_m \cup \mathcal{J}_{m+1}) \setminus \mathcal{K}_m, \bullet}(f) \end{pmatrix}$$

that meets the desired boundary conditions and satisfies

$$\mathcal{H}_{\mathcal{K}_m, \bullet}(f) \mathcal{G}_{\bullet, \mathcal{K}_m}(f) = \mathbf{I}_{|\mathcal{K}_f|} \quad \text{and} \quad \mathcal{H}_{(\mathcal{J}_m \cup \mathcal{J}_{m+1}) \setminus \mathcal{K}_m, \bullet}(f) \mathcal{G}_{\bullet, \mathcal{K}_m}(f) = \mathbf{0} \quad (5.46)$$

for $f \in [\gamma_m, \gamma_{m+1}]$. We also define

$$\mathcal{H}_{(\mathcal{J}_m \cup \mathcal{J}_{m+1})^c, \bullet}(f) = \mathbf{0}, \quad f \in [\gamma_m, \gamma_{m+1}]. \quad (5.47)$$

Therefore, Eqs. (5.46) and (5.47) provide us with a continuous extension for $\mathcal{H}(f)$ on $[\gamma_m, \gamma_{m+1}]$ for each $m \in \mathcal{M}$, and hence for the entire interval $[0, 1/T]$. \square

Remarks. Observe the following:

1. A simple necessary condition for perfect reconstruction using continuous reconstruction filters is that $P \geq \max_m |\mathcal{J}_m|$.
2. Note that although the continuity of the entries of $\mathbf{G}(f)$ was essential in the above proof, it is not strictly necessary as it is possible to carefully construct examples where a continuous $\mathbf{H}(f)$ exists even though $\mathbf{G}(f)$ may be discontinuous.

The following example illustrates Theorem 5.2

Example 5.4. Assume that $R = 2$, $T = 4$, and that the input spectra have the same form as in Example 5.2. Then $\mathcal{K}_1 = \{0, 2, 6, 3\}$ and $\mathcal{K}_2 = \{0, 3\}$. In addition the index sets defined in Eq. (5.38) are

$$\mathcal{J}_1 = \mathcal{K}_1 \cup (\mathcal{K}_2 \oplus 2) = \{0, 2, 6, 3, 5\},$$

$$\mathcal{J}_2 = \mathcal{K}_2 \cup \mathcal{K}_1 = \{0, 2, 3, 6\}.$$

Hence, $P \geq \max_m |\mathcal{J}_m| = 5$ is necessary for the existence of a continuous $\mathbf{H}(f)$, and clearly, the transfer function matrix $\mathbf{G}(f)$ of Example 5.2 does not suffice. So let us append a new row beneath the last row of $\mathbf{G}(f)$, thereby making the the MIMO channel a two-input five-output channel:

$$\mathbf{G}(f) = \begin{pmatrix} 1 & 1 \\ 1 & 1 + e^{-j2\pi f} \\ e^{-j2\pi f} & 0.25 + e^{-j4\pi f} \\ 1 + 0.5e^{-j2\pi f} & 1 + e^{-j4\pi f} \\ 0.25 + e^{-j4\pi f} & e^{-j2\pi f} \end{pmatrix}.$$

The rank condition in Eq. (5.36) holds because the matrix $\mathbf{G}_{\bullet, \mathcal{K}_m}(f)$ of Example 5.2 has full column rank, and adding an extra row to $\mathbf{G}(f)$ (and hence to $\mathbf{G}(f)$ also) does not lower the column rank of $\mathbf{G}_{\bullet, \mathcal{K}_m}(f)$. Figure 5.4 depicts the smallest and largest eigenvalues of the matrix

$$\mathbf{S}(f) = \mathbf{G}_{\bullet, \mathcal{K}_f}^H(f) \mathbf{G}_{\bullet, \mathcal{K}_f}(f)$$

as a function of frequency. Note that the discontinuities in these plots are expected because $\mathcal{K}_f(f)$ is piecewise constant with discontinuities at the cell boundaries, i.e., at $f = \gamma_1 = 0.15$ in this case. A numerical calculation yields the following frame bounds for the MIMO sampling scheme.

$$A = \operatorname{ess\,inf}_{f \in [0, \frac{1}{T}]} \lambda_{\min}(T\mathbf{S}(f)) = 0.1251,$$

$$B = \operatorname{ess\,sup}_{f \in [0, \frac{1}{T}]} \lambda_{\max}(T\mathbf{S}(f)) = 1.1105.$$

Hence, the condition number is $\sqrt{B/A} = 2.9790$. The other rank condition in Eq. (5.37) which needs to be verified at cell boundaries, also holds. Now, Theorem 5.2 guarantees the existence of a continuous filter matrix $\mathbf{H}(f)$ that achieves perfect reconstruction of the MIMO channel inputs. In principle, one can construct a continuous $\mathbf{H}(f)$ by following the steps of the proof of Theorem 5.2.

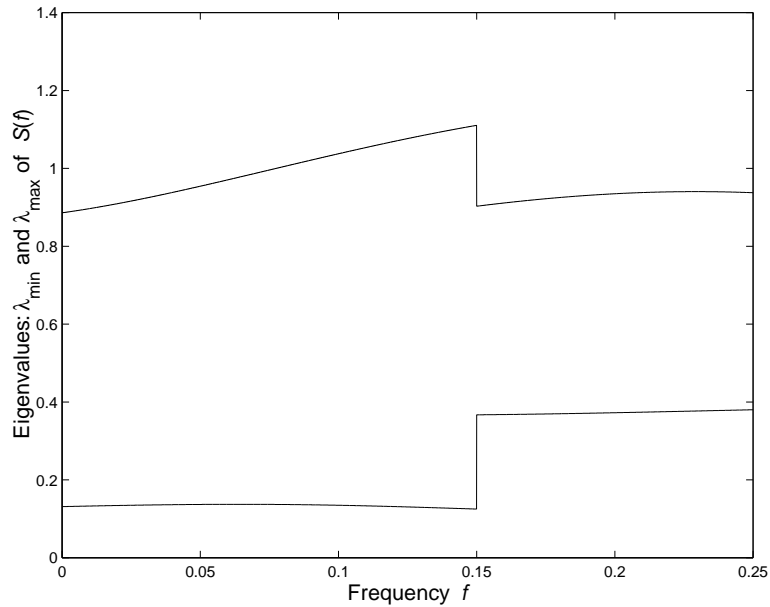


Figure 5.4 Smallest and largest eigenvalues of $S(f)$.

5.5 Summary

In this chapter, we studied the uniform MIMO sampling problem. This scheme encompasses multicoset sampling, Papoulis's generalized sampling, and vector sampling schemes as a special cases. The MIMO problem is motivated from the problem of channel equalization from the sampled channel outputs. We presented necessary and sufficient conditions for perfect reconstruction of the signals, or equivalently, perfect inversion of the channel when the input signals lie in the space of multiband signals with different band structures. We also presented the appropriate conditions for the existence of reconstruction filters continuous in f . The latter result is important from the viewpoint of implementation of the reconstruction system using FIR filters. We address the problem of reconstruction filter design using FIR filters in the next chapter.

CHAPTER 6

FILTER DESIGN FOR MIMO SAMPLING AND RECONSTRUCTION

6.1 Introduction

In this chapter, we address another aspect of MIMO sampling, namely the problem of reconstruction filter design for uniform MIMO sampling. In Chapter 5, we presented necessary and sufficient conditions for perfect reconstruction of the channel inputs. In practice, the channel inputs are continuous-time signals. However, the processing is done digitally, requiring that the channel inputs and outputs be representable as discrete-time sequences. Fortunately, the continuous-time model can be converted to an equivalent discrete-time model, and the discrete-time sequences represent the samples of the continuous-time counterparts at the Nyquist rate or higher.

This is shown rigorously in Appendix B, where we arrive at the following models for the MIMO channel and the reconstruction system. Figure 6.1 depicts the block diagram of the discrete-time MIMO channel with R inputs and P outputs. The inputs to the channel are the sequences $x_r[k]$, $r = 1, \dots, R$, and the outputs are $y_p[k]$, $p = 1, \dots, P$. The channel outputs are then uniformly subsampled by an integer factor $L > 0$ to produce sequences $z_p[n]$. The reconstruction block, depicted in Figure 6.2, produces estimates $\tilde{x}_r[k]$ of the input signals from the quantities $z_p[n]$. We shall consider only uniform subsampling of the channel outputs. This scheme is sufficiently general and it subsumes periodic nonuniform subsampling of the MIMO outputs as a special case of uniform subsampling applied to a hypothetical channel with more rows, as discussed in Chapter 5.

The continuous-time outputs can finally be recovered from the discrete-time sequences $\tilde{x}_r[k]$ using a bank of conventional D/A converters. Thus, the reconstruction filter design problem is one of FIR design.

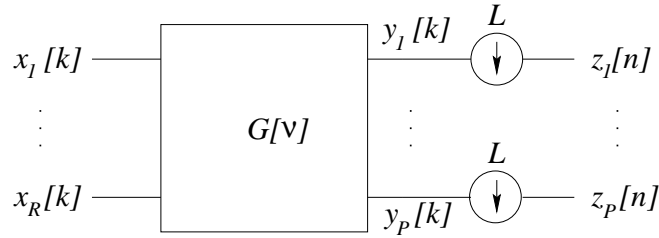


Figure 6.1 Discrete-time model for the MIMO channel.

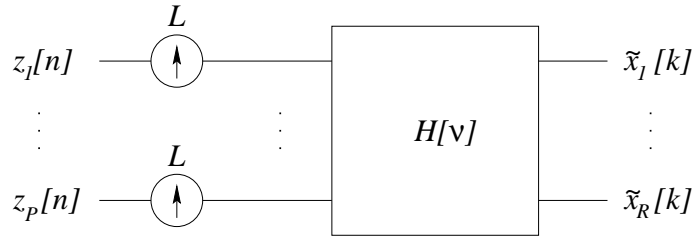


Figure 6.2 Discrete-time model for MIMO reconstruction.

Several sampling schemes can be viewed as special cases of MIMO sampling. For example, in Papoulis’s generalized sampling [12], a single lowpass input signal is passed through a bank of M filters, and the outputs are sampled at $1/M$ th the Nyquist rate. This fits in our framework as a SIMO sampling problem, i.e., $R = 1$. Additionally, if the channel filters are pure delays, we obtain multicoset or periodic nonuniform sampling of the input signal which has been widely studied [14–24], as it allows us to approach the Landau minimum sampling for multiband signals [6]. Seidner and Feder [13] provide a natural generalization of Papoulis’s sampling expansions for a vector input with its components bandlimited to $[-B, B]$. Their sampling scheme is clearly a special case of MIMO sampling. We studied the continuous-time MIMO sampling problem and presented necessary and sufficient conditions for stable sampling in Chapter 5. The purpose of this chapter is to examine the related problem of FIR filter design for MIMO reconstruction filters. We formulate the design problem as a semi-infinite linear program. Semi-infinite formulations have been successfully applied to other multirate filter design problems [54, 55] and solved using standard techniques [34]. Our FIR filter design formulation is fairly general and can be used to design the interpolation filters for those generalized sampling schemes discussed above.

This chapter is organized as follows. Section 6.2, contains some basic notation and definitions. In Section 6.3 we present discrete-time models for the channel and reconstruction block. The channel inputs are modeled as multiband signals. In Section 6.4, we present discrete-time versions of the results derived in Chapter 5. In particular, we specify necessary and sufficient

conditions for the existence of reconstruction filters that are continuous in the frequency domain. This property is important in the context of FIR filter design, as we elaborate on later. Finally, in Section 6.5 we discuss the problem of FIR reconstruction filter design for the MIMO sampling problem. We formulate a cost function in terms of the filter coefficients. Minimizing the cost produces the optimal filter coefficients. The problem may be recast as a semi-infinite linear program. We present two design examples: one for multicoset sampling and another for MIMO sampling with two inputs.

6.2 Preliminaries

We begin with a some basic definitions and notation. Denote the discrete-time Fourier transform of a $x[n] \in l^2$ by the periodic function:

$$X[\nu] = \sum_{k \in \mathbb{Z}} x[k] e^{-j2\pi\nu k}.$$

In general, we denote time signals (either scalar-valued or vector-valued) using lowercase letters, and their Fourier transforms by the corresponding uppercase letters. Let the class complex-valued, finite-energy discrete-time signals bandlimited to the set of frequencies $\mathcal{F} \subseteq [0, 1)$ by

$$\mathcal{B}_d(\mathcal{F}) = \{x[k] \in l^2 : X[\nu] = 0, \forall \nu \in [0, 1) \cap \mathcal{F}^c\}. \quad (6.1)$$

We denote the class of complex-valued matrices of size $M \times N$ by $\mathbb{C}^{M \times N}$, the conjugate-transpose of \mathbf{A} by \mathbf{A}^H , its pseudo inverse by \mathbf{A}^\dagger , and its range space by $\mathcal{R}(\mathbf{A})$. For a given matrix \mathbf{A} , let $\mathbf{A}_{\mathcal{R}, \mathcal{C}}$ denote the submatrix of \mathbf{A} corresponding to rows indexed by the set \mathcal{R} and columns by the set \mathcal{C} . The quantity $\mathbf{A}_{\bullet, \mathcal{C}}$ denotes a submatrix formed by keeping all rows of \mathbf{A} , but only columns indexed by \mathcal{C} , while $\mathbf{A}_{\mathcal{R}, \bullet}$ denotes the submatrix formed by retaining rows indexed by \mathcal{R} and all columns. We use a similar notation for vectors. Hence, $\mathbf{X}_{\mathcal{R}}$ is the subvector of \mathbf{X} corresponding to rows indexed by \mathcal{R} . We always apply the subscripts of a matrix before the superscript. So $\mathbf{A}_{\mathcal{R}, \mathcal{C}}^H$ is the conjugate-transpose of $\mathbf{A}_{\mathcal{R}, \mathcal{C}}$. When dealing with singleton index sets: $\mathcal{R} = \{r\}$ or $\mathcal{C} = \{c\}$, we omit the curly braces for readability. Therefore, $\mathbf{A}_{r, \bullet}$ and $\mathbf{A}_{\bullet, c}$ are the r th row and the c th column of \mathbf{A} , respectively. For convenience, we always number the rows and columns of a finite-size matrix starting from 0. For infinite-size matrices, the row and column indices range over \mathbb{Z} . As a result of the above notation, we have the following straightforward proposition that is used later.

Proposition 6.1. *Suppose that $\mathbf{X} \in \mathbb{C}^L$ and \mathbf{I} is the $L \times L$ identity matrix. Then*

$$\mathbf{X}_{\mathcal{K}} = \mathbf{I}_{\mathcal{K}, \bullet} \mathbf{X} \quad (6.2)$$

for all $\mathcal{K} \subseteq \{0, \dots, L-1\}$. Additionally, if $\mathbf{X}_{\mathcal{K}^c} = \mathbf{0}$, where \mathcal{K}^c is the complement of \mathcal{K} , then

$$\mathbf{X} = \mathbf{I}_{\bullet, \mathcal{K}} \mathbf{X}_{\mathcal{K}}. \quad (6.3)$$

The identity matrix of size $N \times N$ is denoted by \mathbf{I}_N , and the zero matrix by $\mathbf{0}$. Finally suppose that \mathcal{S} is a subset of \mathbb{R} or \mathbb{Z} , and a is an element of \mathbb{R} or \mathbb{Z} , then

$$\begin{aligned} \mathcal{S} \oplus a &= \{s + a : s \in \mathcal{S}\}, \\ \mathcal{S} \ominus a &= \{s - a : s \in \mathcal{S}\}, \\ a\mathcal{S} &= \{as : s \in \mathcal{S}\}, \\ \mathcal{S} \bmod a &= \{s \bmod a : s \in \mathcal{S}\}, \end{aligned}$$

denote the positive and negative translations, scaling, and the modulus of \mathcal{S} by a , respectively.

6.3 Sampling and Reconstruction Models

Figure 6.1 depicts a MIMO channel whose inputs and outputs are discrete-time sequences $\{x_1[k], \dots, x_R[k]\}$ and $\{y_1[k], \dots, y_P[k]\}$, respectively. For convenience, let $\mathcal{R} = \{0, 1, \dots, R-1\}$ and $\mathcal{P} = \{0, 1, \dots, P-1\}$ denote index sets for the channel inputs and outputs. We model $x_r[k]$, $r \in \mathcal{R}$ as multiband signals: $x_r(t) \in \mathcal{B}_d(\mathcal{F}_r)$, where the *spectral support* $\mathcal{F}_r \subseteq [0, 1)$ is a finite union of disjoint intervals:

$$\mathcal{F}_r = \bigcup_{n=1}^{N_r} [a_{rn}, b_{rn}), \quad a_{r1} < b_{r1} < a_{r2} < \dots < a_{rN_r} < b_{rN_r}. \quad (6.4)$$

Let the channel inputs and outputs be expressed in vector form as

$$\begin{aligned} \mathbf{x}[k] &= (x_0[k] \ x_1[k] \ \dots \ x_{R-1}[k])^T, \\ \mathbf{y}[k] &= (y_0[k] \ y_1[k] \ \dots \ y_{P-1}[k])^T. \end{aligned}$$

The MIMO channel is modeled as a linear shift-invariant system, thus enabling us to write

$$\mathbf{y}[k] = \mathbf{g} * \mathbf{x}[k] = \sum_{n \in \mathbb{Z}} \mathbf{g}[k - n] \mathbf{x}[n],$$

where $*$ denotes convolution, and $\mathbf{g}[k] \in \mathbb{C}^{P \times R}$ is the MIMO channel impulse response. Hence, we have

$$\mathbf{Y}[\nu] = \mathbf{G}[\nu] \mathbf{X}[\nu], \quad (6.5)$$

where $\mathbf{X}[\nu]$, $\mathbf{Y}[\nu]$, and $\mathbf{G}[\nu]$ are the Fourier transforms of $\mathbf{x}[k]$, $\mathbf{y}[k]$, and $\mathbf{g}[k]$, respectively. We call $\mathbf{G}[\nu]$ the *channel transfer function matrix*. The channel outputs are uniformly subsampled

by a factor of L , and the resulting sequences are denoted by $\mathbf{z}[n] = \mathbf{y}[nL]$, $n \in \mathbb{Z}$. Using Eq. (6.5), we now have

$$\mathbf{Z}[\nu] = \frac{1}{L} \sum_{l \in \mathbb{Z}} \mathbf{Y} \left[\frac{\nu+l}{L} \right] = \frac{1}{L} \sum_{l \in \mathbb{Z}} \mathbf{G} \left[\frac{\nu+l}{L} \right] \mathbf{X} \left[\frac{\nu+l}{L} \right], \quad \nu \in [0, 1). \quad (6.6)$$

We model the reconstruction block as follows:

$$\tilde{\mathbf{x}}[k] = \sum_{n \in \mathbb{Z}} \mathbf{h}[k - nL] \mathbf{z}[n], \quad (6.7)$$

where $\mathbf{h}[k] \in \mathbb{C}^{R \times P}$ is the impulse response of the reconstruction filter. From Eq. (6.7), it is obvious that the entire system consisting of the channel, the subsampling, and the reconstruction is invariant to time-shifts of any multiple of L , i.e.,

$$\mathbf{x} \rightarrow \tilde{\mathbf{x}} \implies \mathbf{x}[\cdot - nL] \rightarrow \tilde{\mathbf{x}}[\cdot - nL], \quad \forall n \in \mathbb{Z}.$$

Conversely, Eq. (6.7) describes the most general linear transformation that allows this invariance. Taking the Fourier transform of Eq. (6.7), we obtain

$$\tilde{\mathbf{X}}[\nu] = \mathbf{H}[\nu] \mathbf{Z}[L\nu], \quad \nu \in [0, 1), \quad (6.8)$$

where $\mathbf{H}[\nu]$, the Fourier transform of $\mathbf{h}[n]$, is called the *reconstruction filter matrix*. Since $\mathbf{Z}[\nu]$ is a periodic function, we can rewrite Eq. (6.8) as

$$\tilde{\mathbf{X}} \left[\nu + \frac{l'}{L} \right] = \mathbf{H} \left[\nu + \frac{l'}{L} \right] \mathbf{Z}[L\nu], \quad l' \in \mathbb{Z}, \nu \in [0, 1/L). \quad (6.9)$$

We can now write Eqs. (6.6) and (6.9) compactly as

$$\mathbf{Z}[L\nu] = \mathbf{G}[\nu] \mathbf{X}[\nu], \quad (6.10)$$

$$\tilde{\mathbf{X}}[\nu] = \mathbf{H}[\nu] \mathbf{Z}[L\nu] \quad (6.11)$$

for $\nu \in [0, 1/L)$, where $\mathbf{X}[\nu]$ and $\tilde{\mathbf{X}}[\nu]$ are defined as

$$\mathbf{X}_{Rl+r}[\nu] = X_r \left[\nu + \frac{l}{L} \right], \quad (r, l) \in \mathcal{R} \times \mathcal{L}, \quad (6.12)$$

$$\tilde{\mathbf{X}}_{Rl+r}[\nu] = \tilde{X}_r \left[\nu + \frac{l}{L} \right], \quad (r, l) \in \mathcal{R} \times \mathcal{L}, \quad (6.13)$$

while $\mathbf{G}[\nu]$ and $\mathbf{H}[\nu]$ are the *modulated channel and reconstruction matrices* defined as

$$\mathbf{G}_{p, Rl+r}[\nu] = \frac{1}{L} G_{pr} \left[\nu + \frac{l}{L} \right], \quad (p, r, l) \in \mathcal{P} \times \mathcal{R} \times \mathcal{L}, \quad (6.14)$$

$$\mathbf{H}_{Rl+r, p}[\nu] = H_{rp} \left[\nu + \frac{l}{L} \right], \quad (p, r, l) \in \mathcal{P} \times \mathcal{R} \times \mathcal{L}. \quad (6.15)$$

In the next section, we provide precise conditions for stable reconstruction of the channel inputs from the subsampled output sequences. In particular, for FIR implementation reasons, we are interested in a reconstruction filter matrix $\mathbf{H}[\nu]$ whose entries are continuous in ν . Specifically, the continuity guarantees that the approximation error resulting from the FIR implementation can be made arbitrarily small by choosing sufficiently long FIR filters. This point will be elaborated later.

6.4 Conditions for Perfect Reconstruction

In this section, we present the condition for perfect reconstruction from the MIMO channel outputs in the discrete-time setting. More specifically, we provide conditions on the channel transfer function matrix $\mathbf{G}[\nu]$ that guarantee stable reconstruction of the inputs *with/without* the continuity requirement on the reconstruction filter matrix $\mathbf{H}[\nu]$. These results are discrete-time versions of their continuous-time ones presented in Chapter 5.

Let $\mathcal{H} = \mathcal{B}_d(\mathcal{F}_1) \times \cdots \times \mathcal{B}_d(\mathcal{F}_R)$ denote the class of inputs to the MIMO channel. Then \mathcal{H} is a Hilbert space equipped with the following inner product:

$$\langle \mathbf{x}, \mathbf{w} \rangle = \sum_{n \in \mathbb{Z}} \mathbf{w}^H[n] \mathbf{x}[n], \quad \mathbf{x}, \mathbf{w} \in \mathcal{H}.$$

Naturally, the norm on \mathcal{H} is defined as $\|\mathbf{x}\| = \sqrt{\langle \mathbf{x}, \mathbf{x} \rangle}$. We now review an important notion called *stability* of MIMO sampling (see Chapters 4 and 5).

Definition 6.1. The MIMO sampling scheme is called *stable* if there exist constants $A, B > 0$ such that

$$A\|\mathbf{x}\|^2 \leq \sum_{n \in \mathbb{Z}} \|\mathbf{z}[n]\|^2 \leq B\|\mathbf{x}\|^2, \quad (6.16)$$

for all $\mathbf{x} \in \mathcal{H}$.

The implication of Eq. (6.16) is that we can reconstruct the inputs from the outputs samples $\mathbf{z}[n]$ in a stable manner, in the sense that small perturbations in the inputs or the channel output samples, cannot cause large errors in the reconstructed outputs. The quantity $K = \sqrt{B/A} \geq 1$ is called the *condition number* of the sampling scheme, and it is a bound on the amplification of the normalized error energy due to the reconstruction filters. In particular, the notion of stable sampling may be expressed as a frame-theoretic condition. We refer the reader to [2, 46] for more about frames. The theory of frames provides a convenient tool to study sampling [47].

Now, define the following index sets

$$\begin{aligned}\mathcal{K}_\nu &= \{Rl + r : (r, l) \in \mathcal{R} \times \mathcal{L} \text{ and } \nu + l/T \in \mathcal{F}_r\}, \\ \mathcal{K}_\nu^c &= \mathcal{Z} \setminus \mathcal{K}_\nu\end{aligned}\tag{6.17}$$

for $\nu \in [0, 1/L]$, where $\mathcal{Z} = \{0, \dots, RL - 1\}$. Just as in the continuous-time case in Chapter 5, we can decompose the interval $[0, 1/L]$ into a union of intervals, where \mathcal{K}_ν is piecewise constant.

Proposition 6.2. *Suppose that sets \mathcal{F}_r , $r \in \mathcal{R}$ have multiband structure as defined in Eq. (6.4). Then there exists a collection of disjoint intervals \mathcal{I}_m and sets \mathcal{K}_m , $m = 1, \dots, M$ such that*

$$\bigcup_{m=1}^M \mathcal{I}_m = \left[0, \frac{1}{L}\right) \quad \text{and} \quad \mathcal{K}_\nu = \mathcal{K}_m, \quad \forall \nu \in \mathcal{I}_m.$$

This result is easily demonstrated by using an argument very similar to the one in Chapter 2. We write \mathcal{I}_m as

$$\begin{aligned}\mathcal{I}_m &= [\gamma_m, \gamma_{m+1}), \quad m \in \mathcal{M}, \\ \gamma_1 &< \gamma_2 < \dots < \gamma_{M+1},\end{aligned}$$

such that $\gamma_1 = 0$ and $\gamma_{M+1} = 1/L$. For convenience we also define

$$q_m \stackrel{\text{def}}{=} |\mathcal{K}_m|.$$

Equation (6.17) implies that all nonzero entries of $\mathcal{X}[\nu]$ are captured in $\mathcal{X}_{\mathcal{K}_\nu}[\nu]$. Hence, from Eqs. (6.10) and (6.11) we conclude that $\mathcal{H}_{\mathcal{K}_\nu, \bullet}[\nu] \mathcal{G}_{\bullet, \mathcal{K}_\nu}[\nu] = \mathbf{I}_{|\mathcal{K}_\nu|}$ and $\mathcal{H}_{\mathcal{K}_\nu^c, \bullet}[\nu] \mathcal{G}_{\bullet, \mathcal{K}_\nu}[\nu] = \mathbf{0}$ hold a.e. This can be written compactly as

$$\mathcal{H}[\nu] \mathcal{G}_{\bullet, \mathcal{K}_\nu}[\nu] = \mathbf{I}_{\bullet, \mathcal{K}_\nu},\tag{6.18}$$

where \mathbf{I} is the $RL \times RL$ identity matrix. Since $\mathcal{G}_{\bullet, \mathcal{K}_\nu}[\nu] \in \mathbb{C}^{P \times |\mathcal{K}_\nu|}$, we require that $\mathcal{G}_{\bullet, \mathcal{K}_\nu}(\nu)$ have full column rank a.e.

As in Proposition 5.2, it can be easily verified that $\mathbf{H}[\nu]$ is continuous if and only if $\mathcal{H}[\nu]$ is continuous on $[0, 1/L]$, and the following ‘‘boundary conditions’’ hold:

$$\mathcal{H}_{\mathcal{K}, \bullet} \left[\frac{1}{L} \right] = \mathcal{H}_{\mathcal{K}', \bullet} [0]\tag{6.19}$$

for all $\mathcal{K} \subseteq \mathcal{Z}$, where $\mathcal{K}' = (\mathcal{K} \oplus R) \bmod RL$. As we shall see later, in order to achieve continuity of $\mathbf{H}[\nu]$, it is convenient to impose continuity on $\mathbf{G}[\nu]$, and this produces a similar condition on

$\mathcal{G}[\nu]$. Specifically, if $G_{pr}[\nu]$ is continuous on $\overline{\mathcal{F}_r}$ (the closure of \mathcal{F}_r), then $\mathcal{G}_{\bullet, \mathcal{K}_m}[\nu]$ is continuous on $\overline{\mathcal{I}_m}$, and

$$\mathcal{G}_{\bullet, \mathcal{K}}\left[\frac{1}{L}\right] = \mathcal{G}_{\bullet, \mathcal{K}'}[0], \quad (6.20)$$

for all $\mathcal{K} \subseteq \mathcal{Z}$.

The following theorems, which are discrete-time versions of similar results presented in Chapter 5, provide precise conditions for stable and perfect reconstruction of the channel inputs. We do not prove them as they can be deduced in a manner very similar to their continuous-time counterparts. Before stating the results, we point out that ess inf and ess sup denote the essential infimum and supremum, respectively, i.e.,

$$\begin{aligned} \text{ess inf}_t g(t) &= \sup\{\gamma : g(t) \geq \gamma \text{ a.e.}\}, \\ \text{ess sup}_t g(t) &= \inf\{\gamma : g(t) \leq \gamma \text{ a.e.}\}. \end{aligned}$$

for any real function g .

Theorem 6.1. *Suppose that $\mathbf{G}[\nu]$ is such that $G_{pr}[\nu]$ is continuous for $\nu \in \overline{\mathcal{F}_r}$, and $\mathcal{G}_{\bullet, \mathcal{K}_m}[\nu]$ has full column rank for all $m \in \mathcal{M}$, $\nu \in \overline{\mathcal{I}_m} = [\gamma_m, \gamma_{m+1}]$, then the MIMO sampling scheme is stable, and the stability bounds are given by*

$$A = L \text{ess inf}_{\nu \in [0, 1/L]} \lambda_{\min}(\mathcal{G}_{\bullet, \mathcal{K}_\nu}^H[\nu] \mathcal{G}_{\bullet, \mathcal{K}_\nu}[\nu]), \quad (6.21)$$

$$B = L \text{ess sup}_{\nu \in [0, 1/L]} \lambda_{\max}(\mathcal{G}_{\bullet, \mathcal{K}_\nu}^H[\nu] \mathcal{G}_{\bullet, \mathcal{K}_\nu}[\nu]). \quad (6.22)$$

Theorem 6.2. *Suppose that channel transfer function matrix $\mathbf{G}[\nu]$ is such that $G_{pr}[\nu]$ is continuous for $\nu \in \overline{\mathcal{F}_r}$, then there exists a reconstruction filter matrix $\mathbf{H}[\nu]$ continuous in ν that achieves stable and perfect reconstruction of the MIMO channel inputs if and only if*

$$\text{rank}(\mathcal{G}_{\bullet, \mathcal{K}_m}[\nu]) = |\mathcal{K}_m|, \quad \forall \nu \in \text{int } \mathcal{I}_m = (\gamma_m, \gamma_{m+1}), \quad (6.23)$$

$$\text{rank}(\mathcal{G}_{\bullet, \mathcal{J}_m}(\gamma_m)) = |\mathcal{J}_m|, \quad m \in \mathcal{M}. \quad (6.24)$$

where

$$\begin{aligned} \mathcal{J}_m &= \mathcal{K}_m \cup \mathcal{K}_{m-1}, \quad m = 2, \dots, M, \\ \mathcal{J}_1 &= \mathcal{K}_1 \cup ((\mathcal{K}_M \oplus R) \bmod RL). \end{aligned} \quad (6.25)$$

Theorem 6.1 guarantees stability of reconstruction, but not continuity of $\mathbf{H}[\nu]$, while Theorem 6.2 guarantees both stability and continuity of at least one solution $\mathbf{H}[\nu]$. The continuity requirement is desirable from the viewpoint of implementation, as we see in Section 6.5. A simple necessary condition for perfect reconstruction using continuous reconstruction filters is that $P \geq \max_m |\mathcal{J}_m|$. In Theorem 6.2, the assumption that $\mathbf{G}[\nu]$ is continuous in ν is made for convenience; it is possible for continuous perfect reconstruction filter matrix $\mathbf{H}[\nu]$ to exist, despite the lack of continuity of $\mathbf{G}[\nu]$. However, this is rare, and the conditions in the general case are cumbersome.

Finally, under certain conditions, perfect reconstruction is realizable using FIR filters. We say that a filter is FIR if its impulse response has a finite number of nonzero terms. An FIR filter need not be causal, but can be made causal by adding a finite delay. Let

$$\mathbf{G}^*[z] = \sum_{k \in \mathbb{Z}} \mathbf{g}[k] z^{-k}$$

denote the Z -transform of $\mathbf{g}[k]$. We use the superscript “ \star ” here to distinguish between the Z -transform and the discrete-time Fourier transform $\mathbf{G}[\nu]$. Then clearly

$$\mathbf{G}[\nu] = \mathbf{G}^*[\exp(j2\pi\nu)], \quad \nu \in \mathbb{R}.$$

Let $\mathbf{H}^*[z]$ denote the Z -transform of $\mathbf{h}[k]$. Finally, let $\mathcal{G}^*[z]$ and $\mathcal{H}^*[z]$ be the Z -domain analogues of the modulated matrices $\mathcal{G}[\nu]$ and $\mathcal{H}[\nu]$.

Theorem 6.3. *Suppose that channel impulse response $\mathbf{g}[k]$ is a finite sequence, and let*

$$\mathcal{K} = \bigcup_{m=1}^M \mathcal{K}_m, \quad Q = |\mathcal{K}|.$$

Then perfect reconstruction using an FIR reconstruction filter matrix $\mathbf{H}^[z]$ is possible if and only if $P \geq Q$, and all the $Q \times Q$ minors of $\mathcal{G}_{\bullet, \mathcal{K}}^*[z]$ have no common zeros except $z = 0$ or $z = \infty$.*

Proof. Suppose that $P \geq Q$ and the minors share no zeros except $z = 0$ or $z = \infty$. For every $\mathcal{J} \subseteq \mathcal{P}$ such that $|\mathcal{J}| = Q$, let

$$D_{\mathcal{J}}[z] = \det(\mathcal{G}_{\mathcal{J}, \mathcal{K}}^*[z]).$$

Then, by Bezout’s identity, there exist polynomials $A_{\mathcal{J}}[z]$ such that

$$\sum_{\mathcal{J} \subseteq \mathcal{P}: |\mathcal{J}|=Q} A_{\mathcal{J}}[z] D_{\mathcal{J}}[z] = z^d \tag{6.26}$$

for some $d \in \mathbb{Z}$. Let $\tilde{\mathcal{H}}_{\mathcal{J}}[z]$ denote the adjoint of $\mathcal{G}_{\mathcal{J},\mathcal{K}}^*[z]$ so that

$$\tilde{\mathcal{H}}_{\mathcal{J}}[z]\mathcal{G}_{\mathcal{J},\mathcal{K}}^*[z] = D_{\mathcal{J}}[z]\mathbf{I}, \quad (6.27)$$

where \mathbf{I} is the $Q \times Q$ identity matrix. Define

$$\mathcal{H}_{\mathcal{K},\bullet}^*[z] = z^{-d} \sum_{\mathcal{J} \subseteq \mathcal{P}: |\mathcal{J}|=Q} A_{\mathcal{J}}[z] \tilde{\mathcal{H}}_{\mathcal{J}}[z] \mathbf{I}_{\mathcal{J},\bullet} \quad \text{and} \quad \mathcal{H}_{\mathcal{K}^c,\bullet}^*[z] = \mathbf{0}.$$

where $\mathcal{K} = \bigcup_m \mathcal{K}_m$. Then $\mathcal{H}^*[z]$ clearly corresponds to an FIR reconstruction filter matrix $\mathbf{H}^*[z]$. Therefore,

$$\begin{aligned} \mathcal{H}_{\mathcal{K},\bullet}^*[z]\mathcal{G}_{\bullet,\mathcal{K}}^*[z] &= z^{-d} \sum_{\mathcal{J}} A_{\mathcal{J}}[z] \tilde{\mathcal{H}}_{\mathcal{J}}[z] \mathbf{I}_{\mathcal{J},\bullet} \mathcal{G}_{\bullet,\mathcal{K}}^*[z] \\ &= z^{-d} \sum_{\mathcal{J}} A_{\mathcal{J}}[z] \tilde{\mathcal{H}}_{\mathcal{J}}[z] \mathcal{G}_{\mathcal{J},\mathcal{K}}^*[z] = \mathbf{I} \end{aligned}$$

where the last step follows from Eqs. (6.26) and (6.27). We also obviously have

$$\mathcal{H}_{\mathcal{K}^c,\bullet}^*[z]\mathcal{G}_{\bullet,\mathcal{K}}^*[z] = \mathbf{0}.$$

Combining the last two results, we obtain $\mathcal{H}^*[z]\mathcal{G}_{\bullet,\mathcal{K}}^*[z] = \mathbf{I}_{\bullet,\mathcal{K}}$. From this it follows that

$$\mathcal{H}[\nu]\mathcal{G}_{\bullet,\mathcal{K}_m}[\nu] = \mathbf{I}_{\bullet,\mathcal{K}_m}, \quad \forall \nu \in \mathcal{I}_m. \quad (6.28)$$

which is essentially equivalent to Eq. (6.18). Thus, we have found an FIR realization of perfect reconstruction filters.

Conversely, suppose that $\mathbf{h}[k]$ is an FIR filter achieving perfect reconstruction. Then $\mathcal{G}[\nu]$ and $\mathcal{H}[\nu]$ are entire functions since both $\mathbf{g}[k]$ and $\mathbf{h}[k]$ are finite sequences. Hence, Eq. (6.28) implies that

$$\mathcal{H}[\nu]\mathcal{G}_{\bullet,\mathcal{K}_m}[\nu] = \mathbf{I}_{\bullet,\mathcal{K}_m}$$

holds for all $\nu \in \mathbb{R}$, rather than just $\nu \in \mathcal{I}_m$. Therefore, we obtain $\mathcal{H}[\nu]\mathcal{G}_{\bullet,\mathcal{K}}[\nu] = \mathbf{I}_{\bullet,\mathcal{K}}$ for all $\nu \in \mathbb{R}$, where $\mathcal{K} = \bigcup_m \mathcal{K}_m$. Equivalently, we have

$$\mathcal{H}^*[z]\mathcal{G}_{\bullet,\mathcal{K}}^*[z] = \mathbf{I}_{\bullet,\mathcal{K}} \quad (6.29)$$

in the Z -domain. If $P < Q$ then $\text{rank}(\mathcal{G}_{\bullet,\mathcal{K}}^*[z]) \leq Q - 1$, implying that Eq. (6.29) fails to hold. Similarly, if all the minors of $\mathcal{G}_{\bullet,\mathcal{K}}^*[z]$ share a common factor of the form $(z - z_0)$ where $z_0 \neq 0$, then $\mathcal{G}_{\bullet,\mathcal{K}}^*[z]$ loses rank at $z = z_0$, and this contradicts Eq. (6.29) because $\mathcal{H}^*[z]$ is FIR. This proves the converse statement. \square

The proof of Theorem 6.3 is partly based on similar results in [56, 57]. The import of this result is that perfect reconstruction is possible using FIR filters provided the channel impulse response is FIR, and that the modulated channel matrix in the Z -domain $\mathcal{G}^*[z]$ is sufficiently “diverse” in the sense its null space is empty for all $z \notin \{0, \infty\}$. Of course, we do not care about the cases $z = 0$ or $z = \infty$ because no causality requirement is imposed on FIR filters. Suppose that $P = Q$, then $\mathcal{G}_{\bullet, \mathcal{K}}^*[z]$ is a $Q \times Q$ matrix and the necessary and sufficient condition for perfect reconstruction using FIR filters reduces to

$$\det \mathcal{G}_{\bullet, \mathcal{K}}^*[z] = Kz^{-d}, \quad K \neq 0, \quad d \in \mathbb{Z}.$$

This condition is similar to the perfect reconstruction condition for filter banks.

The problem in [57] deals with existence of FIR equalizer filters in the absence of decimation of channel outputs, while in classical filter bank problem deals with a single-input multiple-output channel whose outputs are decimated. In the present problem the existence of an FIR reconstruction filter matrix depends not only on the channel transfer function matrix $\mathbf{G}[\nu]$ (as in the work in [57]), but also on the decimation factor L (as in the filter bank problem), and band-structure of the inputs through \mathcal{K} . Thus, Theorem 6.3 generalized all these problems simultaneously.

6.5 Reconstruction Filter Design

In this section, we study the problem of reconstruction filter design for a given MIMO sampling scheme. We have seen in Section 6.4 that under certain conditions on the channel and the class of input signals, perfect reconstruction is possible. Unfortunately these ideal filters are not necessarily FIR filters. Conversely FIR filters do not generally guarantee perfect reconstruction of the channel inputs. Nevertheless, we can approximate the ideal reconstruction filters using FIR filters chosen judiciously so that an appropriate cost function, such as the end-to-end distortion, is minimized.

We model the input signals as discrete-time multiband functions $X_r[\nu] = 0$, $\nu \notin \mathcal{F}_r$ with $\mathbf{x} \in \mathcal{C}$, where \mathcal{C} is the constraint set for the channel inputs:

$$\mathbf{x} \in \mathcal{C} = \{\mathbf{x} : \|\mathbf{x}_r\| \leq \gamma_r\},$$

i.e., the input signal energies are upper bounded. The reconstruction filters are approximated by FIR filters, i.e., we enforce the following parameterization on $\mathbf{H}[\nu]$:

$$H_{rp}[\nu] = \sum_{k \in \mathcal{Q}_{rp}} \alpha_{rpk} e^{-j2\pi\nu k}, \quad r \in \mathcal{R}, \quad p \in \mathcal{P}, \quad (6.30)$$

where \mathcal{Q}_{rp} is a finite set representing the locations of the nonzero filter coefficients of $H_{rp}[\nu]$. We choose

$$\mathcal{Q}_{rp} = \{k : \kappa_{rp} \leq k \leq l_{rp} + \kappa_{rp} - 1\},$$

where l_{rp} is the length of the FIR reconstruction filter $H_{rp}[\nu]$ and κ_{rp} is the position of the first filter coefficient. This FIR parameterization no longer guarantees perfect reconstruction, and the objective is to minimize the norm of the resulting reconstruction error $\mathbf{e}[k] = \tilde{\mathbf{x}}[k] - \mathbf{x}[k]$. Define

$$\mathcal{E}[\nu] = \tilde{\mathcal{X}}[\nu] - \mathcal{X}[\nu], \quad \nu \in \left[0, \frac{1}{L}\right]. \quad (6.31)$$

We shall now derive an expression for $\mathcal{E}[\nu]$ as a function of the input signals, the channel and reconstruction filters alone. Define index sets

$$\mathcal{I}_r = (R\mathcal{L}) \oplus r = \{Rl + r : l \in \mathcal{L}\}, \quad (6.32)$$

$$\mathcal{K}_{r,\nu} = \mathcal{K}_\nu \cap \mathcal{I}_r = \left\{Rl + r : l \in \mathcal{L} \text{ and } \left(\nu + \frac{l}{L}\right) \in \mathcal{F}_r\right\} \quad (6.33)$$

for each $r \in \mathcal{R}$. It is clear from Eqs. (6.12), (6.13), and (6.32) that

$$\begin{aligned} \mathcal{X}_{\mathcal{I}_r}[\nu] &= \left(X_r[\nu] \quad X_r\left[\nu + \frac{1}{L}\right] \quad \cdots \quad X_r\left[\nu + \frac{L-1}{L}\right]\right)^T, \\ \tilde{\mathcal{X}}_{\mathcal{I}_r}[\nu] &= \left(\tilde{X}_r[\nu] \quad \tilde{X}_r\left[\nu + \frac{1}{L}\right] \quad \cdots \quad \tilde{X}_r\left[\nu + \frac{L-1}{L}\right]\right)^T \end{aligned}$$

for each $r \in \mathcal{R}$; i.e., these quantities are the length- L vectorized representations of $X_r[\nu]$ and $\tilde{X}_r[\nu]$, respectively. Hence, the energy of e_r can be expressed as a function of $\mathcal{E}[\nu]$ using Parseval's theorem:

$$\|e_r\|^2 = \int_{[0,1]} |E_r[\nu]|^2 d\nu = \int_{[0, \frac{1}{L}]} \|\mathcal{E}_{\mathcal{I}_r}[\nu]\|^2 d\nu. \quad (6.34)$$

Similar relations hold for x_r and other signals in terms of the vectorized version of their Fourier transforms. Now for each $r \in \mathcal{R}$ and $\nu \in [0, 1/L]$, Eqs. (6.10) and (6.11) yield

$$\begin{aligned} \tilde{\mathcal{X}}_{\mathcal{I}_r}[\nu] &= \mathcal{H}_{\mathcal{I}_r, \bullet}[\nu] \mathcal{G}[\nu] \mathcal{X}[\nu] \\ &= \sum_{s \in \mathcal{R}} \mathcal{H}_{\mathcal{I}_r, \bullet}[\nu] \mathcal{G}_{\bullet, \mathcal{I}_s}[\nu] \mathcal{X}_{\mathcal{I}_s}[\nu], \end{aligned} \quad (6.35)$$

where the second step holds because the sets $\{\mathcal{I}_r\}$ partition $\{0, 1, \dots, RL - 1\}$. Therefore, Eqs. (6.31) and (6.35) give us

$$\begin{aligned} \mathcal{E}_{\mathcal{I}_r}[\nu] &= \tilde{\mathcal{X}}_{\mathcal{I}_r}[\nu] - \mathcal{X}[\nu] \\ &= \sum_{s \in \mathcal{R}} \mathcal{H}_{\mathcal{I}_r, \bullet}[\nu] \mathcal{G}_{\bullet, \mathcal{I}_s}[\nu] \mathcal{X}_{\mathcal{I}_s}[\nu] - \mathcal{X}[\nu] \\ &= \sum_{s \in \mathcal{R}} \left(\mathcal{H}_{\mathcal{I}_r, \bullet}[\nu] \mathcal{G}_{\bullet, \mathcal{I}_s}[\nu] - \delta_{rs} \mathbf{I}_L \right) \mathcal{X}_{\mathcal{I}_s}[\nu], \end{aligned} \quad (6.36)$$

where δ_{rs} is the Kronecker delta function and \mathbf{I}_L is the identity matrix of size $L \times L$. We know from Eq. (6.2) that

$$\boldsymbol{\mathcal{X}}_{\mathcal{K}_{s,\nu}}[\nu] = \mathbf{I}_{\mathcal{K}_{s,\nu},\mathcal{I}_s} \boldsymbol{\mathcal{X}}_{\mathcal{I}_s}[\nu], \quad (6.37)$$

where \mathbf{I} is the identity matrix of size $LR \times RL$. Since $\boldsymbol{\mathcal{X}}_{\mathcal{K}_{s,\nu}}[\nu]$ captures all the nonzero components of $\boldsymbol{\mathcal{X}}_{\mathcal{I}_s}[\nu]$, we can invoke Eq. (6.3) to write

$$\boldsymbol{\mathcal{X}}_{\mathcal{I}_s}[\nu] = \mathbf{E}_{\mathcal{I}_s,\mathcal{K}_{s,\nu}} \boldsymbol{\mathcal{X}}_{\mathcal{K}_{s,\nu}}[\nu]. \quad (6.38)$$

Combining Eqs. (6.37) and (6.38) we obtain

$$\boldsymbol{\mathcal{X}}_{\mathcal{I}_s}[\nu] = \mathbf{E}_{s,\nu} \boldsymbol{\mathcal{X}}_{\mathcal{I}_s}[\nu], \quad (6.39)$$

where

$$\mathbf{E}_{s,\nu} \stackrel{\text{def}}{=} \mathbf{I}_{\mathcal{I}_s,\mathcal{K}_{s,\nu}} \mathbf{I}_{\mathcal{K}_{s,\nu},\mathcal{I}_s} \quad (6.40)$$

is a diagonal matrix with zeros or ones on the diagonal. Hence, Eqs. (6.36) and (6.39) yield

$$\boldsymbol{\mathcal{E}}_{\mathcal{I}_r}[\nu] = \sum_{s \in \mathcal{R}} \mathbf{T}^{rs}[\nu] \boldsymbol{\mathcal{X}}_{\mathcal{I}_s}[\nu], \quad (6.41)$$

$$\mathbf{T}^{rs}[\nu] = \left(\boldsymbol{\mathcal{H}}_{\mathcal{I}_r,\bullet}[\nu] \boldsymbol{\mathcal{G}}_{\bullet,\mathcal{I}_s}[\nu] - \delta_{rs} \mathbf{I}_L \right) \mathbf{E}_{s,\nu}. \quad (6.42)$$

We point out that if $\mathbf{H}[\nu]$ is a perfect reconstruction filter matrix, then using Eq. (6.18), it is easily shown that

$$\mathbf{T}^{rs}[\nu] = \left(\boldsymbol{\mathcal{H}}_{\mathcal{I}_r,\bullet}[\nu] \boldsymbol{\mathcal{G}}_{\bullet,\mathcal{I}_s}[\nu] - \delta_{rs} \mathbf{I}_L \right) = \mathbf{0}. \quad (6.43)$$

For simplicity we rewrite Eq. (6.41) as

$$e_r = \sum_{s \in \mathcal{R}} \mathbf{T}^{rs} x_s, \quad (6.44)$$

where \mathbf{T}^{rs} is the linear operator equivalent of $\mathbf{T}^{rs}[\nu]$ acting on x_s . Then,

$$\begin{aligned} \|\mathbf{T}^{rs}\|^2 &= \max_{\|x_s\| \leq 1} \|\mathbf{T}^{rs} x_s\|^2 \\ &= \max_{\nu \in [0, \frac{1}{L}]} \int \|\mathbf{T}^{rs}[\nu] \boldsymbol{\mathcal{X}}_{\mathcal{I}_s}[\nu]\|^2 d\nu \quad \text{s.t.} \quad \int_{\nu} \|\boldsymbol{\mathcal{X}}_{\mathcal{I}_s}[\nu]\|^2 d\nu \leq 1. \end{aligned}$$

Note that $\boldsymbol{\mathcal{X}}_{\mathcal{I}_s}[\nu]$ is not an arbitrary vector in $C^{L \times 1}$ for each ν because some entries of $\boldsymbol{\mathcal{X}}_{\mathcal{I}_s}[\nu]$ always vanish due to Eq. (6.39) because $\mathbf{E}_{s,\nu}$ is a diagonal matrix with zeros or ones on the diagonal. From Eqs. (6.42) and (6.40), it is clear that if the k th component of $\boldsymbol{\mathcal{X}}_{\mathcal{I}_s}[\nu]$ vanishes for some k , then the k th column of $\mathbf{T}^{rs}[\nu]$ vanishes; i.e., the range space of $(\mathbf{T}^{rs}[\nu])^H$ equals

the signal space for input s (namely $X_s[\nu]$) so that each row of $\mathbf{T}^{rs}[\nu]$. Hence, we can conclude that

$$\|\mathbf{T}^{rs}\|^2 = \max_{\nu \in [0, \frac{1}{L}]} \|\mathbf{T}^{rs}[\nu]\|^2 = \max_{\nu \in [0, \frac{1}{L}]} \sigma_{\max}(\mathbf{T}^{rs}[\nu]), \quad (6.45)$$

where $\|\mathbf{T}^{rs}[\nu]\|$ is the spectral norm of $\mathbf{T}^{rs}[\nu]$, and $\sigma_{\max}(\cdot)$ is the largest singular value.

6.5.1 The cost function

Our problem is to design an FIR reconstruction filter matrix $\mathbf{H}[\nu]$ such that a measure of the reconstruction error \mathbf{e} is minimized. Using Eq. (6.15) we see that

$$\mathcal{H}_{\mathcal{I}_r, \bullet}[\nu] = \begin{pmatrix} \mathbf{H}_{r, \bullet}[\nu] \\ \mathbf{H}_{r, \bullet}[\nu + \frac{1}{L}] \\ \vdots \\ \mathbf{H}_{r, \bullet}[\nu + \frac{L-1}{L}] \end{pmatrix}$$

depends only on the r th row of $\mathbf{H}[\nu]$, namely $\mathbf{H}_{r, \bullet}[\nu]$. We also see from Eq. (6.30) that $\mathbf{H}_{r, \bullet}[\nu]$ is a linear combination parameterized by the coefficients

$$\boldsymbol{\alpha}^r = \{\alpha_{rpk} : p \in \mathcal{P}, k \in \mathcal{Q}_{rp}\},$$

which is a subset of the entire set of filter coefficients. Therefore, $\mathcal{H}_{\mathcal{I}_r, \bullet}[\nu]$ depends only on $\boldsymbol{\alpha}^r$. In view of Eq. (6.42), $\mathbf{T}^{rs}[\nu]$ depends only on $\boldsymbol{\alpha}^r$ and the channel transfer function matrix $\mathbf{G}[\nu]$. It follows from Eqs. (6.34) and (6.41) that

$$\|e_r\|^2 = \int_{[0, \frac{1}{L}]} \left\| \sum_{s \in \mathcal{R}} \mathbf{T}^{rs}[\nu] \mathcal{X}_{\mathcal{I}_s}[\nu] \right\|^2 d\nu, \quad (6.46)$$

which is completely parameterized by $\boldsymbol{\alpha}^r$. Consequently, for each $r \in \mathcal{R}$, the set of coefficients $\boldsymbol{\alpha}^r$ (or equivalently the r th row of $\mathbf{H}[\nu]$) can be optimized independently of the others by minimizing a cost that measures the fidelity of reconstruction of the r th input. Our choice of the cost function is the norm of the error in the worst case when $\mathbf{x} \in \mathcal{C}$, i.e.,

$$C_r(\boldsymbol{\alpha}^r) = \max \|e_r\| \quad \text{s.t.} \quad \|x_s\| \leq \gamma_s, \quad s \in \mathcal{R}. \quad (6.47)$$

It turns out that Eq. (6.47) is difficult to minimize directly, so we look for an alternate expression for the cost such as a bound on $C_r(\boldsymbol{\alpha}^r)$. The following proposition, which is proved in Appendix A, provides upper and lower bounds on the cost function.

Proposition 6.3. *The cost function $C_r(\boldsymbol{\alpha}^r)$ can be bounded as*

$$\frac{1}{\sqrt{R}} \bar{C}_r(\boldsymbol{\alpha}^r) \leq C_r(\boldsymbol{\alpha}^r) \leq \bar{C}_r(\boldsymbol{\alpha}^r),$$

where

$$\bar{C}_r(\boldsymbol{\alpha}^r) \stackrel{\text{def}}{=} \sum_{s \in \mathcal{R}} \gamma_s \|T^{rs}\| = \sum_{s \in \mathcal{R}} \gamma_s \max_{\nu \in [0, \frac{1}{L}]} \|\mathbf{T}^{rs}[\nu]\|.$$

Instead of minimizing $C_r(\boldsymbol{\alpha}^r)$ to compute the optimal filter coefficients $\boldsymbol{\alpha}^r$, we minimize $\bar{C}_r(\boldsymbol{\alpha}^r)$ as it produces a considerably simpler algorithms to implement. Therefore, the approximate optimal filter coefficients are given by

$$\begin{aligned} \boldsymbol{\alpha}_o^r &= \arg \min_{\boldsymbol{\alpha}^r} \bar{C}_r(\boldsymbol{\alpha}^r), \\ \bar{C}_r(\boldsymbol{\alpha}^r) &= \sum_{s \in \mathcal{R}} \gamma_s \max_{\nu \in [0, \frac{1}{L}]} \|\mathbf{T}^{rs}[\nu]\|. \end{aligned} \tag{6.48}$$

Owing to Proposition 6.3, the approximate solution will produce a cost that is greater by a factor of not more than \sqrt{R} times the true minimum, i.e.,

$$\min_{\boldsymbol{\alpha}^r} C_r(\boldsymbol{\alpha}^r) \leq \bar{C}_r(\boldsymbol{\alpha}_o^r) \leq \sqrt{R} \min_{\boldsymbol{\alpha}^r} C_r(\boldsymbol{\alpha}^r).$$

An important question pertaining to the FIR design is whether the resulting approximation error goes to zero when the filter lengths go to infinity. Under some conditions, we can answer affirmatively, as the following theorem shows.

Theorem 6.4. *Suppose that $\mathbf{G}[\nu]$ is continuous and that $\mathbf{H}[\nu]$ has an FIR parameterization described in Eq. (6.30). If there exists a perfect reconstruction filter matrix continuous in ν , then*

$$\min_{\boldsymbol{\alpha}^r} C_r(\boldsymbol{\alpha}^r) \rightarrow 0$$

as $\kappa_{rp} \rightarrow -\infty$ and $\kappa_{rp} + l_{rp} \rightarrow \infty$.

Proof. In view of Proposition 6.3, it suffices to prove that

$$\lim_{\tau \rightarrow \infty} \min_{\boldsymbol{\alpha}^r} \|T^{rs}\| \rightarrow 0$$

for all $r, s \in \mathcal{R}$, where

$$\tau = \min \left(\{-\kappa_{rp} : r \in \mathcal{R}, p \in \mathcal{P}\} \cup \{\kappa_{rp} + l_{rp} : r \in \mathcal{R}, p \in \mathcal{P}\} \right).$$

Suppose that $\mathbf{H}^\circ[\nu]$ is continuous in ν and achieves perfect reconstruction. Also let $\mathcal{H}^\circ[\nu]$ be the modulated reconstruction matrix corresponding to $\mathbf{H}^\circ[\nu]$. From Eq. (6.43) we conclude that

$$\left(\mathcal{H}_{\mathcal{I}_r, \bullet}^\circ[\nu] \mathcal{G}_{\bullet, \mathcal{I}_s}[\nu] - \delta_{rs} \mathbf{I}_L \right) \mathbf{E}_{s, \nu} = \mathbf{0} \tag{6.49}$$

for all $r, s \in \mathcal{R}$ because we would be guaranteed perfect reconstruction if we choose $\mathcal{H}[\nu] = \mathcal{H}^\circ[\nu]$. Then, combining Eqs. (6.42) and (6.49) we obtain

$$\mathbf{T}^{rs}[\nu] = \left(\mathcal{H}_{\mathcal{I}_r, \bullet}[\nu] - \mathcal{H}_{\mathcal{I}_r, \bullet}^\circ[\nu] \right) \mathcal{G}_{\bullet, \mathcal{I}_s}[\nu] \mathbf{E}_{r, \nu}$$

for any reconstruction matrix $\mathcal{H}[\nu]$. Therefore,

$$\begin{aligned} \max_{\nu \in [0, \frac{1}{L}]} \|\mathbf{T}^{rs}[\nu]\| &\leq \max_{\nu \in [0, \frac{1}{L}]} \|\mathcal{H}_{\mathcal{I}_r, \bullet}[\nu] - \mathcal{H}_{\mathcal{I}_r, \bullet}^\circ[\nu]\| \cdot \|\mathcal{G}_{\bullet, \mathcal{I}_s}[\nu] \mathbf{E}_{r, \nu}\| \\ &\leq C \max_{\nu \in [0, \frac{1}{L}]} \|\mathcal{H}_{\mathcal{I}_r, \bullet}[\nu] - \mathcal{H}_{\mathcal{I}_r, \bullet}^\circ[\nu]\|, \end{aligned}$$

where

$$C = \sup_{\nu \in [0, 1/L]} \|\mathcal{G}_{\bullet, \mathcal{I}_s}[\nu] \mathbf{E}_{r, \nu}\|$$

is finite because $\mathcal{G}[\nu]$ is a continuous function on the compact set $[0, 1/L]$, and $\mathbf{E}_{r, \nu}$ is a constant on each \mathcal{I}_m . Using Eqs. (6.15) and (6.32) we obtain

$$\begin{aligned} \max_{\nu \in [0, \frac{1}{L}]} \|\mathbf{T}^{rs}[\nu]\| &\leq CL \max_{\nu \in [0, 1]} \|\mathbf{H}_{r, \bullet}[\nu] - \mathbf{H}_{r, \bullet}^\circ[\nu]\| \\ &\leq CL \sqrt{P} \max_p \max_{\nu \in [0, 1]} \|H_{rp}[\nu] - H_{rp}^\circ[\nu]\|. \end{aligned} \quad (6.50)$$

Now suppose that $\mathbf{H}[\nu]$ has an FIR parameterization as in Eq. (6.30), i.e.,

$$H_{rp}[\nu] = \sum_{k \in \mathcal{Q}_{rp}} \alpha_{rp k} e^{-j2\pi \nu k},$$

where $\mathcal{Q}_{rp} = \{\kappa_{rp}, \dots, \kappa_{rp} + l_{rp}\}$. Then clearly each entry of $\mathbf{H}[\nu]$ can be expressed as a trigonometric polynomial of degree at least τ . Moreover, the coefficients of the polynomial can be individually controlled by changing the parameters $\boldsymbol{\alpha}^r$. Equivalently, we can reparameterize so that the new parameters are the coefficients of the trigonometric polynomials (rather than the filter coefficients). Now, by the Stone-Weierstrass theorem [58], we obtain

$$\min_{\boldsymbol{\alpha}^r} \max_{\nu \in [0, 1]} \|H_{rp}[\nu] - H_{rp}^\circ[\nu]\| \leq \epsilon \quad (6.51)$$

for any $\epsilon > 0$ if τ is sufficiently large. Combining Eqs. (6.50) and (6.51) we obtain the desired result:

$$\lim_{\tau \rightarrow \infty} \min_{\boldsymbol{\alpha}^r} \max_{\nu \in [0, \frac{1}{L}]} \|\mathbf{T}^{rs}[\nu]\| = 0.$$

Incidentally this also proves that $\lim_{\tau \rightarrow \infty} \min_{\boldsymbol{\alpha}^r} \bar{C}_r(\boldsymbol{\alpha}^r) = 0$ by Proposition 6.3. \square

Theorem 6.4 guarantees the existence of continuous FIR solutions $\mathbf{H}[\nu]$ that can get arbitrarily close to perfect reconstruction, provided that there exists a continuous $\mathbf{H}^\circ[\nu]$ with the perfect reconstruction property.

6.5.2 Semi-infinite linear program formulation

In this section, we present an algorithm to compute the optimal solution to the problem in Eq. (6.48). We show that this problem can be reduced to a *semi-infinite linear program* which can then be solved by a standard method.

We begin by expressing the matrices $\mathbf{T}^{rs}[\nu]$ as functions of the filter coefficients $\boldsymbol{\alpha}^r$.

Proposition 6.4. *The quantity $\mathbf{T}^{rs}[\nu]$ defined in Eq. (6.42) can be written as*

$$\mathbf{T}^{rs}[\nu] = \mathbf{F}_0^{rs}[\nu] + \sum_{p \in \mathcal{P}} \sum_{k \in \mathcal{Q}_{rp}} \alpha_{rp k} \mathbf{F}_{pk}^{rs}[\nu] \quad (6.52)$$

for appropriate matrices $\mathbf{F}_0^{rs}[\nu]$ and $\mathbf{F}_{pk}^{rs}[\nu]$.

Proof. Observe from Eqs. (6.15) and (6.30) that the (l, p) entry of $\mathcal{H}_{\mathcal{I}_r, \bullet}[\nu]$ is given by

$$[\mathcal{H}_{\mathcal{I}_r, \bullet}[\nu]]_{lp} = H_{rp} \left[\nu + \frac{l}{L} \right] = \sum_{k \in \mathcal{Q}_{rp}} \alpha_{rp k} e^{-j2\pi(\nu + l/L)k}.$$

In other words $\mathcal{H}_{\mathcal{I}_r, \bullet}[\nu]$ can be written as the following linear combination

$$\mathcal{H}_{\mathcal{I}_r, \bullet}[\nu] = \sum_{p \in \mathcal{P}} \sum_{k \in \mathcal{Q}_{rp}} \alpha_{rp k} \mathbf{K}^{rp k}[\nu], \quad (6.53)$$

where $\mathbf{K}^{rp k}[\nu]$ are matrices whose entries are

$$[\mathbf{K}^{rp k}[\nu]]_{lp'} = \delta_{pp'} e^{-j2\pi(\nu + l/L)k}.$$

Combining Eqs. (6.42) and (6.53), we obtain the desired affine form in Eq. (6.52), where

$$\begin{aligned} \mathbf{F}_0^{rs}[\nu] &= -\delta_{rs} \mathbf{E}_{r, \nu}, \\ \mathbf{F}_{pk}^{rs}[\nu] &= \mathbf{K}^{rp k}[\nu] \mathbf{G}_{\bullet, \mathcal{I}_s}[\nu] \mathbf{E}_{r, \nu}. \end{aligned}$$

□

Proposition 6.4 shows that $\mathbf{T}^{rs}[\nu]$ has an affine form in terms of the filter coefficients $\boldsymbol{\alpha}^r$. The exact expressions for the matrices involved are provided for the sake of completeness. Next, for a fixed index r , we rewrite the optimization in Eq. (6.48) as

$$\min \sum_{s \in \mathcal{R}} \gamma_s \delta_s \quad \text{s.t.} \quad \delta_s \geq \Re(\mathbf{y}^H \mathbf{T}^{rs}[\nu] \mathbf{x}), \quad \forall s \in \mathcal{R}, \forall \nu \in \left[0, \frac{1}{L}\right], \text{ and } \forall \mathbf{x}, \mathbf{y} \in \mathcal{B}_\circ, \quad (6.54)$$

where \mathcal{B}_\circ is the unit ball for length- L vectors:

$$\mathcal{B}_\circ = \{\mathbf{v} \in \mathbb{C}^L : \|\mathbf{v}\| \leq 1\}.$$

For convenience, we treat $\boldsymbol{\alpha}^r$ as a row-vector (with any ordering of coefficients), i.e.,

$$\boldsymbol{\alpha}_{j(p,k)}^r = \alpha_{rpk},$$

where $j(p,k)$ is an invertible mapping that takes the pair of indices $p \in \mathcal{P}$ and $k \in \mathcal{Q}_{rp}$ to a single index j in the set \mathcal{J}_r defined as

$$\mathcal{J}_r = \{0, \dots, J_r - 1\}, \quad J_r \stackrel{\text{def}}{=} \sum_{p \in \mathcal{P}} |\mathcal{Q}_{rp}| = \sum_{p \in \mathcal{P}} l_{rp}.$$

Recall that $\mathcal{Q}_{rp} = \{k : \kappa_{rp} \leq k \leq l_{rp} + \kappa_{rp} - 1\}$. Hence, an example of one such mapping is

$$j(p,k) = \sum_{p'=0}^{p-1} l_{rp'} + (k - \kappa_{rp}).$$

Define a row-vector $\boldsymbol{\delta} = [\delta_0 \ \dots \ \delta_{R-1}]$. Using the FIR representation in Eq. (6.52), we can rewrite Eq. (6.54) as

$$\min \sum_{s \in \mathcal{R}} \gamma_s \delta_s \quad \text{s.t.} \quad \Re \left(\delta_s - \sum_{p \in \mathcal{P}} \sum_{k \in \mathcal{Q}_{rp}} \alpha_{rpk} (\mathbf{y}^H \mathbf{F}_{pk}^{rs} [\nu] \mathbf{x}) \right) \geq \Re \left(\mathbf{y}^H \mathbf{F}_0^{rs} [\nu] \mathbf{x} \right), \quad \forall (s, \nu, \mathbf{x}, \mathbf{y}) \in \mathcal{U},$$

where $\mathcal{U} = \mathcal{R} \times [0, \frac{1}{L}] \times \mathcal{B}_\circ \times \mathcal{B}_\circ$. This problem can be recast as a semi-infinite linear program:

$$\min \Re(\mathbf{c}\boldsymbol{\xi}) \quad \text{s.t.} \quad \Re(\mathbf{a}(\mathbf{u})\boldsymbol{\xi}) \geq \Re(b(\mathbf{u})), \quad \forall \mathbf{u} \in \mathcal{U}, \quad (6.55)$$

where $\boldsymbol{\xi} = [\boldsymbol{\delta} \ \boldsymbol{\alpha}^r]$ is the set of program variables, $\mathbf{u} = (s, \nu, \mathbf{x}, \mathbf{y}) \in \mathcal{U}$ parameterizes the constraints, and $b(\mathbf{u})$ is a complex-scalar. The quantities $\mathbf{a}(\mathbf{u})$ and \mathbf{c} are row-vectors of length $R + J_r$ whose first R entries are real, and the remaining J_r entries are complex-valued:

$$\mathbf{a}_n(\mathbf{u}) = \begin{cases} 1, & \text{if } n = s, \\ 0, & \text{if } n \in \mathcal{R}, \quad l \neq s, \\ -\mathbf{y}^H \mathbf{F}_{pk}^{rs} [\nu] \mathbf{x}, & \text{if } l = R + j(p, k), \end{cases}$$

$$b(\mathbf{u}) = \mathbf{y}^H \mathbf{F}_0^{rs} [\nu] \mathbf{x},$$

$$\mathbf{c}_n = \begin{cases} \gamma_s, & \text{if } n = s, \\ 0, & \text{otherwise.} \end{cases}$$

The semi-infinite program in Eq. (6.55) is in a nonstandard form, since it contains a mixture of real and complex variables. Nevertheless, it can be converted to the standard real form by decomposing all complex variables into their real and imaginary parts. Finding the dual of this real program, and reconverting to the complex form produces the following dual program:

$$\max \int_{\mathcal{U}} b(\mathbf{u}) dw(\mathbf{u}) \quad \text{s.t.} \quad \mathbf{c} = \int_{\mathcal{U}} \mathbf{a}(\mathbf{u}) dw(\mathbf{u}), \quad w \geq 0, \quad (6.56)$$

where w is a real and positive measure on \mathcal{U} . The dual problem can be solved using a simplex-type algorithm for semi-infinite programs [34].

Recall that whenever the technical conditions in Theorem 6.1 are satisfied, the set

$$\mathcal{S}_H = \{\mathbf{H}[\nu] : \text{perfect reconstruction is achieved.}\}$$

is nonempty. However \mathcal{S}_H need not be a singleton set, because the perfect reconstruction filter matrices are not necessarily unique. The optimization always produces the FIR filter matrix that is “closest” to the set of reconstruction filter matrices \mathcal{S}_H . If the conditions in Theorem 6.2 are satisfied, then \mathcal{S}_H contains a continuous $\mathbf{H}[\nu]$, and guarantees, by Theorem 6.4, that the approximation error can be made arbitrarily small by using sufficiently long FIR filters.

6.5.3 Design example

In this section, we consider two FIR filter design examples. In the first example, we design reconstruction filters for the multicoset sampling scheme which is a special case of MIMO sampling. In the second example, we consider MIMO sampling using a channel having two inputs and five outputs.

Example 6.1. In this example, we design FIR reconstruction filters for multicoset sampling. Let $\mathcal{F} = [0, 0.15) \cup [0.75, 1.0)$, as illustrated in Figure 6.3, be the spectral support for the class of sampled signals.

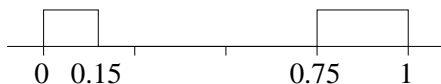


Figure 6.3 Indicator function of the spectral support \mathcal{F} .

Let

$$\Lambda = \bigcup_{n \in \mathbb{Z}} \{4n, 4n + 1\}$$

denote the multicoset sampling set for $\mathcal{B}_d(\mathcal{F})$; i.e., the sampling pattern is $\mathcal{C} = \{0, 1\}$. This sampling scheme can be recast as a uniform MIMO sampling scheme with $L = 4$ and

$$\mathbf{G}[\nu] = \begin{pmatrix} 1 \\ e^{-j2\pi\nu} \end{pmatrix}.$$

This is a single-input double-output channel, and we seek the optimal FIR reconstruction filter matrix

$$\mathbf{H}[\nu] = [H_1[\nu] \ H_2[\nu]]$$

of length 15 centered at the origin, i.e., $\mathcal{Q}_{1p} = \{-7, \dots, 7\}$, $p = 1, 2$. Since $R = 1$, we can take $\gamma_1 = 1$ without loss of generality. Applying the semi-infinite algorithm, we obtain the optimal FIR filters $H_1[\nu]$ and $H_2[\nu]$ shown in Figure 6.4. The resulting maximum approximation error $\|\mathbf{T}^{rs}[\nu]\|$ at optimality is shown for $\nu \in [0, 1/4)$ in Figure 6.5. The equal-ripple nature of this plot is due to the minimax criterion:

$$\delta = \min_{\boldsymbol{\alpha}^1} C_1(\boldsymbol{\alpha}^1) = \min_{\boldsymbol{\alpha}^1} \max_{\nu} \|\mathbf{T}^{1s}[\nu]\|.$$

The optimal cost is $\delta = 0.0483$.

Example 6.2. Consider a MIMO channel with $R = 2$ inputs and $P = 5$ outputs. Suppose that the inputs $x_1[k]$ and $x_2[k]$ have spectral supports illustrated in Figure 6.6, namely,

$$\mathcal{F}_1 = [0, 0.4) \cup [0.75, 1.0) \quad \text{and} \quad \mathcal{F}_2 = [0.25, 0.5).$$

Let $\gamma_1 = \gamma_2 = 0.5$ be the weights and $L = 4$ the subsampling factor. For this choice we have $M = 2$, $\mathcal{I}_1 = [0, 0.15)$ and $\mathcal{I}_2 = [0.15, 0.25)$. Using Eqs. (6.17) and (6.25), it is easy to check that

$$\begin{aligned} \mathcal{K}_1 &= \{0, 2, 3, 6\}, \\ \mathcal{K}_2 &= \{0, 3, 6\}, \\ \mathcal{J}_1 &= \mathcal{K}_1 \cup ((\mathcal{K}_2 \oplus 2) \bmod 8) = \{0, 2, 3, 5, 6\}, \\ \mathcal{J}_2 &= \mathcal{K}_2 \cup \mathcal{K}_1 = \{0, 2, 3, 6\}. \end{aligned}$$

Hence, by Theorem 6.1, $P \geq \max_m |\mathcal{K}_m| = 4$ is required for the existence of a reconstruction filter matrix $\mathbf{H}[\nu]$ that achieves perfect reconstruction. If we also require that the filters be continuous, Theorem 6.2 states that $P \geq \max_n |\mathcal{J}_n| = 5$ is necessary. Let $\mathbf{G}[\nu]$ denote the following continuous channel transfer function matrix with $P = 5$ outputs:

$$\mathbf{G}[\nu] = \begin{pmatrix} 1 & 1 \\ 1 & 1 + z^{-1} \\ z^{-1} & 0.25 + z^{-2} \\ 1 + 0.5z^{-1} & 1 + z^{-2} \\ 0.25 + z^{-2} & z^{-1} \end{pmatrix}, \quad \text{where } z = e^{j2\pi\nu}. \quad (6.57)$$

It can be verified numerically that Eqs. (6.23) and (6.24) in Theorem 6.2 are satisfied. Hence, the existence of a perfect reconstruction filter matrix $\mathbf{H}[\nu]$ that is continuous in ν is guaranteed.

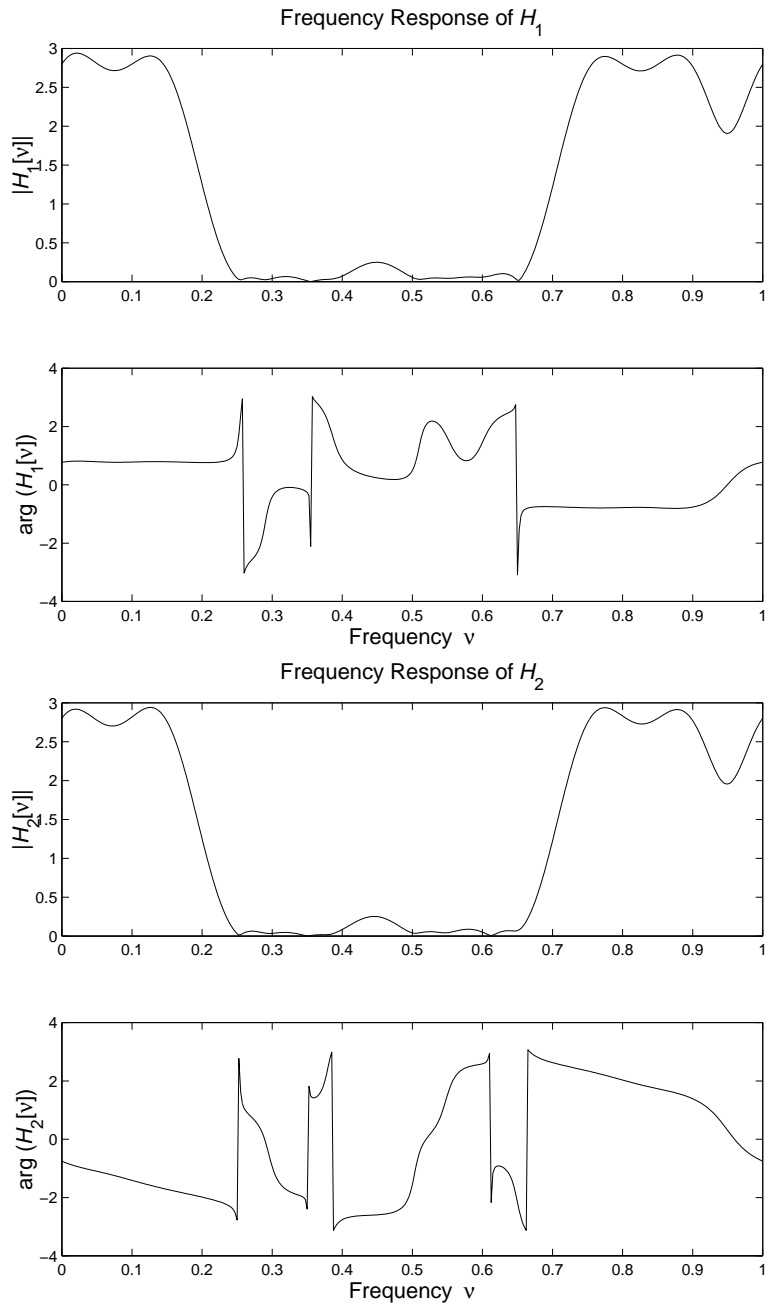


Figure 6.4 Magnitude and phase responses of the optimal FIR filters $H_1[\nu]$ and $H_2[\nu]$.

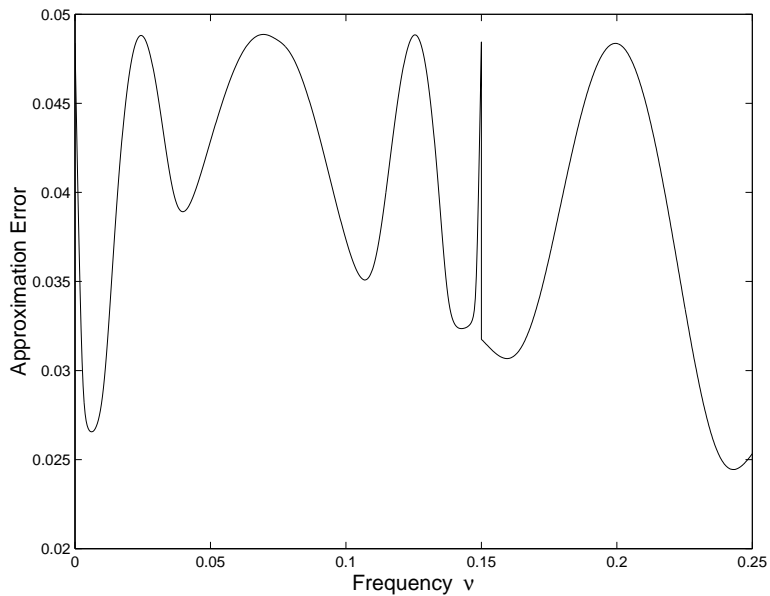


Figure 6.5 Approximation error $\|\mathbf{T}^{rs}[\nu]\|$ at optimality.

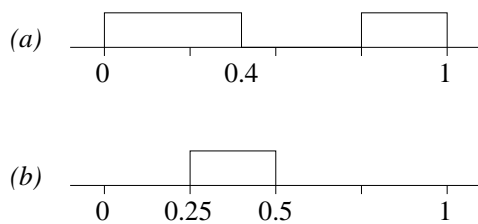


Figure 6.6 (a) Spectral support of $X_1[\nu]$, and (b) spectral support of $X_2[\nu]$.

As a consequence of Theorem 6.4, the approximation error approaches zero as the filter lengths are increased. Using a semi-infinite algorithm, we design six sets of reconstruction filters of varying filter lengths, indexed by $\tau \in \{1, 2, \dots, 6\}$, having the following specifications:

$$l_{rp} = 2\tau + 1$$

$$\kappa_{rp} = \begin{cases} 0 - \tau & \text{if } p \in \{0, 1\}, \\ 1 - \tau & \text{if } p \in \{2, 3, 4\}. \end{cases}$$

In other words, all the FIR reconstruction filters for a given τ have equal lengths $(2\tau + 1)$. Furthermore the filters $g_{pr}[k]$ are centered at $k = 0$ for $p = 0, 1$, and at $k = 1$ for $p = 2, 3$, and 4. Table 6.1 and Figure 6.7 show the cost function for of the two outputs and the six design cases. Observe that the cost falls of quickly as the filter lengths increase. In this example, the costs would converge to zero as $\tau \rightarrow \infty$, since the conditions required in Theorem 6.2 are satisfied.

Table 6.1 Cost functions $\bar{C}_0(\boldsymbol{\alpha}_o^0)$ and $\bar{C}_1(\boldsymbol{\alpha}_o^1)$ at optimality for FIR reconstruction filters of length $2\tau + 1$, $1 \leq \tau \leq 6$.

$2\tau+1$	3	5	7	9	11	13
$\bar{C}_0(\boldsymbol{\alpha}_o^0)$	0.4835	0.3643	0.1093	0.0836	0.0716	0.0329
$\bar{C}_1(\boldsymbol{\alpha}_o^1)$	0.3554	0.1690	0.0637	0.0124	0.0076	0.0034

6.6 Summary

In this chapter, we examined the problem of FIR reconstruction filter design for uniform MIMO sampling. In practice, the reconstruction system would be implemented digitally, meaning that the filter design problem would be one of FIR design. Of course, we would use D/A converters at the far end of the system to reconstruct continuous-time estimates of the inputs. We showed how to convert the continuous-time channel model to a hypothetical discrete-time one. The advantage of this conversion is that it allows us to pretend that the entire system is a discrete-time system, and this facilitates the analysis.

We then presented necessary and sufficient conditions for perfect reconstruction of the channel inputs when the inputs are modeled as multiband signals with different band structures. We stated appropriate conditions for the existence of reconstruction filters that are continuous in the frequency domain. The continuity property was shown to be important from an implementation viewpoint, as it allows to design where the errors due to the FIR approximation

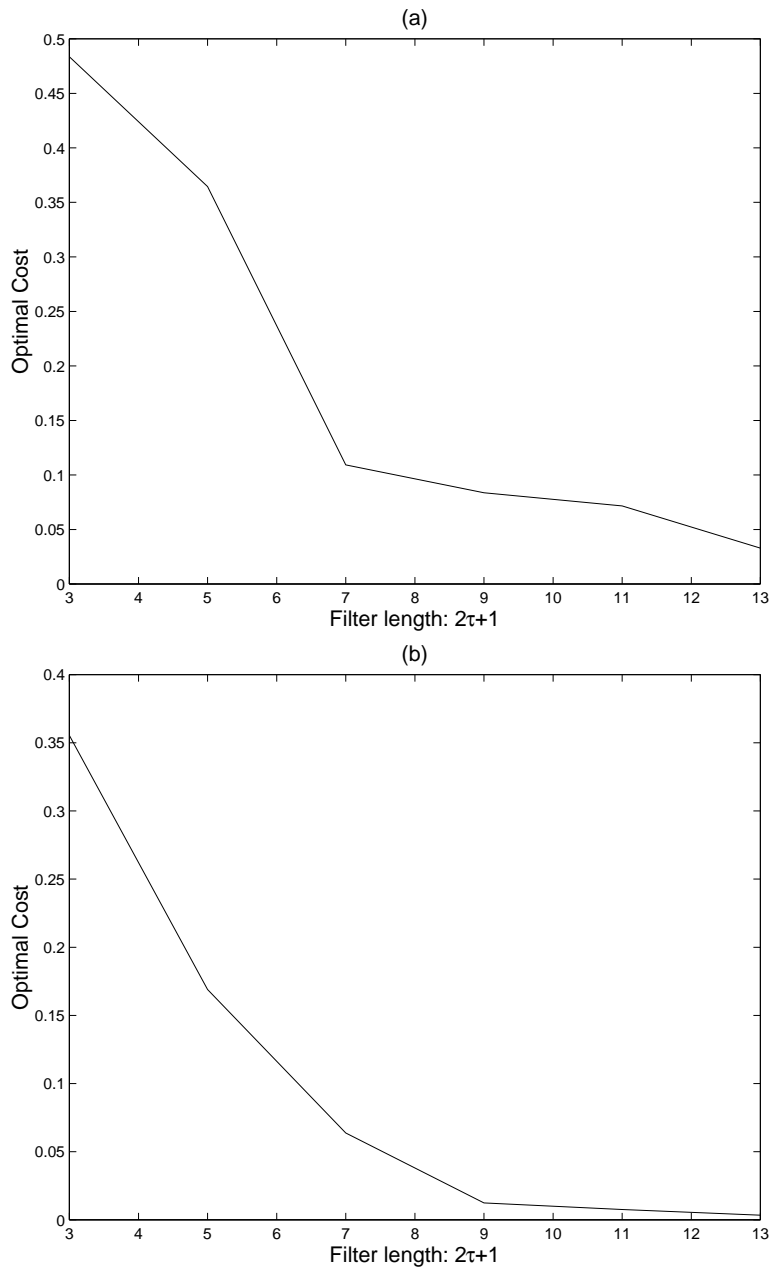


Figure 6.7 Optimal costs (a) $\bar{C}_0(\alpha_0^0)$, and (b) $\bar{C}_1(\alpha_0^1)$ for FIR reconstruction filters of length $2\tau + 1$, $1 \leq \tau \leq 6$.

can be made arbitrarily small by choosing sufficiently long filters. Finally, we formulated the reconstruction filter design problem as a minimax optimization, which was recast as a standard semi-infinite linear program and solved efficiently by computer. The generality of the MIMO setting allows this algorithm to be used for various other sampling schemes that fit into the MIMO framework as special cases. We provided design examples for multicoset and general MIMO sampling schemes.

CHAPTER 7

CONCLUSION

In this dissertation, we addressed several issues pertaining to two sampling schemes, namely, *multicoset sampling* and *MIMO sampling* of multiband input signals. Chapters 2 and 3 dealt with the multicoset sampling problem, which is essentially a nonuniform periodic sampling scheme. The main advantage of multicoset sampling is that it allows sub-Nyquist perfect reconstruction for the class of multiband inputs whose spectra are supported on finite union of intervals. In fact, multicoset sampling achieves the Landau minimum sampling rate in the limit $L \rightarrow \infty$, where L is the period of the sampling pattern. However, for many spectra, the minimum rate can be achieved for a finite L . Typically, this scheme is useful for sampling signals with sparse and nonpackable spectra.

In Chapter 2, we deduced necessary and sufficient conditions for perfect reconstruction of a signal from its multicoset samples, and provided an explicit reconstruction formula. We analyzed the performance of the sampling scheme. Specifically, we computed bounds on the aliasing error occurring in the event that the signal lies outside the valid class of multiband signals and determined the sensitivity to input sample noise. These bounds serve as performance measures for multicoset sampling, and they reveal that some sampling patterns are better than others.

In Chapter 3, we studied *optimality* of sub-Nyquist sampling and reconstruction. The interpolation equation for multicoset sampling derived in Chapter 2 is not unique when there is oversampling relative to Landau's minimum rate. We use this freedom to compute the optimal reconstruction filters that obtain the best performance in terms the measures of performance derived in Chapter 2, namely the aliasing error bounds or the noise sensitivity. The error bounds depend on the multicoset sampling patterns, thereby indicating that some patterns may be better than others. We studied the optimal sampling pattern design using two methods: a *greedy* search algorithm and an *exhaustive* search algorithm. The greedy algorithm, that works by selectively adding new sampling points to a preexisting set greedily, is a suboptimal

algorithm. On the other hand, the exhaustive search algorithm is optimal, but computationally very expensive. We also solved the problem of choosing the optimal base sampling frequency that minimizes the average sampling rate for a given sampling period L .

We also demonstrated that (a) for packable spectral supports, uniform sampling yields a better performance than a general periodic nonuniform sampling scheme, and (b) for non-packable signals, where uniform sampling is not applicable, there is a penalty associated with nonuniform sampling relative to uniform sampling of a packable signal of the same occupancy. However, for signals with nonpackable spectra, these penalties can be controlled by optimal design and by backing off slightly from the minimum rate. The resulting lower error sensitivities and the significant reduction in the sampling rate over the Nyquist rate of our numerical examples suggest that these techniques have considerable practical potential.

Chapters 4, 5, and 6 dealt with MIMO sampling of multiband inputs. In Chapter 4, we formulated the MIMO sampling scheme. The channel inputs are multiband signals whose spectral supports are arbitrary real sets of finite measure. This scheme is motivated by problems in multichannel deconvolution, where the objective is to recover a set of inputs to a MIMO channel by measuring the outputs. The MIMO sampling scheme encompasses various other sampling schemes and is important in its own right. Our primary objective was to derive analogues of Landau's classical sampling and interpolation density results [6, 7] for the MIMO sampling problem. We defined notions of stable sampling and consistent reconstruction in the MIMO setting. Here, *consistent reconstruction* is the MIMO analogue of *interpolation*. We also generalized the definitions of upper and lower sampling densities to *collections* of sampling sets.

Strengthening an idea of Gröchenig and Razafinjato [45], we deduced necessary density conditions for stable sampling and for consistent reconstruction in the MIMO setting. For both problems, we find that a family of $2^P - 1$ density bounds hold, where P is the number of output channels. More specifically, stable sampling dictates that the joint lower densities of each nonempty set of output sampling sets be lower bounded. Similarly, for the consistency problem, the joint upper densities are upper bounded. Like Landau's results, these bounds are fundamentally important results. They are easily computable, and they automatically apply to sampling schemes subsumed by MIMO sampling such as Papoulis's generalized sampling and multicoset sampling.

In Chapter 5, we studied a special case of MIMO sampling of multiband signals where the outputs are sampled either uniformly or on *commensurate* periodic nonuniform sampling sets. The input spectral supports are assumed to be finite disjoint unions of intervals. Despite the restrictions, the sampling scheme still encompasses Papoulis's generalized sampling

and periodic nonuniform sampling schemes as a special cases. We showed that commensurate periodic nonuniform sampling is really uniform sampling in disguise. We presented necessary and sufficient conditions for perfect reconstruction of the inputs *with* and *without* requiring the continuity of the reconstruction filters in the frequency domain. This continuity requirement is desirable from the perspective of FIR reconstruction filter design.

In Chapter 6 we presented the solution to the reconstruction filter design problem in the context of uniform MIMO sampling. We formulated a discrete-time version of the MIMO sampling problem. The resulting reconstruction filter design becomes a problem of FIR filter design. We first presented conditions for perfect reconstruction for the discrete-time problem including the conditions for the existence of reconstruction filters continuous in frequency, and then formulated the design problem as a semi-infinite linear program which is solved using a standard algorithm.

7.1 Directions for Future Research

7.1.1 Sampling pattern design and asymptotic analysis

Our current method of multicoset sampling pattern design is to minimize an appropriate cost function using an exhaustive search over all valid sampling patterns. Unfortunately this solution has complexity that is exponential in L . One could use the inherent structure in the matrices to develop an algorithm of lower complexity to solve the problem either exactly or approximately.

Another interesting problem is to study the behavior of the various bounds or performance measures as we allow the parameter $L \rightarrow \infty$ in the context of multicoset sampling. Presently the only clear thing is that, for any given class of input signals, increasing L causes the system performance to improve, provided that we use the “best sampling pattern” for each L . An exact solution to this problem would be related to the sampling pattern design problem because we pick the best sampling pattern for any L ; the solution would reveal fundamental bounds on the performance of the reconstruction system.

7.1.2 Sufficient density conditions

Multicoset sampling and other periodic nonuniform sampling schemes demonstrate that for a multiband signal whose spectral support is a union of intervals, we can either approach Landau’s lower bound on the sampling density asymptotically or attain it. In the MIMO sampling problem, the necessary density conditions provide an outer bound on the achievable set of den-

sities. A natural question still unanswered is whether all the points in this region are attainable or reachable asymptotically. Otherwise, what is the precise region of achievable sampling densities? The results in Chapter 5 provide conditions for achieving perfect reconstruction using uniform or commensurate periodic nonuniform sampling. Although we can interpret these as sufficient conditions, they are not explicit conditions on the densities themselves.

APPENDIX A

PROOFS AND CALCULATIONS

A.1 Proof of Lemma 2.1

Lemma A.1. *If u, v are integers and $\alpha, \beta \in [0, 1/LT)$ satisfy*

$$\frac{u}{LT} + \alpha < \frac{v}{LT} + \beta, \quad (\text{A.1})$$

then $u \leq v$. Furthermore, if $u = v$ then $\alpha < \beta$ follows trivially.

Proof. Equation (A.1) implies that $(u - v)/LT < \beta - \alpha < 1/LT$, where the strictness of the second inequality comes from the fact that $[0, 1/LT)$ is open on the right. Hence, $u - v < 1$, or equivalently, $u \leq v$. \square

Proof of Lemma 2.1. Let r and m be fixed. Then for each $i \in \{1, 2, \dots, n\}$ we can express a_i and b_i uniquely as

$$a_i = \frac{u_i}{LT} + \alpha_i \quad \text{and} \quad b_i = \frac{v_i}{LT} + \beta_i, \quad (\text{A.2})$$

where u_i and v_i are integers and α_i and β_i are elements of Γ , with α_i and β_i in $[0, 1/LT)$. Now we shall prove by contradiction that exactly one of the two conditions $(r/LT) \oplus \mathcal{G}_m \subset [a_i, b_i)$ and $(r/LT) \oplus \mathcal{G}_m \cap [a_i, b_i) = \emptyset$ holds. It is clear that both statements cannot be true simultaneously. So if neither holds, then either one or both of the following must hold:

$$\gamma_m + r/LT < a_i < \gamma_{m+1} + r/LT,$$

$$\gamma_m + r/LT < b_i < \gamma_{m+1} + r/LT.$$

If the first condition holds, then Eq. (A.2) along with Lemma A.1 implies that $r \leq u_i \leq r$. Therefore, $r = u_i$ and $\gamma_m < \alpha_i < \gamma_{m+1}$. The last observation contradicts $\alpha_i \in \Gamma$ because the γ 's are arranged in increasing order. Similarly the second statement above would also lead to a contradiction. This proves our claim that the subcell $(r/LT) \oplus \mathcal{G}_m$ is either contained in or disjoint from $[a_i, b_i)$. This fact, being true for each i , now implies that either $(f + r/LT) \in \mathcal{F}$

for every $f \in \mathcal{G}_m$, or it is so for no such f . Therefore, $\chi(f + r/LT \in \mathcal{F})$ is constant over the interval \mathcal{G}_m . \square

A.2 Proof of Theorem 2.1

Observe that the quantity $q(f)$ in Eq. (2.10) equals the number of nonzero entries in

$$\{X_r(f) : r = 0, 1, \dots, L-1\}.$$

Hence, the summation in Eq. (2.8) (repeated below) contains $q(f)$ nonzero terms, for each $f \in \mathcal{F}_0$:

$$\underline{X}_{c_i}(e^{j2\pi fT}) = \frac{1}{LT} \sum_{r=0}^{L-1} \exp\left(\frac{j2\pi c_i r}{L}\right) X_r(f), \quad i = 1, \dots, p. \quad (\text{A.3})$$

These form a set of p linear equations with $q(f)$ unknown variables on the right-hand side, and solving them requires $p \geq q(f)$. Hence, $p \geq q(f)$ for all $f \in \mathcal{F}_0$ is necessary for reconstruction of the spectral components $X_r(f)$. Next, using Eq. (2.10) we bound the average sampling density p/LT from below by the Landau minimum rate:

$$\frac{p}{LT} \geq \int_0^{\frac{1}{LT}} q(f) df = \mu(\mathcal{F}),$$

with the equality holding if and only if $p = q(f)$ for all $f \in \mathcal{F}_0$. \square

A.3 Proof of Theorem 2.2

To derive the interpolation equations, we begin by expressing Eq. (2.15) in scalar form:

$$\begin{aligned} [\mathbf{x}_m^+(f)]_l &= \sum_{i=1}^p [\mathbf{A}_m^{-1}]_{li} [\mathbf{y}(f)]_i \\ [\mathbf{x}_m^-(f)]_l &= \sum_{i=1}^p [\mathbf{C}_m]_{li} [\mathbf{y}(f)]_i \end{aligned} \quad f \in \mathcal{G}_m.$$

We use the expressions for $\mathbf{y}(f)$, $\mathbf{x}_m^+(f)$ and $\mathbf{x}_m^-(f)$ from Eq. (2.13) to obtain

$$\begin{aligned} X_{k_m(l)}(f) &= T\sqrt{L} \sum_{i=1}^p [\mathbf{A}_m^{-1}]_{li} \underline{X}_{c_i}(e^{j2\pi fT}) \chi(f \in \mathcal{G}_m), \quad 1 \leq l \leq q_m, \\ X_{k_m^c(l)}(f) &= T\sqrt{L} \sum_{i=1}^p [\mathbf{C}_m]_{li} \underline{X}_{c_i}(e^{j2\pi fT}) \chi(f \in \mathcal{G}_m), \quad 1 \leq l \leq L - q_m, \end{aligned}$$

for $f \in \mathcal{G}_m$ and all m . Or equivalently, using Eq. (2.12) we have

$$X(f) = \begin{cases} T\sqrt{L} \sum_{i=1}^p [\mathbf{A}_m^{-1}]_{li} \underline{\mathbf{X}}_{c_i}(e^{j2\pi(f - \frac{k_m(l)}{LT})T}) & \text{if } f \in k_m(l)/LT \oplus \mathcal{G}_m, \\ T\sqrt{L} \sum_{i=1}^p [\mathbf{C}_m]_{li} \underline{\mathbf{X}}_{c_i}(e^{j2\pi(f - \frac{k_m^c(l)}{LT})T}) & \text{if } f \in k_m^c(l)/LT \oplus \mathcal{G}_m. \end{cases}$$

for each m , which in view of Eq. (2.7), leads to

$$X(f) = \begin{cases} T\sqrt{L} \sum_{i=1}^p [\mathbf{A}_m^{-1}]_{li} e^{j2\pi \frac{c_i k_m(l)}{L}} \underline{\mathbf{X}}_{c_i}(e^{j2\pi f T}) & \text{if } f \in k_m(l)/LT \oplus \mathcal{G}_m, \\ T\sqrt{L} \sum_{i=1}^p [\mathbf{C}_m]_{li} e^{j2\pi \frac{c_i k_m^c(l)}{L}} \underline{\mathbf{X}}_{c_i}(e^{j2\pi f T}) & \text{if } f \in k_m^c(l)LT \oplus \mathcal{G}_m. \end{cases} \quad (\text{A.4})$$

for $1 \leq m \leq M$. Equation (A.4) specifies the spectrum $X(f)$ over the active subcells $(k_m(l)/LT) \oplus \mathcal{G}_m$ that partition \mathcal{F} . For $f \notin \mathcal{F}$, we have $X(f) = 0$ by our choice of \mathbf{C}_m 's. We multiply the expressions on the right-hand side of Eq. (A.4) by the indicator functions corresponding to their regions of validity and add them together. This gives us a single equation for $X(f)$:

$$\begin{aligned} X(f) &= T\sqrt{L} \sum_{m=1}^M \sum_{l=1}^{q_m} \sum_{i=1}^p [\mathbf{A}_m^{-1}]_{li} e^{j2\pi \frac{c_i k_m(l)}{L}} \underline{\mathbf{X}}_{c_i}(e^{j2\pi f T}) \chi\left(f \in \frac{k_m(l)}{LT} \oplus \mathcal{G}_m\right) \\ &\quad + T\sqrt{L} \sum_{m=1}^M \sum_{l=1}^{L-q_m} \sum_{i=1}^p [\mathbf{C}_m]_{li} e^{j2\pi \frac{c_i k_m^c(l)}{L}} \underline{\mathbf{X}}_{c_i}(e^{j2\pi f T}) \chi\left(f \in \frac{k_m^c(l)}{LT} \oplus \mathcal{G}_m\right) \\ &\equiv \sum_{i=1}^p \Phi_i(f) \underline{\mathbf{X}}_{c_i}(e^{j2\pi f T}), \end{aligned}$$

where

$$\begin{aligned} \Phi_i(f) &= T\sqrt{L} \sum_{m=1}^M \sum_{l=1}^{q_m} [\mathbf{A}_m^{-1}]_{li} e^{j2\pi \frac{c_i k_m(l)}{L}} \chi\left(f \in \frac{k_m(l)}{LT} \oplus \mathcal{G}_m\right) \\ &\quad + T\sqrt{L} \sum_{m=1}^M \sum_{l=1}^{L-q_m} [\mathbf{C}_m]_{li} e^{j2\pi \frac{c_i k_m^c(l)}{L}} \chi\left(f \in \frac{k_m^c(l)}{LT} \oplus \mathcal{G}_m\right) \\ &= \begin{cases} T\sqrt{L} [\mathbf{A}_m^{-1}]_{li} e^{j2\pi \frac{c_i k_m(l)}{L}} & \text{if } f \in k_m(l)/LT \oplus \mathcal{G}_m, \\ T\sqrt{L} [\mathbf{C}_m]_{li} e^{j2\pi \frac{c_i k_m^c(l)}{L}} & \text{if } f \in k_m^c(l)/LT \oplus \mathcal{G}_m. \end{cases} \end{aligned}$$

Each filter $\Phi_i(f)$, $1 \leq i \leq p$ has a piecewise constant frequency response. Therefore, the reconstruction equation is

$$\begin{aligned} x(t) &= \sum_{i=1}^p \sum_{n=-\infty}^{\infty} \underline{\mathbf{x}}_{c_i}(nT) \phi_i(t - nT) \\ &= \sum_{i=1}^p \sum_{j=-\infty}^{\infty} x((c_i + Lj)T) \phi_i(t - (c_i + Lj)T), \end{aligned}$$

where $\phi_i(t)$ is the inverse Fourier transform of $\Phi_i(f)$. □

A.4 Proof of Theorem 2.3

The following equations (for each m and $f \in \mathcal{G}_m$) are equivalent to Eq. (2.21) rewritten in scalar form:

$$\begin{aligned}\tilde{X}_{k_m(r)}(f) &= X_{k_m(r)}(f) + \sum_{l=1}^{L-q_m} [\mathbf{D}_m]_{rl} X_{k_m^c(l)}(f), & 1 \leq r \leq q_m, \\ \tilde{X}_{k_m^c(r)}(f) &= X_{k_m^c(r)}(f) + \sum_{l=1}^{L-q_m} [\mathbf{F}_m]_{rl} X_{k_m^c(l)}(f), & 1 \leq r \leq L - q_m.\end{aligned}$$

Consider the spectral components $E_{k_m(l)}(f)$ and $E_{k_m^c(l)}(f)$ of the aliasing error

$$E(f) \stackrel{\text{def}}{=} \tilde{X}(f) - X(f)$$

defined exactly as in Eq. (2.12) with $E(f)$ in place of $X(f)$:

$$\begin{aligned}E_{k_m(r)}(f) &= \sum_{l=1}^{L-q_m} [\mathbf{D}_m]_{rl} X_{k_m^c(l)}(f), \\ E_{k_m^c(s)}(f) &= \sum_{l=1}^{L-q_m} [\mathbf{F}_m]_{sl} X_{k_m^c(l)}(f)\end{aligned}\tag{A.5}$$

for $f \in \mathcal{G}_m$, $1 \leq r \leq q_m$, $1 \leq s \leq L - q_m$ and each m . When expressed in the time domain, Eq. (A.5) becomes

$$\begin{aligned}e_{k_m(r)}(t) &= \sum_{l=1}^{L-q} [\mathbf{D}_m]_{rl} [x_{k_m^c(l)}(t)], \\ e_{k_m^c(s)}(t) &= \sum_{l=1}^{L-q} [\mathbf{F}_m]_{sl} [x_{k_m^c(l)}(t)].\end{aligned}\tag{A.6}$$

The total aliasing error can be obtained by modulating the errors on each subcell appropriately and adding. The result is that $e(t) = \sum_{m=1}^M e^{(m)}(t)$ where

$$e^{(m)}(t) = \sum_{l=1}^{q_m} e_{k_m(l)}(t) e^{\frac{j2\pi k_m(l)t}{LT}} + \sum_{l=1}^{L-q_m} e_{k_m^c(l)}(t) e^{\frac{j2\pi k_m^c(l)t}{LT}}.$$

Employing Eq. (A.6) in the above equation gives

$$\begin{aligned}e(t) &= \sum_{m=1}^M \sum_{r=1}^{q_m} e^{\frac{j2\pi k_m(r)t}{LT}} \left(\sum_{l=1}^{L-q_m} [\mathbf{D}_m]_{rl} x_{k_m^c(l)}(t) \right) \\ &\quad + \sum_{m=1}^M \sum_{r=1}^{L-q_m} e^{\frac{j2\pi k_m^c(r)t}{LT}} \left(\sum_{l=1}^{L-q_m} [\mathbf{F}_m]_{rl} x_{k_m^c(l)}(t) \right) \\ &\equiv \sum_{m=1}^M \sum_{l=1}^{L-q_m} \eta_{m,l}(t) x_{k_m^c(l)}(t),\end{aligned}\tag{A.7}$$

where $\eta_{m,l}(t)$ for each $1 \leq m \leq M$ and $1 \leq l \leq L - q_m$ are continuous, LT -periodic functions defined as

$$\eta_{m,l}(t) = \sum_{r=1}^{L-q_m} [\mathbf{F}_m]_{rl} e^{\frac{j2\pi k_m^c(r)t}{LT}} + \sum_{r=1}^{q_m} [\mathbf{D}_m]_{rl} e^{\frac{j2\pi k_m(r)t}{LT}}.$$

The sup-norm of $e(t)$ can be computed directly from Eq. (A.7) as follows

$$\begin{aligned} \sup_t |e(t)| &\leq \left(\max_{m,l,t} |\eta_{m,l}(t)| \right) \sum_{m=1}^M \sum_{l=1}^{L-q_m} \sup_t |x_{k_m^c(l)}(t)| \\ &\leq \left(\max_{m,l,t} |\eta_{m,l}(t)| \right) \sum_{m=1}^M \sum_{l=1}^{L-q_m} \int |X_{\bar{k}_m(l)}(f)| df \\ &= \max_{m,l,t} |\eta_{m,l}(t)| \sum_{m=1}^M \sum_{l=1}^{L-q_m} \int_{[\mathcal{F}]} |X(f)| \chi\left(f \in \frac{k_m^c(l)}{LT} \oplus \mathcal{G}_m\right) df. \end{aligned}$$

The double summation of the integrals reduces to the integral of $|X(f)|$ over the union of the subcells $\{(k_m^c(l)/LT) \oplus \mathcal{G}_m\}$, or equivalently, over the out-of-band region $[\mathcal{F}] \setminus \mathcal{F}$. Hence,

$$\sup_t |e(t)| \leq \psi \int_{[\mathcal{F}] \setminus \mathcal{F}} |X(f)| df, \quad (\text{A.8})$$

where ψ is the constant

$$\psi \stackrel{\text{def}}{=} \max_m \left(\max_{1 \leq l \leq L-q_m, t \in [0, LT]} |\eta_{m,l}(t)| \right).$$

We have used the fact that $\eta_{m,l}(t)$ is a periodic function of period LT to restrict the range for t in the above maximization. We demonstrate that ψ is the smallest possible coefficient in the bound in Eq. (A.8) for the sup-norm of $e(t)$. First note that $\psi = |\eta_{m_0, l_0}(t_0)|$ for some $m_0 \in \{1, \dots, M\}$, $l_0 \in \{1, 2, \dots, L - q_{m_0}\}$, and $t_0 \in [0, LT]$ because $\eta_{m,l}(t)$ is continuous on $[0, LT]$. Now define

$$X(f) = \begin{cases} \exp(-j2\pi f t_0) & \text{if } f \in k_{m_0}^c(l_0)/LT \oplus \mathcal{G}_{m_0}, \\ 0 & \text{otherwise.} \end{cases} \quad (\text{A.9})$$

In the time domain this is equivalent to

$$\begin{aligned} x(t) &= \mu(\mathcal{G}_{m_0}) \text{sinc}(\mu(\mathcal{G}_{m_0})(t - t_0)) \\ &\quad \times \exp\left(j2\pi \left(\frac{k_{m_0}^c(l_0)}{LT} + \frac{1}{2}(\gamma_{m_0} + \gamma_{m_0+1})\right)(t - t_0)\right), \end{aligned} \quad (\text{A.10})$$

where $\text{sinc } t = \sin t/(\pi t)$. For the choice of $X(f)$ in Eq. (A.9), it is clear that there is only one nonzero term in the right-hand side of Eq. (A.7), namely, the term corresponding to $m = m_0$

and $l = l_0$. Hence, we obtain

$$\begin{aligned} \sup_t |e(t)| &= \sup_t |\eta_{m_0, l_0}(t) x_{k_{m_0}^c}(l_0)(t)| \\ &\geq |\eta_{m_0, l_0}(t_0)| \times |x_{k_{m_0}^c}(l_0)(t_0)| \\ &= \psi \times \mu(\mathcal{G}_{m_0}) = \psi \int_{[\mathcal{F}] \setminus \mathcal{F}} |X(f)| df. \end{aligned}$$

In fact, both sides of the above inequality are equal since Eq. (A.8) holds. This proves that the bound in Eq. (A.8) is sharp with the extremal $x(t)$ in Eq. (A.10) achieving the bound. \square

A.5 Proof of Theorem 2.4

We shall now derive a bound on the energy of the error $e(t)$. First observe that by Parseval's theorem

$$\begin{aligned} \int_{-\infty}^{\infty} e^2(t) dt &= \int_{[\mathcal{F}]} |E(f)|^2 df = \int_{[\mathcal{F}] \setminus \mathcal{F}} |E(f)|^2 df + \int_{\mathcal{F}} |E(f)|^2 df \\ &= \sum_{m=1}^M \sum_{r=1}^{L-q_m} \int_{\frac{k_m^c(r)}{LT} \oplus \mathcal{G}_m} |E(f)|^2 df + \sum_{m=1}^M \sum_{r=1}^{q_m} \int_{\frac{k_m(r)}{LT} \oplus \mathcal{G}_m} |E(f)|^2 df \\ &= \sum_{m=1}^M \sum_{r=1}^{L-q_m} \int_{\mathcal{G}_m} |E_{k_m^c(r)}(f)|^2 df + \sum_{m=1}^M \sum_{r=1}^{q_m} \int_{\mathcal{G}_m} |E_{k_m(r)}(f)|^2 df. \end{aligned}$$

Now it readily follows from Eqs. (A.5), (2.13), and the above equation that

$$\begin{aligned} \int_{-\infty}^{\infty} e^2(t) dt &= \sum_{m=1}^M \int_{\mathcal{G}_m} (\mathbf{x}_m^-(f))^* (\mathbf{F}_m^* \mathbf{F}_m + \mathbf{D}_m^* \mathbf{D}_m) \mathbf{x}_m^-(f) df \\ &= \sum_{m=1}^M \sum_{l=1}^{L-q_m} \int_{\mathcal{G}_m} |X_{k_m^c(l)}(f)|^2 df = \int_{\mathcal{H}_m} |X(f)|^2 df, \end{aligned} \quad (\text{A.11})$$

where the last step follows from the definition of $\mathbf{x}_m^-(f)$. Here, \mathcal{H}_m is defined as

$$\mathcal{H}_m = \bigcup_{l=1}^{L-q_m} \frac{k_m^c(l)}{LT} \oplus \mathcal{G}_m. \quad (\text{A.12})$$

Note that the union of these sets, $\bigcup_m \mathcal{H}_m$, equals the total out-of-band region $[\mathcal{F}] \setminus \mathcal{F}$. Therefore, we deduce from Eqs. (A.11) and (A.12) that

$$\int_{-\infty}^{\infty} e^2(t) dt \leq \sum_{m=1}^M \lambda_{\max}(\mathbf{F}_m^* \mathbf{F}_m + \mathbf{D}_m^* \mathbf{D}_m) \int_{\mathcal{H}_m} |X(f)|^2 df.$$

This bound is not very useful in this form. We can weaken it a little to express it in terms of the out-of-band signal energy \mathcal{E}_{out} :

$$\int_{-\infty}^{\infty} e^2(t)dt \leq \max_m [\lambda_{\max}(\mathbf{F}_m^* \mathbf{F}_m + \mathbf{D}_m^* \mathbf{D}_m)] \mathcal{E}_{\text{out}}, \quad (\text{A.13})$$

where \mathcal{E}_{out} is defined as

$$\mathcal{E}_{\text{out}} = \sum_{m=1}^M \int_{\mathcal{H}_m} |X(f)|^2 df \equiv \int_{[\mathcal{F}] \setminus \mathcal{F}} |X(f)|^2 df. \quad (\text{A.14})$$

By a very similar argument, we obtain the following lower bound on the energy of $e(t)$

$$\int_{-\infty}^{\infty} e^2(t)dt \geq \min_m [\lambda_{\min}(\mathbf{F}_m^* \mathbf{F}_m + \mathbf{D}_m^* \mathbf{D}_m)] \mathcal{E}_{\text{out}}. \quad (\text{A.15})$$

These bounds are indeed sharp. The constants multiplying \mathcal{E}_{out} are the best. To demonstrate this, we construct extremal functions satisfying each of the above bounds. It is sufficient to specify the active and inactive spectral components, $\mathbf{x}_m^+(f)$ and $\mathbf{x}_m^-(f)$, rather than $X(f)$. After all, one can be determined in terms of the other. Consider the bound in Eq. (A.13) first. Let $m_0 = \arg \max_m (\lambda_{\max}(\mathbf{F}_m^* \mathbf{F}_m + \mathbf{D}_m^* \mathbf{D}_m))$. For each m , define

$$\mathbf{x}_m^+(f) = \mathbf{0} \quad f \in \mathcal{G}_m,$$

$$\mathbf{x}_m^-(f) = \begin{cases} \mathbf{0} & \text{if } m \neq m_0 \\ \mathbf{p}_{m_0} & \text{if } m = m_0, \end{cases} \quad f \in \mathcal{G}_{m_0},$$

where \mathbf{p}_{m_0} is the an eigenvector of $[\mathbf{F}_{m_0}^* \mathbf{F}_{m_0} + \mathbf{D}_{m_0}^* \mathbf{D}_{m_0}]$ corresponding to its largest eigenvalue. Starting from Eq. (A.11), one can easily verify that the above function is an extremal for the bound in Eq. (A.13). An extremal for Eq. (A.15) is constructed analogously. \square

A.6 Proof of Theorem 2.5

Recall that

$$\tilde{w}(t) = \sum_{i=1}^p \sum_{j=-\infty}^{\infty} w((c_i + Lj)T) \phi_i(t - (c_i + Lj)T).$$

It is clear that $E[w^*((Lj + c_i)T)w((Lj' + c_{i'})T)] = \sigma^2 \delta_{jj'} \delta_{ii'}$. Hence, distinct terms in the above summation are uncorrelated and we obtain the expression

$$E|\tilde{w}(t)|^2 = \sigma^2 \sum_{i=1}^p \sum_{j=-\infty}^{\infty} |\phi_i(t - LjT - c_iT)|^2$$

for the output noise power at time t . The above expression, although not necessarily independent of time, is certainly periodic with period LT . Hence, $\tilde{w}(t)$ is periodically stationary and its *average* noise power can be computed as follows

$$\begin{aligned} \langle E|\tilde{w}(t)|^2 \rangle_t &= \frac{1}{LT} \int_0^{LT} E|\tilde{w}(t)|^2 dt \\ &= \frac{\sigma^2}{LT} \int_0^{LT} \sum_{i=1}^p \sum_{j=-\infty}^{\infty} |\phi_i(t - LTj - c_i T)|^2 dt \\ &\equiv \frac{\sigma^2}{LT} \sum_{i=1}^p \int_{-\infty}^{\infty} |\phi_i(t - c_i T)|^2 dt = \frac{\sigma^2}{LT} \sum_{i=1}^p \mathcal{E}_{\phi_i}, \end{aligned} \quad (\text{A.16})$$

where \mathcal{E}_{ϕ_i} is the energy contained in $\phi_i(t)$. Using Parseval's theorem and Eq. (2.18) we compute \mathcal{E}_{ϕ_i}

$$\begin{aligned} \mathcal{E}_{\phi_i} &= \int |\Phi_i(f)|^2 df \\ &= T^2 L \sum_{m=1}^M \mu(\mathcal{G}_m) \left(\sum_{l=1}^{q_m} |[A_m^{-1}]_{li}|^2 + \sum_{l=1}^{L-q_m} |[C_m]_{li}|^2 \right). \end{aligned} \quad (\text{A.17})$$

This computation was quite simple because $\Phi_i(f)$ is piecewise constant. Combining Eqs. (A.16) and (A.17) gives

$$\begin{aligned} \langle E|\tilde{w}(t)|^2 \rangle_t &= \sigma^2 T \sum_{i=1}^p \sum_{m=1}^M \mu(\mathcal{G}_m) \left(\sum_{l=1}^{q_m} |[A_m^{-1}]_{li}|^2 + \sum_{l=1}^{L-q_m} |[C_m]_{li}|^2 \right) \\ &= \sigma^2 \psi_n, \quad \text{where} \quad \psi_n = T \sum_{m=1}^M \mu(\mathcal{G}_m) (\|A_m^{-1}\|_F^2 + \|C_m\|_F^2). \end{aligned}$$

The norm $\|\cdot\|_F$ above is the Frobenius norm. □

A.7 Proof of Lemma 3.1

Let $\mathbf{Y} = \mathbf{X} + \mathbf{R}\mathbf{Q}^\dagger$. Rewriting in terms of \mathbf{Y} followed by squaring, the objective function gives us an equivalent problem: $\min_{\mathbf{Y}} \|\mathbf{R} + (\mathbf{Y} - \mathbf{R}\mathbf{Q}^\dagger)\mathbf{Q}\|_2^2 = \min_{\mathbf{Y}} \|\mathbf{R}\mathbf{P}_Q^\perp + \mathbf{Y}\mathbf{Q}\|_2^2$, where $\mathbf{P}_Q^\perp = \mathbf{I} - \mathbf{Q}^\dagger\mathbf{Q}$, is the orthogonal projection operator onto $R(\mathbf{Q})^\perp$. Hence, using $\mathbf{P}_Q^\perp\mathbf{Q} = \mathbf{0}$, transforms the problem to

$$\begin{aligned} &\min_{\mathbf{Y}} \lambda_{\max}((\mathbf{R}\mathbf{P}_Q^\perp + \mathbf{Y}\mathbf{Q})(\mathbf{R}\mathbf{P}_Q^\perp + \mathbf{Y}\mathbf{Q})^*) \\ \implies &\min_{\mathbf{Y}} \lambda_{\max}(\mathbf{R}\mathbf{P}_Q\mathbf{Q}^*\perp\mathbf{R}^* + \mathbf{Y}\mathbf{Q}\mathbf{Q}^*\mathbf{Y}^*). \end{aligned}$$

The choice $\mathbf{Y} = \mathbf{0}$ (or $\mathbf{X} = -\mathbf{R}\mathbf{Q}^\dagger$) is clearly optimal since $\mathbf{Y}\mathbf{Q}\mathbf{Q}^*\mathbf{Y}^*$ is a positive semidefinite perturbation. In fact, all singular values of $(\mathbf{R} + \mathbf{X}\mathbf{Q})$ are simultaneously minimized. □

A.8 Proof of Lemma 3.2

The proof of Lemma 3.2 relies on the following result:

Lemma A.2. *Let \mathbf{A} and \mathbf{B} have the same number of rows and satisfy $\mathbf{A}\mathbf{A}^* + \mathbf{B}\mathbf{B}^* = \mathbf{I}$, and define $\mathbf{P} \stackrel{\text{def}}{=} \mathbf{I} - \mathbf{A}\mathbf{A}^\dagger = \mathbf{I} - \mathbf{A}(\mathbf{A}^*\mathbf{A})^{-1}\mathbf{A}^*$. Then the pseudo-inverse of $\mathbf{M} = \mathbf{P}\mathbf{B}$ is $\mathbf{M}^\dagger = \mathbf{B}^*\mathbf{P}$.*

Proof. It suffices to check that the asserted pseudo-inverse \mathbf{M}^\dagger satisfies

$$\begin{aligned} (a) \quad \mathbf{M}^\dagger \mathbf{M} &= \mathbf{P}_{R(\mathbf{M}^\dagger)} \\ (b) \quad \mathbf{M}\mathbf{M}^\dagger &= \mathbf{P}_{R(\mathbf{M})}, \end{aligned}$$

where $\mathbf{P}_{R(\mathbf{U})}$ denotes the orthogonal projection operator onto the range space of any matrix \mathbf{U} . Note that \mathbf{P} , being the orthogonal projection matrix onto the null space of \mathbf{A}^* , satisfies the following properties which are easily verified: $\mathbf{P}^* = \mathbf{P}^2 = \mathbf{P}^\dagger = \mathbf{P}\mathbf{P}\mathbf{A} = \mathbf{0}$ and $\mathbf{A}^*\mathbf{P} = \mathbf{0} = \mathbf{A}^\dagger\mathbf{P} = \mathbf{0}$. We use these properties without explicitly stating them. To verify (a), let $\mathbf{Q} = \mathbf{M}^\dagger\mathbf{M} = \mathbf{B}^*\mathbf{P}\mathbf{P}\mathbf{B} = \mathbf{B}^*\mathbf{P}\mathbf{B}$. A standard way to check that \mathbf{Q} is an orthonormal projection operator is to verify that $\mathbf{Q}^2 = \mathbf{Q}$ and $\mathbf{Q}^* = \mathbf{Q}$. It is evident from its definition that \mathbf{Q} is Hermitian. Next, we examine the quantity \mathbf{Q}^2 :

$$\begin{aligned} \mathbf{Q}^2 &= (\mathbf{B}^*\mathbf{P}\mathbf{B})^2 = \mathbf{B}^*\mathbf{P}\mathbf{B}\mathbf{B}^*\mathbf{P}\mathbf{B} \\ &= \mathbf{B}^*\mathbf{P}(\mathbf{I} - \mathbf{A}\mathbf{A}^*)\mathbf{P}\mathbf{B} = \mathbf{B}^*\mathbf{P}\mathbf{B} = \mathbf{Q}, \end{aligned}$$

which follows from $\mathbf{A}\mathbf{A}^* + \mathbf{B}\mathbf{B}^* = \mathbf{I}$ and the properties of \mathbf{P} . The equation $\mathbf{Q} = \mathbf{B}^*\mathbf{P}\mathbf{B} = \mathbf{M}^\dagger\mathbf{B}$ yields $R(\mathbf{Q}) \subset R(\mathbf{M}^\dagger)$. Conversely, $\mathbf{Q}\mathbf{B}^*\mathbf{P} = \mathbf{B}^*\mathbf{P}\mathbf{B}\mathbf{B}^*\mathbf{P} = \mathbf{B}^*\mathbf{P} = \mathbf{M}^\dagger$ implies that $R(\mathbf{M}^\dagger) \subset R(\mathbf{Q})$. This proves that $R(\mathbf{Q}) = R(\mathbf{M}^\dagger)$ and therefore completes the verification of (a). We may check (b) similarly. Let $\bar{\mathbf{Q}} = \mathbf{M}\mathbf{M}^\dagger = \mathbf{P}\mathbf{B}\mathbf{B}^*\mathbf{P} = \mathbf{P}$. Then $\bar{\mathbf{Q}}$ is clearly a projection operator. As before, we have $R(\mathbf{M}) \subseteq R(\mathbf{P})$ since $\mathbf{M} = \mathbf{P}\mathbf{B}$, while $R(\mathbf{P}) \subseteq R(\mathbf{M})$ since $\mathbf{M}\mathbf{M}^\dagger = \mathbf{P}$. Thus, (b) is verified and the lemma is proved. \square

Proof of Lemma 3.2. Any matrix \mathbf{C} that satisfies $\mathbf{C}\mathbf{A} = \mathbf{0}$ can be expressed as $\mathbf{C} = \mathbf{Y}\mathbf{P}$ for a suitable matrix \mathbf{Y} of the same size as \mathbf{C} . Conversely the matrix $\mathbf{Y}\mathbf{P}$ is a valid “ \mathbf{C} -matrix” since $\mathbf{Y}\mathbf{P}\mathbf{A} = \mathbf{0}$. The upshot is that we can replace \mathbf{C} by $\mathbf{Y}\mathbf{P}$ in the minimization, thereby eliminating the constraint $\mathbf{C}\mathbf{A} = \mathbf{0}$ altogether. By a similar argument we can replace \mathbf{A}^{-1} by $\mathbf{A}^\dagger + \mathbf{X}\mathbf{P}$. The sizes of \mathbf{X} and \mathbf{Y} are $q \times (L - q)$ and $(L - q) \times (L - q)$, respectively. Therefore, Eq. (3.13) transforms to

$$\min_{\mathbf{X}, \mathbf{Y}} \left\| \begin{pmatrix} (\mathbf{A}^\dagger + \mathbf{X}\mathbf{P})\mathbf{B} \\ \mathbf{Y}\mathbf{P}\mathbf{B} - \mathbf{I} \end{pmatrix} \right\|_2 \equiv \min_{\mathbf{X}, \mathbf{Y}} \left\| \begin{pmatrix} \mathbf{A}^\dagger\mathbf{B} \\ -\mathbf{I} \end{pmatrix} + \begin{pmatrix} \mathbf{X} \\ \mathbf{Y} \end{pmatrix} \mathbf{P}\mathbf{B} \right\|_2.$$

We can now apply Lemma 3.1 to the above problem to obtain the minimizing solution

$$\begin{pmatrix} \mathbf{X}_\star \\ \mathbf{Y}_\star \end{pmatrix} = - \begin{pmatrix} \mathbf{A}^\dagger \mathbf{B} \\ -\mathbf{I} \end{pmatrix} (\mathbf{P}\mathbf{B})^\dagger. \quad (\text{A.18})$$

Next observe that $(\mathbf{A} \ \mathbf{B})$ is a $q \times L$ submatrix of the $L \times L$ DFT matrix with possible rearrangements of columns. Therefore, its rows are orthonormal and it satisfies $\mathbf{A}\mathbf{A}^* + \mathbf{B}\mathbf{B}^* = \mathbf{I}$. Combining Lemma A.2 with Eq. (A.18), yields the minimizing solution: $\mathbf{X}_\star = \mathbf{A}^\dagger \mathbf{B}\mathbf{B}^* \mathbf{P}$ and $\mathbf{Y}_\star = -\mathbf{B}^* \mathbf{P}$. Again, using $\mathbf{A}\mathbf{A}^* + \mathbf{B}\mathbf{B}^* = \mathbf{I}$ and the properties of \mathbf{P} , we find that $\mathbf{X}_\star = \mathbf{A}^\dagger \mathbf{B}\mathbf{B}^* \mathbf{P}$ simplifies to zero. Hence, the choice $\mathbf{A}_\star^{-1} = \mathbf{A}^\dagger$ and $\mathbf{C}_\star = \mathbf{B}^* \mathbf{P}^2 \equiv \mathbf{B}^* \mathbf{P}$ minimizes $\|\mathbf{S}\|_2$. Note that this solution also simultaneously minimizes all the singular values of \mathbf{S} and therefore also its Frobenius norm. We now compute the minimum norm of \mathbf{S} at optimality, namely $\|\mathbf{S}_\star\|_2$ where

$$\mathbf{S}_\star = \begin{pmatrix} \mathbf{D}_\star \\ \mathbf{F}_\star \end{pmatrix} = \begin{pmatrix} \mathbf{A}^\dagger \mathbf{B} \\ \mathbf{B}^* \mathbf{P}\mathbf{B} - \mathbf{I} \end{pmatrix}. \quad (\text{A.19})$$

From the proof of Lemma A.2, we know that $\mathbf{Q} = \mathbf{B}^* \mathbf{P}\mathbf{B}$ is a projection operator. Therefore, $-\mathbf{F}_\star = \mathbf{I} - \mathbf{Q}$ is also an orthogonal projection operator. The case $p = L$ is trivial and it is easy to check that $\mathbf{S}_\star = \mathbf{0}$ for this case. Moreover, \mathbf{F}_\star is nonzero if and only if $p < L$. We assume that $p < L$ (and hence $\mathbf{F}_\star \neq \mathbf{0}$) in the rest of the proof. The spectral norm of \mathbf{S}_\star can be bounded from above as follows

$$\begin{aligned} \|\mathbf{S}_\star\|_2^2 &= \lambda_{\max}(\mathbf{D}_\star^* \mathbf{D}_\star + \mathbf{F}_\star^* \mathbf{F}_\star) \\ &\leq \lambda_{\max}(\mathbf{D}_\star^* \mathbf{D}_\star) + \lambda_{\max}(\mathbf{F}_\star^* \mathbf{F}_\star) = 1 + \lambda_{\max}(\mathbf{D}_\star^* \mathbf{D}_\star). \end{aligned} \quad (\text{A.20})$$

Now observe that

$$-\mathbf{F}_\star^* \mathbf{D}_\star^* = \mathbf{D}_\star^* - \mathbf{B}^* \mathbf{P}\mathbf{B}\mathbf{B}^* (\mathbf{A}^\dagger)^* = \mathbf{D}_\star^* - \mathbf{B}^* \mathbf{P} (\mathbf{A}^\dagger)^* = \mathbf{D}_\star^*$$

Therefore, $R(\mathbf{D}_\star^*) \subset R(\mathbf{F}_\star^*)$, or equivalently, $R(\mathbf{D}_\star^* \mathbf{D}_\star) \subset R(\mathbf{F}_\star^* \mathbf{F}_\star)$. Let $\boldsymbol{\xi}$ be an eigenvector corresponding to the largest eigenvalue of $\mathbf{D}_\star^* \mathbf{D}_\star$, i.e., $\mathbf{D}_\star^* \mathbf{D}_\star \boldsymbol{\xi} = \lambda_{\max}(\mathbf{D}_\star^* \mathbf{D}_\star) \boldsymbol{\xi}$. Then $\mathbf{F}_\star^* \mathbf{F}_\star \boldsymbol{\xi} = \boldsymbol{\xi}$ because $\boldsymbol{\xi} \in R(\mathbf{F}_\star^* \mathbf{F}_\star)$. Therefore,

$$(\mathbf{D}_\star^* \mathbf{D}_\star + \mathbf{F}_\star^* \mathbf{F}_\star) \boldsymbol{\xi} = (1 + \lambda_{\max}(\mathbf{D}_\star^* \mathbf{D}_\star)) \boldsymbol{\xi},$$

implying that $\|\mathbf{S}_\star\|_2^2 \geq 1 + \lambda_{\max}(\mathbf{D}_\star^* \mathbf{D}_\star)$. Combining this with Eq. (A.20) we obtain

$$\|\mathbf{S}_\star\|_2^2 = 1 + \lambda_{\max}(\mathbf{D}_\star^* \mathbf{D}_\star). \quad (\text{A.21})$$

Finally, a simple calculation reveals that

$$\begin{aligned} \mathbf{D}_\star^* \mathbf{D}_\star^* &= \mathbf{A}^\dagger \mathbf{B}\mathbf{B}^* (\mathbf{A}^\dagger)^* = \mathbf{A}^\dagger (\mathbf{I} - \mathbf{A}\mathbf{A}^*) (\mathbf{A}^\dagger)^* = \mathbf{A}^\dagger (\mathbf{A}^\dagger)^* - \mathbf{I} \\ &= (\mathbf{A}^* \mathbf{A})^{-1} \mathbf{A}^* \mathbf{A} (\mathbf{A}^* \mathbf{A})^{-1} - \mathbf{I} = (\mathbf{A}^* \mathbf{A})^{-1} - \mathbf{I}. \end{aligned} \quad (\text{A.22})$$

Therefore, $\lambda_{\max}(\mathbf{D}_\star^* \mathbf{D}_\star) = \lambda_{\max}(\mathbf{D}_\star^* \mathbf{D}_\star) = \lambda_{\max}((\mathbf{A}^* \mathbf{A})^{-1}) - 1$, and hence Eq. (A.21) yields $\|\mathbf{S}_\star\|_2 = \sqrt{\lambda_{\max}((\mathbf{A}^* \mathbf{A})^{-1})}$, for $p < L$. \square

A.9 Proof of Theorem 3.3

We can rewrite the optimization as

$$\min_{\alpha \geq \alpha_0} \left(\alpha \max_{f \in [0, \alpha]} \sum_{r=0}^{L-1} \nu(f + r\alpha) \right), \quad (\text{A.23})$$

where $\nu(f) = \chi(f \in \mathcal{F})$, $\alpha = 1/LT$, and $\alpha_0 = 1/LT_0$. The set $\mathcal{F} = \bigcup_i [a_i, b_i)$ is assumed to satisfy $0 = a_1 < b_1 < a_2 < \dots < a_n < b_n = 1/T_0$. The function $\nu(f)$ is right continuous and has jump discontinuities of $+1$ and -1 at a_i and b_i , respectively. Hence, we obtain the following properties of $\nu(f)$: (a) $\bar{\exists} a_i \in (f_1, f_2] \implies \nu(f_1) \geq \nu(f_2)$ and (b) $\bar{\exists} b_i \in (f_1, f_2] \implies \nu(f_1) \leq \nu(f_2)$. We use these properties without explicitly stating them. Now suppose that the optimum value α_\star does not satisfy $k\alpha_\star = b_j - a_i$ for any $i \leq j$ and $k \geq 0$. We will show the choice $\alpha = \alpha_\star - \delta$ yields a smaller objective function than $\alpha = \alpha_\star$, for a sufficiently small δ , which is a contradiction. In particular, we prove that $\bar{q} \leq q$, where q and \bar{q} are defined as

$$\begin{aligned} q &\stackrel{\text{def}}{=} \max_{f \in [0, \alpha_\star]} \sum_{r=0}^{L-1} \nu(f + r\alpha_\star), \\ \bar{q} &\stackrel{\text{def}}{=} \max_{f \in [0, \alpha_\star - \delta]} \sum_{r=0}^{L-1} \nu(f + r(\alpha_\star - \delta)), \end{aligned} \quad (\text{A.24})$$

for an appropriately chosen δ , and this implies that $(\alpha_\star - \delta)\bar{q} \leq \alpha_\star q$. Hence, the optimality of α_\star is contradicted. We start by choosing δ :

$$0 < \delta < \frac{1}{L} \min\{|b_j - a_i - k\alpha_\star| : i \leq j, 0 < k \leq L\}. \quad (\text{A.25})$$

Since $\delta < L^{-1}|b_n - a_1 - L\alpha_\star|$, we see that $\alpha \stackrel{\text{def}}{=} \alpha_\star - \delta \geq (b_n - a_1)/L \equiv \alpha_0$ is feasible to the optimization in Eq. (A.23). Let $f \in [0, \alpha_\star - \delta)$ be fixed. If there does not exist a b_j such that $b_j \in (f + r(\alpha_\star - \delta), f + r\alpha_\star]$ for any $r \in \mathcal{L} = \{0, \dots, L-1\}$, then it follows that $\nu(f + r(\alpha_\star - \delta)) \leq \nu(f + r\alpha_\star)$ holds for every $r \in \mathcal{L}$ and, hence, $\bar{q} \leq q$ follows from Eq. (A.24). Otherwise, let r_0 be the largest integer in \mathcal{L} such that

$$f + r_0(\alpha_\star - \delta) < b_{j_0} \leq f + r_0\alpha_\star \quad (\text{A.26})$$

for some b_{j_0} . We now claim that there do not exist an $r \in \{0, \dots, r_0 - 1\}$ and a_i such that

$$f + r\alpha_\star - r\delta \geq a_i > f + r\alpha_\star - r_0\delta. \quad (\text{A.27})$$

This is easily justified because subtracting Eq. (A.27) from Eq. (A.26) gives

$$\begin{aligned} (r_0 - r)\alpha_\star + (r - r_0)\delta &< b_{j_0} - a_i < (r_0 - r)\alpha_\star + r_0\delta \\ \implies (r - r_0)\delta &< b_{j_0} - a_i - (r_0 - r)\alpha_\star < r_0\delta \\ \implies |b_{j_0} - a_i - (r_0 - r)\alpha_\star| &< \max(r_0, r_0 - r)\delta < L\delta, \end{aligned}$$

which contradicts the choice of δ in Eq. (A.25). Consequently,

$$\nu(f + r\alpha_\star - r\delta) \leq \nu(f + r\alpha_\star - r_0\delta), \quad 0 \leq r < r_0. \quad (\text{A.28})$$

Next, for $r_0 \leq r \leq L-1$, the definition of r_0 implies that there does not exist a $b_j \in (f + r(\alpha_\star - \delta), f + r\alpha_\star] \supset (f + r(\alpha_\star - \delta), f + r\alpha_\star - r_0\delta]$. Hence,

$$\nu(f + r\alpha_\star - r\delta) \leq \nu(f + r\alpha_\star - r_0\delta), \quad r_0 \leq r \leq L-1. \quad (\text{A.29})$$

Summing Eqs. (A.28) and (A.29) over their respective ranges and adding together yields

$$\sum_{r=0}^{L-1} \nu(f + r\alpha_\star - r\delta) \leq \sum_{r=0}^{L-1} \nu(f' + r\alpha_\star) \leq q, \quad (\text{A.30})$$

where $f' = f - r_0\delta$. The second inequality in Eq. (A.30) follows from the definition of q . Of course, we need to verify that $f' \geq 0$. This is true because, if $f' = f - r_0\delta < 0$, the choice $r = 0$, $a_i = a_1 = 0$ would serve as a counter example to the claim. Since Eq. (A.30) holds for each $f \in [0, \alpha_\star - \delta)$, we obtain $\bar{q} \leq q$. This proves the original statement that $1/LT_\star = (b_j - a_i)/k$ for some $1 \leq i \leq j \leq n$ and $0 < k \leq L$. Furthermore, the condition $T \leq T_0$ restricts k to $0 < k \leq T_0L(b_j - a_i) \leq L$ for given indices i and j . \square

A.10 Proof of Proposition 4.1

Let \mathcal{S}_1 and \mathcal{S}_2 be the null spaces of $\mathbf{G}_{\mathcal{A} \cap \mathcal{B}, \bullet}$ and $\mathbf{G}_{\mathcal{B}, \bullet}$, respectively. Then obviously $\mathcal{S}_2 \subseteq \mathcal{S}_1$ implying that $\mathbf{P}_{\mathcal{S}_2} = \mathbf{P}_{\mathcal{S}_1} \mathbf{P}_{\mathcal{S}_2}$, where $\mathbf{P}_{\mathcal{S}_2}$ and $\mathbf{P}_{\mathcal{S}_1}$ are the orthogonal projection operator onto the spaces \mathcal{S}_1 and \mathcal{S}_2 , respectively. Then we have

$$\begin{aligned} \text{rank}(\mathbf{G}_{\mathcal{A}, \bullet}) &= \text{rank} \begin{pmatrix} \mathbf{G}_{\mathcal{A} \cap \mathcal{B}^c, \bullet} \\ \mathbf{G}_{\mathcal{A} \cap \mathcal{B}, \bullet} \end{pmatrix} = \text{rank} \begin{pmatrix} \mathbf{G}_{\mathcal{A} \cap \mathcal{B}^c, \bullet} \mathbf{P}_{\mathcal{S}_1} \\ \mathbf{G}_{\mathcal{A} \cap \mathcal{B}, \bullet} \end{pmatrix} \\ &= \text{rank}(\mathbf{G}_{\mathcal{A} \cap \mathcal{B}^c, \bullet} \mathbf{P}_{\mathcal{S}_1}) + \text{rank}(\mathbf{G}_{\mathcal{A} \cap \mathcal{B}, \bullet}), \end{aligned}$$

where the last step follows because every row of $\mathbf{G}_{\mathcal{A} \cap \mathcal{B}^c, \bullet} \mathbf{P}_{\mathcal{S}_1}$ is orthogonal to every row of $\mathbf{G}_{\mathcal{A} \cap \mathcal{B}, \bullet}$. Hence, we have

$$\text{rank}(\mathbf{G}_{\mathcal{A} \cap \mathcal{B}^c, \bullet} \mathbf{P}_{\mathcal{S}_1}) = \text{rank}(\mathbf{G}_{\mathcal{A}, \bullet}) - \text{rank}(\mathbf{G}_{\mathcal{A} \cap \mathcal{B}, \bullet}). \quad (\text{A.31})$$

Similarly, we can show that

$$\text{rank}(\mathbf{G}_{\mathcal{A} \cap \mathcal{B}^c, \bullet} \mathbf{P}_{\mathcal{S}_2}) = \text{rank}(\mathbf{G}_{\mathcal{A} \cup \mathcal{B}, \bullet}) - \text{rank}(\mathbf{G}_{\mathcal{B}, \bullet}). \quad (\text{A.32})$$

Finally, using $\mathbf{P}_{\mathcal{S}_2} = \mathbf{P}_{\mathcal{S}_1} \mathbf{P}_{\mathcal{S}_2}$, we obtain

$$\begin{aligned} \text{rank}(\mathbf{G}_{\mathcal{A} \cap \mathcal{B}^c, \bullet} \mathbf{P}_{\mathcal{S}_2}) &= \text{rank}(\mathbf{G}_{\mathcal{A} \cap \mathcal{B}^c, \bullet} \mathbf{P}_{\mathcal{S}_1} \mathbf{P}_{\mathcal{S}_2}) \\ &\leq \text{rank}(\mathbf{G}_{\mathcal{A} \cap \mathcal{B}^c, \bullet} \mathbf{P}_{\mathcal{S}_1}). \end{aligned} \quad (\text{A.33})$$

Combining Eqs. (A.31), (A.32), and (A.33), we obtain Eq. (4.4). \square

A.11 Proof of Proposition 4.2

If $D^+(\Lambda) < \infty$, then every interval contains finitely many points of Λ , implying that

$$K_0 = \inf_{\delta > 0} \nu_{\delta}^+(\Lambda) \quad (\text{A.34})$$

is well defined. We can also assume that $\{\lambda_n\} \in \Lambda$ is an increasing sequence. Since $\nu_{\delta}^+(\Lambda)$ is an integer, we can find $\delta_0 > 0$ such that

$$\nu_{\delta_0}^+(\Lambda) = K_0, \quad (\text{A.35})$$

i.e., every interval of length $2\delta_0$ contains no more than K_0 points of Λ . Let $K \geq K_0$. Define sets

$$\Lambda_k = \{\lambda_{nK+k} : n \in \mathbb{Z}\}$$

for $k = 0, \dots, K-1$, so that $\Lambda = \bigcup_k \Lambda_k$. Clearly, the interval $[\lambda_{nK+k}, \lambda_{(n+1)K+k}]$ contains exactly $(K+1)$ points of Λ because $\{\lambda_n\}$ is an increasing sequence. Hence, in order to satisfy Eq. (A.35), we must have

$$\lambda_{(n+1)K+k} - \lambda_{nK+k} > 2\delta_0,$$

proving that each Λ_k is uniformly discrete. For every interval $\mathcal{B}_{\gamma}(\tau)$, a simple counting argument yields

$$K \#(\mathcal{B}_{\gamma}(\tau) \cap \Lambda_k) - (K-1) \leq \#(\mathcal{B}_{\gamma}(\tau) \cap \Lambda) \leq K \#(\mathcal{B}_{\gamma}(\tau) \cap \Lambda_k) + (K-1).$$

Using Eq. (4.22), we obtain

$$D^{\pm}(\Lambda_k) = \frac{1}{K} D^{\pm}(\Lambda).$$

The proof of the converse statement is trivial. To see that K_0 is the smallest such K , consider the following argument. Let Λ be a union of K uniformly discrete sets. Equation (A.34) implies

that for any $\delta > 0$ there exists an interval of length 2δ containing K_0 points of Λ . If $K < K_0$, clearly not all these points can belong to different Λ_k , implying that some Λ_k are not uniformly discrete. Thus $K \geq K_0$.

Now let $\epsilon > 0$ be arbitrary. By the definition of upper density, we can find a sufficiently large $\delta > 0$ such that every interval of length 2δ contains no more than $2\delta(D^+(\Lambda) + \epsilon)$ points of Λ . Hence, $\nu_\delta^+(\Lambda) \leq K$, where K is an integer such that

$$K \leq 2\delta(D^+(\Lambda) + \epsilon) < K + 1.$$

Using the same argument as before, we can write Λ as a union of K uniformly discrete sets $\{\Lambda_k : k = 0, \dots, K - 1\}$ of separation of δ . Then clearly

$$\frac{K}{2\delta} \leq D^+(\Lambda) + \epsilon.$$

Finally, note that $D^+(\Lambda_k) \leq 1/(2\delta)$ because each Λ_k has separation of δ . Consequently,

$$D^+(\Lambda) \leq \sum_{k=0}^{K-1} D^+(\Lambda_k) \leq \frac{K}{2\delta}.$$

□

A.12 Proof of Proposition 4.3

Suppose that $d^+ = D^+(\Lambda_1, \dots, \Lambda_P) < \infty$. Let $\epsilon > 0$ and $\gamma > 0$ be arbitrary. Then Eq. (4.23) guarantees the existence of $\tau \in \mathbb{R}$ and $\gamma' \geq \gamma/\epsilon$ such that

$$\sum_{p=1}^P \#(\Lambda_p \cap B_{\gamma'}(\tau)) \geq 2\gamma'(d^+ - \epsilon).$$

Let $n \in \mathbb{Z}$ be such that $\gamma'/\gamma \leq n < \gamma'/\gamma + 1$. Suppose we divide the interval $\mathcal{I} = B_{\gamma'}(\tau)$ into n equal intervals of width $2\gamma'/n$, then it is clear that for at least one interval, say \mathcal{I}_0 , we have

$$\sum_{p=1}^P \#(\Lambda_p \cap \mathcal{I}_0) \geq 2\gamma'(d^+ - \epsilon)/n.$$

Therefore, our choices for γ' and n imply that

$$\begin{aligned} \sum_{p=1}^P \#(\Lambda_p \cap \mathcal{I}_0) &\geq \frac{2\gamma'(d^+ - \epsilon)}{1 + \gamma'/\gamma} = \frac{2\gamma(d^+ - \epsilon)}{1 + \gamma/\gamma'} \\ &\geq \frac{2\gamma(d^+ - \epsilon)}{1 + \epsilon}. \end{aligned}$$

Since $m(\mathcal{I}_0) = 2\gamma'/n \leq 2\gamma$, it follows that

$$\nu_\gamma^+(\Lambda_1, \dots, \Lambda_P) \geq \frac{2\gamma(d^+ - \epsilon)}{1 + \epsilon}$$

for all $\gamma > 0$, and we obtain Eq. (4.25) because $\epsilon > 0$ is arbitrary. If $d^+ = \infty$, then for every $\epsilon > 0$, we can find $\gamma' \geq \gamma/\epsilon$ such that

$$\sum_{p=1}^P \#(\Lambda_p \cap B_{\gamma'}(\tau)) \geq 2\gamma'/\epsilon.$$

Proceeding as before, we find that there exists an interval \mathcal{I}_0 such that $m(\mathcal{I}_0) \leq 2\gamma$ and

$$\sum_{p=1}^P \#(\Lambda_p \cap \mathcal{I}_0) \geq \frac{2\gamma}{\epsilon(1 + \epsilon)}.$$

Since $\epsilon > 0$ is arbitrary, we obtain $\nu_\gamma^+(\Lambda_1, \dots, \Lambda_P) = \infty$. The proof of Eq. (4.26) is very similar. Thus, the limits in Eqs. (4.23) and (4.24) can be replaced by simple limits. \square

A.13 Proof of Lemma 5.1

Observe that $\mathbf{C}^H(f) = \mathbf{C}(f)$ is nonsingular for all $f \in [\alpha, \beta]$ because $\text{rank } \mathbf{C}(f) = q$. In fact

$$\mathbf{C}^H(f)\mathbf{C}(f) > \epsilon^2 \mathbf{I}_q, \quad f \in [\alpha, \beta],$$

where ϵ is the minimum value of the smallest singular value of $\mathbf{C}(f)$ on $[\alpha, \beta]$:

$$\epsilon = \inf_{f \in [\alpha, \beta]} \sigma_{\min}(\mathbf{C}(f)) = \min_{f \in [\alpha, \beta]} \sigma_{\min}(\mathbf{C}(f)) > 0.$$

This is because $\mathbf{C}(f)$ is continuous, implying that $\sigma_{\min}(\mathbf{C}(f))$, which is also continuous on the compact set $[\alpha, \beta]$, attains its infimum. Therefore,

$$\begin{aligned} \mathbf{C}^\dagger(f) &= (\mathbf{C}^H(f)\mathbf{C}(f))^{-1}\mathbf{C}^H(f), \\ \mathbf{P}_{\mathcal{R}(\mathbf{C}(f))} &= \mathbf{C}(f)(\mathbf{C}^H(f)\mathbf{C}(f))^{-1}\mathbf{C}^H(f), \end{aligned}$$

are also a continuous functions of f . Note that $\mathcal{R}(\mathbf{C}(f))$ is the projection onto the range space of $\mathbf{C}(f)$. Define

$$\begin{aligned} \mathbf{E}_1 &:= \mathbf{E}_\alpha - \mathbf{D}(\alpha)\mathbf{C}^\dagger(\alpha), \\ \mathbf{E}_2 &:= \mathbf{E}_\beta - \mathbf{D}(\beta)\mathbf{C}^\dagger(\beta). \end{aligned}$$

It follows that $\mathbf{E}_1\mathbf{C}(\alpha) = \mathbf{E}_2\mathbf{C}(\beta) = \mathbf{0}$, implying that

$$\mathbf{E}_1\mathbf{P}_{\mathcal{R}(\mathbf{C}(\alpha))} = \mathbf{E}_2\mathbf{P}_{\mathcal{R}(\mathbf{C}(\beta))} = \mathbf{0}. \quad (\text{A.36})$$

Now take

$$\mathbf{E}(f) := \mathbf{D}(f)\mathbf{C}^\dagger(f) + \left(\frac{(f-\alpha)}{(\beta-\alpha)}\mathbf{E}_2 + \frac{(\beta-f)}{(\beta-\alpha)}\mathbf{E}_1 \right) (\mathbf{I}_q - \mathbf{P}_{\mathcal{R}(\mathbf{C}(f))}).$$

This is a valid solution because it is continuous and meets the requirements:

$$\mathbf{E}(f)\mathbf{C}(f) = \mathbf{D}(f) + \left(\frac{(f-\alpha)}{(\beta-\alpha)}\mathbf{E}_2 + \frac{(\beta-f)}{(\beta-\alpha)}\mathbf{E}_1 \right) (\mathbf{C}(f) - \mathbf{P}_{\mathcal{R}(\mathbf{C}(f))}\mathbf{C}(f)) = \mathbf{D}(f),$$

$$\mathbf{E}(\alpha) = \mathbf{D}(\alpha)\mathbf{C}^\dagger(\alpha) + \mathbf{E}_1 - \mathbf{E}_1\mathbf{P}_{\mathcal{R}(\mathbf{C}(\alpha))} = \mathbf{E}_\alpha,$$

$$\mathbf{E}(\beta) = \mathbf{D}(\beta)\mathbf{C}^\dagger(\beta) + \mathbf{E}_2 - \mathbf{E}_2\mathbf{P}_{\mathcal{R}(\mathbf{C}(\beta))} = \mathbf{E}_\beta.$$

The last two equations follow from Eq. (A.36). \square

A.14 Proof of Proposition 6.3

From Eqs. (6.44) and (6.47) we obtain an upper bound on the cost function:

$$\begin{aligned} C_r(\boldsymbol{\alpha}^r) &= \max \left\| \sum_{s \in \mathcal{R}} T^{rs} x_s \right\| \quad \text{s.t.} \quad \|x_s\| \leq \gamma_s, \quad s \in \mathcal{R} \\ &\leq \max \sum_{s \in \mathcal{R}} \|T^{rs} x_s\| \quad \text{s.t.} \quad \|x_s\| \leq \gamma_s, \quad s \in \mathcal{R} \\ &= \sum_{s \in \mathcal{R}} \gamma_s \|T^{rs}\| = \sum_{s \in \mathcal{R}} \gamma_s \max_{\nu \in [0, \frac{1}{L}]} \|T^{rs}[\nu]\|, \end{aligned}$$

where the last step follows from Eq. (6.45). Hence, $C_r(\boldsymbol{\alpha}^r) \leq \bar{C}_r(\boldsymbol{\alpha}^r)$. We now prove the other inequality. start by choosing a set of signals x'_s , $s \in \mathcal{R}$ such that $\|x'_s\| = \gamma_s$ and $\|T^{rs}x'_s\| = \gamma_s\|T^{rs}\|$. In other words, x'_s is the right singular vector of T^{rs} corresponding to its largest singular value. First let $\bar{x}_0 = x'_0$. Then, for $s = 1, 2, \dots, R-1$, let \bar{x}_s be either x'_s or $-x'_s$ such that

$$\left\langle T^{rs}\bar{x}_s, \sum_{\sigma=0}^{s-1} T^{r\sigma}\bar{x}_\sigma \right\rangle \geq 0. \quad (\text{A.37})$$

Hence, we have $\|\bar{x}_s\| = \gamma_s$ and $T^{rs}\bar{x}_s = \|T^{rs}\|\bar{x}_s$. Therefore, Eq. (A.37) implies that for any $s \in \mathcal{R}$

$$\begin{aligned} \left\| \sum_{\sigma=0}^s T^{r\sigma}\bar{x}_\sigma \right\|^2 &= \|T^{rs}\bar{x}_s\|^2 + 2 \left\langle T^{rs}\bar{x}_s, \sum_{\sigma=0}^{s-1} T^{r\sigma}\bar{x}_\sigma \right\rangle + \left\| \sum_{\sigma=0}^{s-1} T^{r\sigma}\bar{x}_\sigma \right\|^2 \\ &\geq \|T^{rs}\bar{x}_s\|^2 + \left\| \sum_{\sigma=0}^{s-1} T^{r\sigma}\bar{x}_\sigma \right\|^2. \end{aligned} \quad (\text{A.38})$$

Then,

$$\begin{aligned}
C_r(\boldsymbol{\alpha}^r)^2 &\stackrel{(a)}{\geq} \left\| \sum_{\sigma=0}^{R-1} T^{r\sigma} \bar{x}_\sigma \right\|^2 \\
&\stackrel{(b)}{\geq} \sum_{s \in \mathcal{R}} \|T^{rs} \bar{x}_s\|^2 \\
&\stackrel{(c)}{=} \sum_{s \in \mathcal{R}} \gamma_s^2 \|T^{rs}\|^2
\end{aligned} \tag{A.39}$$

where (a) follows from the definition of $C_r(\boldsymbol{\alpha}^r)$, (b) by recursively applying Eq. (A.38) starting with $s = R - 1$, and (c) by the choice of \bar{x}_s . Now, using the Cauchy-Schwarz inequality, we have

$$\sum_{s \in \mathcal{R}} \gamma_s^2 \|T^{rs}\|^2 \geq \frac{1}{R} \left(\sum_{s \in \mathcal{R}} \gamma_s \|T^{rs}\| \right)^2 = \frac{1}{R} \bar{C}_r(\boldsymbol{\alpha}^r)^2. \tag{A.40}$$

Finally, combining Eqs. (A.39) and (A.40), we obtain the other desired inequality:

$$C_r(\boldsymbol{\alpha}^r) \geq \frac{1}{\sqrt{R}} \bar{C}_r(\boldsymbol{\alpha}^r).$$

□

APPENDIX B

JUSTIFICATION FOR DISCRETE-TIME MODELS

The purpose of this appendix is to justify the discrete-time models for the MIMO channel and the reconstruction system in Chapter 6. More specifically, we show that the MIMO channel can be replaced by a hypothetical discrete-time channel. The reconstruction system, which is implemented by digital signal processing, also has a discrete-time model, and the continuous-time outputs can eventually be reconstructed by using D/A converters at the of the digital processing stage.

B.1 Channel Model

Suppose that the MIMO channel and its inputs have continuous-time models as described in Chapter 5. Then the input-output relation for the channel is

$$\mathbf{Y}(f) = \mathbf{G}(f)\mathbf{X}(f), \quad (\text{B.1})$$

Now, each component of the input $\mathbf{x}(t)$ is a multiband signal whose Fourier transform $\mathbf{X}(f)$ has a bounded support \mathcal{F}_r . Hence, by the classical sampling theorem, $\mathbf{x}(t)$ is representable in terms of its samples on taken uniformly at a sufficiently high rate (the Nyquist rate). Suppose that

$$\mathcal{F} = \bigcup_{r \in \mathcal{R}} \mathcal{F}_r, \quad f_{\max} = \sup_{f \in \mathcal{F}} f, \quad f_{\min} = \inf_{f \in \mathcal{F}} f,$$

and that $L \in \mathbb{Z}$ such that $(f_{\max} - f_{\min}) \leq L/T$. Hence, it follows that

$$|f - f'| \geq \frac{L}{T} \implies \mathbf{J}(f)\mathbf{J}(f') = 0, \quad (\text{B.2})$$

where $\mathbf{J}(f)$ is the following diagonal matrix:

$$\mathbf{J}(f) = \text{diag}(\chi(f \in \mathcal{F}_1), \dots, \chi(f \in \mathcal{F}_R)). \quad (\text{B.3})$$

Observe that

$$\mathbf{J}(f)\mathbf{X}(f) = \mathbf{X}(f) \quad (\text{B.4})$$

because $X_r(f) = 0$ for $f \notin \mathcal{F}_r$. Next, using Eqs. (B.2) and (B.4), we have

$$|f' - f| \geq L/T \implies \mathbf{J}(f)\mathbf{X}(f') = \mathbf{J}(f)\mathbf{J}(f')\mathbf{X}(f') = 0. \quad (\text{B.5})$$

So let us define sequences $\mathbf{x}[k]$, $\mathbf{y}[k]$, and a discrete-time transfer function $\mathbf{G}[\nu]$ as follows:

$$\begin{aligned} \mathbf{x}[k] = \mathbf{x}\left(\frac{kT}{L}\right) &\iff \mathbf{X}[\nu] = \frac{L}{T} \sum_{l \in \mathbb{Z}} \mathbf{X}\left(\frac{L(\nu+l)}{T}\right) \\ \mathbf{y}[k] = \mathbf{y}\left(\frac{kT}{L}\right) &\iff \mathbf{Y}[\nu] = \frac{L}{T} \sum_{l \in \mathbb{Z}} \mathbf{Y}\left(\frac{L(\nu+l)}{T}\right) \\ \mathbf{G}[\nu] &= \frac{T}{L} \sum_{l \in \mathbb{Z}} \mathbf{G}\left(\frac{L(\nu+l)}{T}\right) \mathbf{J}\left(\frac{L(\nu+l)}{T}\right) \end{aligned} \quad (\text{B.6})$$

Notice that discrete-time sequences (and their Fourier transforms) use square brackets, while continuous-time quantities use round brackets. The quantity $\mathbf{X}_r[\nu]$ is clearly supported on the set $\mathcal{F}_r^d = (T/L)\mathcal{F}$. We can assume, without loss of generality, that $\mathcal{F}_r^d \subseteq [0, 1]$. Taking the Fourier transform of $\mathbf{y}[k]$, we obtain

$$\begin{aligned} \mathbf{Y}[\nu] &= \frac{T}{L} \sum_{l \in \mathbb{Z}} \mathbf{Y}\left(\frac{L(\nu+l)}{T}\right) \\ &\stackrel{(a)}{=} \frac{T}{L} \sum_{l \in \mathbb{Z}} \mathbf{G}\left(\frac{L(\nu+l)}{T}\right) \mathbf{J}\left(\frac{L(\nu+l)}{T}\right) \mathbf{X}\left(\frac{L(\nu+l)}{T}\right) \\ &\stackrel{(b)}{=} \frac{T}{L} \sum_{l \in \mathbb{Z}} \mathbf{G}\left(\frac{L(\nu+l)}{T}\right) \mathbf{J}\left(\frac{L(\nu+l)}{T}\right) \sum_{\nu' \in \mathbb{Z}} \mathbf{X}\left(\frac{L(\nu+l')}{T}\right) \\ &= \mathbf{G}[\nu] \mathbf{X}[\nu], \quad \nu \in [0, 1], \end{aligned} \quad (\text{B.7})$$

where (a) follows from Eq. (B.1) and Eq. (B.4), while (b) holds because

$$l \neq l' \implies \mathbf{J}\left(\frac{L(\nu+l)}{T}\right) \mathbf{X}\left(\frac{L(\nu+l')}{T}\right) = 0,$$

which itself is a consequence of Eq. (B.5). Finally note that the actual observations from the channel output samples $\mathbf{z}[n]$ can be obtained by down-sampling $\mathbf{y}[k]$ by a factor of L , i.e., $\mathbf{z}[n] = \mathbf{y}(nT) = \mathbf{y}[nL]$. Hence,

$$\mathbf{Z}[\nu] = \frac{1}{L} \sum_{l \in \mathcal{L}} \mathbf{Y}\left[\frac{\nu+l}{L}\right], \quad \nu \in [0, 1], \quad (\text{B.8})$$

where $\mathcal{L} = \{0, 1, \dots, L-1\}$. In other words, everything to the left of the dashed line in Figure 5.1 can be represented by a discrete-time system shown in Figure B.1. The block represents a discrete linear shift-invariant system with transfer function $\mathbf{G}[\nu]$.

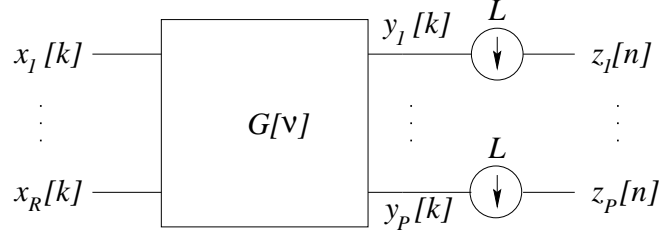


Figure B.1 Discrete-time model for the MIMO channel.

Finally, observe that only one term of the summation in Eq. (B.6) is nonzero for $\nu \in [0, 1)$, because the terms do not overlap at any frequency ν due to Eq. (B.2). Therefore, if $G_{pr}(f)$ is continuous on the set $\overline{\mathcal{F}}_r$ (the closure of \mathcal{F}_r), then clearly $G_{pr}[\nu]$ is continuous on $\overline{\mathcal{F}}_r$. Hence, the continuity property, which is desirable for implementation reasons, is preserved.

B.2 Reconstruction Model

Assume that the continuous-time reconstructed output $\tilde{\mathbf{x}}(t)$ lies in \mathcal{H} . This is a reasonable assumption because, after all $\tilde{\mathbf{x}}(t)$ is an estimate of $\mathbf{x}(t) \in \mathcal{H}$. Therefore, the sampling theorem implies that $\tilde{\mathbf{x}}(t)$ is fully represented by the sampled sequence $\tilde{\mathbf{x}}(kT/L)$. So, we model our reconstruction system as a discrete-time system producing an output $\tilde{\mathbf{x}}[k] = \tilde{\mathbf{x}}(kT/L)$, because it suffices to reconstruct $\tilde{\mathbf{x}}(t)$. Note that $\tilde{\mathbf{x}}(t) \in \mathcal{H}$ if each column of $\mathbf{h}(t)$ lies in \mathcal{H} . From Eq. (5.6) we see that

$$\tilde{\mathbf{x}}[k] = \sum_{n \in \mathbb{Z}} \mathbf{h}\left(\frac{(k - nL)T}{L}\right) \mathbf{z}[n] \equiv \sum_{k \in \mathbb{Z}} \mathbf{h}[k - Lk] \mathbf{z}[k], \quad (\text{B.9})$$

where

$$\mathbf{h}[k] = \mathbf{h}\left(\frac{kT}{L}\right).$$

We can rewrite Eq. (B.9) in the frequency domain as

$$\tilde{\mathbf{X}}[\nu] = \mathbf{H}[\nu] \mathbf{Z}[L\nu], \quad (\text{B.10})$$

where

$$\mathbf{H}[\nu] = \frac{T}{L} \sum_{l \in \mathbb{Z}} \mathbf{H}\left(\frac{L(\nu + l)}{T}\right). \quad (\text{B.11})$$

Therefore, the reconstruction block, shown to the right of the dashed line in Figure 5.1, can be replaced by the discrete-time system illustrated in Figure B.2. Equation (B.6) describes the hypothetical discrete-time channel that replaces the continuous-time model, while Eq. (B.11)

describes the real reconstruction system. Finally, since the discrete-time sequences $\tilde{\mathbf{x}}_r[k]$ represent samples of $\tilde{\mathbf{x}}_r(t)$ at a rate higher than the Nyquist rate, we can reconstruct $\tilde{\mathbf{x}}_r(t)$ by using D/A converters.

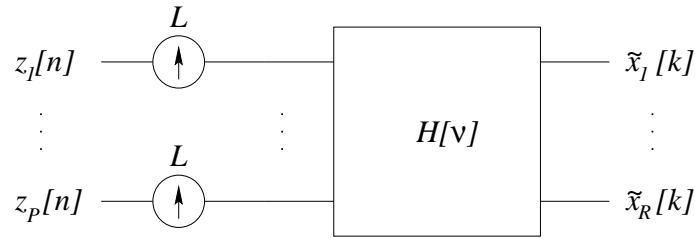


Figure B.2 Discrete-time model for MIMO reconstruction.

If the channel has a discrete-time model as shown in Figure B.1, then the reconstruction block in Figure B.2 is the most general structure with the property that the entire MIMO system (consisting of the channel, the down- and up-samplers, and the reconstruction filters) is invariant to shifts by multiples of L samples:

$$\mathbf{x}(k) \rightarrow \tilde{\mathbf{x}}(k) \implies \mathbf{x}(k - nL) \rightarrow \tilde{\mathbf{x}}(k - nL), \quad \forall k, n \in \mathbb{Z}.$$

The models presented here are applicable whether the discrete-time inputs represent underlying continuous-time function or whether they are genuinely discrete-time by nature.

Finally, we point out that the sets \mathcal{F}_r are not used in the discrete-time setting, there by obviating the need for the superscript in \mathcal{F}^d , i.e., we denote the spectral support of $x_r[k]$ by \mathcal{F}_r .

REFERENCES

- [1] C. E. Shannon, "Communication in the presence of noise," in *IRE Proc.*, vol. 37, pp. 10–21, January 1949.
- [2] J. R. Higgins, *Sampling Theory in Fourier and Signals Analysis Foundations*. New York: Oxford Science Pub., 1996.
- [3] R. J. Marks II, Ed., *Advanced Topics in Shannon Sampling and Interpolation Theory*. New York: Springer-Verlag, 1993.
- [4] A. J. Jerri, "The Shannon sampling theorem—its various extensions and applications: A tutorial review," *Proc. IEEE*, vol. 65, no. 11, pp. 1565–1596, November 1977.
- [5] A. Zayed, *Advances in Shannon's Sampling Theory*, CRC Press, Boca Raton, FL, 1993.
- [6] H. Landau, "Necessary density conditions for sampling and interpolation of certain entire functions," *Acta Math.*, vol. 117, pp. 37–52, 1967.
- [7] H. J. Landau, "Sampling, data transmission, and the Nyquist rate," *Proc. IEEE*, vol. 55, pp. 1701–1706, October 1967.
- [8] R. N. Bracewell, *Two Dimensional Imaging*. Englewood Cliffs, NJ: Prentice Hall, 1994.
- [9] Z. P. Liang and P. C. Lauterbur, *Principles of Magnetic Resonance Imaging*. New York: IEEE Press, 2000.
- [10] M. Soumekh, *Synthetic Aperture Radar Signal Processing with MATLAB Algorithms*. New York: John Wiley & Sons, 1999.
- [11] R. J. Korzig and S. A. Kassam, "Synthetic aperture pulse-echo imaging with rectangular bounded arrays," *IEEE Trans. Image Process.*, vol. 2, no. 1, pp. 68–79, January 1993.
- [12] R. J. Papoulis, "Generalized sampling expansions," *IEEE Trans. Circuits Syst.*, vol. CAS-24, pp. 652–654, November 1977.

- [13] D. Seidner and M. Feder, "Vector sampling expansions," *IEEE Trans. Sig. Process.*, vol. 48, no. 5, pp. 1401–1416, May 2000.
- [14] J. L. Brown Jr., "Sampling expansions for multi-band signals," *IEEE Trans. Acoust. Speech Signal Process.*, vol. 33, pp. 312–315, February 1985.
- [15] R. E. Kahn and B. Liu, "Sampling representations and the optimum reconstruction of signals," *IEEE Trans. Info. Theory*, vol. 11, no. 3, pp. 339–347, July 1965.
- [16] K. Cheung and R. Marks, "Image sampling below the Nyquist density without aliasing," *J. Opt. Soc. Am. A*, vol. 7, no. 1, pp. 92–105, January 1990.
- [17] K. Cheung, "A multidimensional extension of Papoulis' generalized sampling expansion with the application in minimum density sampling," in *Advanced Topics in Shannon Sampling and Interpolation Theory*, R. J. Marks II, Ed. New York: Springer-Verlag, 1993, pp. 85–119.
- [18] P. Feng and Y. Bresler, "Spectrum-blind minimum-rate sampling and reconstruction of multi-band signals," in *Proc. IEEE Int. Conf. Acoust. Speech, Sig. Process.*, Atlanta, GA, May 1996.
- [19] Y. Bresler and P. Feng, "Spectrum-blind minimum-rate sampling and reconstruction of 2-D multiband signals," in *Proc. 3rd IEEE Int. Conf. on Image Processing, ICIP'96*, Lausanne, Switzerland, vol. I, pp. 701–704, September 1996.
- [20] P. Vaidyanathan and V. Liu, "Efficient reconstruction of band-limited sequences from non-uniformly decimated versions by use of polyphase filter banks," *IEEE Trans. Acoust., Speech Signal Process.*, vol. 38, pp. 1927–1936, November 1990.
- [21] B. Foster and C. Herley, "Exact reconstruction from periodic nonuniform sampling of signals with arbitrary frequency support," in *Proc. IEEE Int. Conf. Acoust. Speech Sig. Process.*, Detroit, MI, May 1998.
- [22] S. C. Scoluar and W. J. Fitzgerald, "Periodic nonuniform sampling of multi-band signals," *Signal Process.*, vol. 28, no. 2, pp. 195–200, August 1992.
- [23] C. Herley and P. W. Wong, "Minimum rate sampling of signals with arbitrary frequency support," in *Proc. IEEE Int. Conf. Image Process.*, Lausanne, Switzerland, September 1996.

- [24] R. G. Shenoy, “Nonuniform sampling of signals and applications,” in *Int. Symposium on Circuits and Systems*, London, vol. 2, pp. 181–184, May 1994.
- [25] J. R. Higgins, “Some gap sampling series for multiband signal,” *Signal Process.*, vol. 12, no. 3, pp. 313–319, April 1986.
- [26] M. G. Beaty and J. R. Higgins, “Aliasing and Poisson summation in the sampling theory of Paley-Wiener spaces,” *J. Fourier Anal. Appl.*, vol. 1, pp. 67–85, 1994.
- [27] A. Papoulis, *Probability, Random Variables, and Stochastic Processes*, 3rd edition, New York: McGraw-Hill, 1991.
- [28] C. Herley and P. W. Wong, “Minimum rate sampling and reconstruction of signals arbitrary frequency support,” *IEEE Trans. Info. Theory*, vol. 45, no. 5, pp. 1555–1564, July 1999.
- [29] H. G. Feichtinger and K. Gröchenig, “Theory and practice of irregular sampling,” in *Wavelets: Mathematics and Applications*, J. Benedetto and M. W. Frazier, Eds. Boca Raton, FL: CRC Press, 1994. pp. 305–364.
- [30] K. Gröchenig, “Reconstruction algorithms in irregular sampling theory,” *Comput. Math.*, vol. 59, pp. 181–194, 1992.
- [31] J. J. Benedetto, “Irregular sampling and frames,” in *Wavelets—A Tutorial in Theory and Applications*, C. K. Chui, Ed. Boston: Academic Press, 1992, pp. 445–507.
- [32] Y. C. Eldar and A. V. Oppenheim, “Filter bank reconstruction of bandlimited signals from nonuniform and generalized sampling,” *IEEE Trans. Sig. Process.*, vol. 48, no. 10, pp. 2864–2875, October 2000.
- [33] K. Gosse and P. Duhamel, “Perfect reconstruction versus MMSE filter banks in source coding,” *IEEE Trans. Sig. Process.*, vol. 45, no. 9, pp. 2188–2202, September 1997.
- [34] E. J. Anderson and P. Nash, *Linear Programming in Infinite-Dimensional Spaces*. Chichester: John Wiley & Sons, 1987.
- [35] P. J. S. G. Ferreira, “The eigenvalues of matrices that occur in certain interpolation problems,” *IEEE Trans. Sig. Process.*, vol. 45, pp. 2115–2120, August 1997.
- [36] M. M. Dodson and A. M. Silva, “Fourier analysis and the sampling theorem,” *Proc. Royal Irish Acad.*, vol. 85, pp. 81–108, 1985.

- [37] G. B. Giannakis and R. W. Heath Jr., “Blind identification of multichannel FIR blurs and perfect image restoration,” *IEEE Trans. Image Process.*, vol. 9, no. 11, pp. 1877–1896, November 2000.
- [38] G. Harikumar and Y. Bresler, “Perfect blind restoration of images blurred by multiple filters: theory and efficient algorithms,” *IEEE Trans. Image Process.*, vol. 8, no. 2, pp. 202–219, February 1999.
- [39] S. Zazo and J. M. Páez-Borrillo, “Blind multichannel equalization using a novel subspace method,” *IEEE Trans. Sig. Process.*, vol. 48, no. 8, pp. 2458–2462, August 2000.
- [40] E. Moulines, P. Duhamel, J.-F. Cardoso, and S. Mayrargue, “Subspace methods for the blind identification of multichannel FIR filters,” *IEEE Trans. Sig. Process.*, vol. 43, no. 2, pp. 516–525, February 1995.
- [41] S. Shamsunder and G. B. Giannakis, “Multichannel blind signal separation and reconstruction,” *IEEE Trans. Speech Audio Process.*, vol. 5, no. 6, pp. 515–528, 1997.
- [42] J. Idier and Y. Goussard, “Multichannel seismic deconvolution,” *IEEE Trans. Geoscience Remote Sensing*, vol. 31, no. 5, pp. 961–979, September 1993.
- [43] A. González and J. J. López, “Fast transversal filters for deconvolution in multichannel sound reproduction,” *IEEE Trans. Speech Audio Process.*, vol. 9, no. 4, pp. 429–440, May 2001.
- [44] M. Unser and J. Zerubia, “Generalized sampling: Stability and analysis,” *IEEE Trans. Sig. Process.*, vol. 45, no. 12, pp. 2941–2950, December 1997.
- [45] K. Gröchenig and H. Razafinjato, “On Landau’s necessary density conditions for sampling and interpolation of bandlimited functions,” *J. London Math. Soc.*, vol. 2, no. 54, pp. 557–565, 1996.
- [46] R. M. Young, *An Introduction to Nonharmonic Fourier Analysis*. New York: Academic Press, 2001.
- [47] J. Benedetto and P. J. S. G. Ferreira, Eds., *Modern Sampling Theory: Mathematics and Applications*. Boston: Birkhäuser, 2001.
- [48] J. Ramanathan and T. Steger, “Incompleteness of sparse coherent states,” *J. Appl. Comp. Harm. Anal.*, vol. 2, pp. 148–153, 1995.

- [49] J. Edmonds, “Submodular functions, matroids and certain polyhedra,” in *Proc. Calgary Int. Conf. Combinatorial Structures and Applications*, Calgary, Alberta, June 1969, pp. 69–87.
- [50] D. N. C. Tse and S. V. Hanly, “Multiaccess fading channels—Part I: Ploymatroid structure, optimal resource allocation and throughput capacities,” *IEEE Trans. Info. Theory*, vol. 44, no. 7, pp. 2796–2815, November 1998.
- [51] Y. I. Lyubarskii and K. Seip, “Sampling and interpolating sequences for multiband-limited functions and exponential bases on disconnected sets,” *J. Fourier Anal.*, vol. 3, no. 5, pp. 597–615, September 1997.
- [52] S. Avdonin and W. Moran, “Sampling and interpolation of functions with multiband spectra and controllability problems,” in *Optimal Control of Partial Differential Equations (Chemnitz, 1998)*, vol. 133 of *International Series of Numerical Mathematics*. Basel: Birkhäuser, 1999, pp. 43–51.
- [53] V. E. Katnelson, “Sampling and interpolation for functions with multi-band spectrum: the mean periodic continuation method,” in *Signal and Image Reproduction in Combined Spaces*, vol. 7 of *Wavelet analysis and Applications*. San Diego: Academic Press, 1998, pp. 525–553.
- [54] P. Moulin, M. Anitescu, K. O. Kortanek, and F. A. Potra, “The role of linear semi-infinite programming in signal-adapted QMF bank design,” *IEEE Trans. Sig. Process.*, vol. 45, no. 9, pp. 2160–2174, September 1997.
- [55] R. G. Shenoy, D. Burnside, and T. W. Parks, “Linear periodic systems and multirate filter design,” *IEEE Trans. Sig. Process.*, vol. 42, no. 9, pp. 2242–2255, September 1994.
- [56] C. A. Berenstein and D. C. Struppa, “On explicit solutions to the Bezout equation,” *Systems and Control Letters*, vol. 4, no. 1, pp. 33–39, February 1984.
- [57] R. Rajagopal, “Exact FIR inverses of FIR filters,” M.S. thesis, Ohio state University, 2000.
- [58] W. Rudin, *Principles of Mathematical Analysis*. New York: McGraw-Hill, 1976.

VITA

Raman C. Venkataramani was born in Anamalai, India, on June 19, 1974. He received the Bachelor of Technology degree from the Indian Institute of Technology, Madras in 1995, and the Master of Science in Engineering degree from Johns Hopkins University in 1996, both in electrical engineering. He was a teaching assistant at Johns Hopkins University from 1995 to 1997. He has been a graduate research assistant at the Coordinated Science Laboratory at the University of Illinois since 1997. He spent the summer of 2000 as an intern at Bell Labs in New Jersey. His current research interests are statistical signal and image processing, signal representation and interpolation, inverse problems, information and coding theory. After the completion of his doctoral program, he will start work for Bell Labs in the Mathematical Science Research Center.